Ankara Üniversitesi Veteriner Fakültesi Dergisi

Veterinary Journal of Ankara University

E-ISSN 1308-2817 Cilt/Volume 68 ● Sayı/Number 3 ● 2021

Ankara Univ Vet Fak Derg - vetjournal.ankara.edu.tr - Open Acsess

E-ISSN 1308-2817

Ankara Üniversitesi Veteriner Fakültesi Dergisi

Veterinary Journal of Ankara University

Cilt/Volume **68** • **Sayı**/Number **3** • **2021**

Ankara Üniversitesi Veteriner Fakültesi Dergisi
Cilt / *Volume*: 68 • Sayı / *Number*: 3 • 2021
Veterinary Journal of Ankara University
Üç ayda bir yayımlanır / *Published three monthly*
E-ISSN 1308-2817

Sahibi
Ankara Üniversitesi Veteriner Fakültesi Adına
Prof. Dr. Ender YARSAN
Dekan

Yönetim Yeri
Adres / *Address*

Ankara Üniversitesi Veteriner Fakültesi Dekanlığı
Yayın Alt Komitesi
06 110 Ankara, Türkiye
Tel: 90 312 317 03 15, **Fax:** 90 312 316 44 72
Sürdürüm ve iletişim: vfdergi@veterinary.ankara.edu.tr
URL: http://vetjournal.ankara.edu.tr
Yayın Türü: Yaygın süreli ve hakemli

"Bu dergi Thomson Reuters®'in **SCI-EXP** ve **JCR** ile Uluslararası CABI yayınlarının **CAB Abstracts, Global Health**, **CAB Direct, Database Subsets; Scopus** ve **Ulakbim** (Yaşam Bilimleri) veri tabanları kapsamındadır.

This journal is covered by **SCI-EXP** and **JCR** of Thomson Reuters®, **CAB Abstracts**, **Global Health**, **CAB Direct, Database Subsets; Scopus** and **Ulakbim** (Life Sciences) database systems.

İnternet Adresi / *Web Address*
http://vetjournal.ankara.edu.tr
Yayım Tarihi: 30.06.2021

Ankara Üniversitesi Veteriner Fakültesi Dergisi
Cilt / *Volume*: 68 • Sayı / *Number*: 3 • 2021
Veterinary Journal of Ankara University

İÇİNDEKİLER / *CONTENTS*

Ankara Univ Vet Fak Derg, **68**, 213-222, 2021
DOI: 10.33988/auvfd.775971

Examination of the morphometric features and three-dimensional modelling of the skull in Van cats by using computed tomographic images

Osman YILMAZ[1,a,✉], İsmail DEMİRCİOĞLU[2,b]

[1]Van Yüzüncü Yıl University, Faculty of Veterinary Medicine, Department of Anatomy, Van; [2]Harran University, Faculty of Veterinary Medicine, Department of Anatomy, Şanlıurfa, Turkey.
[a]ORCID: 0000-0003-2013-9213; [b]ORCID: 0000-0002-0724-3019

✉Corresponding author: osman_40_5@hotmail.com
Received date: 30.07.2020 - Accepted date: 08.09.2020

Abstract: This study was conducted to make the three-dimensional modelling of the skull in Van cats by using computed tomographic images and to determine the morphometric features between sexes. The skulls of 16 adult Van cats were used in the study. The skulls of the anesthetized animals were scanned by using a Computed Tomography (CT) device and their images were obtained. These images were converted to a three-dimensional structure using MIMICS 20.1 software and their morphometric measurements were calculated. It was determined in the study that total length of the skull (TLS), facial length (FCL), upper neurocranium length (UNCL), greatest length of the nasal (GLN), maximum zygomatic width (MZW), condylobasal length (CBL), basal length (BL), median palatal length (MPL), palatal length (PL), least palatal breadth (LPB), length of the cheek tooth row (LCR), greatest inner height of the orbit (GIHO), skull height (SH), and volumetric measurement values were statistically significantly higher in the male cats; whereas, breadth dorsal to the external auditory meatus (BEAM) and neurocranium length (NL) measurement values were statistically significantly higher in the female cats ($P<0.05$). In conclusion, the statistical differences between the sexes in terms of biometric values of skull of Van cats were determined. Present study would be beneficial to veterinary physicians in the surgical and clinical practice fields and to the studies in the field of zooarchaeology as well as being guiding for determining the typology of Van cats among the cat species and its differences from other species.
Keywords: Computed tomography, morphometry, skull, three-dimensional modelling, Van cat.

Van kedilerinde kafatasının bilgisayarlı tomografi görüntüleri kullanılarak üç boyutlu modellenmesi ve morfometrik özelliklerinin incelenmesi

Özet: Bu çalışma, Van kedilerinde kafatasının bilgisayarlı tomografi görüntüleri kullanılarak üç boyutlu modellemesini yapmak ve cinsiyetler arasındaki morfometrik özelliklerini belirlemek amacıyla yapıldı. Çalışmada 16 adet erişkin Van kedisi kafatası kullanıldı. Anestezi altındaki hayvanların kafatasları Bilgisayarlı Tomografi (BT) cihazı ile taranarak görüntüleri elde edildi. Bu görüntüler MIMICS 20.1 programı aracılığıyla üç boyutlu yapıya dönüştürüldü ve morfometrik ölçümleri hesaplandı. Çalışmada kafatasının total uzunluğu (TLS), facial uzunluk (FCL), üst neurocranium uzunluğu (UNCL), en büyük nasal uzunluk (GLN), maksimum zygomatic genişlik (MZW), condylobasal uzunluk (CBL), basal uzunluk (BL), median palatal uzunluk (MPL), palatal uzunluk (PL), en küçük palatal genişlik (LPB), yanak diş sırasının uzunluğu (LCR), orbita'nın en büyük iç yüksekliği (GIHO), kafatası yüksekliği (SH) ve volüm ölçüm değerlerinin erkek kedilerde; meatus acusticus externus'un dorsal genişliği (BEAM) ve neurocranium uzunluğu (NL) ölçüm değerlerinin ise dişi kedilerde istatistik olarak önemli düzeyde daha yüksek olduğu saptandı ($P<0.05$). Sonuç olarak, Van kedilerinde kafatasının biyometrik değerlerinin istatistiksel olarak cinsiyetler arasındaki farklılıkları tespit edildi. Sunulan çalışmanın, Van kedilerinin kedi türleri arasındaki tipolojisinin belirlenmesinde ve diğer türler arasındaki farkılıklarının tespit edilmesine rehberlik etmesinin yanında, cerrahi ve klinik uygulama alanlarında veteriner hekimlere ve zooarkeoloji alanındaki çalışmalara faydalı olabileceği düşünülmektedir.
Anahtar sözcükler: Bilgisayarlı tomografi, kafatası, morfometri, üç boyutlu modelleme, Van kedisi.

Introduction

Van cats are an endemic cat species that live around the city of Van in eastern Turkey and named after here. In recent years, these cats have attracted attention due to their unique physical properties both in Turkey and throughout the world. Having a special place among worldwide cat species, these cats are known for their different eye colors (their eyes may be amber or blue or they may have

heterochromia), moderately long straight nose, round face, pointed ear, triangular-shaped head, superior learning ability, and intelligence (3, 16, 47).

Skull is a strong structure composed of many bones which are paired, but some of them which are median-located and single. This structure includes the sense organs such as sight, olfactory, balance, and taste as well as upper respiratory and digestive tracts together with the brain. Cranial bones are joined with each other through sutures and with mandibulae and apparatus hyoideus through joints (12). The morphometric and morphological studies conducted on the skull not only reflect the effects of the genetic and environmental factors (such as genetic and ecophenotypic variations in general) on individual development but also underlie the clinical and surgical applications related to the region (43). Also, the morphometric measurement values of skull may show many individual differences among species and including breed, age, and the structure specific to the animal (5).

Significant changes have taken place in anatomy education by means of the technological developments in medical imaging and computer-aided learning fields, various software developed, and three-dimensional modelling (2). Especially in small pets such as cats, the computed tomography and three-dimensional modelling programs are used as a standard imaging method in the imaging of skull and the anatomic structures around it and monitoring the changes in these structures (14, 17). Also, skull and various extracranial and intracranial pathological structures around it may be determined and the effectiveness of treatment may be evaluated using these imaging methods and three-dimensional modelling software (17, 44). In addition, these imaging methods are commonly used in anthropological studies such as determining the osteometric features of the crania obtained in the excavation works conducted in various regions and obtaining their measurement values (32, 33).

The measurements obtained from the skull using computed tomography (CT) and three-dimensional modelling software may be mostly used in revealing the biometric differences between sexes (34). For this purpose, many studies have been conducted in veterinary medicine (7, 23, 37). No study was found on the skull of Van cats in the literature reviews.

This study was conducted to perform the three-dimensional modelling of the skull in Van cats by using computed tomography, display their anatomic structures, obtain their morphometric measurement values, and reveal the biometric differences of these measurement values between sexes.

Material and Methods

Animal materials: In the study, a total of 16 adult Van cats (8 males and 8 females) which had a weight of 4810 - 7050 gram, were aged between 3 and 8 years, were procured from Van Yüzüncü Yıl University Van Cat Research and Application Center. Drinking water and standard cat food were given ad libitum to the Van cats until one day before the study. This study was approved by Van Yüzüncü Yıl University Animal Experiments Local Ethics Committee (Decision no: 2020/02 and Date: 27. 02. 2020).

Anesthesia: The Van cats included in the study were numbered and they were not given any food one day before the study. On the day of examination, the combination of Ketamine (15 mg/kg, IM, Ketasol® 10% injectable, İnterhas Veterinary Drugs, Ankara) and Xylazine (1-2 mg/kg, IM, Alfazyne® 2% injectable, Ege-Vet Veterinary Drugs, İzmir) was used for the anesthesia of the cats.

Computed tomography imaging: The 16-slice computed tomography (CT) device (Somatom Sensation 16; Siemens Medical Solutions, Erlangen, Germany) available in Van Yüzüncü Yıl University Faculty of Medicine Radiology Department was used for the Computed Tomography (CT) examinations of the cats. The cats under anesthesia were positioned symmetrically in a prone head-first position on a "disposable" cover spread in the gantry of the machine. During scan, the CT device parameters were determined as KV / Effective mAs / Rotation time (sec) values 120 / 120 / 0.75; gantry rotation period 420 ms; physical detector collimation, 16 × 0.6 mm; section thickness, 0.5 mm; final section collimation 32 × 0.63 mm; feed/rotation, 6 mm; Kernel, U90u; increment 0.5 mm; and resolution 512 × 512 pixels. Dosage parameters and scanning were performed in accordance with standard protocols found in published literature (11, 31). The images obtained were recorded in DICOM format.

Three-dimensional modelling of the images and performing their measurements: Then, the modelling of these images was performed by transferring them to MIMICS 20.1 (The Materialise Group, Leuven, Belgium), a three-dimensional modelling software. Osteometric measurements were taken for 34 different parameters on the skulls whose three-dimensional modelling was performed. The morphometric measurements were taken based on the measurement points specified in the literature (4, 20, 21, 25, 42). After completing the morphometric measurements, the surface area and volumetric values of the remaining part of the skull other than mandibulae were calculated. Nine different indices were calculated using osteometric measurements. While Table 1 shows the linear measurement points obtained from the dorsal, lateral, and ventral surfaces of the skull, Table 2 shows the formula of the indices calculated by using these measurement points. Nomina Anatomica Veterinaria was used as terminology in the study (15). Also, a digital scale (TESS®, RP - LCD, Çomak Terazi, İstanbul) was used for the weight measurements of the cats used in the study.

Table 1. Studied cranial parameters (mm).

Parameter	Abbreviation	Definition
1	TLS	Total length of the skull: the distance between akrokranion-prosthion
2	FCL	Facial length: frontal midpoint-prosthion
3	UNCL	Upper neurocranium length: akrokranion-frontal midpoint
4	CL	Cranial length: akrokranion-nasion
5	VL	Viscerocranial length: nasion-prosthion
6	GLN	Greatest length of the nasals: nasion-rhinion
7	LBO	Least breadth between the orbits: entorbitale-entorbitale
8	GFB	Greatest frontal breadth: ectorbitale-ectorbitale
9	LBS	Least breadth of skull: breadth at the postorbital constriction
10	MWN	Maximum width of neurocranium: euryon-euryon
11	MZW	Maximum zygomatic width: zygion-zygion
12	CBL	Condylobasal length: caudal border of occipital condyles-prosthion
13	BL	Basal length: basion-prosthion
14	MPL	Median palatal length: staphylion-prosthion
15	LHP	Length of the horizontal part of the palatine: staphylion-palatinoorale
16	LHP-1	Length of the horizontal part of the palatine-1: the median point of intersection of the line joining the deepest indentations of the choana-palatinoorale
17	PL	Palatal length: the median point of intersection of the line joining the deepest indentations of the choana-prosthion
18	GBP	Greatest breadth of the palate: maximum width of the distal ends of the alveolus of upper P3
19	LPB	Least palatal breadth
20	BCA	Breadth at the canine alveoli
21	LPR	Length of the premolar row
22	LMR	Length of the molar row
23	LCR	Length of the cheektooth row
24	GDAB	Greatest diameter of the auditory bulla: from the most aboral point of the bulla on the suture with the jugular processes up to the external carotid foramen
25	BEAM	Breadth dorsal to the external auditory meatus: breadth between external auditory porus
26	GIHO	Greatest inner height of the orbit
27	NL	Neurocranium length: basion-nasion
28	SH	Skull height: basion-external occipital crest
29	HOT	Height of the occipital triangle: akrokranion-basion
30	HFM	Height of the foramen magnum: basion-opisthion
31	GWFM	Greates breadth of the foramen magnum
32	GBOC	Greatest breadth of the occipital condyles
33	GBJP	Greatest breadth of the bases of the jugular processes
34	GMB	Greatest mastoid breadth: otion-otion

Table 2. Indices and formulas of the skulls.

Studied indexes	Formulas
Skull index	Greatest frontal breadth (var.8) / total length of the skull (var. 1) x 100.
Cranial index	Maximum width of neurocranium (var. 10) / Cranial length (var. 4) x 100.
For. magnum index	Height of the for. magnum (var. 30) / greatest breadth of the for. magnum (var. 31) x 100.
Facial index-1	Maximum zygomatic width (var. 11) / Viscerocranial length (var. 5) x 100.
Facial index-2	Greatest breadth of the palate (var. 18) / greatest length of the nasals (var. 6) x 100.
Basal indeks-1	Maximum width of neurocranium (var. 10) / basal length (var. 13) x 100.
Basal indeks-2	Maximum zygomatic width (var. 11) / basal length (var. 13) x 100.
Palatal index-1	Greatest breadth of the palate (var. 18) / median palatal length (var. 14) x 100.
Palatal index-2	Greatest breadth of the palate (var. 18) / palatal length (var. 17) x 100.

Statistical analysis: Shapiro-Wilk test (n<50) was used to determine whether the measurement mean values were normally distributed in this study conducted to obtain the three-dimensional modelling of the skull in Van cats using computed tomographic images and examine its morphometric features. Nonparametric tests were applied as the measurement values of the variables did not generally have a normal distribution. The descriptive statistics for the measurement values in the present study were represented as mean, standard deviation, minimum and maximum. Mann-Whitney U test was used for the comparisons between sexes based on the measurements. Spearman's correlation coefficients were used in determining the correlation between the measurements, separately for each sex. The statistical significance level (α) was taken as 5% in the calculations and SPSS (IBM SPSS for Windows, Ver. 23) statistical software was used for the calculations.

Results

In the present study, 34 parameters of the skull were measured (Figure 1, 2, 3, and 4). The statistical analysis was performed to determine the group averages of the morphometric measurement values in the males and females in terms of the continuous variables and the differences between sexes. Upon the examination of the statistical results, statistically significant differences were determined between the measurement values of skull (P<0.05). Tables 3 - 5 show the measurement values assessed.

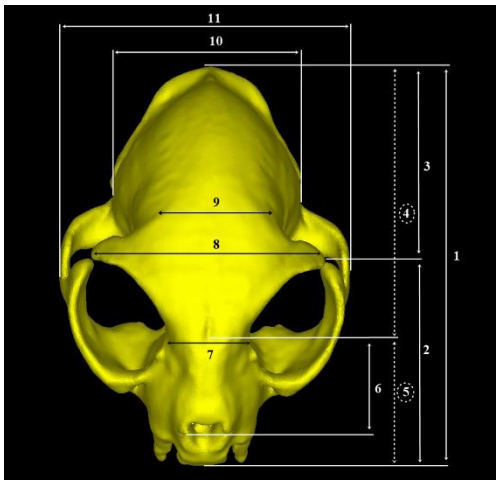

Figure 1. Measurement points of the skull in Van cats (craniodorsal view).

1- TLS: Total length of the skull; 2- FCL: Facial length; 3- UNCL: Upper neurocranium length; 4- CL: Cranial length; 5- VL: Viscerocranial length; 6- GLN: Greatest length of the nasals; 7- LBO: Least breadth between the orbits; 8- GFB: Greatest frontal breadth; 9- LBS: Least breadth of skull; 10- MWN: Maximum width of neurocranium; 11- MZW: Maximum zygomatic width**.**

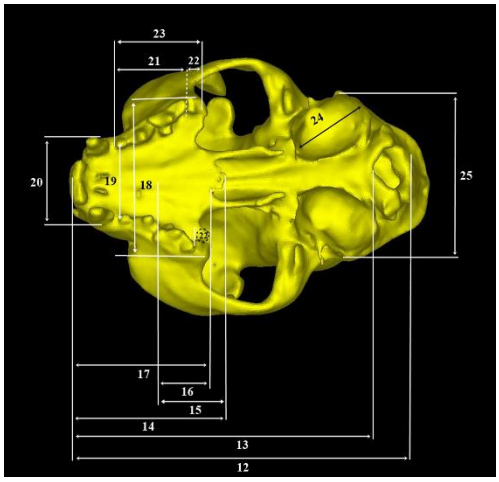

Figure 2. Measurement points of the skull in Van cats (ventral view).

12- CBL: Condylobasal length; 13- BL: Basal length; 14- MPL: Median palatal length; 15- LHP: Length of the horizontal part of the palatine; 16- LHP - 1: Length of the horizontal part of the palatine - 1; 17- PL: Palatal length; 18- GBP: Greatest breadth of the palate; 19- LPB: Least palatal breadth; 20- BCA: Breadth at the canine alveoli; 21- LPR: Length of the premolar row; 22- LMR: Length of the molar row; 23- LCR: Length of the cheektooth row; 24- GDAB: Greatest diameter of the auditory bulla; 25- BEAM: Breadth dorsal to the external auditory meatus.

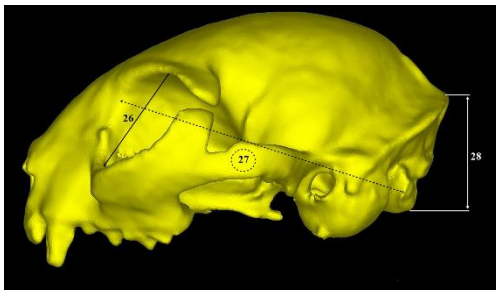

Figure 3. Measurement points of the skull in Van cats (lateral view).

26- GIHO: Greatest inner height of the orbit; 27- NL: Neurocranium length; 28- SH: Skull height.

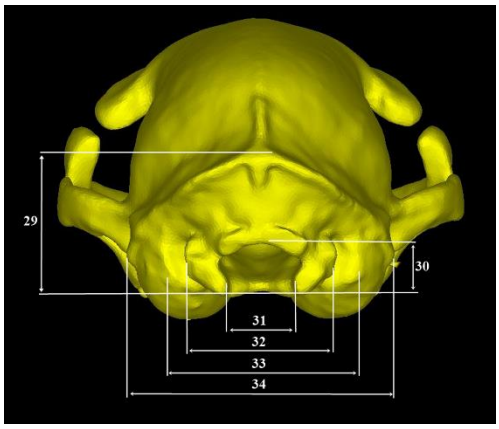

Figure 4. Measurement points of the skull in Van cats (caudal view).

29- HOT: Height of the occipital triangle; 30- HFM: Height of the foramen magnum; 31- GWFM: Greatest breadth of the foramen magnum; 32- GBOC: Greatest breadth of the occipital condyles; 33- GBJP: Greatest breadth of the bases of the jugular processes; 34- GMB: Greatest mastoid breadth.

Table 3. Descriptive statistics of the measurements of the skull according to gender.

	MALE			FEMALE			
Parameter	**Mean±S.E.**	**Min.**	**Max.**	**Mean±S.E.**	**Min.**	**Max.**	***P**
Age(A)	5.00±2.00	3.00	8.00	5.00±2.00	3.00	8.00	1.00
Weight(W) kg	6.08±0.70	5.30	7.05	5.28±0.28	4.81	5.63	0.027
TLS	96.16±6.38	89.38	108.44	87.38±2.71	83.93	93.08	0.002
FCL	52.14±2.99	49.08	58.85	48.91±2.77	43.27	52.23	0.036
UNCL	56.41±2.93	53.95	61.53	51.32±1.93	48.49	53.37	0.001
CL	73.32±3.05	68.79	78.17	72.12±2.76	67.80	74.83	0.600
VL	26.38±1.67	23.78	28.72	24.79±2.39	22.10	29.62	0.074
GLN	20.37±2.11	18.43	24.95	17.77±1.14	15.54	19.33	0.003
LBO	21.82±1.08	20.44	23.40	20.16±2.02	16.90	23.07	0.074
GFB	49.48±2.41	46.08	52.62	48.28±2.34	45.85	51.85	0.248
LBS	32.04±1.62	30.00	34.97	32.37±1.04	30.95	34.07	0.599
MWN	41.87±1.44	40.19	45.01	46.37±10.39	38.99	64.56	0.834
MZW	66.64±3.66	62.50	72.24	56.11±8.81	41.38	62.33	0.001
CBL	86.42±4.55	78.52	93.39	80.83±4.64	71.16	86.74	0.027
BL	79.86±4.34	73.43	87.36	73.96±2.99	69.53	79.08	0.012
MPL	37.39±1.54	34.63	39.70	34.37±2.13	32.20	38.44	0.015
LHP	15.78±2.76	12.95	21.08	14.50±0.96	13.33	16.34	0.462
LHP-1	13.65±2.33	11.11	17.06	13.35±1.27	12.14	16.11	0.916
PL	34.63±2.32	30.21	37.95	32.83±2.06	30.17	37.09	0.046
GBP	37.78±2.28	34.89	41.56	37.33±2.44	34.42	41.88	0.636
LPB	22.96±1.00	21.93	24.68	21.64±.90	20.19	23.37	0.009
BCA	22.17±1.67	20.08	25.09	21.49±1.56	18.94	23.87	0.753
LPR	16.46±1.13	14.34	17.78	15.46±1.12	13.86	17.21	0.083
LMR	7.83±0.89	6.77	9.31	8.62±0.97	7.34	9.64	0.115
LCR	23.52±1.10	22.12	25.26	21.49±1.72	18.77	23.77	0.016
GDAB	18.85±1.48	17.61	21.05	18.60±0.87	17.06	19.85	0.916
BEAM	33.36±2.45	29.85	36.37	37.35±1.26	34.97	38.71	0.002
GIHO	25.67±0.50	24.79	26.22	24.47±1.12	23.17	26.38	0.027
NL	61.36±2.52	58.44	64.43	64.34±3.72	59.22	71.23	0.046
SH	29.72±2.68	25.65	32.99	24.25±1.76	21.74	27.02	0.002
HOT	26.04±0.73	25.01	27.10	25.27±1.08	22.88	26.28	0.115
HFM	11.47±1.09	10.25	13.09	12.38±0.59	11.54	13.57	0.126
GWM	13.69±0.75	12.85	14.88	13.49±0.79	12.43	14.67	0.640
GBOC	20.87±1.19	19.40	22.42	21.08±1.18	19.26	22.67	0.605
GBJP	28.00±1.82	25.69	30.78	28.13±2.00	25.39	31.57	0.916
GMB	41.39±1.66	38.73	43.21	40.21±1.06	38.25	41.72	0.093
Volume(cm^3)	28.44±4.36	25.28	35.56	22.96±2.03	19.96	26.20	0.003
Area (cm^2)	329.41±26.07	290.04	375.02	303.80±37.49	226.30	354.75	0.172

*P<0.05; Mann whitney U test; S.E.: Standard error of mean.

Table 4. Correlation between skull measurements according to gender.

		MALE		FEMALE	
Parameter		**A**	**W**	**A**	**W**
W	r	0.957**		0.390	
TLS	r	0.781*	0.814*	-0.195	0.667
FCL	r	0.537	0.611	0.000	0.738*
UNCL	r	0.732*	0.707	-0.123	0.240
CL	r	0.927**	0.946**	0.000	0.262
VL	r	0.146	0.096	0.245	0.024
GLN	r	0.878**	0.898**	0.049	0.310
LBO	r	0.732*	0.635	0.439	0.262
GFB	r	0.732*	0.683	0.293	0.119
LBS	r	-0.146	-0.407	0.515	-0.144
MWN	r	0.732*	0.707	-0.098	-0.286
MZW	r	0.586	0.623	0.390	0.619
CBL	r	0.781*	0.886**	-0.146	0.262
BL	r	0.634	0.755*	0.195	0.357
MPL	r	0.293	0.263	0.195	0.381
LHP	r	-0.195	-0.252	-0.244	-0.214
LHP-1	r	-0.293	-0.431	0.439	0.071
PL	r	0.781*	0.766*	0.146	0.500
GBP	r	0.781*	0.826*	0.634	0.286
LPB	r	0.634	0.515	-0.172	-0.707
BCA	r	0.683	0.503	0.098	0.095
LPR	r	0.293	0.419	-0.146	-0.262
LMR	r	-0.390	-0.431	0.098	-0.500
LCR	r	0.146	0.036	-0.244	-0.167
GDAB	r	0.732*	0.659	0.390	0.500
BEAM	r	-0.098	-0.084	-0.244	0.024
GIHO	r	0.390	0.383	0.293	0.238
NL	r	0.830*	0.946**	-0.491	0.311
SH	r	0.488	0.575	-0.098	-0.333
HOT	r	0.927**	0.898**	0.390	0.167
HFM	r	-0.293	-0.419	-0.293	-0.429
GWM	r	-0.049	-0.084	-0.195	-0.143
GBOC	r	0.683	0.671	-0.439	0.190
GBJP	r	0.736*	0.795*	0.146	0.429
GMB	r	0.933**	0.934**	0.342	0.095

**P<0.01; *P<0.05; r: Spearman's rho Nonparametric Correlations Coefficients.

Table 5. Descriptive statistics of the measurements of the craniofacial indices according to gender.

	MALE			FEMALE			
Parameter	**Mean±S.E.**	**Min.**	**Max.**	**Mean±S.E.**	**Min.**	**Max.**	***P**
Skull index	51.62±3.64	43.43	55.91	55.27±2.41	52.73	58.70	0.021
Cranial index	57.14±1.46	55.00	59.28	64.85±17.37	52.97	95.22	0.674
For. magnum index	83.74±5.89	77.67	93.54	91.97±5.48	81.46	99.12	0.016
Facial index-1	253.63±23.00	230.40	291.51	228.39±43.29	155.56	282.04	0.462
Facial index-2	186.17±9.08	166.57	195.77	210.44±13.53	194.35	238.03	0.002
Basal indeks-1	52.50±1.80	50.59	55.47	63.01±15.67	52.87	92.85	0.021
Basal indeks-2	83.53±3.84	76.89	88.91	75.81±11.27	55.63	86.75	0.115
Palatal index-1	101.15±6.84	94.10	112.48	108.76±6.31	97.77	114.93	0.027
Palatal index-2	109.34±7.17	102.47	122.24	113.77±5.02	106.87	122.61	0.115

*P<0.05; Mann whitney U test; S.E.: Standard error of mean.

Table 3 shows the morphometric measurement values of the skull based on sex. Accordingly, it was observed that W, TLS, FCL, UNCL, GLN, MZW, CBL, BL, MPL, PL, LPB, LCR, GIHO, SH, and volumetric measurement values were higher in the male cats compared to the female cats. Furthermore, it was determined that BEAM and NL measurement values were higher in the female cats compared to the male cats. These differences in the male and female Van cats were statistically significant ($P<0.05$).

Table 4 shows the correlation between the morphometric measurement values of the skull in male and female Van cats and their ages and body weights. Accordingly, a positive significant correlation was determined between age and W, TLS, UNCL, CL, GLN, LBO, GFB, MWN, CBL, PL, GBP, GDAB, NL, HOT, GBJP, and GMB measurement values in the male cats ($P<0.05$). Also, a positive significant correlation was found between body weight and TLS, CL, GLN, CBL, BL, PL, GBP, NL, HOT, GBJP, and GMB measurement values ($P<0.05$). In the female cats, a positive significant correlation was observed only between body weight and FCL measurement value ($P<0.05$).

Table 5 illustrates the craniofacial index measurement values obtained from the morphometric measurement value of the skull based on sex. Accordingly, it was determined that the skull index, foramen magnum index, facial index-2, basal index-1, and palatal index-1 measurement values were statistically significantly higher in the female cats compared to the male cats ($P<0.05$).

Discussion and Conclusion

The morphometric measurements of the skull in animals may be used to investigate different species among the animal genera and to determine the morphological variations in a species (46). The shape of the skull is one of the most important criteria used in determining the standard cat breeds. Especially the size and shape of skulls between the domestic and wild cats are significantly compared to the other mammals (36). Also, the skull indices obtained from these cranial measurements are quite effective in distinguishing or identifying morphological types (22). For this reason, various craniometric measurements have been used in the studies in determining the morphological variations between the domestic and wild cat species (6, 7, 14, 30, 35-37). The medical imaging methods such as computed tomography is used commonly in displaying a skull and the related complex anatomic structures especially in the pets such as cat, obtaining craniometric and volumetric measurement values from these images, and assessing the pathological conditions in the region (14, 17). The present study is the first attempt to determine the morphometric and volumetric values of the skull using CT and three-dimensional modelling in adult Van cats and reveal the biometric differences of these values between the males and the females.

In general, it has been determined that the craniometric measurement values are higher mostly in males compared to females in both humans and animals (8, 24, 26, 30, 34, 46). It was also determined that 28 measurement parameters among 37 measurement parameters obtained in Van cats together with the volumetric measurement value and the surface area of the skull were higher in the male cats compared to the female cats, which is compatible with the literature data. These measurement values are present in Table 2. This pointed out that the skull was larger in males compared to females.

It has been reported that the morphometric measurements of the skull or cranium are used for sex determination in most mammal species (40). However, in the morphometric study conducted by Pitakarnnop et al. (30), on 38 dried domestic cat skulls to determine the sexual dimorphism between sexes they determined that there no statistically significant difference in the parameters of the skull measured between males and females. However, the fact that the morphometric measurements of the skull cannot be used in sexual dimorphism although the animals have been adults in the studies has varied based on age and body weight (6, 38). In the present study, it was determined that W, TLS, FCL, UNCL, GLN, MZW, CBL, BL, MPL, PL, LPB, LCR, GIHO, SH, and volumetric measurement values were higher in the male cats compared to the female cats; on the other hand BEAM and NL measurement values were higher in the female cats compared to the male cats. It was observed that these differences in the male and female Van cats were statistically significant ($P<0.05$).

Age and body weight are quite important in the morphometric measurements of the skull. It has been generally reported in the studies that there is mostly a positive correlation between the morphometric measurement parameters of the skull and the age and body weight of the male and female animals (13, 38). In parallel with this information, it was observed in the present study that the measurement parameters of the skull in the males and females had mostly a positive correlation with age and body weight. Among these measurement parameters, it was determined that there was a positive significant correlation between age and W, TLS, UNCL, CL, GLN, LBO, GFB, MWN, CBL, PL, GBP, GDAB, NL, HOT, GBJP, and GMB measurement values and between body weight and TLS, CL, GLN, CBL, BL, PL, GBP, NL, HOT, GBJP, and GMB measurement values in the male cats ($P<0.05$). In the female cats, on the other hand, no significant correlation was found between age and skull

measurement parameters and a positive significant correlation was observed only between body weight and FCL measurement value ($P<0.05$).

In their study, Saber et al. (35), grouped the Australian domestic cats as flat-head and round-head skull based on their head types and calculated the cranial, skull, and facial indices from the craniometric measurements and determined that these measurement values were 56.0 ± 4.0, 71.1 ± 4.4, 298.1 ± 34.0 in flat-head skull cats and 66.6 ± 4.9, 71.3 ± 2.4, 279.8 ± 31.9 in round-head skull cats, respectively. In another study conducted by Saber and Gummow (36) on cats, they found these values as 121.24 ± 18.29, 80.79 ± 6.08, and 121.67 ± 19.51, respectively. In Van cats, mean values were calculated as 60.99 ± 9.41 for the cranial index, 53.44 ± 3.02 for the skull index, 241.01 ± 33.14 for the facial index-1, and 198.30 ± 11.30 for the facial index-2. Additionally, no basal index and palatal index measurements have been found in cats in the literature review. In Van cats, mean values were determined as 57.75 ± 1.68 for the basal index-1, 79.67 ± 7.55 for basal index-2, 104.95 ± 6.57 for palatal index-1, and 111.55 ± 6.09 for palatal index-2. Also, it was found in the present study that the skull index, facial index-2, basal index-1, and palatal index-1 measurement values among these measurement indices were statistically significantly higher in the female cats compared to the male cats ($P<0.05$).

In their study, Uddin et al. (41), determined that in domestic cats for. magnum index (average: 90.72 ± 4.93) was 86.98 ± 2.78 in the males and 94.42 ± 3.52 in the females. They found that this difference between male and female cats was statistically significant ($P<0.001$). Also, in parallel with the finding of that study, the results of the present study revealed that for. magnum index (average: 87.85 ± 5.68) was 83.74 ± 5.89 in the male cats and 91.97 ± 5.48 in the female cats and this difference was statistically significant. In addition, for. magnum index has been calculated in many studies on mole rat 88.41 (27), Pekingese dog 93.4 (39), German Shepherd dogs 92.67 - 93.51 (24), Red fox 80.84 - 74.63 (21), rabbit 74.78 (10), African giant rat 81.42 (19), West African dwarf goat 102.5 (18), One-Humped Camel 108.72 (45), Australian domestic cats 128 (35), and gazelles 92.84 (46).

The measurement values of the skull and the anatomic structures around it such as volume and surface area especially in small pets such as dogs and cats can be calculated using CT and various software and the quantitative data of the normal anatomic structure are obtained and the diagnosis and treatment activities of various pathological situations can be assessed (1, 17). In the present study, the CT images of the cats were used and the volume and surface areas of the skull were calculated by using 3D modelling software. It was determined that the volume of the skull was determined to be 22.96 ± 2.03 cm^3 in females and 28.44 ± 4.36 cm^3 in males. Its surface area was 303.80 ± 37.49 cm^2 in females and 329.41 ± 26.07 cm^2 in males. In addition, Piechocki (29) reported that the cranial volumes were 32.5 - 50 cm^3 in the wild cats and were 20 - 25 cm^3 in domestic cats. Also, Saber et al. (35) determined in their study that the cranial volume value was 30 ± 5.2 cm^3 in the flat-headed skull cats and 25.2 ± 3.8 cm^3 in the round-head skull cats. Thus, it can be asserted that Van cats are generally domestic and more likely to have a round-head skull.

The images of the relevant anatomic structure of animals can be obtained with a desired thickness, without giving any physical harm under anesthesia by using the computed tomography and the three-dimensional modelling software and the morphometric and volumetric measurements of these anatomic structures can be calculated easily and quickly (2, 17). Due to these properties, computed tomography imaging and three-dimensional modelling software are increasingly and commonly used in the field of veterinary anatomy in recent times together with computer-aided technological developments (9, 28, 47).

Consequently, the statistical differences in biometric values of the skull between male and female Van cats were determined using CT and three-dimensional modelling software. The recent technological developments in the field of medical imaging methods have provided opportunities to obtain broader and comprehensive data on cranial morphometry. It is thought that the results of this study may be used as a guide in the assessment of the CT images of Van cats with various extracranial and intracranial pathological disorders related to the skull and they may be used in determining the taxonomic classification of Van cats among the cat species and sex determination. Also, we think that the present study would be beneficial to veterinary physicians in the surgical and clinical practice fields, primarily the anatomy education related to skull of Van cats and to the studies in the field of zooarchaeology.

Ethical Statement

This study was approved by Van Yüzüncü Yıl University Animal Experiments Local Ethics Committee (Decision no: 2020/02 and Date: 27.02.2020).

Conflict of Interest

The authors declared that there is no conflict of interest.

Finacial Support

This research received no grant from any funding agency/sector.

References

1. **Breiman RS, Beck JW, Korobkin M, et al** (1982): *Volume determinations using computed tomography*. Am J Roentgenol, **138**, 329-333.
2. **Brenton H, Hernandez J, Bello F, et al** (2007): *Using multimedia and web 3D to enhance anatomy teaching*. Comput Educ, **49**, 32-53.
3. **Cak B** (2017): *Turkish Van cat and Turkish Angora cat: a review*. J Agric Sci Technol A, **7**, 151-159.
4. **Dayan MO, Gürbüz İ, Demiraslan Y, et al** (2017): *Craniometric measurements of the male Eurasian Lynx from Turkey*. Anim Vet Sci, **5**, 15-20.
5. **Dyce KM, Sack WO, Wensing CJG** (2010): Textbook of Veterinary Anatomy. 32-99. 4th Edition, Saunders Elsevier Inc, Missouri, United States.
6. **Farhadinia MS, Kaboli M, Karami M, et al** (2014): *Patterns of sexual dimorphism in the Persian Leopard (Panthera pardus saxicolor) and implications for sex differentiation.* Zool Middle East, **60**, 195-207.
7. **Gordon CR, Marchant TW, Lodzinska J, et al** (2018): *Morphological variation of the caudal fossa of domestic cat skulls assessed with CT and geometric morphometrics analysis*. J Feline Med Surg, **20**, 752-758.
8. **Gündemir O, Duro S, Jashari T, et al** (2020): *A study on morphology and morphometric parameters on skull of the Bardhoka autochthonous sheep breed in Kosovo*. Anat Histol Embryol, **49**, 365-371.
9. **İnce NG, Demircioğlu İ, Yılmaz B, et al** (2018): *Martılarda (Laridae spp.) cranium'un üç boyutlu modellemesi.* Harran Univ Vet Fak Derg, **7**, 98-101.
10. **Kahvecioğlu KO, Onar V, Alpak H, et al** (2000): *The morphometry of the foramen magnum in rabbits and its correlation with craniometric measurements*. Folia Vet, **44**, 62-69.
11. **Kalra MK, Maher MM, Toth TL, et al** (2004): *Strategies for CT radiation dose optimization*. Radiology, **230**, 619-628.
12. **Liebich HG, König HE** (2007): Axial skeleton. 49-85. In: Veterinary Anatomy of Domestic Mammals: Text Book and Colour Atlas. 3rd Edition, Schattauer, Germany.
13. **Mo G, Zotti A, Agnesi S, et al** (2009): *Age classes and sex differences in the skull of the Mediterranean monk seal, Monachus monachus (Hermann, 1779). A study based on bone shape and density.* Anat Rec, **292**, 544-556.
14. **Moselhy AA, Mahdy EA** (2019): *Comparative three-dimensional computed tomography (CT) scans and anatomical investigation of rabbit (Oryctolagus cuniculus) and cat (Felis domestica) skull.* Slov Vet Res, **56**, 365-379.
15. **Nomina Anatomica Veterinaria** (2017): International Committee on Veterinary Gross Anatomical Nomenclature (ICVGAN), Published by the Editorial Committee, Hannover.
16. **Odabaşıoğlu F, Ateş CT** (2000): Van Cats. 1st Edition, Selcuk University Printing Office, Konya, Turkey.
17. **Ohlerth S, Scharf G** (2007): *Computed tomography in small animals-basic principles and state of the art applications.* Open Vet J, **173**, 254-271.
18. **Olopade JO, Onwuka SK** (2005): *Morphometric study of the skull of the West African dwarf goat from South West Nigeria.* Niger Vet J, **26**, 18-21.
19. **Olude MA, Olopade JO, Fatola IO, et al.** (2009): *Some aspects of the neurocraniometry of the African giant rat (Cricetomys gambianus Waterhouse).* Folia Morphol, **68**, 224-227.
20. **Onar V** (1999*): A morphometric study on the skull of the German shepherd dog (Alsatian)*. Anat Histol Embryol, **28**, 253-256.
21. **Onar V, Belli O, Owen PR** (2005): *Morphometric examination of red fox (Vulpes vulpes) from the Van-Yoncatepe Necropolis in Eastern Anatolia*. Int J Morphol, **23**, 253-260.
22. **Onar V, Güneş H** (2003): *On the variability of skull shape in German Shepherd (Alsatian) puppies.* Anat Rec A Discov Mol Cell Evol Biol, **272**, 460-466.
23. **Onar V, Kahvecioğlu KO, Cebi V** (2002): *Computed tomographic analysis of the cranial cavity and neurocranium in the German shepherd dog (Alsatian) puppies.* Vet Arh, **72**, 57-66.
24. **Onar V, Mutuş R, Kahvecioğlu KO** (1997): *Morphometric analysis of the foramen magnum in German shepherd dogs (Alsatians)*. Ann Anat, **179**, 563-568.
25. **Onar V, Ozcan S, Pazvant G** (2001): *Skull typology of adult male Kangal dogs.* Anat Histol Embryol, **30**, 41-48.
26. **Özkadif S, Eken E** (2016): *Craniometric measurements of New Zealand rabbits skull from three-dimensional reconstruction images.* ARC J Anim Vet Sci, **2**, 9-14.
27. **Özkan ZE** (2007): *Macro-anatomical investigations on the skeletons of mole-rat (Spalax leucodon Nordmann) III. Skeleton axiale*. Vet Arh, **77**, 281-289.
28. **Papadopoulos MA, Jannowitz C, Boettcher P, et al** (2005): *Three-dimensional fetal cephalometry: an evaluation of the reliability of cephalometric measurements based on three-dimensional CT reconstructions and on dry skulls of sheep fetuses.* J Cranio Maxill Surg, **33**, 229-237.
29. **Piechocki R** (1990): Die Wildkatze Felis Silvestris - Die Neue Brehm Bücherei A. 232. Ziemsen Verlag, Wittenberg.
30. **Pitakarnnop T, Buddhacha K, Euppayo T, et al** (2017): *Feline (Felis catus) skull and pelvic morphology and morphometry: gender-related difference?* Anat Histol Embryol, **46**, 294-303.
31. **Prokop M** (2003): *General principles of MDCT*. Eur J Radiol, **45**, S4-S10.
32. **Raghina DT, Perlea P, Marinescu M** (2017): *Forensic anthropology from skeletal remains to CT scans: a review on sexual dimorphism of human skull*. Rom J Leg Med, **25**, 287-292.
33. **Ramamoorthy B, Pai MM, Ullal S, et al** (2020): *Discriminant function analysis of craniometric traits for sexual dimorphism and its implication in forensic anthropology.* J Anat Soc India, **68**, 260-268.
34. **Rooppakhun S, Surasith P, Vatanapatimakul N, et al** (2010): *Craniometric study of Thai skull based on three-dimensional computed tomography (CT) data*. J Med Assoc Thai, **93**, 90-98.
35. **Saber A, Cacec T, Gummow B, et al** (2016): *Morphometric studies on the skull of the Australian domestic cat (F. catus) and its clinical implications for regional anesthesia*. J Vet Med, **9**, 1-24.
36. **Saber AS, Gummow B** (2015): *Skull morphometry of the lion (Panthera leo), dog (Canis lupus familiaris) and cat (Felis catus).* J Vet Med, **8**, 13-30.

37. **Segura V** (2015): *A three-dimensional skull ontogeny in the bobcat (Lynx rufus) (Carnivora: Felidae): a comparison with other carnivores.* Can J Zool, **93**, 225-237.
38. **Shukla BB, Kumar R, Upadhyay AK, et al** (2003): *Relationship of age with body weight in orphaned leopard cubs*. Zoos Print J, **18**, 1058.
39. **Simoens P, Poels P, Lauwers H** (1994): *Morphometric analysis of the foramen magnum in Pekingese dogs*. Am J Vet Res, **55**, 34-39.
40. **Travaini A, Juste J, Novaro AJ, et al** (2000): *Sexual dimorphism and sex identification in the South American culpeo fox, Pseudalopex culpaeus (Carnivora: Canidae)*. Wildlife Res, **27**, 669-674.
41. **Uddin M, Sarker MHR, Hossain ME, et al** (2013): *Morphometric investigation of neurocranium in domestic cat (Felis catus).* Bangl J Vet Med, **11**, 69-73.
42. **Von Den Driesch A** (1976): A guide to the measurement of animal bones from archaeological sites. Peabody Museum Bulletin 1. Cambridge, MA, Harvard University.
43. **Wehausen JD, Ramey RR** (2000): *Cranial morphometric and evolutionary relationships in the nothern range of Ovis canadensis.* J Mammal, **81**, 145-161.
44. **Wisner ER, Zwingenberger AL** (2015): Atlas of small animal CT and MRI. 55-68. Willey-Blackwell Publishing, USA.
45. **Yahaya A, Olopade JO, Kwari HD** (2013): *Morphological analysis and osteometry of the foramen magnum of the one-humped camel (Camelus dromedarius).* Anat Histol Embryol, **42**, 155-159.
46. **Yılmaz B, Demircioğlu İ, Bozkaya F, et al** (2020): *Three-dimensional tomographic reconstruction and morphometric analysis of skull in gazelles (Gazella subgutturosa).* Ankara Univ Vet Fak Derg, **67**, 161-168.
47. **Yilmaz O, Soyguder Z, Yavuz A, et al** (2020): *Three-dimensional computed tomographic examination of pelvic cavity in Van Cats and its morphometric investigation*. Anat Histol Embryol, **49**, 60-66.

Ankara Univ Vet Fak Derg, **68**, 223-228, 2021
DOI: 10.33988/auvfd.727842

Molecular identification of *Paramphistomidae* obtained from ruminants in Van province

Yusuf PADAK[1,a], Ayşe KARAKUŞ[2,b,✉]

[1]Ozalp District Health Directorate, Van; [2]Van Yüzüncü Yıl University, Faculty of Veterinary Medicine, Department of Parasitology, Van, Turkey
[a]ORCID: 0000-0002-5785-9129; [b]ORCID: 0000-0002-7151-8777

✉Corresponding author:vetci.sona@hotmail.com
Received date: 27.04.2020 - Accepted date: 10.10.2020

Abstract: This study was aimed to identify *Paramphistomum* species from infected ruminants (sheep and cattle) by molecular methods between March 2018 and September 2018 at Van municipality slaughterhouse. In the research, the rDNA ITS-2 gene region of adult Paramphistomums was amplified by PCR method. Amplicons 399 bp long were viewed in agarose gel. As a result of bidirectional sequence analysis made from PCR amplicons, *Paramphistomum leydeni* and *Calicophoron daubneyi* species were identifyed. Amplicon sequences were compared by BLAST with reference sequences from Genbank. Phylogenetic tree was created with the Neighbor-Joining method by using the MEGA 7 program. Genotypes obtained from isolates were compared for exact or closest similarities. In conclusion, *C. daubneyi*, which was previously detected by morphological methods in Turkey, in this study, it was identified for the first time by using molecular methods. Also in this study, P. leydeni was reported for the first time in Turkey.
Keywords: Molecular identification, *Paramphistomum* spp., PCR, Van.

Van ilindeki ruminatlardan elde edilen *Paramphistomidae*'lerin moleküler olarak belirlenmesi

Özet: Bu çalışmada, Mart 2018-Eylül 2018 tarihleri arasında Van belediyesi mezbahasında enfekte ruminantlardan (koyun ve sığır) elde edilen *Paramphistomum* türlerinin moleküler yöntem kullanılarak belirlenmesi amaçlanmıştır. Araştırmada, erişkin *Paramphistomum*'ların rDNA ITS-2 gen bölgesi PCR yöntemi ile çoğaltıldı. Agaroz jelde, 399 bp uzunluğunda amplikonlar görüntülendi. PCR amplikonlarından yapılan çift yönlü sekans analizi sonucunda *Paramphistomum leydeni* ve *Calicophoron daubneyi* türleri belirlendi. Amplicon dizileri, BLAST ile Genbank'taki referans dizilerle karşılaştırıldı. MEGA 7 programı kullanılarak Neighbor-Joining yöntemi ile filogenetik ağaç oluşturuldu. İzolatlardan elde edilen genotipler tam yada en yakın benzerlikleri karşılaştırıldı. Sonuç olarak, Türkiye'de daha önce morfolojik yöntemlerle tespit edilen *C. daubneyi*, bu çalışmada moleküler yöntemler kullanılarak ilk kez tespit edildi. Ayrıca bu çalışmada, Türkiye'de ilk kez *P. leydeni* bildirildi.
Anahtar sözcükler: Moleküler belirleme, *Paramphistomum* spp., PCR, Van.

Introduction

Paramphistomosis or amphistomiasis is known as a disease caused by parasites classified in *Paramphistomidae* and infects various domestic and wild ruminant species. The adult form of the parasite resides in the rumen and reticulum and the young form resides in the small intestine. While small numbers of adult parasites do not cause serious problems in the hosts, larger numbers of parasites damage the rumen tissue. Clinical symptoms might not be present despite the damage and loss in the rumen papillae caused by the adult parasites. Young and immature paramphistomes, resident in the first part of the duodenum and ileum, cause severe hemorrhage and necrosis in this region. Although mature flukes of paramphistomum species are not very pathogenic, immature flukes are trematodes that can cause serious pathological disorders, loss of yield, clinical symptoms and adversely affect animal health. (2, 3, 5, 20, 26).

Species of the genus *Paramphistomum* live in the stomach (rumen-reticulum) and rarely in the bile ducts of the ruminants. They are observed in countries with tropical and subtropical climates. Several studies reported two sub-genera such as *Paramphistomum* and *Explanatum*, based on the ratio between the mouth sucker and posterior sucker sizes (26).

Although the disease is identified worldwide, it is known to be more common in tropical and subtropical regions, especially in Africa, Asia, Austria and Western

Europe. The prevalence of *Paramphistomum* species varies between regions depending on various variables such as host, intermediate host, active species and meteorological and environmental factors. Therefore, different prevalence rates have been reported in studies conducted in various countries. The most common type in Turkey is *Paramphistomum cervi*, followed by *Paramphistomum ichikawai* and *Calicophoron daubneyi* (10, 15, 20).

The traditional method for identifying these economically significant helminths is based on common morphological features. Furthermore, the traditional diagnostic method is challenging and error-prone, particularly for soft-bodied parasites such as trematodes, which are morphologically similar but genetically diverse in terms of resistance and sensitivity. It could eliminate such challenges in identifying these structural parasites through the use of ultra-structural observations (9, 18, 24).

Histomorphological identification of parasites was conducted with the examination of "median-sagittal" sections that pass through the center of muscular organs such as pharynx, genital hole and acetabulum. However, these morphological differences are highly challenging and have several disadvantages. Molecular methods, especially those used in phylogenetic studies, were proposed as an alternative method for the differentiation of the species. ITS-2 gene region sequence could be used as a specific marker for this purpose. For instance, polymerase chain reaction (PCR) could facilitate the diagnosis through studying highly preserved molecular markers such as ITS-2 rDNA (11, 21, 22).

Given that *Paramphistomum* species could be morphologically similar, molecular biological techniques could be helpful in the classification and identification of these species. Itagaki et al. (8) and Rinaldi et al. (17) characterized several *Paramphistomum* genera and species by molecular methods and by focusing on the ITS-2 gene region that characterized the species (19).

This study aimed to determine the molecular characterization of paramphistomoid parasites infecting cattle and sheep using molecular methods in the province of Van in Turkey.

Materials and Methods

In this study, were examined the rumen and reticulum of sheep and cattle slaughtered by regular visits to the Van Municipality Slaughterhouse 4 times a month between March 2018 and September 2018. A total of 2600 sheep and 1335 cattle were examined after slaughtering, 169 sheep and 195 cattle were identified as infected. An average of 30-40 adult flukes were collected from the rumen and/or reticulum of naturally infected ruminants and placed in labeled containers.

The collected adult flukes were washed with PBS (Phosphate-buffer saline) and placed in 70% ethanol. The samples were kept at -20°C until the tests were conducted at the Department of Parasitology, the Faculty of Veterinary Medicine, Van Yüzüncü Yıl University, Turkey.

Molecular analysis: Paramphistomes, which were initially preserved with 20 ml of ethanol, were washed 5 times with PBS for genomic DNA isolation. Subsequently, paramphistomes were thoroughly crushed in a homogenizer (Brand: Qiagen Model: Tissue LyserII). The tissues, crushed based on the kit procedure, were transferred to Eppendorf tubes. The DNA purification was conducted manually based on the general guidelines provided by the Thermo Scientific GeneJET Genomic DNA Purification Kit (Catalog number: K0722).

Paramphistomum spp. were identified using ITS-2 F 5′-AGAACATCGACATCTTGAAC-3' (1) and R 5′TATGCTTAAATTCAGCGGGT-3′ (13) primers by PCR. The total volume of 25 µl PCR was prepared with 2.5 µl 10X PCR buffer, 1 µl 25mM $MgCl_2$, 0.5 µl 25mM dNTP, 0.5 µl from each primer, 5U/µl 0.2 µlTaq DNA polymerase, 5 µl genomic DNA and 14.8 µl dH_2O. The cycling conditions used were 94°C for 5 min (initial denaturation), then 94°C for 1 min (denaturation), 50°C for 35 s (annealing), 72°C for 1 min (extension) for 30 cycles, and a final extension at 72°C for 10 min. (Brand: BIO-RAD, Model: Power pac Basic). The PCR product was run on 2% agarose gel at 100 volts for 1 hour (Electrophoresis: BİO-RAD, Model: Power pac Basic). The samples were imaged under UV light (Figure 1).

Sequence analysis and phylogenetic analysis: 25µl of those PCR products that were run on agarose gel and exhibited a DNA sequence placed into PCR tubes and 2 µl primer (10 pmol) was used for each sample. The tubes were tagged and sent to Medsantek (Istanbul, Turkey) for sequence analysis. The amplicons purified at Medsantek were duplex sequence analysis with an Applied Biosystems 377 DNA Sequencer device. Phylogenetic tree was created via the neighbor joining method and the Bootstrap test (100 repetitions). The evolutionary closeness between the obtained *P. leydeni* and the sequences of *C. daubneyi* isolates was created an UPGMA dendrogram using the MEGA 7 program and the neighbor joining model (Figure 2). The phylogenetic tree obtained by comparing the sequences of the amplified ITS-2 region with KP201674, AY790883, LN610457, KP201674, KX668976, KX668943, KX668944, MH558675, KJ995529,HM209064, KF564869 and KC503920 are presented in Figure 2. *Schistoma haematobium* was used as the outer group (KT354669).

Results

A product size of 399 bp was obtained from the PCR products ran on electrophoresis (Figure 1). As a result of sequence analysis of amplicons obtained from adult parasites; *Paramphistomum leydeni* was identified from 5 sheep and 3 cattle, and the *Calicophoron daubneyi* was identified from 2 cattle.

ITS-2 sequences for all isolates were successfully amplified and the sequences produced were registered to GenBank. Access numbers of GenBank registered isolates are shown in Figure 2. Depending on the upper class of *Paramphistomatidae* in Dendogram; Evolutionary proximity between *P. leydeni*, *C. daubneyi*, *P. cervi*, *Explanatum explanatum*, *Cotylophoron* spp. and the *C. clavula* species, that are supported by a high boostrap value 100% in the *C. daubneyi* and 96% in the *P. leydeni*. It was observed that the *P. leydeni* and *C. daubneyi* isolates obtained from cattle and sheep showed 100% similarity in terms of nucleotide sequences among themselves. In the comparative nucleotide sequences of the ITS-2 gene region of the our isolates, no genetic differences were observed between *P. leydeni* 8 isolates and *C. daubneyi* 2 isolates (Figure 3).

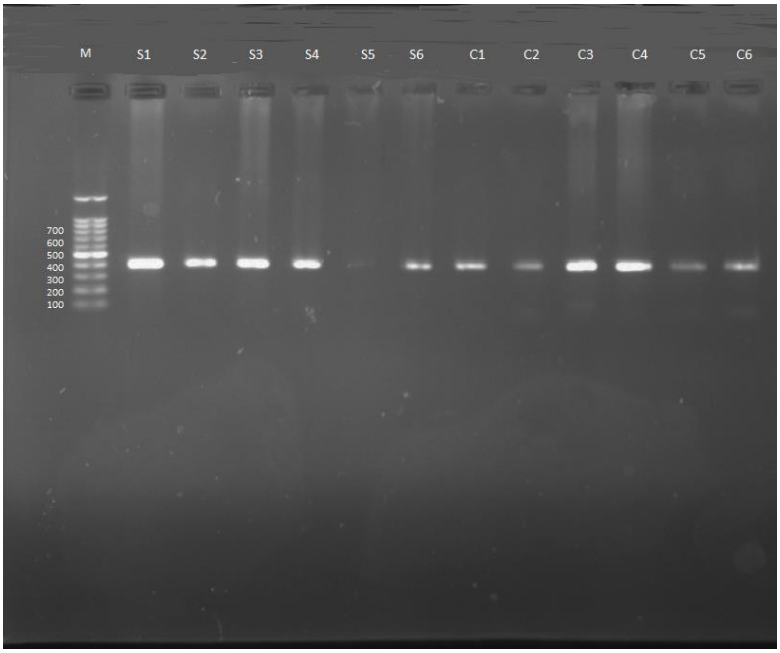

Figure 1. PCR amplification of rDNA ITS2 gene region in *Paramphistomum* species found in sheep and cattle (Amplicon length 399 bp).
S (1-2-3-4-6): PCR amplicons of adult parasites from sheep.
C (1-2-3-4-5): PCR amplicons of adult parasites from cattle.

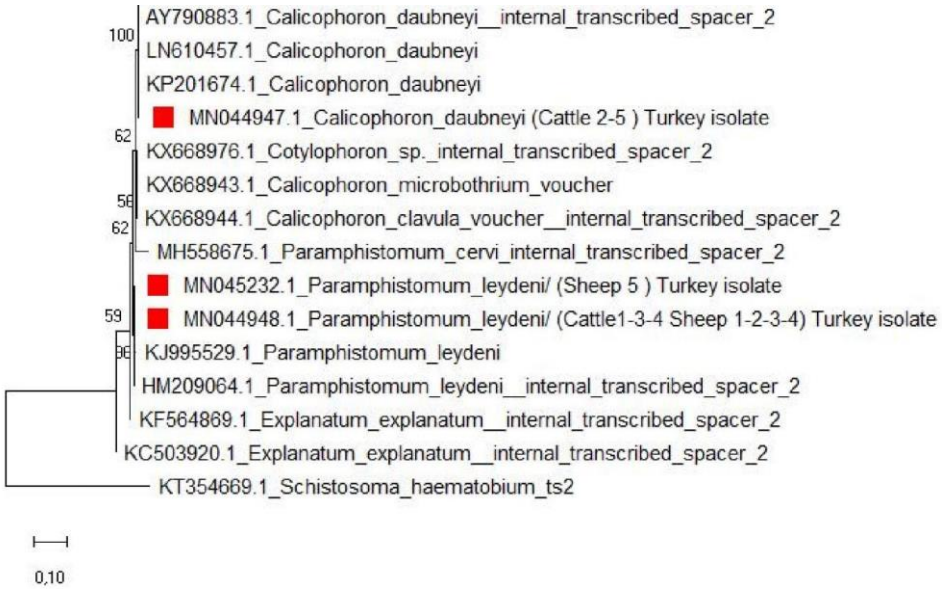

Figure 2. Phylogenetic relationship of the sequences obtained in the study and the sequences obtained from GenBank.
The tree was constructed by the neighbor -joining analysis (NJ) with genetic distance of 0.10.

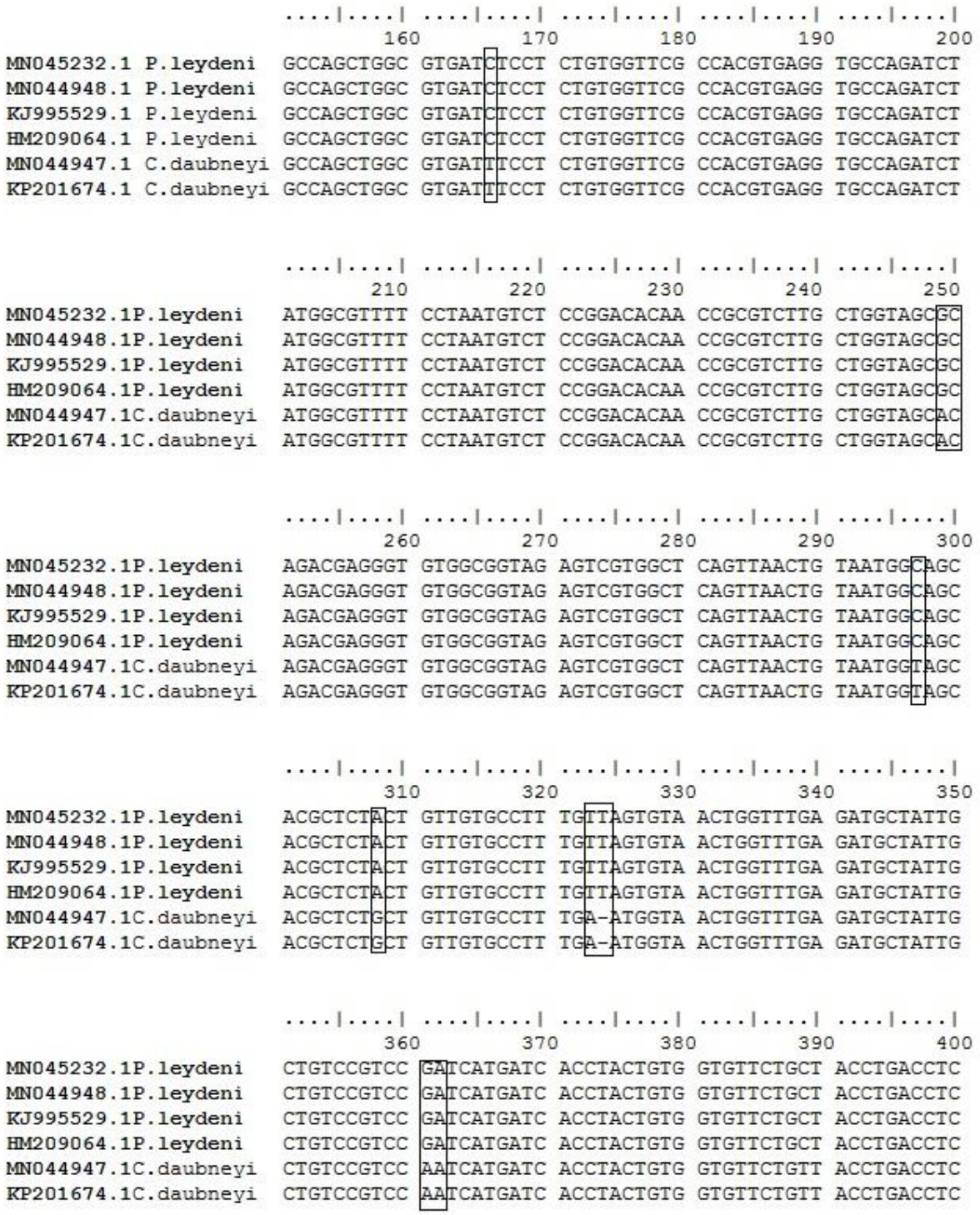

Figure 3. Comparative nucleotide sequences of the ITS-2 gene region of the isolates.

Discussion and Conclusion

Paramphistomoid worms are difficult to identify because most have thick robust bodies in which the internal organs are hard to see. Specific identification becomes more difficult, as the immature flukes responsible for the disease are not sexually mature. Therefore, the researcher can make a dubious diagnosis to identify the few mature flukes that can be found in the animal's rumen. Because of such problems, better alternative approaches need to be developed to identify the species in this group. A variety of molecular tools now complemented traditional diagnostic techniques in parasitology to help in resolving the vexing taxonomic issues associated with describing new species or strains

based on phenotypic characteristics and/or epidemiological observations in particular endemic areas. PCR-based techniques that provide rDNA ITS-2 sequences have proven to be a reliable tool to identify digenean species and restore phylogenetic relationships. In addition, ITS-2 has been found to be a useful marker for species identification of parampistomes (4, 6, 8, 9, 12, 16, 17, 25, 27, 28).

A variety of molecular methods are used in epidemiological parasitology studies in certain endemic regions to assist in solving complex taxonomic problems associated with conventional diagnostic assays or the identification of new species and strains based on the origin of phenotypic features (25). In this study, DNA analyzes of *Paramphistomum* spp. collected from ruminants (cattle and sheep) in Van province was performed, studied by PCR (polymerase chain reaction) method, and the rDNA ITS-2 gene region was characterized. As a result of sequence analysis of amplicons, *Calicophoron daubneyi* from 2 cattle, *Paramphistomum leydeni* from 3 cattle and 5 sheep were identified. The presence of *C. daubneyi* was previously reported in Turkey by morphological diagnosis method, and its presence was reported using molecular methods in this study.

In the molecular study on paramphistomum eggs in Ireland; *C. daubneyi* and *P. leydeni* have been reported (14). In this study, the *C. daubneyi* sequences matched with sequences isolated from Ireland (14), Algeria (27) and southern Italy (17).

Some researchers have investigated possible intra-specific variations of ITS-2, due to the fact that length differences were not observed in PCR products of *C. daubneyi* samples. The study also did not see any intra-specific variations between the samples. In the study, confirmed by the ITS-2 sequence analyses, which indicated 100% homologies. The finding of the present study suggests that ITS-2 can serve as an effective genetic marker for the molecular identification of paramphistomes, as already demonstrated for other parasitic helminths (17).

Paramhistomum parasites collected from a reindeer in Croatia reported *P.cervi* and *P. leydeni* as a result of sequence analysis conducted in the rDNA ITS-2 gene region by molecular methods (23). Sanabria et al. (19) *Paramphistomum leydeni* was identified molecular using 5.8S and 28S partial ITS-2 rDNA sequences. Ichikawa et al. (7) studied fluke parasites cattle and water buffalo from Myanmar for morphological and molecular characterization using ITS-2, partial 5.8S and 28S rDNA sequences. ITS-2 sequences of *Explanatum explanatum* specimens showed similarity and variability at 7 nucleotide sites compared to *Paramphistomum leydeni*. In this study, unlike previously described species as macroscopically in Turkey that, *P. leydeni* was reported for the first time using molecular methods. The *P. leydeni* sequences in this study matched those isolated from cattle from Uruguay (unpublished), cattle from Argentina (19).

In conclusion, paramphistomiasis in ruminants is still a widespread parasitic infection that leads to economic losses in the Van region of Turkey. Molecular methods, which provide accurate results, have the potential to contribute to the taxonomic identification and epidemiological studies of paramphistomiasis. The results of the present study confirm that ITS-2 is a useful molecular marker for species identification of paramphistomes and can be used to determine the relationship of samples within the different taxa of *Paramphistomoidea*. The use of the ITS-2 rDNA gene region for the identification of *Paramphistomum* species was carried out for the first time in Turkey by PCR method, and a species not previously reported in Turkey was identified with this study. Since there are few studies focusing on the taxonomic and morphological description of *Paramphistomum* in Turkey, the importance of a careful review of previous findings on paramphistomum infections was emphasized. We believe that this study will be an important resource for interspecies variation studies of paramphistomas and will provide an exemplary study for comparative ribosomal genomic and systematic studies of digeneans in Turkey.

Acknowledgments

The authors are thankful to Van Yüzüncü Yıl University Scientific Research Projects Department.

Financial Support

This study has been supported by Van Yüzüncü Yıl University Scientific Research Projects Department with TYL 2018-6882 project code.

Ethical Statement

This study does not present any ethical concerns.

Conflict of Interest

The authors have no conflict of interest.

References

1. **Anderson GR, Barker SC** (1998): *Inference of phylogeny and taxonomy within the didymozoidae (Digenea) from the second internal transcribed spacer ITS2 of ribosomal DNA.* Syst Parasitol, **41**, 87-94.
2. **Celep A, Açıcı M, Çetindağ M, et al** (1990): *Samsun yöresi sığırlarında helmintolojik araştırmalar.* Etlik Vet Mikrobiyol Derg, **6**, 117-30.
3. **Coşkun ŞZ** (1988): *The discovery and spread of Paramphistomum species in ruminants.*Turk J Vet Anim Sci, **12**, 168-179.

4. **Goswami LM, Prasad PK, Tandon V, et al** (2009): *Molecular characterization of Gastrodiscoides hominis (Platyhelminthes: Trematoda: Digenea) inferred from ITS rDNA sequence analysis.* Parasitol Res, **104**, 1485-1490.
5. **Güralp N** (1981): The Helminthology. Ankara University Faculty of Veterinary Medicine. Ankara University Press, Ankara, Turkey.
6. **Horak IG** (1971): *Paramphistomiasis of domestic ruminants*. Adv Parasitol, **9**, 33-72.
7. **Ichikawa M, Kondoh D, Bawn S, et al** (2013): *Morphological and molecular characterization of Explanatum explanatum from cattle and buffaloes in Myanmar*. JVMS, **75,** 309-314.
8. **Itagaki T, Tsumagari N, Tsutsumi K, et al** (2003): *Discrimination of three amphistome species by PCR-RFLP based on rDNA ITS2 markers.* J Vet Med Sci, **65**, 931-933.
9. **Jones A** (1990): *Techniques for hand-sectioning thick-bodied Platyhelminths.* Syst Parasitol, **15**, 211-218.
10. **Khan UJ** (2008): Epidemiology, Economic Importance and Therapy of Paramphistomosis in Cattle and Buffaloes. PhD Thesis Department of zoology, University of Punjap, Lahor, Pakistan.
11. **Lotfy WM, Brant SV, Ashmawy KI, et al** (2010): *A molecular approach for identification of paramphistomes from Africa and Asia*. Vet Parasitol, **174**, 234-240.
12. **Lotfy WM, Brant SV, DeJong RJ, et al** (2008): *Evolutionary origins, diversification, and biogeography of liver flukes (Digenea, Fasciolidae)*. Am J Trop Med Hyg, **79**, 248-255.
13. **Luton K, Walker D, Blair D** (1992): *Comparisons of ribosomal internal transcribed spacers from two congeneric species of flukes (Piatyhelminthes: Trematoda: Digenea).* Mol Biochem Parasit, **56**, 323-328.
14. **Martínez-Ibeas AM, González-Warleta M, Martínez-Valladares M, et al** (2013): *Rumen fluke in Irish sheep: prevalence, risk factors and molecular identification of two paramphistome species.* BMC Vet Res, **12**, 143.
15. **Özdal N, Gül A, İlhan F, et al** (2010): *Prevalence of Paramphistomum infection in cattle and sheep in Van Province, Turkey*. Helminthologia, **47**, 20-24.
16. **Reinitz DM, Yoshino TP, Cole RA** (2007): *A Ribeiroia spp. (Class: Trematoda)-specific PCR-based diagnostic.* J. Parasitol, **93**, 1234-1238.
17. **Rinaldi L, Perugini AG, Capuano F, et al** (2005): *Characterization of the second internal transcribed spacer of ribosomal DNA of Calicophoron daubneyi from various hosts and locations in southern Italy.* Vet Parasitol, **131**, 247-253.
18. **Roy B, Tandon V** (1993): *Morphological and microtopographical train variations among Fasciolopsis buski originating from different geographical areas*. Acta Parasitol, **38**, 72-77.
19. **Sanabria R, More G, Romero J** (2011): *Molecular characterization of the ITS-2 fragment of Paramphistomum leydeni (Trematoda: Paramphistomidae).* Vet Parasitol, **177**, 182-185.
20. **Şenlik B** (2013): Helminth Diseases Seen in Digestive System in Cattle. In: Ozcel MA (Ed). Parasitic Diseases in Veterinary Medicine. Meta Printing Printing Services. İzmir.
21. **Sharma S, Lyngdoh D, Roy B, et al** (2016): *Differential diagnosis and molecular characterization of Hymenolepis nana and Hymenolepis diminuta (Cestoda: Cyclophyllidea: Hymenolepididae) based on nuclear rDNA ITS2 gene marker.* Parasitol Res, **5**, 4293-4298.
22. **Sharma S, Lyngdoh D, Roy B, et al** (2016): *Molecular phylogeny of Cyclophyllidea (Cestoda:Eucestoda): An in-silico analysis based on mtCOI gene.* Parasitol Res, **115**, 3329-3335.
23. **Sindičić M, Martinkovic F, Striskovic T, et al** (2017): *Molecular identification of the rumen flukes Paramphistomum leydeni and Paramphistomum cervi in a concurrent infection of the red deer Cervus elaphus*. J Helminthol, **91**, 637-641.
24. **Tandon V, Roy B** (2002): SEM Pictorial Guide to Trematodes of Live Stock In India. Regency Publication. New Delhi, India.
25. **Thompson RCA, Zarlenga DS, La Rosa G** (2004): *Molecular systematics and diagnosis.* Vet Parasitol, **125**, 69-92.
26. **Tınar R, Umur Ş, Köroğlu E, et al** (2006): The Helmintology. In: Tınar R (Ed). Nobel, Ankara, Turkey.
27. **Titi A** (2013): La paramphistomose gastro-duodenales des ruminants dans le nord-est algerien: investigations sur les bovins et le mollusque hote PhD thesis, Constantine University, Algeria.
28. **Van Van K, Dalsgaard A, Blair D, et al** (2009): *Haplorchis pumilio and H. taichui in Vietnam discriminated using ITS-2 DNA sequence data from adults and larvae*. Exp Parasitol, **123**, 146-151.

Ankara Univ Vet Fak Derg, **68**, 229-235, 2021
DOI: 10.33988/auvfd.754619

An evaluation of the efficiency of beekeeping enterprises in Hatay province with data envelopment analysis

Ufuk KAYA[1,a,✉], İsmayil Safa GÜRCAN[2,b]

[1]Hatay Mustafa Kemal University, Faculty of Veterinary Medicine, Department of Biostatistics, Hatay; [2]Ankara University, Faculty of Veterinary Medicine, Department of Biostatistics, Ankara, Turkey
[a]ORCID: 0000-0002-4805-0993; [b]ORCID: 0000-0002-0738-1518

✉Corresponding author: u.kaya@mku.edu.tr
Received date: 19.06.2020 - Accepted date: 13.10.2020

Abstract: This study was aimed to determine technical and economic efficiency in beekeeping enterprises and to reveal the factors effecting the efficiency scores. The material of the current study consisted of the data obtained from 46 enterprises in Hatay province. Efficiency scores for technical and economical properties were determined with data envelopment analysis. The truncated regression model was used to determine the factors effecting the efficiency scores. The efficiency scores for technical and economical properties were calculated as 0.97 and 0.94, respectively. The results showed that 'experience', 'race of bee', 'education level' and 'number of colony' variables were found to be statistically significant factors on efficiency of technical properties. No significant factors were found on efficiency of economic properties. In conclusion, it was revealed what conditions should be had in terms of technical and economical properties to be performed an efficient beekeeping activity in Hatay province.
Keywords: Beekeeping, data envelopment analysis, efficiency, truncated regression model.

Hatay ili arıcılık işletmelerinin etkinliklerinin veri zarflama analizi ile değerlendirilmesi

Özet: Bu çalışmada arıcılık işletmelerinde teknik ve ekonomik etkinliğin belirlenmesi, etkinlik skorlarına etki eden faktörlerin ortaya konulması amaçlanmıştır. Çalışmanın materyalini, Hatay ilindeki 46 adet arıcılık işletmesinden elde edilen veriler oluşturmaktadır. Teknik ve ekonomik özellikler açısından işletmelerin etkinlik skorları veri zarflama analizi ile belirlenmiştir. Etkinlik skorları üzerine etki eden faktörlerin belirlenmesi amacıyla kesilmiş regresyon modelinden yararlanılmıştır. Teknik ve ekonomik özellikler bakımından etkinlik skorları sırasıyla, 0,97 ve 0,94 bulunmuştur. Teknik özelliklerin etkinlik skorları üzerine, 'deneyim', 'arı ırkı', 'eğitim seviyesi' ve 'koloni sayısı' parametreleri istatistiksel olarak anlamlı faktörler olarak tespit edilmiştir. Ekonomik özelliklerin etkinlik skorları üzerine, istatistiksel olarak anlamlı bir faktör bulunmamıştır. Sonuç olarak, Hatay ilinde etkin bir arıcılık faaliyeti yapılabilmesi için teknik ve ekonomik özellikler bakımından hangi şartlara sahip olunması gerektiği ortaya konulmuştur.
Anahtar sözcükler: Arıcılık, etkinlik, kesilmiş regresyon modeli, veri zarflama analizi.

Introduction

Beekeeping is a sub-sector of livestock, in which products with great importance for human health such as pollen, propolis, royal jelly, and especially honey, which provide economic value and profit, are produced by blending plants, honeybee, and labor (13). Compared to other livestock sectors, it holds advantages such as requiring less manpower and little dependence on the land (13, 19, 36). All over the world, beekeeping is a common activity and it keeps developing each year. According to FAO data in 2017, China was ranked first in terms of honey production, beehive number, and honey yield per hive. As for Turkey, although it was ranked second in terms of the total number of beehives and honey production, it was ranked quite at the bottom among the leading countries in honey yield per hive (17). Thanks to being rich in plants, Turkey is able to produce various types of honey and honeybee products (16, 31). However, due to the factors such as breeding wrong races, mistaken struggles against honeybee pests and diseases, lack of knowledge about colony management, Turkey cannot fully reflect its potential (11). At this point, it is quite important for the beekeeping sector in Turkey to have modern enterprises which work efficiently and effectively (20).

In Hatay province in 2017, the total number of hives, number of beekeeping enterprises, and honey yield per hive (kg) were reported as 95 943, 554, and 10.58 kg, respectively (35).

Performing this study in the field of beekeeping and examining the beekeeping enterprises in detail was very important for the veterinary medicine and beekeeping sector. In this study, it was aimed to determine the activities of beekeeping enterprises both technically and economically using data envelopment analysis. Furthermore, influential factors on efficiency scores of beekeeping enterprises were determined with a truncated regression model.

Materials and Methods

The study material was consisted of information gathered from 46 enterprises, which were registered under the Ministry of Agriculture and Forestry and Hatay Beekeeping Association and operate actively. The sample size was determined using a stratified random sampling method (33). In the analysis, demographic information about the enterprise and its owner, technical properties of the enterprises included in the study, bee feeding cost, auxiliary material cost, marketing and packaging cost, transportation and hive accommodation cost, drug cost, maintenance-repair cost, and other cost were used as inputs, and the income from honey sales, incidental income, and government supports were used as outputs (3, 6, 13, 16).

Data Envelopment Analysis (DEA) was aimed to measure the efficiency of decision making units by using present similar inputs and outputs. Through this analysis, efficient and non-efficient units were determined and solutions were developed to turn non-efficient units into efficient ones. At the same time, in order to become efficient, non-efficient decision making units try to assimilate themselves to the clusters consisting of efficient decision making units that were called the reference set (21, 30).

A certain efficient frontier is formed with DEA, and thus the distance of decision making units can be determined. The decision making units which are formed as a result of DEA and which have the function equal to 1 in value are called “efficient”, and those which have a function smaller than 1 in value are called “non-efficient” decision making units (30). The efficiency of decision making unit in DEA is obtained as follows;

$$\frac{\sum_{r=1}^{s} u_r y_{r0}}{\sum_{i=1}^{m} v_i x_{i0}} \qquad \frac{\sum_{r=1}^{s} u_r y_{rj}}{\sum_{i=1}^{m} v_i x_{ij}} \leq 1$$

$$u_r \geq 0 \quad , \quad v_i \geq 0$$

Here “s” stands for the number of output, “m” stands for the number of input, and “j” stands for decision making unit (24). In addition to these; x_{ij}: stands for i. the input amount used by j. decision making units, y_{rj}: stands for r. the output amount used by j. decision making units, u_r: stands for the weight given to r. output by decision making unit, v_i: stands for the weight given to i. input by decision making units (8, 10).

BCC (Banker, Charnes, Cooper) model, developed by Banker, Charnes and Cooper in 1984, is defined as the DEA model, which has been generated because the technical efficiency and scale efficiency are confused with each other in CCR (Charnes, Cooper, Rhodes) model, and whose hypothesis variable return to scale, which is defined as the imbalance between the increase in the input amount and the increase in the output amount in a decision making unit is valid (5, 8, 9). It can be analyzed in two different forms, namely input or output oriented models. The aim of input oriented models is to minimize the input variables in order to produce a certain output in the most effective way (10, 30, 34).

DEA produces no results as to why non-efficient enterprises are non-efficient. For this reason, a truncated regression model was used to determine which factors have impacts on the efficiency in the second stage. The truncated regression model was used to solve the problem of bias due to correlation between input, output variables, and factors, to reduce sampling errors compared to other models, and to predict stronger confidence intervals (18, 22, 32).

Within the scope of this study, primarily, descriptive statistics of all collected variables were calculated. DEA was used to calculate the efficiency of enterprises. In the study, input oriented BCC model was used as it is more flexible compared to CCR model, for its ease of interpretation, as it is the most suitable model to apply for beekeeping, and as it is field-oriented. In the study, statistic package programs were used such as SPSS 14.01 (License Number: 9869264) for descriptive statistics, MaxDEA 7 Basic for the determination of efficiency scores as a result of data envelopment analysis and Stata 12/MP4 (Licence Number: 50120500264) for the determination of factors effecting the efficiency scores.

Results

The average colony number of all enterprises included in the study was 188. It was found that the enterprise owners were an average of 20.33 years of experience, 67.4% of them had only primary education, 73.9% of them worked with crossbreed bee races, 32.6% of them saved records of their enterprises and 26.1% of them changed the queen in beehives in a time longer than 2 years.

The annual means for the input variables for the technical properties of beekeeping enterprises were calculated as follows: 185 beehives, 65 kilograms of beeswax to process, 20 sacks of sugar, 2.5 cans of sugar syrup, 1 staff and 50 cans. The annual means for the output

variables were calculated as 1 215 kilograms of honey and 4 kilograms of pollen produced in a year.

The target values for technical properties of beekeeping enterprises according to the input oriented BCC model were shown in Table 1. In the study, 40 of these beekeeping enterprises (87%) were found as efficient. The average efficiency value was calculated as 0.97. Among the efficient enterprises, the ones to give the most number of references (11 references) were enterprises numbered 7 and 32 (Table 5). Enterprises, whose efficiency values are below 1, were defined as non-efficient enterprises. These enterprises had to take efficient enterprises as a reference to become efficient. For instance, in order for the enterprise numbered 11 to become efficient, it needed to take enterprises numbered 1, 15, 17, and 28 as references (Table 5). Accordingly, enterprise numbered 11 could become efficient by reducing the number of hives by 5, the amount of processed beeswax by 50 kg, the sugar used by approximately half a sack, the number of staff by 2, the number of packages by 24, and by increasing the pollen production by 5 kg.

The annual means of input variables for the economic properties of beekeeping enterprises were calculated as follows: 3476.48 Turkish Lira (₺) for bee feeding cost, 1069.89 ₺ for auxiliary material cost, 597.72 ₺ for marketing and packaging cost, 3704.35 ₺ for transportation and hive accommodation cost, 725 ₺ for drug cost, 1661.52 ₺ for other cost and 563.04 ₺ for maintenance-repair cost. As for output variables, they were calculated as follows: 1746.74 ₺ as government support, 30804.13 ₺ as honey sales income, and 1006.30 ₺ as incidental income (1 USD= 3.8466 ₺ in December, 2017).

Table 1. Target values of technical properties of non-efficient enterprises.

Enterprise number	Efficiency score	Input variables						Output variables	
		Beehives	Beeswax	Sugar	Sugar syrup	Staff	Cans	Honey	Pollen
11	0.98	- 5	- 50	- 0.5	0	- 2	- 24	0	+ 5.31
16	0.58	- 118	- 21	- 13	- 9	- 1	- 61	0	0
24	0.66	- 58	- 15	- 1.5	- 2	- 1	- 18	0	+ 1.77
29	0.92	- 53	- 84	- 1	0	- 1	- 5	0	0
36	0.64	- 140	- 30	- 3.5	- 1	- 1	- 14	0	+ 1.85
44	0.92	- 74	- 45	- 1	0	- 1	- 4	0	0

Table 2. Target values of economical properties of non-efficient enterprises (₺/Year).

Enterprise No.	Efficiency Score	Input variables							Output variables		
		Bee feeding	Auxiliary material	Marketing and packaging	Transportation and accommodation	Drug	Maintenance-repair	Others	Government support	Honey sales	Incidental
11	0.90	-5071	-1226	-614	-2615	-143	-1352	-33	+1259	0	+131
12	0.69	-493	-218	-156	-62	-467	-438	-116	+749	0	+74
13	0.95	-90	-39	-171	-20	-15	-165	-10	+1181	0	+329
14	0.58	-1334	-683	-875	-2117	-207	-415	-215	0	+7360	0
16	0.62	-2811	-1642	-267	-18000	-381	-2935	-198	0	0	+3302
19	0.88	-294	-79	-403	-2141	-1250	-1536	-42	0	+24884	+1102
20	0.76	-536	-38	-758	-644	-120	-93	-60	0	+5250	+538
21	0.79	-1082	-128	-763	-373	-227	-3962	-107	0	+7195	+500
34	0.89	-728	-62	-47	-127	-32	-62	-78	0	0	+466
37	0.77	-821	-678	-277	-914	-213	-473	-23	0	+4213	+1507
38	0.98	-147	-2	-72	-1477	-6	-489	-56	+10	0	0
39	0.80	-357	-48	-83	-3322	-89	-149	-378	+148	0	+764
40	0.95	-118	-5	-106	-71	-190	-55	-7	0	0	+573
43	0.87	-334	-13	-19	-1767	-590	-47	-20	0	+4130	+1089
45	0.84	-449	-98	-69	-441	-512	-163	-573	0	0	+486

Table 3. Parameters effecting the efficiency scores of technical properties.

Parameters	Coefficient	Std. Error	Z	P	95% CI
Experience	0.0022	0.0009	2.41	0.016	0.0004 – 0.0039
Race of bee	-0.691	0.027	-25.21	<0.001	(-0.745) – (-0.637)
Education level	0.375	0.010	35.6	<0.001	0.354 – 0.396
Number of colony	0.0053	0.0001	32.47	<0.001	0.0050 – 0.0056

Table 4. Parameters effecting the efficiency scores of economical properties.

Parameters	Coefficient	Std. Error	Z	P	95% CI
Experience	0.006	0.005	1.02	0.306	-0.005 – 0.017
Race of bee	-0.156	0.118	-1.31	0.189	-0.389 – 0.076
Education level	-0.066	0.094	-0.70	0.482	-0.251 – 0.118
Number of colony	-0.0011	0.0006	-1.72	0.086	-0.0023 - 0.0001
Record-keeping status	0.058	0.096	0.60	0.552	-0.132 – 0.248
Frequency of changing queen	-0.159	0.086	-1.83	0.067	-0.328 – 0.011

Tablo 5. Reference sets for technical and economical properties.

Enterprise number	Technical properties	Economical properties	Enterprise number	Technical properties	Economical properties
1	-	-	24	1, 10, 27, 32, 45	-
2	-	-	25	-	-
3	-	-	26	-	-
4	-	-	27	-	-
5	-	-	28	-	-
6	-	-	29	9, 17, 32	-
7	-	-	30	-	-
8	-	-	31	-	-
9	-	-	32	-	-
10	-	-	33	-	-
11	1, 15, 17, 28	29, 33, 46	34	-	1, 7, 9, 23, 27, 32, 33
12	-	5, 7, 27, 32, 41	35	-	-
13	-	1, 5, 7, 27, 32, 46	36	1, 9, 12, 17, 32	-
14	-	1, 3, 4, 17, 23, 32	37	-	30, 31, 32
15	-	-	38	-	23, 33, 41
16	7, 15, 17, 28, 45	1, 3, 4, 17, 32, 46	39	-	4, 18, 31, 32, 33
17	-	-	40	-	18, 23, 24, 30, 41, 42
18	-	-	41	-	-
19	-	32, 36, 44, 46	42	-	-
20	-	23, 24, 28, 30, 36	43	-	18, 30, 32, 36, 41, 42
21	-	32, 41, 44, 46	44	9, 17, 32	-
22	-	-	45	-	1, 5, 7, 32, 33, 36, 44
23	-	-	46	-	-

- : Efficient

The target values for economic properties of beekeeping enterprises according to input-oriented BCC method were shown in Table 2. In the study, 31 of the beekeeping enterprises (67%) were found to be efficient. The average efficiency value was calculated as 0.94. Among the efficient enterprises, the one to give the most number of references (11 references) was the enterprise numbered 32 (Table 5). For example, the enterprise numbered 14 had to take enterprises numbered 1, 3, 4, 17, 23, and 32 as references to become efficient (Table 5). Accordingly, it could become efficient by reducing the cost of bee feeding by 1334 ₺, the cost of auxiliary material by 683 ₺, the cost of marketing and packaging by 875 ₺, the cost of transportation and hive accommodation by 2117 ₺, the cost of the drug by 208 ₺, the cost of other expenses by 415 ₺ and maintenance-repair cost by 215 ₺, and by increasing the income from honey sales by 7360 ₺.

After the determination of the efficiency of beekeeping enterprises by DEA, the determination of parameters estimated to affect the efficiency scores were calculated using truncated regression analysis. The variables that effects the technical and economic properties efficiency scores of beekeeping enterprises and results were shown in Tables 3 and 4. It was determined that in terms of technical properties of enterprises, the owner's beekeeping experience ($P<0.05$), educational level ($P<0.001$), and the number of a colony ($P<0.001$) were in positive effect and had a statistically significant on efficiency scores, and race of bee ($P<0.001$) was in negative effect and had a statistically significant on efficiency scores (Table 3).

It was determined that, in terms of economic properties of enterprises, the influence of the owner's beekeeping experience ($P>0.05$) and record-keeping status ($P>0.05$) on efficiency scores of enterprises were in positive effect, but were not statistically significant. It was also determined that the influence of the enterprise owner's educational level ($P>0.05$), number of colonies ($P>0.05$), race of bee ($P>0.05$), frequency of changing the queen (changing the queen for more than 2 years) ($P>0.05$) was in negative effect and statistically non-significant on efficiency scores of enterprises (Table 4).

Discussion and Conclusion

In various studies carried out using DEA (14, 16, 29), it was observed that the economic properties of enterprises were analyzed rather than their technical properties. It is quite important and instructive to analyze enterprises in terms of their technical properties along with economic parameters. Examining the technical properties of enterprises using DEA models has the characteristics of foresight for an enterprise that is planned to be started.

According to the DEA results of technical and economic properties of beekeeping enterprises, the enterprises which were shown as references the most are identified as number 7 and 32 by 11 times and number 32 by 11 times, respectively. Enterprise number 32 was said to use its technical and economic inputs more effectively compared to other enterprises. In different researches, reference sets were formed and it was reported that in order for the non-efficient decision making units to become efficient, they must resemble efficient decision making units (1, 4, 14). The reference set that consists of efficient units is of great importance for the non-efficient units to reach their target values.

According to input-oriented BCC model results of technical and economic properties of beekeeping enterprises respectively 40 enterprises (87%) and 31 enterprises (67%) were found to be efficient. Efficient enterprises in different fields of livestock were determined using different DEA models (4, 14, 15, 23, 28). Accordingly, in terms of ease of interpretation and field feasibility, researchers are able to use whichever DEA model they want, without any obligation or conditions.

In the input-oriented BCC model for technical and economic properties of beekeeping enterprises, the average efficiency score was calculated as 0.97 and 0.94, respectively. In a study conducted in Turkey on beekeeping (16), the researcher identified the technical efficiency score as 0.84, and the economic efficiency score as 0.63. The average efficiency scores in beekeeping enterprises were calculated as, 0.55 in Nigeria (3), as 0.89 in Ghana (2), as 0.57 in Greece (25), and as 0.85 in Adana (27). It was understood that, when compared to other studies, technical and economic efficiency scores were high. The reasons for this are thought to be the place of study, the difference between the input and output variables, different approaches about beekeeping in different countries and regions and the alteration of efficiency scores according to the applied DEA model.

In various studies about efficiency analysis, it was seen that regression models such as classical regression, Tobit regression and truncated regression were used in relation to analyzing parameters, which were considered to be influential on efficiency (6, 7, 15, 16, 23, 27, 28). The experience of the enterprise owner, included in the study, was similar to the study in which its relation to efficiency was analyzed (2). It was not similar to the study by Olarinde et al. (26).

In the study, in terms of technical properties that the owner's experience was found significant, makes us think that he is experienced in matters such as following the beekeeping production and technology about breeding, and being open to any kind of scientific innovation about honey production. The reason why this did not reflect economic efficiency was thought to be that the input costs increase over time and that government support for beekeeping is not satisfactory enough. In our study, it was

determined that, technically, colony number was a significant factor and had a positive effect on efficiency, that it was economically non-significant but had a negative effect. It was similar to studies (12, 16, 27). It was considered that a rise in the number of colonies, will thus increase honey production and incidental incomes, namely the technical efficiency. Economically, however, it will not be quite possible to experience an increase in output amount for reasons such as that the honey sale price was not high in the market and the government support was not satisfactory, and besides that due to the increase in the number of colonies, input costs will considerably increase. In the study, it was seen that the race of bees was a technically significant factor in efficiency, but it was not economically significant. Technically, choosing race of bee which are compatible with the conditions in the area of beekeeping and which are able to adapt quickly makes a positive contribution. Though found to be economically non-significant, by the increase in the number of enterprises included in the research, it is expected that this variable will become significant.

Consequently, an efficient beekeeping enterprise technically must have hives between 180 and 200, between 30 and 50 kilograms of processed beeswax, between 2 and 7 sacks of sugar used for feeding bees, 1 staff, and between 30 and 45 cans to store honey. Economically, the cost of bee feeding should be between 500 and 2000 ₺, the cost of transportation and hive accommodation should be 500 and 2000 ₺ and other expenses should be between 1000 and 1500 ₺. For Hatay province, crossbreed bee races should be used, enterprises should not use the queen bee for more than 2 years, and they must certainly produce bee products except honey. In order to promote efficiency in beekeeping enterprises, the beekeepers must manage the input use well. When producers produce beekeeping bee products as well as honey, their contribution both to the national economy and to their own economy will become even bigger. Enterprises, not only in the field of beekeeping but also in all sectors related to livestock, must be analyzed using data envelopment analysis, and the loss resulted from the wrong use of sources must be prevented by taking necessary precautions.

Acknowledgements

This manuscript is derived from the PhD thesis of the first author. We would like to thank The Turkish Association of Beekeepers (TAB) for their kindly help in field studies and coordination with the beekeeping enterprises.

Finacial support

This research received no grant from any funding agency/sector.

Ethical Statement

This study does not present any ethical concerns.

Conflict of Interest

The authors declared that there is no conflict of interest.

References

1. **Abacıoğlu S, Ünal İH** (2017): *Veri zarflama ve sıralı lojistik regresyon analizi ile şirketlerin etkinliklerinin belirlenmesi: Dokuma, giyim eşyası ve deri sektörü üzerine bir uygulama.* ASEAD, **12**, 1-19.
2. **Abdul-Malik A, Mohammed A** (2012): *Technical efficiency of beekeeping farmers in Tolon-Kumbungu district of Northern region of Ghana.* J Dev Agric Econ, **4**, 304-310.
3. **Aburime IL, Omotesho OA, Ibrahim HY** (2006): *An analysis of technical efficiency of beekeeping farms in Oyo state, Nigeria.* Eur J Soc Sci, **4**, 1-8.
4. **Akçay A, Çelik E, Sarıözkan S** (2017): Veri zarflama analizi ile koyunculuk işletmelerinin etkinliklerinin belirlenmesi: Yozgat ili örneği. 184-195. II. Ulusal Hayvancılık Ekonomisi Kongresi. Antalya, Turkey.
5. **Banker RD, Charnes A, Cooper WW** (1984). *Some models for estimating technical and scale inefficiencies in data envelopment analysis*. Manage Sci, **30**, 1078-1092.
6. **Barlovic N, Kezic J, Osmanagic Benedik N, et al** (2009): *Economic efficiency of beekeeping in Croatia.* Agric Conspec Sci, **74**, 51-54.
7. **Ceyhan V, Canan S, Yıldırım Ç, et al** (2017): *Economic structure and services efficiency of Turkish Beekeepers' Association.* Eur J Sustain Dev, **6**, 53-64.
8. **Charnes A, Cooper WW, Lewin AY, et al** (1994): Data Envelopment Analysis: Theory, Methodology, and Application. Springer Science+Business Media, LLC, USA.
9. **Cooper WW, Seiford LM, Tone K** (2007): Data Envelopment Analysis – A Comprehensive Text with Models, Applications, References and DEA-Solver Software, Second Edition. Springer Science+Business Media, LLC, USA.
10. **Çağlar A** (2003): Veri zarflama analizi ile belediyelerin etkinlik ölçümü. Doktora Tezi, Hacettepe Üniversitesi Fen Bilimleri Enstitüsü, Ankara.
11. **Çevrimli MB, Sakarya E** (2018): *Arıcılık işletmelerinin yapısal özellikleri ve sorunları; Ege Bölgesi örneği.* Eurasian J Vet Sci, **34**, 83-91.
12. **Çevrimli MB** (2019): *Assessment of the effects of subsidies to the beekeeping sector in Turkey on the number of hives and amount of honey produced.* Vet Hekim Der Derg, **90**, 115-121.
13. **Çevrimli MB, Sakarya E** (2019): *Economic analysis of beekeeping enterprises in Aegean Region, Turkey*. Ankara Univ Vet Fak Derg, **66**, 109-115.
14. **Demir P, Derbentli Ö, Sakarya E** (2012): *Kars ilinde bulunan mandıraların etkinliğinin veri zarflama analizi ile ölçülmesi.* Kafkas Univ Vet Fak Derg, **18**, 169-176.
15. **Doğan N** (2017): Konya ilinde yumurta tavukçuluğu yapan işletmelerin teknik ve ekonomik analizi. Doktora Tezi, İstanbul Üniversitesi Sağlık Bilimleri Enstitüsü, İstanbul.

16. **Emir M** (2015): Türkiye'de arıcıların sosyo-ekonomik yapısı ve üretim etkinliği. Doktora Tezi, Ondokuz Mayıs Üniversitesi Fen Bilimleri Enstitüsü, Samsun.
17. **FAO** (2017): Food and Agricultural Organization, Animal production. Available at: http://www.fao.org/faostat/en/#data. (Accessed December 10, 2019).
18. **Fernandes FDS, Stasinakis C, Bardarova V** (2018): *Two-stage DEA-Truncated Regression: Application in banking efficiency and financial development.* Expert Syst Appl, **96**, 284-301.
19. **Fıratlı Ç, Gençer HV** (1995): Dünya Arıcılığı ve Türkiye'nin Yeri. TC Ziraat Bankası Kültür Yayınları, No:28, Ankara, Turkey.
20. **Fıratlı Ç, Karacaoğlu M, Gençer HV, et al** (2010): Türkiye arıcılığının yapısal analizi. TMMOB Ziraat Mühendisleri Odası, Türkiye Ziraat Mühendisliği VI. Teknik Kongresi, Ankara, Turkey.
21. **Gören KB** (2012): Veri zarflama analizi ile kanola bitkisinin üretim maliyetleri ve ekonomik verimliliğinin ölçülmesi. Yüksek Lisans Tezi, Trakya Üniversitesi Sosyal Bilimleri Enstitüsü, Edirne.
22. **Kai D, Worthington AC, Zelenyuk V** (2018): *Data envelopment analysis, truncated regression and double-bootstrap for panel data with application to Chinese banking.* Eur J Oper Res, **265**, 748-764.
23. **Kaygısız F, Evren A, Koçak Ö, et al** (2018): *İstanbul'un Çatalca ilçesindeki mandacılık işletmelerinin etkinlik analizi.* Ankara Univ Vet Fak Derg, **65**, 291-296.
24. **Kirigia JM, Emrouznejad A, Sambo LG, et al** (2004): *Using data envelopment analysis to measure the technical efficiency of public health centers in Kenya.* J Med Syst, **28**, 155-166.
25. **Makri P, Papanagiotou P, Papanagiotou E** (2015): *Efficieny and economic analysis of Greek beekeeping farms.* Bulg J Agric Sci, **21**, 479-484.
26. **Olarinde LO, Ajao AO, Okunola SO** (2008): *Determinants of technical efficiency in bee-keeping farms in Oyo state, Nigeria: A stochastic production frontier approach.* Res J Agric Biol Sci, **4**, 65-69.
27. **Ören MN, Alemdar T, Parlakay O, et al** (2010): Adana İlinde Arıcılık Faaliyetinin Ekonomik Analizi. Yayın no: 178. Tarımsal Ekonomi Araştırma Enstitüsü, Ankara.
28. **Özden A** (2016): *Veri zarflama analizi ile süt sığırcılığı işletmelerinin performans düzeylerinin belirlenmesi.* Tarım Ekonomisi Dergisi, **22**, 49-55.
29. **Ritten CJ, Peck D, Ehmke M, et al** (2018): *Firm efficiency and retuns-to-scale in the honey bee pollination services industry.* J Econ Entomol, **111**, 1014-1022.
30. **Sarı Z** (2015): Veri zarflama analizi ve bir uygulama. Yüksek Lisans Tezi, Hacettepe Üniversitesi Fen Bilimleri Enstitüsü, Ankara.
31. **Sarıözkan S, İnci A, Yıldırım A, et al** (2009): *Kapadokya'da arıcılık.* Erciyes Univ Vet Fak Derg, **6**, 143-155.
32. **Simar L, Wilson P** (2007): *Estimation and inference in two-stage semiparametric models of production processes.* J Econom, **136**, 31-64.
33. **Sümbüloğlu K, Sümbüloğlu V** (1997): Örnekleme Yöntemleri. Hatipoğlu Yayınevi, Ankara.
34. **Şener C** (2013): Veri zarflama analizi ve Malmquist endeksi ile Avrupa Birliği ülkelerinin sağlık performanslarının incelenmesi. Yüksek Lisans Tezi, Gazi Üniversitesi Fen Bilimleri Enstitüsü, Ankara.
35. **TÜİK** (2018): Arıcılık verileri. Available at: http://www.tuik.gov.tr/Start.do. (Accessed November 10, 2019).
36. **Yeninar H, Akyol E, Şahinler N, et al** (2010): Taşıma ve çevre şartlarının gezginci arıcılık koşullarında, bal arısı kolonileri üzerine etkilerinin belirlenerek uygun taşımacılık ve kışlama yöntemlerinin geliştirilmesi. Available at: https://app.trdizin.gov.tr/publication/show/pdf/project/TVRBMU5qRXg. (Accessed October 12, 2020).

Ankara Univ Vet Fak Derg, **68**, 237-244, 2021
DOI: 10.33988/auvfd.680747

The effect of dietary supplementation of natural antioxidants and coated calcium butyrate on carcass traits, serum biochemical parameters, lipid peroxidation in meat and intestinal histomorphology in broilers

Erinç GÜMÜŞ[1,a,✉], Seher KÜÇÜKERSAN[2,b], Alev Gürol BAYRAKTAROĞLU[3,c], Tevhide SEL[4,d]

[1]Aksaray University, Eskil Vocational School, Aksaray; [2]Ankara University, Faculty of Veterinary Medicine, Department of Animal Nutrition and Nutritional Disease, Ankara; [3]Ankara University, Faculty of Veterinary Medicine, Department of Histology and Embryology, Ankara; [4]Ankara University, Faculty of Veterinary Medicine, Department of Biochemistry, Ankara, Turkey.
[a]ORCID: 0000-0002-6839-8428; [b]ORCID: 0000-0002-2882-9203; [c]ORCID: 0000-0001-9248-8370;
[d]ORCID: 0000-0002-9753-779X

✉Corresponding author: erincgumus@aksaray.edu.tr
Received date: 27.01.2020 - Accepted date: 14.10.2020

Abstract: The aim of this study was to investigate the effects of vitamin E, grape seed extract and green tea extract with or without supplementation of coated calcium butyrate in broilers based on carcass traits, some biochemical parameters, intestinal histomorphology, and lipid peroxidation in meat. Two hundred fifty-two one-day-old broiler chicks were divided into nine groups, one control and eight experimental. Control group fed only a basal diet (control). The experimental groups' diets contained feed additives as; coated calcium butyrate (CCB), vitamin E (VitE), grape seed extract (GSE), green tea extract (GTE), a combination of vitamin E with coated calcium butyrate (VitE+CCB), grape seed extract with coated calcium butyrate (GSE+CCB), green tea extract with coated calcium butyrate (GTE+CCB), and a combination of grape seed extract, green tea extract, and coated calcium butyrate (GSE+GTE+CCB) respectively. According to the study results; no significant differences were observed in gut histomorphology and serum biochemical parameters. The broilers fed with GSE and GTE with/without CCB had significantly higher hot carcass yield than control, VitE, and VitE+CCB. Furthermore, all groups showed significantly lesser lipid peroxidation in meat than control; however, the VitE group had the lowest malondialdehyde (MDA) levels. It can be concluded that the combination of CCB with natural antioxidants could be used to improve carcass traits and meat antioxidant capacity in broilers.
Keywords: Broiler, coated calcium butyrate, intestinal histomorphology, lipid peroxidation, natural antioxidants.

Etçi piliç rasyonlarına doğal antioksidanlar ve kaplanmış kalsiyum bütirat ilavesinin karkas özellikleri, serum biyokimyasal parametreleri, ette lipid peroksidasyon ve bağırsak histomorfolojisi üzerine etkileri

Özet: Bu çalışmanın amacı, vitamin E, üzüm çekirdeği ekstraktı ve yeşil çay ekstraktının tek başına veya kaplanmış kalsiyum bütirat ile birlikte kullanılmasının etçi piliçlerde karkas özellikleri, bazı biyokimyasal parametreleri, bağırsak histomorfolojisi ve ette lipid peroksidasyon düzeyi üzerindeki etkisini araştırmaktır. Bir günlük 252 civciv, bir kontrol ve sekiz deneme grubu olmak üzere dokuz gruba ayrılmıştır. Kontrol grubuna sadece temel rasyon verilmiştir (Kontrol). Deneme gruplarının yemleri sırasıyla kaplanmış kalsiyum bütirat (CCB), vitamin E (VitE), üzüm çekirdeği ekstraktı (GSE), yeşil çay ekstraktı (GTE), vitamin E ile kaplanmış kalsiyum bütirat (VitE+CCB), üzüm çekirdeği ekstraktı ile kaplanmış kalsiyum bütirat (GSE+CCB), yeşil çay ekstraktı ile kaplanmış kalsiyum bütirat (GTE+CCB) ve üzüm çekirdeği + kaplanmış kalsiyum bütirat + yeşil çay ekstraktının (GSE+GTE+CCB) birlikte olduğu yem katkılarını içermektedir. Çalışma sonuçlarına göre; bağırsak histomorfolojisi ve serum biyokimyasal parametreler açısından gruplar arasında anlamlı bir fark tespit edilememiştir. GSE ve GTE tek başına veya CCB ile verildiği etçi piliçlerde, Kontrol, VitE ve VitE+CCB kombinasyonu verilen gruplara göre sıcak karkas randımanın anlamlı derecede yüksek olduğu gözlenmiştir. Ayrıca, bütün gruplar kontrol grubuna göre ette önemli düzeyde daha düşük lipid peroksidasyonu gösterdi, fakat VitE grubu en düşük MDA seviyesine sahipti. Sonuç olarak etçi piliçlerde CCB'nin doğal antioksidanlarla kombine olarak kullanılmasının karkas özellikleri ve et antioksidan kapasitesini iyileştirmek için kullanılabileceği sonucuna varılabilmektedir.
Anahtar sözcükler: Bağırsak histomorfolojisi, doğal antioksidanlar, etlik piliç, kaplanmış kalsiyum bütirat, lipid peroksidasyon.

Introduction

Oxidation is a natural part of the metabolism's biological activity, yet a high intake of poly-unsaturated fatty acids (PUFA), oxidized lipids, or ingesting an insufficient amount of nutrients essential for the antioxidant defense system could cause excessive level of lipid peroxidation (16, 29). The commonly used energy and protein sources in poultry diets, such as fishmeal and vegetable oils, are rich with PUFA. They also increase susceptibility to lipid peroxidation and account for the loss in the nutritional value and shelf life of poultry meat and meat products (29, 35). These kind of unwanted side effects could be reduced with antioxidant supplementation in poultry nutrition (15).

Although synthetic antioxidants are commonly used in animal nutrition due to their effectiveness and low cost, more attention is being given to natural antioxidants due to increasing consumer concerns (7). Similarly, the broiler industry has been investigating new sources of natural antioxidants to establish antioxidant stability in meat tissues (29, 35). Most natural antioxidants consist of lipid soluble phenolics, such as tocopherols or phenolic extracts prepared from plants like rosemary, sage, green tea, grape seed, and oregano (35). Green tea and grape by-products or extracts are two of the most important polyphenol-rich sources due to their mass production, easy accessibility, and ability to capture free radicals (26, 33).

Protecting the intestinal health of poultry is critical in order to reach target body weight gain and feed conversion ratio (3, 36). Butyric acid, one of the short-chain fatty acids, has been shown to have a significant effect on the proliferation, growth, and differentiation of intestinal mucosa cells by means of its influence on gene expression and protein synthesis (10). Salt forms of butyric acid are preferred in animal nutrition due to the butyric acid's strong unpleasant odor (10). Salt forms of butyric acid also significantly improve the intestinal histomorphology of broilers in different phases of growth (3, 10, 22). Due to the fact that non-protected butyrate salts are mostly absorbed in the upper part of the gastrointestinal tract, microencapsulation is used to protect butyrate salts until they reach the broiler intestines (31).

The aim of this study was to investigate the effects of alone and combined dietary use of coated calcium butyrate (CCB) with three important natural antioxidants; vitamin E (VitE), grape seed extract (GSE), and green tea extract (GTE) based on carcass traits, serum biochemical parameters, intestinal histomorphology, and muscular antioxidant activity in broilers.

Material and Method

***Bird Husbandry and Diets*:** This research was conducted in the Ankara University Veterinary Faculty Research and Application Farm and approved by the Ankara University Ethics Committee (decision no. 2015-18-201). The feeding trial was carried out on 252 male Ross 308 broiler chicks (initial weight 43.66 ± 0.05 g) assigned to nine groups. Every treatment group consisted of four replicates of seven chicks each. All chickens were placed in wired cages and were held in an environmentally controlled room. The temperature of the environment was kept at 32ºC (±1) for the first week and then decreased to 25ºC the days after. Feed and water were offered ad libitum to the chickens. Basal diets were formulated for starter (1-14 days) and finisher (15-41 days) periods. The diets were produced in a local feed mill, based on corn and soybeans, and formulated to be isocaloric and isonitrogenous for starter and finisher periods in order to meet all nutritional requirements (23). The ingredients and calculated chemical composition of the basal diet are shown in Table 1. All diets were supplemented with 250 mg/kg CCB, except for the control group. The CCB used in the study was a commercial product consisting of 860 g/kg salt (160 g Ca and 700 g butyric acid) and coated with a matrix of vegetable oils (Globamax B700, Sanita Sağlık Ürünleri A.Ş.). In order to better understand the effect of the natural antioxidants in the diet, no antioxidant other than 45 mg vitamin E, 70 mg zinc, and 0.3 mg selenium per kg in the vitamin and mineral premix was used in the study.

The control group was fed only with basal diet (Control). The experimental diets were supplemented with CCB, VitE, GSE, GTE and a combination of CCB and natural antioxidants: VitE+CCB, GSE+CCB, GTE+CCB, and GSE+GTE+CCB mixture, respectively. The VitE (Vimar Gıda Tarım Hayvancılık A.Ş., İstanbul, Turkey), GSE (Nor-Grape, Vimar Gıda Tarım Hayvancılık A.Ş., İstanbul, Turkey), and GTE (Balen, Arı Mühendislik Ltd. Şti, Ankara, Turkey) were procured from commercial products. The polyphenols and alpha-tocopherol were added as 200 mg/kg, as described by Vossen et al. (35) and the CCB was added 250 mg/kg into the diet, based on the study of Van Den Borne et al. (31).

Traits measured: Twelve broilers were selected, weighed, and slaughtered from each group on the day 41 of the experiment. Afterward, blood samples were taken from the jugular vein and were centrifuged to collect serum. The carcasses were weighed to calculate hot carcass yield. The heart, spleen, liver, abdominal fat, gizzard, proventriculus, and bursa of Fabricius were also weighed. Their relative weights of them were calculated by dividing into slaughtering weight. Breast meat samples were taken from the hot carcasses of broilers. The serum and breast meat samples were stored at -20°C until the time the analyses were carried out.

The serum samples were analyzed for levels of alkaline phosphatase (ALP), alanine amino transferase

(ALT), aspartate amino transferase (AST), total cholesterol, triglyceride, high-density lipoprotein (HDL), and low-density lipoprotein (LDL) by an automatic analyzer (BT 3000, Biotechnica Instruments, Italy) with commercial kits (Randox RX series, Randox Laboratories Ltd., London, United Kingdom).

A 25-mg of breast meat from each animal was mixed with a 250-µ RIPA buffer and sonicated (Bandelin Sonoplus HD 3100 Homogeniser). The blend was centrifuged at 1.600 x g for four minutes at 4°C, and supernatants were taken to determine the malondialdehyde (MDA) levels. The SpectraMax®i3 Plate Reader (Molecular Devices, Sunnyvale, CA, USA) was used to measure the absorbance at 540 nm with TBARS Assay Kits (Molecular Devices, Sunnyvale, CA, USA).

The small intestine tissue samples were taken from the jejunum and ileum according to the method described by Calik et. al (8). The samples were fixed in a 10% neutral buffered formalin for 24h. Thereafter, following routine histological process, samples were embedded in paraffin and then stained with Mallory's modified triple stain in order to visualize general morphology (5). The histological sections were examined under a light microscope (Leica DM 2500, Leica Microsystems GmbH, Wetzlar, Germany) and captured with the Leica DFC450 (Leica Microsystems, Heerbrugg, Germany) digital microscope camera. Morphometric indices were evaluated using the ImageJ software (Image J, US National Institutes of Health, Bethesda, MD, USA) as described by Calik et. al (8).

Statistical analysis: All received data were analyzed by the one-way analysis of variance (ANOVA) procedure of the SPSS version 20 (Inc., Chicago IL, USA) (12). The differences among the groups were examined with a post-hoc Tukey test. Any statistical differences were considered significant at $P<0.05$.

Table 1. The ingredients and chemical composition of the basal diets (as-fed basis).

Ingredients (%)	Starter diet (1-14 days)	Finisher diet (15-41 days)
Corn	46.59	51.86
Corn gluten meal	2.55	3.60
Wheat	5.00	10.00
Full fat soya	0.00	4.50
Soybean meal	37.50	23.50
Monocalcium phosphate	0.99	0.66
Limestone	1.89	1.27
Sodium butyrate	0.30	0.08
Salt	0.30	0.32
Soybean Oil	4.00	3.50
Methionine	0.30	0.22
Lysine	0.24	0.23
Threonine	0.12	0.07
Choline chloride (%75)	0.07	0.05
Vitamin-mineral mix*	0.10	0.10
Enzyme (6-Phytase)	0.05	0.05
Total	100.00	100.00
Calculated composition		
Crude Protein, %	23.00	21.00
Ether extract, %	6.00	6.50
Crude Ash, %	6.00	5.00
Crude fibre, %	3.50	4.00
Sodium, %	0.22	0.16
Calcium, %	1.10	0.90
Phosphorus, %	0.50	0.45
Total Lysine, %	1.44	1.24
Total Met + Sis, %	1.07	0.95
ME** (kcal/kg)	3,100	3,200

* Vitamin – mineral mix supplied the following per kg of diet: Vitamin A 15000 IU. Vitamin D3 3000 IU. Vitamin E 45 mg, Manganese 100 mg, Iron 100 mg, Zinc 70 mg, Copper 15 mg, Iodine 1.5 mg, Cobalt 0.5 mg, Selenium 0.3 mg. ** Metabolizable energy content of diets was calculated according to the equation of Carpenter and Clegg (9)

Results

The effect of natural antioxidants and CCB supplementation on the carcass yield and percentages of organs are shown in Table 2. The carcass yield (P<0.001) and relative liver weight (P<0.05) was significantly affected by polyphenol supplementation with/without CCB. However, no significant interaction between the groups was found for the percentages of heart, spleen, bursa of Fabricius, gizzard, proventriculus and abdominal fat (P>0.05).

The serum biochemical analysis results showed that dietary supplement of natural antioxidants with or without CCB does not affect serum ALT, ALP, AST, total cholesterol, triglyceride, LDL, and HDL levels in broiler chickens at day 41 (Table 3) (P>0.05).

Table 2. The effects of natural antioxidant and coated calcium butyrate supplementation on carcass yield and relative weight percentages (g/100 g BW) of internal organs.

Treatments	Slaughter weight (g)	Hot carcass yield (%)	Heart (%)	Spleen (%)	Liver (%)	Bursa of Fabricius (%)	Abdominal fat (%)	Gizzard (%)	Pro-ventriculus (%)
Control	2332.75±97.72^{d}	69.85±0.51^{b}	0.40±0.04	0.12±0.03	2.09±0.05^{a}	0.18±0.01	1.62±0.11	1.21±0.13	0.33±0.02
CCB	2404.92±69.83^{cd}	70.79±0.44^{ab}	0.38±0.04	0.11±0.03	1.99±0.06^{ab}	0.14±0.01	1.59±0.09	1.26±0.03	0.29±0.01
VitE	2471.25±65.12^{abc}	70.58±0.49^{ab}	0.39±0.04	0.11±0.02	2.07±0.04^{a}	0.16±0.02	1.64±0.11	1.18±0.04	0.29±0.01
GSE	2557.25±94.20^{a}	71.60±0.71^{a}	0.38±0.06	0.12±0.04	1.96±0.05^{ab}	0.14±0.01	1.56±0.06	1.20±0.04	0.30±0.03
GTE	2528.58±74.56^{ab}	71.99±1.10^{a}	0.39±0.07	0.11±0.02	1.88±0.05^{b}	0.14±0.02	1.51±0.13	1.18±0.03	0.29±0.04
VitE+ CCB	2458.50±61.80^{bc}	70.85±0.36^{ab}	0.38±0.04	0.11±0.02	1.94±0.06^{ab}	0.17±0.01	1.57±0.10	1.21±0.05	0.31±0.01
GSE+ CCB	2559.58±36.67^{a}	71.59±0.54^{a}	0.38±0.07	0.10±0.03	1.89±0.06^{b}	0.13±0.02	1.58±0.07	1.21±0.06	0.30±0.04
GTE+ CCB	2520.50±85.51^{ab}	71.59±0.36^{a}	0.39±0.07	0.12±0.05	1.86±0.04^{b}	0.14±0.02	1.54±0.10	1.27±0.02	0.31±0.05
GSE+ GTE+ CCB	2479.17±73.38^{abc}	71.34±0.34^{a}	0.38±0.13	0.11±0.05	1.98±0.04^{ab}	0.16±0.01	1.55±0.13	1.34±0.05	0.32±0.05
P	<0.001	<0.001	0.983	0.703	0.034	0.132	0.992	0.171	0.094

$^{a,b,c,d:}$Means within a column with different letters are significantly different (P<0.05). VitE, Vitamin E; CCB, Coated Calcium Butyrate; GSE, Grape Seed Extract; GTE, Green Tea Extract.

Table 3. The effects of natural antioxidants and coated calcium butyrate supplementation on some serum biochemical parameters.

Treatments	ALT (IU/L)	ALP (IU/L)	AST (IU/L)	Total cholesterol (mg/dL)	Triglyceride (mg/dL)	LDL (mg/dL)	HDL (mg/dL)
Control	3.36±0.74	1934.55±269.08	215.42±12.05	111.10±3.66	43.00±2.54	26.87±5.73	73.58±3.85
CCB	2.82±0.42	1945.10±270.79	216.91±17.51	103.80±5.56	43.38±6.57	17.25±3.50	67.33±3.65
VitE	3.63±0.73	2063.20±270.79	237.00±28.60	107.13±6.80	51.50±5.39	23.45±6.69	63.55±3.69
GSE	2.89±0.45	1871.00±210.85	240.00±25.25	106.00±6.87	48.90±4.63	19.13±7.81	63.18±3.85
GTE	3.13±0.73	1739.78±213.76	265.43±26.68	107.13±9.22	50.70±4.63	20.71±9.20	69.18±3.85
VitE+CCB	2.78±0.40	1827.08±134.38	241.33±19.06	101.36±6.80	41.56±5.59	27.63±3.87	70.38±3.85
GSE+CCB	2.22±0.40	1708.63±191.01	208.78±26.25	98.00±4.10	47.10±3.96	14.62±2.63	67.30±3.85
GTE+CCB	2.58±0.53	1960.25±161.60	228.27±26.44	103.00±5.87	44.75±2.33	18.52±4.31	72.23±3.85
GSE+GTE+ CCB	2.30±0.42	1845.88±108.84	209.50±16.49	100.20±6.23	44.80±4.37	17.38±6.52	77.90±3.85
P	0.661	0.977	0.670	0.907	0.647	0.655	0.127

VitE, Vitamin E; CCB, Coated Calcium Butyrate; GSE, Grape Seed Extract; GTE, Green Tea Extract.

Table 4 illustrates the effects of natural antioxidant administration with or without CCB on villus height and crypt depth in the jejunum and ileum of broiler chickens at day 41. Ileum crypt depth decreased significantly in the groups fed with VitE, GSE, VitE+CCB, and GTE+CCB supplementation at the end of the study (P<0.05). Lowest values were recorded from the birds supplemented with GSE and VitE+CCB. There was no significant difference in jejunum villus height, jejunum crypt depth, jejunum villus height/crypt depth ratio, ileum villus height, and ileum villus height/crypt depth ratio between the control group and the experimental groups (P>0.05).

MDA concentrations in the breast meat of broiler chickens are presented in Figure 1. A positive improvement in MDA-reduced levels was examined in the broilers supplemented with natural antioxidants with or without CCB compared to the ones fed with basal diet (P<0.05). The best value was recorded from the group that received dietary VitE supplementation.

Table 4. The effects of natural antioxidant and coated calcium butyrate supplementation on the jejunum and ileum histomorphology of broiler chickens at day 41.

Treatments	Jejunum			Ileum		
	Villus height (µm)	Crypt depth (µm)	Villus height/ crypt depth	Villus height (µm)	Crypt depth (µm)	Villus height/ crypt depth
Control	1127.30±97.93	194.20±4.90	5.82±0.52	792.00±64.04	176.77±7.99^{a}	4.46±0.25
CCB	1153.27±36.77	209.97±19.12	5.62±0.39	748.30±68.83	175.80±9.39^{a}	4.30±0.36
VitE	1187.60±101.89	206.70±10.14	5.72±0.41	671.20±46.46	161.90±4.78^{ab}	4.15±0.21
GSE	1236.20±73.83	222.20±2.69	5.58±0.37	685.00±59.72	156.73±5.80^{b}	4.35±0.24
GTE	1228.03±73.28	213.90±8.86	5.75±0.28	782.2±29.37	179.04±7.95^{a}	4.39±0.21
VitE+ CCB	1247.30±76.23	205.50±5.45	6.12±0.49	631.70±36.07	157. 67±3.87^{b}	4.02±0.25
GSE+CCB	1224.30±49.94	224.80±10.25	5.49±0.36	788.00±39.08	176.10±7.24^{a}	4.49±0.23
GTE+CCB	1443.10±21.68	227.53±5.84	6.36±0.23	771.60±17.82	164.47±2.08^{ab}	4.69±0.12
GSE+GTE+CCB	1350.10±35.97	216.73±4.84	6.25±0.25	773.43±47.90	179.80±4.48^{a}	4.29±0.21
P	0.093	0.218	0.725	0.139	0.045	0.714

$^{a,b:}$Means within a column with different letters are significantly different (P<0.05). VitE, Vitamin E; CCB, Coated Calcium Butyrate; GSE, Grape Seed Extract; GTE, Green Tea Extract.

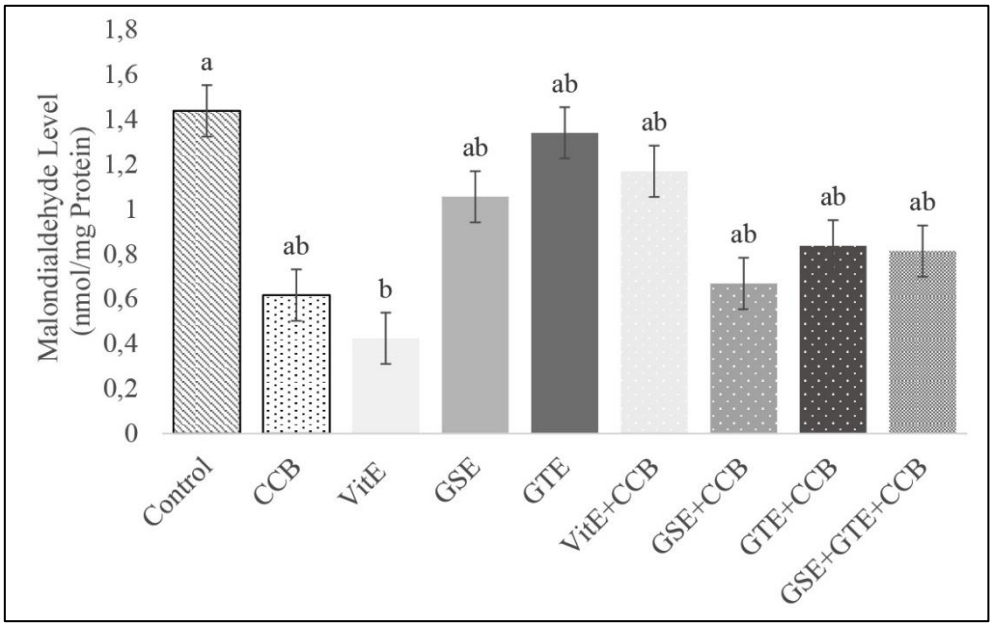

Figure 1. The effects of natural antioxidant and coated calcium butyrate supplementation on MDA levels on breast meat of broiler chickens at day 41.

^{a,b}: For each treatment, bars with different letters are significantly different (P<0.05). VitE, Vitamin E; CCB, Coated Calcium Butyrate; GSE, Grape Seed Extract; GTE, Green Tea Extract.

Discussion and Conclusion

The experiment showed that both supplementation of CCB and natural antioxidants in broiler diets improved slaughter weight and carcass yield, compared to the control group. Especially, broilers fed with GSE and GSE+CCB supplementation showed the best slaughter weights. Similar results were found for the positive effect of dietary grape by-product supplementation on the final body weight of broilers (1) and rabbits (18). In addition, several studies also reported positive effect of VitE (26, 32), GTE (6, 26), and butyrate salts (3, 10, 24) on the final body weight of broilers. The movement-retarding effects of tannins in intestines to improve nutrient absorption might be one possible reason for this result (1). Furthermore, butyrate salts are known to improve protein and energy digestibility by enhancing gut health (24). In this experiment, hot carcass yields were affected positively by the dietary supplementation of CCB and antioxidants. These results are in line with previous studies stating that supplementation of grape seed by-products (1, 27), VitE (39), and butyric acid (21, 24) positively affected hot carcass yield in broilers. Relative liver size was found smaller in the groups fed with GSE, GTE, and CCB. Similar results were observed by Biswas and Wakita (6) and Brenes et al. (7). The liver is an important organ for digestive processes. Bile production and relative liver weight correlates with its secretory activity (2). The inhibitory effect of polyphenols on lipid absorption in intestines might negatively affect liver weight (6). However, Vlaicu et al. (34) reported relative liver size of broilers fed with grape seed oil increased in chronic heat stress. Aghazadeh and Taha Yazdi (2) also reported butyric acid supplementation improved liver size in broilers.

In this study, serum biochemical parameters did not change with the dietary supplementation of natural antioxidants with/without CCB. Parallel to our study, similar findings were found for triglyceride (11, 17, 30), lipoprotein (11, 14), and liver enzyme (1) levels. Total cholesterol level was lower in groups fed with natural antioxidant and CCB combination, compared to the control group and those without CCB supplementation, although this low level of cholesterol exists only numerically. Polyphenols and condensed tannins in natural antioxidants are known for their ability to bind cholesterol and prevent the absorption in the intestines (14). Yin et al. (37) also reported that butyric acid affects adipogenesis and lipid metabolism in young broilers and decreases cholesterol content in serum and tissues.

The intestines are an important part of the broiler's gastrointestinal tract and are essential in keeping them healthy and productive (33). Both butyric acid and dietary polyphenols or related phenolic components are used to modulate gut activity (3, 31). However, supplementation of natural antioxidants with/without CCB did not affect jejunum villus height, jejunum crypt depth, jejunum villus height/crypt depth ratio, ileum villus height, and ileum villus height/crypt depth ratio in this study. Also, the ileum crypt depth was adversely altered, especially by the dietary supplementation of GSE and VitE+CCB. Several reports have also documented adverse effects of grape seed products (13, 33) and VitE (38) in broilers. Ebrahimzadeh et al. (13) indicated that crypts mainly responsible for the intestinal cell proliferation and lower crypt depth might have a positive effect on the performance of poultry due to decreasing nutrient requirements for intestinal maintenance. Contrary to our findings, previous studies reported that the supplementation of natural antioxidants (13, 17, 19) and butyric acid salts (3, 24, 28) had constructive effects on villus height and crypt depth of jejunum in broilers. The discrepancies between the studies might be due to the variety of the dietary feed additive (pomace, extract, powder, microencapsulated, etc), polyphenol content, experimental conditions, and slaughter age.

The TBARS method is commonly used to detect MDA levels, one of the by-products of the lipid peroxidation reaction (29). In this study, the lowest MDA level was recorded in the group fed with VitE. Alpha-tocopherol is accepted as the most powerful lipid-soluble antioxidant due to the ready donation of hydrogen from the hydroxyl (-OH) group on the ring structure to free radicals (4, 29). Other researchers also found similar results to our study in terms of the comparative effects of natural antioxidants. Smet et al. (29) reported that breast meat obtained from broilers fed with 200 mg/kg alpha-tocopherol had lower MDA levels than the broilers fed with green tea, grape seed, tomato, or rosemary. Brenes et al. (7) and Goñí et al. (16) also showed that dietary VitE supplementation delayed lipid peroxidation in meat, compared to grape pomace. Likewise, dietary inclusion of alpha-tocopherol showed better antioxidant activity, compared to green tea polyphenol supplementation in growing pigs (4). In agreement with previous studies in broilers (20, 36, 40), the groups supplemented with CCB also showed significantly low MDA levels in our experiment. Although there are limited data on antioxidant effect of butyrate, it is estimated that butyric acid reduces MDA levels in tissues by suppressing I-kappa-B kinase production and stimulating antioxidant enzymes such as superoxide dismutase and catalase (40). Despite both VitE and CCB groups having the MDA levels, broilers fed with VitE+CCB showed higher lipid peroxidation in breast meat. Rietjens et al. (25) reported that natural antioxidants may show pro-oxidative effects and increase oxidative stress on tissues in certain conditions or at higher doses. In

the same study, researchers emphasized that the increasing level of tocopherol radicals could generate lipid peroxidation by themselves.

In conclusion, this study showed that supplementation of natural antioxidants with or without CCB did not impair serum biochemical parameters and intestinal histomorphology in broiler chickens. However, they did have a beneficial effect on hot carcass yield and reducing MDA levels in breast meat. Therefore, a combination of CCB and natural antioxidants could be used in poultry nutrition to improve carcass performance and to reduce oxidative rancidity to increase the shelf life of meat products.

Acknowledgment

This manuscript is based on PhD thesis of Erinç GÜMÜŞ. The authors wish to acknowledge Beypi A.Ş. for chicks and Vimar A.Ş. for grape seed extract, Vitamin E and Sanita Sağlık Ürünleri A.Ş. for coated calcium butyrate supply.

Financial Support

This research was supported by Ankara University Research Fund (Project No: 16L0238002).

Ethical Statement

This study was approved by the Ankara University Ethics Committee (2015-18-201).

Conflict of Interest

The authors declared that there is no conflict of interest.

References

1. **Abu Hafsa SH, Ibrahim SA** (2018): *Effect of dietary polyphenol-rich grape seed on growth performance, antioxidant capacity and ileal microflora in broiler chicks.* J Anim Physiol Anim Nutr, **102**, 268–275.
2. **Aghazadeh A, Taha Yazdi M** (2012): *Effect of butyric acid supplementation and whole wheat inclusion on the performance and carcass traits of broilers.* S Afr J Anim Sci, **42**, 241–248.
3. **Antongiovanni M, Buccioni A, Petacchi F, et al** (2007): *Butyric acid glycerides in the diet of broiler chickens: effects on gut histology and carcass composition.* Ital J Anim Sci, **6**, 19–25.
4. **Augustin K, Blank R, Boesch-Saadatmandi C, et al** (2008): *Dietary green tea polyphenols do not affect vitamin E status, antioxidant capacity and meat quality of growing pigs.* J Anim Physiol Anim Nutr, **92**, 705–711.
5. **Bancroft JD, Gamble M** (2002): Histological Techniques, 5th edition. 182-189. Churchill & Livingstone, London, Philadelphia.
6. **Biswas AH, Wakita M** (2001): *Effect of dietary japanese green tea powder supplementation on feed utilization and carcass profiles in broilers.* J Poult Sci, **38**, 50–57.
7. **Brenes A, Viveros A, Goñi I, et al** (2010): *Effect of grape seed extract on growth performance, protein and polyphenol digestibilities, and antioxidant activity in chickens.* Span J Agric Res, **8**, 326–333.
8. **Calık A, Ceylan A, Ekim B, et al** (2017): *The effect of intra-amniotic and posthatch dietary synbiotic administration on the performance, intestinal histomorphology, cecal microbial population, and short-chain fatty acid composition of broiler chickens.* Poult Sci, **96**, 169–183.
9. **Carpenter KJ, Clegg KM** (1956): *The metabolizable energy of poultry feeding stuffs in relation to their chemical composition.* J Sci Food Agric, **7**, 45-51.
10. **Chamba F, Puyalto M, Ortiz A, et al** (2014): *Effect of partially protected sodium butyrate on performance, digestive organs, intestinal villi and E. coli development in broilers chickens.* Int J Poult Sci, **13**, 390–396.
11. **Chamorro S, Viveros A, Centeno C, et al** (2013): *Effects of dietary grape seed extract on growth performance, amino acid digestibility and plasma lipids and mineral content in broiler chicks.* Animal, **7,** 555–561.
12. **Dawson B, Trapp RG** (2001): Basic & Clinical Biostatistics, 3rd Edition. Lange Medical Books, McGnaw-Hill Medical Publishing Division, New York.
13. **Ebrahimzadeh SK, Navidshad B, Farhoomand P, et al** (2018): *Effects of grape pomace and vitamin E on performance, antioxidant status, immune response, gut morphology and histopathological responses in broiler chickens.* S Afr J Anim Sci, **48**, 324-336.
14. **Farahat M, Abdallah F, Abdel-Hamid T, et al** (2016): *Effect of supplementing broiler chicken diets with green tea extract on the growth performance, lipid profile, antioxidant status and immune response.* Br Poult Sci, **57**, 714–722.
15. **Farahat MH, Abdallah FM, Ali HA, et al** (2017): *Effect of dietary supplementation of grape seed extract on the growth performance, lipid profile, antioxidant status and immune response of broiler chickens.* Animal, **11**, 771–777.
16. **Goñi I, Brenes A, Centeno C, et al** (2007): *Effect of dietary grape pomace and vitamin E on growth performance, nutrient digestibility, and susceptibility to meat lipid oxidation in chickens.* Poult Sci, **86**, 508–516.
17. **Hajati H, Hassanabadi A, Golian AG, et al** (2015): *The effect of grape seed extract and vitamin C feed supplements carcass characteristics, gut morphology and ileal microflora in broiler chickens exposed to chronic heat stress.* Iran J Appl Anim Sci, **5**, 155–165.
18. **Hassan FA, Mahrose KM, Basyony MM** (2014): Influence of grape seeds powder as a natural antioxidant on growth performance, antioxidant status and carass characteristics of rabbits under hot conditions. 395–412. In: The 7th International Conference on Rabbit Production in Hot Climate, Egypt.
19. **Hassanpour H, Zamani Moghaddam AK, Yazdani A, et al** (2010): *Evaluation of intestinal morphology and nitric oxide metabolites in broiler chickens supplemented by green tea.* Comp Clin Path, **19**, 43–47.
20. **Jiang Y, Zhang WH, Gao F, et al** (2015): *Micro-encapsulated sodium butyrate attenuates oxidative stress induced by corticosterone exposure and modulates*

apoptosis in intestinal mucosa of broiler chickens. Anim Prod Sci, **55**, 587–594.

21. **Leeson S, Namkung H, Antongiovanni M, et al** (2005): *Effect of butyric acid on the performance and carcass yield of broiler chickens.* Poult Sci, **84**, 1418–1422.
22. **Mallo JJ, Puyalto M, Rama Rao SV** (2012): *Evaluation of the effect of sodium butyrate addition to broilers diet on energy and protein digestibility, productive parameters and size of intestinal villi of animals.* Feed Livest, **8**, 26–30.
23. **National Research Council** (1994): Nutrient Requirements of Poultry: 9th Revised Edition, 1994. National Academies Press, Washington.
24. **Panda AK, Rao SVR, Raju MVLN, et al** (2009): *Effect of butyric acid on performance, gastrointestinal tract health and carcass characteristics in broiler chickens.* Asian-Australas J Anim Sci, **22**, 1026–1031.
25. **Rietjens IMCM, Boersma MG, Haan L de, et al** (2002): *The pro-oxidant chemistry of the natural antioxidants vitamin C, vitamin E, carotenoids and flavonoids.* Environ Toxicol Pharmacol, **11**, 321–333.
26. **Rowghani E, Tabeidian SA, Abolfathi E** (2016): *The effects of green tea extract and vitamin E on the growth performance and immune response in broiler chicks.* Res Opin Anim Vet Sci, **6**, 200–205.
27. **Sarıca Ş, Ürkmez D** (2016): *The use of grape seed-, olive leaf- and pomegranate peel-extracts as alternative natural antimicrobial feed additives in broiler diets.* Europ Poult Sci, **80**, 1–13.
28. **Sayrafi R, Soltanalinejad F, Shahrooz R, et al** (2011): *Effects of butyric acid glycerides and antibiotic growth promoter on the performance and intestinal histomorphometry of broiler chickens.* J Food Agric Environ, **9**, 285–288.
29. **Smet K, Raes K, Huyghebaert G, et al** (2005): Influence of feed enriched with natural antioxidants on the oxidative stability of broiler meat. 99–106. In: Proc. 17th European Symposium on the Quality of Poultry Meat, Doorwerth, Doorwerth, The Netherlands.
30. **Taherpour K, Moravej H, Shivazad M, et al** (2009): *Effects of dietary probiotic, prebiotic and butyric acid glycerides on performance and serum composition in broiler chickens.* Afr J Biotechnol, **8**, 2329–2334.
31. **Van Den Borne JJGC, Heetkamp MJW, Buyse J, et al** (2015): *Fat coating of Ca butyrate results in extended butyrate release in the gastrointestinal tract of broilers.* Livest Sci, **175**, 96–100.
32. **Villar-Patino G, Diaz-Cruz A, Avila-Gonzalez E, et al** (2002): *Effects of dietary supplementation with vitamin C or vitamin E on cardiac lipid peroxidation and growth performance in broilers at risk of developing ascites syndrome.* Am J Vet Res, **63**, 673–676.
33. **Viveros A, Chamorro S, Pizarro M, et al** (2011): Effects of dietary polyphenol-rich grape products on intestinal microflora and gut morphology in broiler chicks. Poult Sci, **90**, 566–578.
34. **Vlaicu PA, Saracila M, Panaite TD, et al** (2017): *Effect of the dietary grape seeds and rosehip oils given to broilers (14-42 days) reared at 32°C on broiler performance, relative weight of carcass cuts and internal organs and balance of gut microflora.* Arch Zootech, **20**, 77–88.
35. **Vossen E, Ntawubizi M, Raes K, et al** (2011): *Effect of dietary antioxidant supplementation on the oxidative status of plasma in broilers: Dietary antioxidants and oxidative status in broilers.* J Anim Physiol Anim Nutr, **95**, 198–205.
36. **Wu Y, Zhou Y, Lu C, et al** (2016): *Influence of butyrate loaded clinoptilolite dietary supplementation on growth performance, development of intestine and antioxidant capacity in broiler chickens.* PLoS One, **11**, e0154410.
37. **Yin F, Yu H, Lepp D, et al** (2016): *Transcriptome analysis reveals regulation of gene expression for lipid catabolism in young broilers by butyrate glycerides.* PLoS One, **11**, e0160751.
38. **Yoo J, Yi YJ, Koo B, et al** (2016): *Growth performance, intestinal morphology, and meat quality in relation to alpha-lipoic acid associated with vitamin C and E in broiler chickens under tropical conditions.* RBZ, **45**, 113-120.
39. **Zdanowska-Sąsiadek Ż, Michalczuk M, Damaziak K, et al** (2016): *Effect of vitamin E supplementation on growth performance and chicken meat quality.* Europ Poult Sci, **80**, 1–14.
40. **Zhang WH, Jiang Y, Zhu QF, et al** (2011): *Sodium butyrate maintains growth performance by regulating the immune response in broiler chickens.* Br Poult Sci, **52**, 292–301.

Ankara Univ Vet Fak Derg, **68**, 245-250, 2021
DOI: 10.33988/auvfd.798803

Pathomorphological findings of Mortellaro disease in dairy cattle

Arda Selin TUNÇ[1,a,✉], Soner ÇAĞATAY[2,b], Mehmet SAĞLAM[3,c], Osman KUTSAL[1,d]

[1]Ankara University, Faculty of Veterinary Medicine, Department of Pathology, Ankara, Turkey; [2]Near East University, Faculty of Veterinary Medicine, Department of Surgery, Cyprus; [3]Aksaray University, Faculty of Veterinary Medicine, Department of Surgery, Aksaray, Turkey.

[a]ORCID: 0000-0002-4813-7626; [b]ORCID: 0000-0002-7358-4399; [c]ORCID: 0000-0001-8934-8529; [d]ORCID: 0000-0003-3599-6867

✉Corresponding author: scoskan@veterinary.ankara.edu.tr
Received date: 23.09.2020 - Accepted date: 21.10.2020

Abstract: Mortellaro disease is an infection caused by mostly spirochete bacteria in dairy cows, sheep, and goats. The aim of the present study was to define to Mortellaro disease pathomorphologically and immunohistochemically and investigate whether cell-cell adhesion connections are lost in cell proliferation. Tissue samples were collected from underfoots of Holstein (n: 6) and Swiss Brown (n: 15) dairy cattle. The sections were stained with hematoxylin-eosin (H&E) and Warthin-Starry (WS) for isolation of spirochetes histopathologically and with β-catenin and PCNA primary antibodies immunohistochemically. Histopathologically, number of the cells in the stratum spinosum layer increased excessively, and it gave finger-like extensions to the dermis. Black stained spirochetes were detected among enlarged keratinocytes and inflammatory cells in WS staining. β-catenin was strongly positive in the cell membranes of epithelial cells in all slides. PCNA also gave positive reaction moderately (n: 18) and strongly (n: 3) in nuclei of epithelial cells. It was observed that β-catenin cell-cell adhesion connections did not impair in the disease, so this is thought to positively affect the prognosis of the disease. The high expression of PCNA showed that the mitotic activity was high and explained the formation of wart-like. As a result, while the disease does not have a poor prognosis, the disease has a negative economic impact, and the economical results of this disease might be much greater than the treatment costs. It is still seen in our country and causes in loss of yield for the economy of country.

Keywords: Dairy cattle, digital dermatitis, immunohistochemistry, Mortellaro disease, pathomorphology.

Süt sığırlarında Mortellaro hastalığının patomorfolojik bulguları

Özet: Mortellaro hastalığı süt sığırlarında, koyunlarda ve keçilerde şekillenen, çoğunlukla spiroket bakterilerinin neden olduğu bir enfeksiyondur. Bu çalışmanın amacı, Mortellaro hastalığını patolojik ve immünohistokimyasal olarak tanımlanması ve hücre proliferasyonunda hücre-hücre adezyon bağlantılarının kaybolup kaybolmadığının araştırılmasıdır. Çalışmada Holştayn (n: 6) ve İsviçre Esmeri (n: 15) ırkı süt sığırlarından ayakların altından doku örnekleri toplandı. Kesitler, histopatolojik olarak hematoksilen-eozin (H&E) ve spiroketlerin izolasyonu için Warthin-Starry (WS) ile; immünohistokimyasal olarak da β-katenin ve PCNA primer antikorları ile boyandı. Histopatolojik olarak stratum spinosum tabakasındaki hücreler aşırı derecede artmıştı ve dermise parmak benzeri uzantılar vermişti. WS boyamasında genişlemiş keratinositler ve yangı hücreleri arasında siyah renkli spiroketler tespit edildi. β-katenin, tüm olgularda epitel hücrelerinin hücre membranlarında kuvvetli pozitifti. PCNA da epitel hücrelerinin çekirdeklerinde orta derecede (n: 18) ve kuvvetli (n: 3) pozitif reaksiyon verdi. β-katenin hücre-hücre adezyon bağlantılarının hastalıkta kaybolmadığı gözlendi, bu nedenle bu durumun hastalığın prognozunu olumlu etkilediği düşünülmektedir. PCNA'nın yüksek ekspresyonu, mitotik aktivitenin yüksek olduğunu gösterdi ve siğil benzeri oluşumları açıkladı. Sonuç olarak, hastalık kötü bir prognoza sahip değildir ancak ekonomik kayıpları oldukça yüksektir ve bu nedenle bu hastalığın ekonomik sonuçları tedavi maliyetlerinden çok daha fazla olabilir. Ülkemizde halen görülmektedir ve ülke ekonomisinde verim kaybına neden olmaktadır.

Anahtar sözcükler: Dijital dermatitis, immünohistokimya, Mortellaro hastalığı, patomorfoloji, süt sığırı.

Introduction

Mortellaro disease, also known as digital dermatitis, hairy heel warts, strawberry foot, digital warts or interdigital papillomatosis, is an infection caused by mostly spirochete bacteria. It is mostly characterized by a painful papilloma-like-warts on the heel inducing lameness. Mortellaro disease was reported in dairy cows, sheep, and goats both in Turkey and in the world (3, 4, 16, 19, 32).

The pathogenesis is still not clear. On the other hand, predisposing factors such as shelter, feeding conditions, and season play a major role in the occurrence of the

disease. The disease brings about discomfort and often severe lameness that decreases milk production, reproductive efficiency, and the health and welfare of the dairy cattle. This situation causes serious economic losses for dairy producers (6, 20, 25, 29).

The macroscopical appearance of the disease could be either ulcerative, erosive, or proliferative and wart-like with papillary growths. Lesions are circular or oval in shape and the skin is usually red in colored (14, 27).

Few papers were reported about histopathology and immunohistochemistry of the disease. In previous studies, the researchers reported a thickening of the epidermis with necrosis and hyperkeratosis, ulcer formation, hemorrhage, microabscess foci and infiltration of neutrophils, mononuclear cells, and eosinophils in both the epidermis and dermis in histopathological examinations (6, 9, 14, 19, 28).

β-catenin, also known as Catenin beta-1, is encoded by the CTNNB1 gene. It is so significant for cell adhesion and is chiefly existing in the cell membranes. β-catenin is related with regulation and link of cell–cell adhesion and gene transcription. β-catenin also plays an important role in a signaling pathway of progenitor cell proliferation and differentiation (11, 18). β-catenin is used for hyperplasias and many different types of tumors such as mammary, lung, colon, liver (1, 7, 11, 17, 26, 30).

PCNA, 'proliferating cell nuclear antigen', is a cell cycle protein that acts as a processivity factor for DNA polymerase delta in cells of all eukaryotic species. It is also a DNA clamp. Cell proliferation can be determined by the change in the amount of PCNA within the cell. While PCNA expression increases in G phase, it reaches maximum in S phase where DNA is duplicated. A decrease in PCNA expression is observed during the transition to the M stage of cleavage. In this way, the positions of the cells in the division cycle can be determined by PCNA expression (23, 31, 33).

The aim of the present study was to define to Mortellaro disease pathomorphologically and immunohistochemically and investigate whether cell-cell adhesion connections are lost in cell proliferation.

Material and Methods

Tissue samples: In this study, tissue samples from their underfoots were collected from dairy cattle of Holstein (n: 6) and Swiss Brown (n: 15) breed which were suffering from pain and clinical lameness. These samples were taken from the various regions with lesions under local anesthesia with punch biopsy and were treated with topical oxytetracycline hydrochloride spray and lincomycin hydrochloride soluble powder and then sent for routine diagnosis to the Ankara University Department of Pathology.

Microscopical examinations: The samples were fixed in 10% neutral buffered formalin, processed routinely, embedded in paraffin, and sectioned at 5μm thickness. The sections were stained with hematoxylin-eosin (H&E) and Warthin-Starry (WS) for isolation of spirochetes (21).

Immunohistochemical examinations: After deparaffinization and dehydration were provided, peroxidase activity was removed from the tissues on adhesive slides with 3% hydrogen peroxide-methanol solution. Antigen retrieval using microwave heating (10 min; 10 mmol/citrate buffer, pH 6.0) was performed. Nonspecific proteins in tissue were blocked by using a protein blocking solution. All slides were submitted to a Streptavidin Biotin Complex Peroxidase (Strept ABC-P) according to the manufacturer's protocol (Super Sensitive Polymer-HRP Detection System (BioGenex, Fremont, CA, REF: QP300-XAK)). Primary antibodies were selected as β-catenin (Ready to use, Thermo Fisher Scientific) and PCNA (1:200 dilution, PC10, Thermo Fisher Scientific). The slides were incubated for both primary antibodies for 45 min at 56^{o}C in the oven. As chromogen, 3-Amino-9-Ethylcarbazole (AEC) was used, and slides were counterstained with Mayer's hematoxylin and then coverslipped using an aqueous mounting media. For negative controls, PBS was used instead of each primary antibody. All microscopical areas were evaluated and positivities were picked up from 10 areas at the same magnification. The results were scored as mild, moderate, and strong as <10%, 10-50%, >50%, respectively. All results were evaluated under a light microscope (Leica, DM 4000B) and were photographed (Leica DFC-280).

Results

Clinical findings: After the masses were taken for pathological examination, firstly, they were treated only with topical oxytetracycline hydrochloride spray. After one month, four of 21 cows did not recover, and lincomycin hydrochloride soluble powder was added to the treatment options. So, functional recovery was achieved in all cases and no recurrence of digital dermatitis during a follow up period of 15 months were seen.

Macroscopical findings: All masses appeared as a proliferation of single or multiple cauliflower-like. The masses were from 0.3 cm to 2x1x0.5 cm in diameter and had grayish white in color and hard in consistency with lobular in appearance at the cut sections. Some masses had necrotic, ulcerative, and hemorrhagic areas (Figure 1 A-B).

Microscopical findings: The keratin layer on the stratum corneum was thickened and included parakeratosis in some area with the retention of nuclei. It

was noted that the cells increased excessively in the stratum spinosum layer, and it gave finger-like extensions to the dermis. In some areas, microabscesses, ulcers, inflammatory cells, vascularization, degenerative, and necrotic changes in epithelial cells, and proliferation of connective tissue were seen (Figure 2 A-C) and there was also no finding of neoplasia. Visible black stained spirochetes were detected among enlarged keratinocytes and inflammatory cells in WS staining (Figure 2 D).

Immunohistochemical findings: β-catenin was strongly positive in the cell membranes of epithelial cells in all slides (Figure 3 A-B). PCNA also gave positive reaction moderately (n: 18) and strongly (n: 3) in nuclei of epithelial cells (Figure 3 C-D).

Figure 1. A-B. Gross appearance of papilloma-like-warts (arrows) and necrotic, hemorrhagic, ulcerative areas on the heels.

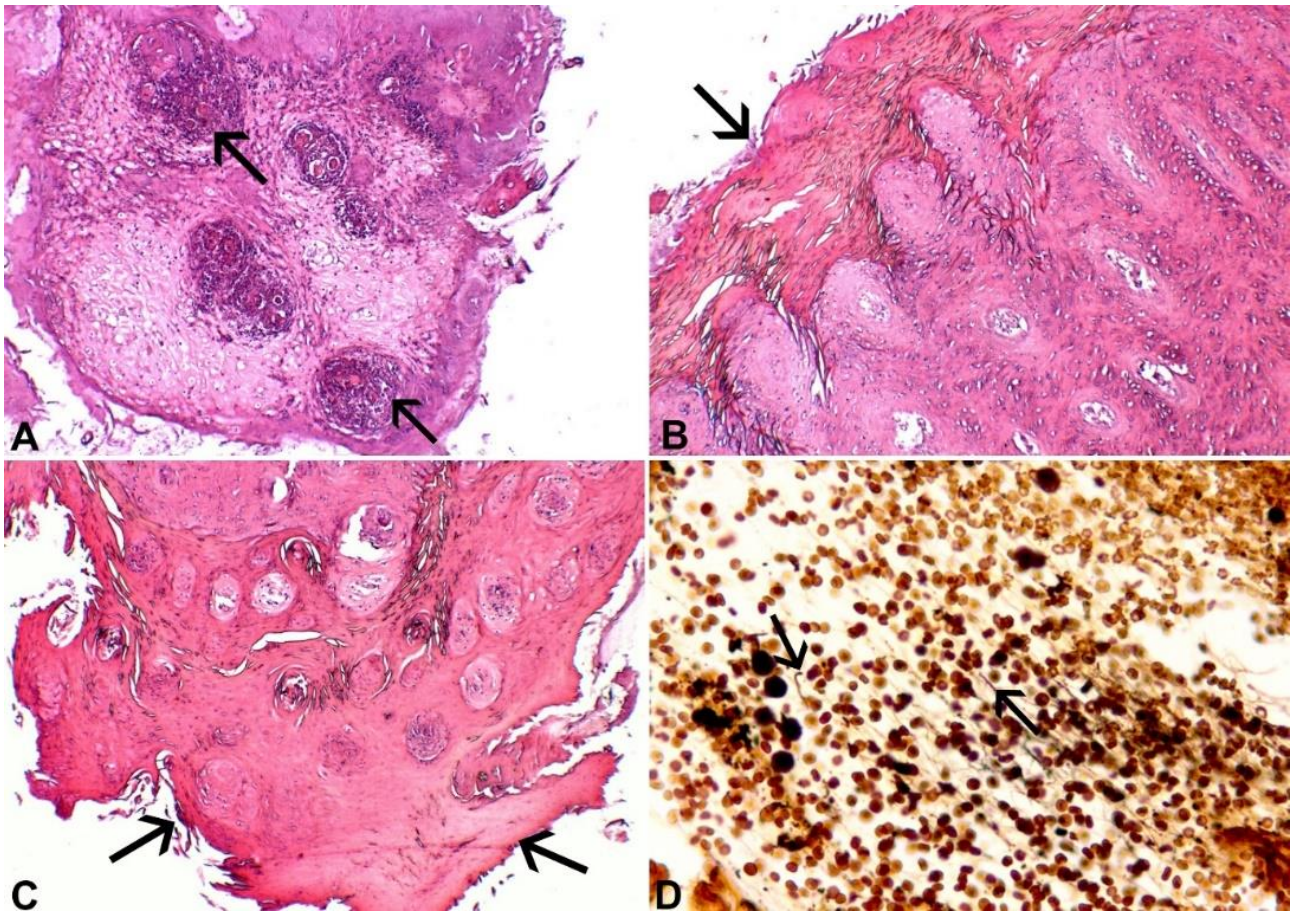

Figure 2. A. Microabscesses (arrows) and the accumulation of inflammatory cells, 4x objective, H&E, **B.** Thickening of the stratum corneum (arrow) and spinosum and acanthosis 10x objective, H&E, **C.** Epidermal protrusions and hyperkeratosis (arrows), 4x objective, H&E, **D.** Black-stained spirochetes (arrows) among enlarged keratinocytes and inflammatory cells, 20x objective, WS.

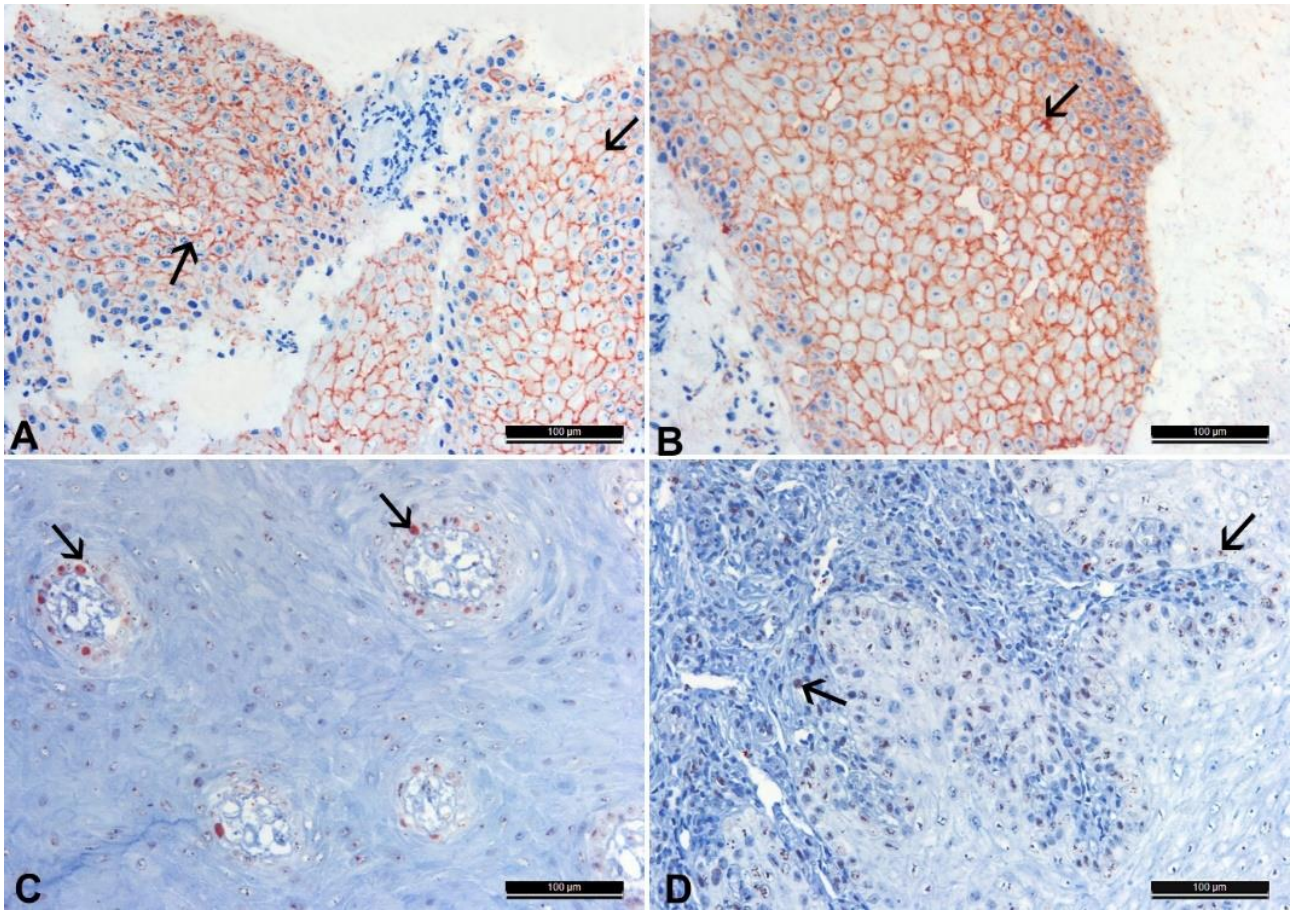

Figure 3. A-B. β-catenin (arrows) strongly positive in the cell membranes of epithelial cells, Bar: 100µm, Strept ABC-P, **C-D.** Strong nuclear expressions in epithelial cells of PCNA (arrows), Bar: 100µm, Strept ABC-P.

Discussion and Conclusion

This disease, defined as contagious ovine digital dermatitis (CODD) in sheep (10) and contagious caprine digital dermatitis (CCDD) in goats (8), is commonly called digital dermatitis, hairy heel warts, strawberry foot, digital warts, or interdigital papillomatosis in cattle (12, 34).

Although the disease has been reported mostly in America, Canada, and England, it has been frequently seen in our country in recent years (2, 13). Predisposing factors such as care, shelter and feeding conditions, seasons, lactation period, mineral deficiencies, and genetic conditions play an important role in the occurrence of the disease (12, 24). However, it was noted that the farm conditions were not suitable in the study. Since the disease improved after the treatment, it was not thought that the disease caused by genetic conditions or mineral deficiencies occurred. The occurrence of the disease was attributed to negative environmental conditions.

While all cattle breeds were sensitive, it was reported that the disease was frequently seen in Holstein cows, and was also emphasized that the lesions were occurred in more hind legs (5, 24, 29) as in this study.

The etiology of the disease is still exactly unknown but could be multifactorial. Bacteria may play an important role in the pathogenesis of the disease. In previous studies, it has been reported that this disease in sheep and cattle is caused by spirochetes such as *Treponema vincentii*, *Treponema phagedenis*, *Treponema denticola*, and *Borrelia burgdorferi* (4, 13, 22, 25). While the spirochetes mostly show growth in microbiology cultures, they can also be detected by immunofluorescence assay, electron microscopy, or PCR (13, 22). The spirochetes were detected by the WS staining in this study, but the species of spirochetes could not be determined. The spirochetes are found between the stratum spinosum and dilated keratinocytes along the dermal papilla at microscopic examination in the study. The disease should sometimes be differentiated from interdigital necrobacillosis. However, severe necrosis and edema were not observed in the feet of these animals as in necrobacillosis. In addition, differential diagnosis must be made with interdigital papilloma/papillomatosis (27). The disease is not defined as a tumor since it shows rapid spread throughout the herd and heals with antibiotics. So, it is easily distinguished from other diseases and tumors.

Likewise, local antibiotics were used in this study. The disease showed recovery in 17/21 cattle using topical oxytetracycline hydrochloride spray, but for the other 4 cattle, lincomycin hydrochloride soluble powder was added to this spray. In this way, full recovery was occurred in all animals.

Grossly, the lesions might be usually characterized by either tumor-like papillomatosis pattern or necrotic, hemorrhagic, and ulcerative areas (14, 15, 27). The ulcerative and hemorrhagic areas with irregular edges were accompanied in some parts by the purulent inflammation that had yellowish-whitish colored in the consistency of cream in the study. Bright red or black circular growth above the heel bulbs with edges forming hairy wart-like growths or sores were observed. In addition to these lesions, ulcerated and hemorrhagic areas were also found in the areas of the sole, toe and/or heel in some cases.

The histopathological findings in the study are compatible with the previous studies (6, 9, 13, 19). Thickening of the stratum corneum and spinosum were remarkable. In this respect, there were areas similar to papilloma. However, spirochetes detected in these areas in WS staining were diagnosed as Mortellaro disease. Necrosis, hemorragia, ulcer, acanthosis, reticular degeneration, and microabscesses were also seen in histopathological sections of some cases.

A few papers have been published about immunohistochemical (6, 9, 28) findings of the Mortellaro disease. Cruz et al. (9) examined to only immunohistochemical findings associated with the microorganisms in the disease. Bruijnis et al. (6) used IL-8 antibody to detect for corneal epithelial cells and keratocytes. In the study, β-catenin and PCNA were examined in Mortellaro disease. High expression of β-catenin and PCNA was assessed at membranes and nuclei of stratum spinosum. The high expression of PCNA showed that the mitotic activity was high and explained the formation of wart-like. In the study, it was observed that there were no alterations in the localization and expression levels of β-catenin. It was noted that β-catenin cell-cell adhesion connections were not destroyed in the disease, so this was thought to positively affect the prognosis of the disease.

In conclusion, in present study, we defined the disease pathomorphologically and showed that despite increased cell proliferation in the disease, cell-cell adhesion connections have not been lost. Although the disease does not have a poor prognosis, its economic lost is quite high and so it is known, the economical results of this disease might be much greater than the treatment costs. It could be still seen in our country, and it causes a loss of yield for the economy of country.

Acknowledgements

This study was presented as a poster in 33rd World Veterinary Congress, 27-31August 2017, Incheon, Korea.

Financial Support

This research received no grant from any funding agency/sector.

Ethical Statement

This study does not present any ethical concerns.

Conflict of Interest

The authors declared that there is no conflict of interest.

References

1. **Ahmad B, Asif M, Ali A, et al** (2020): *Expression of Ki-67 and Beta-Catenin in pseudoepitheliomatous hyperplasia and squamous cell carcinoma in oral mucosal biopsies: an immunohistochemical study*. Asian Pac J Cancer Prev, **21**, 157-161.
2. **Akin I, Akin T** (2018): *Economic impact of digital dermatitis treatment on a dairy farm: an application of the break-even analysis*. Cienc Rural, **48**, 1-8.
3. **Akköse M, İzci C** (2017): *Koyun ve keçilerde digital dermatitis*. Atatürk Üniversitesi Vet Bil Derg, **12**, 99-110.
4. **Angel JW, Crosby-Durrani HE, Duncan JS, et al** (2015): *Histopathological characterization of the lesions of contagious ovine digital dermatitis and immunolabelling of Treponema-like organisms*. J Comp Pathol, **153**, 212-226.
5. **Blowey RW, Sharp MW** (1988): *Digital dermatitis in dairy cattle*. Vet Rec, **122**, 505-508.
6. **Bruijnis MRN, Hogeveen H, Stassen EN** (2010): *Assessing economic consequences of foot disorders in dairy cattle using a dynamic stochastic simulation model*. J Dairy Sci, **93**, 2419-2432.
7. **Bui T, Schade B, Cardiff RD, et al** (2017): *β-Catenin haploinsufficiency promotes mammary tumorigenesis in an ErbB2-positive basal breast cancer model*. PNAS, **114**, E707-E716.
8. **Clegg SR, Sullivan LE, Bell J, et al** (2014): The expanding host range of digital dermatitis treponemes. 55-56. In: Proceedings of the Cattle Lameness Conference, Sixways, Worcester, UK.
9. **Cruz CE, Pescador CA, Nakajima Y, et al** (2005): *Immunopathological investigations on bovine digital epidermitis*. Vet Rec, **157**, 834-840.
10. **Davies IH, Naylor RD, Martin PK** (1999): *Severe ovine foot disease*. Vet Rec, **145**, 646.
11. **De Montpréville VT, Lacroix L, Rouleau E, et al** (2020): *Non-small cell lung carcinomas with CTNNB1 (beta-catenin) mutations: A clinicopathological study of 26 cases*. Ann Diagn Pathol, **46**, 151522.
12. **Demirkan İ** (1997): *Mortellaro hastalığı (digital dermatitis): genel perspektif*. Kafkas Univ Vet Fak Derg, **3**, 123-125.
13. **Demirkan I, Erdoğan M, Çevik Demirkan A, et al** (2018): *Isolation and identification of Treponema pedis and*

Treponema phagedenis-like organisms from bovine digital dermatitis lesions found in dairy cattle in Turkey. J Dairy Sci, **101**, 10317-10326.

14. **Dopfer D, Koopmans A, Meijer FA, et al** (1997): *Histological and bacteriological evaluation of digital dermatitis in cattle, with special reference to spirochaetes and Campylobacter faecalis*. Vet Rec, **140**, 620-623.
15. **Durgun T, İstek Ö** (2004): *Digital dermatitis in the cows*. Fırat Üniversitesi Doğu Araştırmaları Dergisi, **2**, 35-38.
16. **Evans NJ, Murray RD, Carter SD** (2016): *Bovine digital dermatitis: current concepts from laboratory to farm.* Vet J, **211**, 3-13.
17. **Fu X, Zhu X, Qin F, et al** (2018): *Linc00210 drives Wnt/β-catenin signaling activation and liver tumor progression through CTNNBIP1-dependent manner*. Mol Cancer, **17**, 73.
18. **Gao C, Wang Y, Broaddus R, et al** (2018): *Exon 3 mutations of CTNNB1 drive tumorigenesis: a review*. Oncotarget, **9**, 5492-5508.
19. **Görgül OS, Kahraman MM, Çeçen G, et al** (2002): *Sığırlarda digital ve interdigital dermatitis'lerde klinik tanı, sağaltım ve histopatolojik bulgular*. J Res Vet Med, **21**, 115-124.
20. **Hoffman A** (2012): *Footbaths for the treatment or control of hairy heel warts (digital dermatitis) in dairy herds: summary of seven studies.* Washington State University Veterinary Medicine Extension: Washington State University.
21. **Luna GL** (1968): Manual of Histologic Staining Methods of the Armed Forces Institute of Pathology. McGraw Hill Book Co, New York.
22. **Middelveen MJ, Burugu D, Poruri A, et al** (2013): *Association of spirochetal infection with Morgellons disease.* F1000Research, **2**, 25.
23. **Naryzhny SN** (2008): *Proliferating cell nuclear antigen: a proteomics view*. Cell Mol Life Sci, **65**, 3789-3808.
24. **Nowrouzian I** (1994): *Risk factors in the development of digital dermatitis in dairies in Tehran, Iran*. Proc Int Symp Dis Ruminant Digit, **8**, 155.
25. **Palmer MA, O'Connell NE** (2015): *Digital dermatitis in dairy cows: a review of risk factors and potential sources of between-animal variation in susceptibility*. Animals, **5**, 512-535.
26. **Pignatti E, Sining L, Yuchi Y, et al** (2020): *Beta-Catenin causes adrenal hyperplasia by blocking zonal transdifferentiation.* Cell Rep, **31**, 107524.
27. **Read DH, Walker RL** (1998): *Papillomatous digital dermatitis (footwarts) in california dairy cattle: clinical and gross pathologic findings*. J Vet Diagn Invest, **10**, 67-76.
28. **Refaai W, Ducatelle R, Geldhof P, et al** (2013): *Digital dermatitis in cattle is associated with an excessive innate immune response triggered by the keratinocytes.* BMC Vet Res, **9**, 193.
29. **Shearer JK, Amstel S van** (2000): Lameness in Dairy Cattle. 1-12. In: Proceedings from 2000 Kentucky Dairy Conference, USA.
30. **Shiizaki K, Kido K, Mizuta Y** (2019): *Insight into the relationship between arylhydrocarbon receptor and β-catenin in human colon cancer cells*. PLoS ONE, **1**, 1-21.
31. **Strzalka W, Ziemienowicz A** (2011): *Proliferating cell nuclear antigen (PCNA): a key factor in DNA replication and cell cycle regulation.* Ann Bot, **107**, 1127-1140.
32. **Sullivan LE, Evans NJ, Clegg SR, et al** (2014): *Digital dermatitis treponemes associated with a severe foot disease in dairy goats.* Vet Rec, **176**, 283.
33. **Terzioğlu G, Keskin AÜ, Yanıkkaya Demirel G** (2013): *Hücre proliferasyonu ölçüm yöntemleri ve çeşitli ticari proliferasyon kitlerinin karşılaştırılması*. Turk J Immunol, **1**, 74-89.
34. **Wilson-Welder JH, Alt DP, Nally JE** (2015): *Digital dermatitis in cattle: current bacterial and immunological findings.* Animals, **5**, 1114-1135.

Ankara Univ Vet Fak Derg, **68**, 251-258, 2021
DOI: 10.33988/auvfd.717013

The effects of dietary supplementation of olive leaf extract and eggshell with membrane on performance, egg quality, blood biochemical, and bone parameters in laying Japanese quail

Seda İFLAZOĞLU MUTLU[1,a]✉, Yasin BAYKALIR[2,b], Mehmet Ali AZMAN[3,c], Ülkü Gülcihan ŞİMŞEK[2,d], Mehtap ÖZÇELİK[4,e], Oğuz BAYRAKTAR[5,f], Mehmet ÇİFTÇİ[1,g], Zeki ERİŞİR[2,h]

[1]Fırat University, Faculty of Veterinary Medicine, Department of Animal Nutrition and Nutritional Diseases, Elazığ; [2]Fırat University, Faculty of Veterinary Medicine, Department of Animal Science, Elazığ; [3]Balıkesir University, Faculty of Veterinary Medicine, Department of Animal Nutrition and Nutritional Diseases, Balıkesir; [4]Fırat University, Vocational School of Health Services, Elazığ; [5]Ege University, Department of Chemical Engineering, İzmir, Turkey.
[a]ORCID: 0000-0002-6835-2171; [b]ORCID: 0000-0002-9248-6065; [c]ORCID: 0000-0001-9281-9520; [d]ORCID: 0000-0003-2871-3005; [e]ORCID: 0000-0003-2362-4935; [f]ORCID:0000-0003-4210-2825; [g]ORCID: 0000-0002-3009-8710; [h]ORCID: 0000-0003-0420-023X

✉Corresponding author: siflazoglu@firat.edu.tr
Received date: 09.04.2020 - Accepted date: 13.11.2020

Abstract: This study was conducted to determine the effects of dietary supplementation of olive leaf extract (OLE), eggshell with the membrane (ESM), and the ESM that absorbed the OLE (OLE+ESM) on the performance, egg quality, biochemical, and bone parameters in laying Japanese quail. A total of 112 quail, being 45-day-old, were divided into 4 groups with 4 replicates. The quail were fed with four diets: i) basal diet ii) basal diet supplemented with 400 ppm OLE iii) basal diet supplemented with 2% ESM, and iv) basal diet supplemented with 2% ESM that absorbed with 400 ppm OLE. Egg weight was observed to be higher in the OLE group ($P<0.05$). Total feed intake increased in ESM and OLE+ESM groups ($P<0.05$). Egg production and feed conversion ratio were found to be better in control and OLE+ESM groups ($P<0.01$). Shape index was higher in OLE, ESM and OLE+ESM groups ($P<0.05$). Percentages of albumen and shell were significantly lower in ESM group ($P<0.01$). Percentage of yolk, shell thickness, shell ash, and yolk color were not affected by the supplementation of ESM and OLE groups ($P>0.05$). There was no statistical difference in tibia bone parameters ($P>0.05$). The lowest concentration of serum lactate dehydrogenase (LDH) was observed in control group ($P<0.01$). Serum uric acid level decreased in ESM group ($P<0.01$). OLE supplementation had limited impacts on quail nutrition. Consequently, while the individual usage of OLE and ESM did not show remarkable effects, the mixture of OLE and ESM has been found to positively affect the egg quality and performance parameters.

Keywords: Biochemical parameters, eggshell with membrane, olive leaf extract, performance, quail.

Yumurtacı Japon bıldırcınlarında diyete ilave edilen zeytin yaprağı özütü ve zarlı yumurta kabuğunun performans, yumurta kalitesi, kan biyokimyasal ve kemik parametreleri üzerine etkileri

Özet: Bu çalışma, yumurtacı Japon bıldırcınlarında zeytin yaprağı özütü (OLE), zarlı yumurta kabuğu (ESM), zarlı yumurta kabuğuna emdirilmiş zeytin yaprağı özütü (OLE+ESM) ilavesinin performans, yumurta kalitesi, kan ve kemik parametreleri üzerine etkilerini belirlemek için yapılmıştır. Toplam olarak 112 adet 45 günlük yumurtacı bıldırcın, 4 tekerrürlü 4 gruba ayrılmıştır. Bıldırcınlar; i) bazal diyet ii) bazal diyete 400 ppm OLE ilavesi iii) bazal diyete %2 zarlı yumurta kabuğu ilavesi iv) bazal diyete 400 ppm OLE+%2 ESM ilavesi şeklinde 4 diyetle beslenmiştir. Yumurta ağırlığının OLE grubunda daha yüksek olduğu gözlenmiştir ($P<0,05$). Toplam yem tüketimi ESM ve OLE+ESM gruplarında artmıştır ($P<0,05$). Yumurta üretimi ve yem dönüşüm oranı, kontrol ve OLE+ESM gruplarında daha iyi bulunmuştur ($P<0,01$). Şekil indeksi OLE, ESM ve OLE+ESM gruplarında daha yüksek bulunmuştur ($P<0,05$). Ak ve kabuk oranı, ESM grubunda anlamlı olarak düşük tespit edilmiştir ($P<0,01$). ESM ve OLE ilavesi sarı oranı, kabuk kalınlığı, kabuk külü ve sarı rengini etkilememiştir ($P>0,05$). Tibia kemik parametrelerinde istatistiksel fark bulunmamıştır ($P>0.05$). En düşük serum laktat dehidrojenaz konsantrasyonu (LDH) kontrol grubunda gözlenmiştir ($P<0,01$). Serum ürik asit düzeyi ESM grubunda azalmıştır ($P<0,01$). OLE ilavesinin bıldırcın beslenmesi üzerinde sınırlı etkileri olmuştur. Sonuç olarak, OLE ve ESM'nin ayrı ayrı kullanımları önemli etkiler göstermezken, OLE ve ESM karışımının yumurta kalitesini ve performans parametrelerini olumlu yönde etkilediği görülmüştür.

Anahtar sözcükler: Bıldırcın, biyokimyasal parametreler, performans, zarlı yumurta kabuğu, zeytin yaprağı özütü.

Introduction

Agricultural by-products are the the most commonly used feed additives in animal feeding (43). Although oleuropein (OLE), the main phenolic compound of the olive tree, is found in all parts of the olive fruit (pulp, core, membrane), it is contained in the highest level in theleaves. The olive leaf extract includes 19% OLE, 1.8% flavonoid glycosides, and 3-4 dihydroxy-phenethyl esters (1, 15). Moreover, OLE is composed of sub-units of hydroxytyrosol, elenolic acid, and glucose (15).

Recent studies have revealed that OLE has antioxidant, antimicrobial, antiviral, anti-inflammatory, antitumor, neuroprotective, and hepatoprotective effects (3, 15, 19). The addition of herbal extracts to poultry feeds, regulates the digestive system, stimulates digestive juices for enhancing their appetite, increases the feed intake, protects against diseases by its antibacterial effect, and consequently improves the performance of the quail (15, 16).

OLE is susceptible to oxidation and enzymatic reactions during digestion. OLE may show a poor bioavailability in the gastrointestinal tract during oral intake (29). In particular, OLE is an inhibitor of low-density lipoprotein (LDL) oxidation and has stronger antioxidant properties than butylated hydroxytoluene (BHT), vitamin C, and vitamin E (10, 34). OLE significantly reduces serum aspartate aminotransferase (AST) and alanine aminotransferase (ALT) levels and, thus has positive effects on hepatotoxicity (19). In addition, OLE inhibits several enzymes involved in glucose metabolism both *in vivo* and *in vitro* (4, 21).

Eggshell is a by-product of the poultry industry (hatcheries, poultry farms, fast food industries, egg product factories) in addition to household waste and restaurant (30). Eggshell is composed of 10.2% of the whole egg. It contains calcium and other microelements such as magnesium, boron, copper, iron, manganese, molybdenum, sulfur, silicon, and zinc in trace amounts. Calcium in the eggshell is accepted as the best source of natural calcium and can be absorbed by about 90%. A whole medium eggshell contains approximately 750-800 mg elemental calcium (8). The composition of the eggshell is about 98.2%, 0.9%, and 0.9% of calcium carbonate, magnesium, and phosphate, respectively (22).

The eggshell membranes (ESM) also contain 69.2% protein, 2.7% fat, 1.5% moisture, and 27.2% ash (27). The membranes are fibrous structural proteins made up of collagens and keratins. There are also numerous other proteins and peptides with antimicrobial, antioxidant, and immune-modulatory properties such as lysozyme, ovotransferrin, ovalbumin, globulin, ovomucin, and defensin present in these membranes (28).

The studies have shown that the usage of eggshells as a source of calcium in poultry diets is appropriate (18, 38). The eggshell powder is one of the egg by-products that increase egg production and improve the quality of egg shells in laying hens (22). Makkar et al. (28) found that eggshell membrane supplementation to broiler diet had a positive effect on their performance.

Gongruttananun (18) revealed that chicken eggshells can be used as the sole calcium source in layer diets without adverse effects on productive traits, egg and eggshell quality, plasma calcium balance, and bone mineralization. On the other hand, Scheideler (38) reported that there was no significant advantage of supplementation of eggshells in layer diets. Similarly, Olgun et al. (33) found that eggshell supplementation into laying hens' diet was not beneficial in performance.

In this context, the aim of this study was to evaluate the possible usage of OLE and ESM as a feed additive in quail diets and determine the effects of OLE, ESM, and OLE+ESM supplementations on performance, egg quality, blood biochemical, and bone parameters in laying Japanese quail.

Material and Methods

Experimental design and diets: A total of 112 laying Japanese quail (*Coturnix coturnix Japonica*) were obtained from a commercial quail producer company. Ethical approval was approved by Local Ethics Committee (Protocol Number: 2016/68) for this study. The experiment was carried out at the Poultry Unit, Faculty of Veterinary, Fırat University.

Four groups consisting of 28 female quail aged 45 days were assigned into four replicates and each replicate included 7 quail. The quail fed one of four diets: i) Control group was fed with basal diet. ii) ESM group was fed with 2% eggshell with membrane (ESM) which added to the basal diet. iii) OLE group was fed with only 400 ppm olive leaf extract (OLE) added into standard basal diet. iv) OLE+ESM group was fed with 2% ESM that absorbed 400 ppm OLE that added into the standard diet. The ESM used in the study was prepared according to Jia et al. (20). Raw ESM was obtained manually from commercial quail eggs and powdered by grinding with a mortar and pestle. Feed and freshwater were provided as *ad libitum*, and the lighting was implemented as 16L:8D hours/day. The birds were reared in wired cages under a thermal controlled (21-22°C) room for 56 days. Maize and soybean meal-based diets containing 19% crude protein and 2900 kcal/kg metabolizable energy were used in accordance with minimum NRC (31) standards; whereas, only the calcium sources of the diets were different (Table 1). Chemical composition of feed ingredients (dry matter, crude protein, crude ash, and ether extract) was analyzed according to the AOAC procedures (5) and crude fiber was determined by the methods of Crampton and Maynard (11). Carpenter and Clegg (9)’s formula was applied for the calculation of

metabolizable energy. Chemical composition of calcium, available phosphorus, sodium, lysine, and threonine were calculated (31).

Table 1. Ingredients and nutrient composition of experimental diets (%)[1].

Item	Control	ESM
Ingredients (%)		
Maize	58.00	58.29
Soybean meal (44% Crude protein)	31.66	31.22
Sunflower oil	2.65	2.65
Sodium chloride	0.25	0.25
L-Lysine hydrochloride	0.01	0.01
L-Treonine	0.04	0.04
Sodium bicarbonate	0.10	0.10
DL-Methionine	0.12	0.12
Vitamin-Mineral premix[2]	0.35	0.35
Ground limestone	5.42	3.57
Dicalcium phosphate	1.40	1.40
ESM	-	2.00
Nutritional composition (%)		
Dry matter	90.10	90.00
Crude protein	19.00	19.00
Crude fiber	3.49	3.47
Ether extract	4.32	4.32
Crude ash	10.04	9.97
Calcium[3]	2.50	2.50
Available phosphorus[3]	0.36	0.36
Sodium[3]	0.16	0.16
Lysine[3]	1.01	1.00
Threonine[3]	0.75	0.75
ME, kcal/kg[4]	2900	2900

[1]Olive leaf extract (400 mg oleuropein per kg diet) was added to the basal diet. ESM: Eggshell with membrane.
[2]Vitamin-mineral premix (per 1 kg): vitamin A, 8000 IU; vitamin D3, 3000 IU; vitamin E, 25 IU; menadione, 1.5 mg; vitamin B12, 0.02 mg; biotin, 0.1 mg; folacin, 1 mg; niacin, 50 mg; pantothenic acid, 15 mg; pyridoxine, 4 mg; riboflavin, 10 mg; and thiamin, 3 mg copper (copper sulphate), 10 mg; iodine (ethylenediamine dihydriodide), 1.0 mg; iron (ferrous sulphate monohydrate), 50 mg; manganese (manganese sulphate monohydrate), 60 mg; and zinc (zinc sulphate monohydrate), 60 mg, selenium (sodium selenite), 0.42 mg. [3]: Calculated values (34). [4]Calculated, Metabolizable energy (kcal/kg) (9)

OLE used in the study was provided by a commercial company (DUAG, Natural Products Agriculture Machinery Plant and Microbiological Products Research Development Industry and Trade Limited Company, Izmir, Turkey). Phenolic compounds in the olive leaf extract were analyzed by HPLC according to Altinok et al. (2). The antioxidant analysis of the olive leaf extract was also performed by HPLC (6).

Egg production was calculated when the number of total bird reached 5% of hen-day egg production. The hen-day egg production was calculated by dividing the number of daily collected eggs by the number of quail on the same day. Feed intake (g/bird/day) and feed conversion ratios (FCR) were weekly determined. FCR was calculated by using the number of birds and values of egg production, egg weight, and feed intake as g feed/g egg. For egg quality parameters, a total of 288 eggs including 72 eggs from each group (including sub-groups) were collected to beginning from 3rd week in 2 week periods with 2 times. The eggs were kept in room conditions for one day. The whole eggs were weighed and recorded. The shape index was then determined by using a digital caliper (Tresna, 0-300 mm, USA). After the eggs were broken, albumen and yolk were separated gently and weighed. Shells were washed under tap water and dried in the air for 24 hours and then weighed. Shell thickness was determined by a digital micrometer (MMT IP54). Yolk color was determined with a 15-sliced yolk color fan (Roche, Switzerland).

Shape index, albumen, yolk, and shell ratios were calculated following formulas (7);

Shape index: (egg width/egg length)x100
Albumen ratio: (albumen weight/egg weight)x100
Yolk ratio: (yolk weight/egg weight)x100
Shell ratio: (shell weight/egg weight)x100

The crude ash analyses of the eggshells were made according to AOAC (5). Eggshells were burned in ash oven at 550°C for 4 hours.

At the end of the experiment, a total of 24 quail, which were close to the average body weight of the groups, (6 quails from each group) were randomly selected and they were slaughtered with decapitation. Blood samples were taken into tubes during the cutting process. They were centrifuged at 4000 rpm for 10 min and the serums were separated. Serum levels of glucose, triglyceride, high-density lipoprotein (HDL), creatine, uric acid, urea, and lactate dehydrogenase (LDH) were measured by using the autoanalyzer (Olympus AU-600, Tokyo, Japan). Calcium levels of serum were determined by atomic absorption spectrophotometer (Perkin Elmer Analyst 800 Atomic Absorption Spectrometer-Flame). Phosphorus levels were determined according to the modified Youngberg-Youngberg method (23).

The bones of 24 slaughtered quail were scraped thoroughly from meat residues. The bones were stored at 4°C for 12 hours until examined. Right tibial-tarsal bones were used for physical analysis of the bones. Bones first weighed with 0.001 mg precision scale. The length and width of the bones were measured by using a digital caliper (Tresna, 0-300 mm, Guilin, China). The crude ash values of the bones were calculated according to AOAC (5).

Statistical analysis: The data including performance, egg quality, blood biochemical, and bone parameters were subjected to analysis of variance. After carrying out tests of normality (Shapiro-Wilk), One-Way ANOVA test was applied, and significant differences were further compared with Tukey HSD as post-hoc test. The results were considered significant when $P \leq 0.05$. The data were represented as the mean and standard error. Statistical Package for the Social Sciences for Windows (39) was used for all statistical analyses.

Results

Phenolic compounds in olive leaf extract are presented in Table 2. Antioxidant capacity of olive leaf extract was found to be 232 Trolox equivalents antioxidant capacity (mM trolox/g olive leaf extract).

Table 3 shows the effects of olive leaf extract (OLE), eggshell with membrane (ESM), and OLE+ESM on performance parameters of quail. Differences were observed between the groups in terms of egg weight. Egg weight of OLE+ESM group on days 15 to 28 had the lowest egg weight compared to other groups ($P<0.01$). During the total laying cycle, egg weight was found to be higher in the OLE group, which was followed by control, ESM, and OLE+ESM groups, respectively ($P<0.05$).

Table 2. Phenolic compounds in olive leaf extract.

Phenolics	mg/g
Oleuropein	103
Rutin	32
Catechin	1.5
Hydroxytyrosol	12
Caffeic acid	3.6
Vanillic acid	4.1
Vanillin	3.2

Table 3. Effect of eggshell with membrane and olive leaf extract on performance in quail.

Traits	C	ESM	OLE	OLE+ESM	P
Feed intake (g/quail/day)					
15-28 days	24.85^{b}±1.39	30.10^{a}±0.76	28.05^{ab}±0.61	29.65^{a}±0.43	**
29-42 days	32.16±1.42	34.10±0.29	31.78±1.11	32.99±1.21	NS
43-56 days	29.36±1.22	32.55±1.04	31.33±1.31	32.14±0.86	NS
15-56 days	28.79^{b}±1.10	32.25^{a}±0.61	30.39^{ab}±0.80	31.60^{a}±0.59	*
Egg production %					
15-28 days	74.40^{a}±3.50	64.80^{ab}±3.28	60.71^{b}±3.09	69.13^{ab}±2.46	*
29-42 days	80.48±2.47	78.57±3.80	73.72±3.35	77.72±4.14	NS
43-56 days	77.35±2.74	73.72±2.95	77.89±2.65	84.06±3.68	NS
15-56 days	77.41^{a}±2.13	72.37^{ab}±1.48	70.78^{b}±2.36	76.97^{a}±2.35	NS
Egg weight (g)					
15-28 days	12.36^{ab}±0.18	12.56^{a}±0.06	12.53^{a}±0.06	11.95^{b}±0.17	**
29-42 days	12.58±0.35	12.66±0.06	12.82±0.29	12.05±0.14	NS
43-56 days	12.35±0.24	12.67±0.15	12.59±0.10	11.93±0.31	NS
15-56 days	12.43^{ab}±0.18	12.63^{ab}±0.06	12.64^{a}±0.06	11.98^{b}±0.17	*
15-28 days	12.36^{ab}±0.18	12.56^{a}±0.06	12.53^{a}±0.06	11.95^{b}±0.17	**
Feed conversion ratio (g feed/g egg)					
15-28 days	2.70^{b}±0.14	3.70^{a}±0.20	3.69^{a}±0.14	3.59^{a}±0.19	**
29-42 days	3.18±0.16	3.43±0.16	3.37±0.14	3.53±0.20	NS
43-56 days	3.08±0.11	3.49±0.18	3.22±0.18	3.20±0.26	NS
15-56 days	2.99±0.11	43.53±0.12	3.40±0.10	3.43±0.15	NS

C: Control, ESM: Eggshell with membrane, OLE: Olive leaf extract, NS: non-significant, NS: P>0.05. *: P<0.05, **: P<0.01. $^{a\text{-}b}$Mean values with different superscripts within a row differ significantly. n= 112.

Differences in feed intake were observed between 15-28 days. The feed intake was found the lowest in the control group and the highest in the ESM group between 15-28 days (P<0.01). The highest feed intake during the study was determined in the ESM group. Feed intake was similar in control and OLE groups (P>0.05).

Egg production between 15-28 days of control and OLE+ESM groups was higher than the other two groups (P<0.05). There was no difference between ESM and OLE groups in terms of egg production (P>0.05). Similar to egg production; control and OLE+ESM groups resulted in improved feed conversion. The feed conversion ratio was similar in OLE and ESM groups (P>0.05).

Table 4 shows egg quality parameters. Shape index values were found to be different between control and OLE+ESM groups. The shape index was higher in OLE, ESM, and OLE+ESM groups than control (P<0.05). ESM group was different from the other groups in terms of percentage of albumen; the lowest percentage of albumen was seen in the ESM group. Yolk ratio, shell thickness, crude ash, and yolk color were not affected in all groups (P>0.05).

Table 5 shows the levels of serum glucose, triglyceride, high-density lipoprotein (HDL), lactate dehydrogenase (LDH), creatine, uric acid, urea, calcium, and phosphorus. Serum LDH level was lower in the control group (P<0.01). This parameter was similar in ESM, OLE, and OLE+ESM groups. The level of uric acid was found to be lower in the ESM group, which was followed by control, OLE, and OLE+ESM, respectively (P<0.01). Serum glucose, triglyceride, HDL, creatine, urea, calcium, and phosphorus levels were similar among the groups.

Table 6 shows the tibia weight, length, width, and ash values. The tibia weight, length, width, and ash values were found to be similar among the groups.

Table 4. Effect of eggshell with membrane and olive leaf extract on egg parameters in quail.

Egg Parameters	C	ESM	OLE	OLE+ESM	P
Shape index (SI), %	77.21^{b}±0.22	77.93^{ab}±0.21	77.50^{ab}±0.33	78.27^{a}±0.22	*
Albumen ratio (AR), %	51.28^{a}±0.32	49.33^{b}±0.32	50.80^{a}±0.23	50.88^{a}±0.24	**
Yolk ratio (YR), %	31.94±0.17	32.20±0.30	31.80±0.30	31.65±0.20	NS
Shell ratio, %	7.92^{ab}±0.05	7.73^{b}±0.07	7.94^{a}±0.05	7.99^{a}±0.05	**
Shell thickness, mm	0.25±0.00	0.25±0.00	0.25±0.00	0.25±0.00	NS
Shell ash, %	87.77±0.18	86.99±0.17	87.88±0.46	87.42±0.33	NS
Yolk color	5.39±0.07	5.33±0.07	5.22±0.05	5.32±0.07	NS

C: Control, ESM: Eggshell with membrane, OLE: Olive leaf extract, NS: non-significant, NS: P>0.05. *: P<0.05, **: P<0.01. a-bMean values with different superscripts within a row differ significantly. n=288.

Table 5. Effect of eggshell with membrane and olive leaf extract on blood biochemical parameters in quail.

Parameters	C	ESM	OLE	OLE+ESM	P
Glucose, mg/dL	207.10±14.09	181.95±15.40	163.37±10.12	195.00±5.03	NS
Triglyceride, mg/dL	121.67±5.06	122.17±4.13	118.67±6.30	118.17±3.06	NS
HDL, mmol/dL	151.78±5.54	149.92±13.86	145.05±5.54	142.57±5.10	NS
LDH, µkat/L	463.67^{b}±17.03	725.33^{a}±22.92	704.17^{a}±30.13	652.00^{a}±29.43	**
Creatine, mg/dl	0.09±0.02	0.07±0.01	0.07±0.01	0.07±0.01	NS
Uric acid, µmol/dL	4.65^{bc}±0.19	3.98^{c}±0.41	5.50^{ab}±0.53	6.32^{a}±0.22	**
Urea, mg/dL	5.65±0.31	5.39±0.40	6.61±0.41	6.32±0.66	NS
Calcium, mg/dL	8.32±0.68	7.38±0.73	10.26±0.77	8.10±0.78	NS
Phosphorus, mg/dl	4.85±0.67	4.59±0.72	4.88±0.49	4.79±0.37	NS

C: Control, ESM: Eggshell with membrane, OLE: Olive leaf extract, HDL: High density lipoprotein, LDH: Lactate dehydrogenase, NS: non-significant. NS: P>0.05, **: P<0.01. $^{a-b}$Mean values with different superscripts within a row differ significantly. n= 24.

Table 6. Effect of eggshell with membrane and olive leaf extract on some bone parameters in quail.

Bone parameters	C	ESM	OLE	OLE+ESM	P
Tibia weight, g	0.95±0.04	0.89±0.04	0.87±0.04	0.87±0.04	NS
Tibia length, mm	50.43±0.79	51.14±0.53	50.94±1.14	51.38±0.64	NS
Tibia width, mm	2.81±0.08	2.81±0.06	2.82±0.05	2.88±0.13	NS
Tibia ash, %	34.53±1.73	35.86±1.89	37.05±1.06	36.30±1.53	NS

C: Control, ESM: Eggshell with membrane, OLE: Olive leaf extract, NS: non-significant, NS: P>0.05. n=24.

Discussion and Conclusion

The requirement of calcium in layers are influenced by many physiological, metabolic, hormonal, and environmental factors. Therefore, it is important to meet calcium requirement sufficiently in layers. Various calcium sources could be used in poultry nutrition. The eggshell could be used as a calcium source. Moreover, eggshells may be combined with limestone and oyster shells for reducing calcium costs (25, 38).

Studies conducted on determining the effect of calcium sources such as limestone, oyster shell, and eggshells on egg production reported that calcium source did not have a significant effect on egg production, feed intake, and feed conversion ratio (17, 26, 36, 38). On the other hand, feed intake was influenced by different calcium sources. According to Olgun et al. (33), more desirable results were obtained from the oyster shell compared to the eggshell. In this study, quail fed with a diet supplemented with ESM and OLE+ESM exhibited higher feed intake. The groups fed with the 400 ppm OLE and control diet showed the lower feed intake value in comparison to the other groups. Feed conversion was similar in OLE+ESM, OLE, and ESM groups. In the present study, egg production of the experimental groups showed different results. When examining total egg productions, the control and OLE+ESM groups were higher than the ESM and OLE groups.

Different results were obtained from the studies conducted on determining the effects of herbal and other by-products used as feed additives on egg production, feed intake and, feed conversion ratio. Oke et al. (32) found the lowest egg weight and egg production in the OLE group. In this study, quail fed with a diet supplemented with OLE+ESM had the lowest egg weight. The feed intake and FCR were not similar in this study, as noted by Oke et al. (32).

The particle size of the calcium source used in the poultry diet affected both performance and egg quality. In this study, ESM was ground with a mortar and a pestle that particle size was around 1 mm. When the particle of calcium source was more than 0.8 mm, the dissolution of calcium source in the gizzard retarded and its retention time increased. Thus, the availability of sources increased parallelly (26, 44). However, in some studies, egg production and egg quality of laying hens were not affected by the type of calcium source and its particle size (18, 38). However, Lichovnikova (26) reported that different levels of eggshell or oyster shell as supplemental calcium sources significantly increased egg weight in laying hens.

The shape index is influenced by egg weight (14). There was a negative correlation between the shape index and egg weight in laying Japanese quail (24). In this study, the OLE+ESM group resulted in a higher shape index than the other groups. Belonging higher values of the shape index in this group (OLE+ESM) may be associated with their egg weight. The percentage of albumen was the lowest in the ESM group. The percentage of albumen also reduced with aging and an increase in size of the eggs (7). According to the present study, it was observed that egg weights increased in the ESM group at the weekly basis. Therefore, the percentage of albumen values could be affected by both aging and egg size. In this study, the well-grinded eggshell and ground limestone were used as the same amount in all diet groups; thus, the shell thickness was similar in all groups. Similarly, there was no difference in eggshell thickness of laying hens when eggshell was used as a calcium source in laying hen diets (38, 40). This fact was also observed in the bone parameters.

LDH catalyzes the conversion of pyruvate and lactate with an associated interchange of NADH and NAD^+. LDH isoenzymes are released into the bloodstream when a heart, liver, and pulmonary system are damaged (41). Moreover, OLE is also associated with glucose metabolism and has an anti-hyperglycemic effect. Indeed, serum glucose was determined to be low level in the OLE group and LDH in this study. This feature is based on two mechanisms. The first mechanism improves glucose-induced insulin release and the second mechanism increases peripheral uptake of glucose (36, 42).

Uric acid is the final product of purine and protein metabolism in poultry. Uric acid is formed in the liver and excreted by kidneys. It is considered a biomarker for many physiological characteristics in vertebrates and birds that are related to diet, genetics, and diseases (13). It is also an important scale for renal function status. It is well known that OLE has an antioxidant effect and has been documented in many studies (3, 19). However, dietary overdoses phenolic have a pro-oxidant effect on redox-active metal-containing systems. They may lead to the formation of reactive oxygen species and phenoxyl radicals causing oxidative stress (12). Moreover, it was emphasized that LDH can accelerate detoxification reactions (35). Thus, OLE supplemented groups have resulted in higher levels of LDH and uric acid when compared to the control in this study.

In conclusion, the eggshell usage in quail diets as a calcium source had no effect on egg production and quality. The same effect was also seen in the OLE. There is a need for further investigation of an effective dose of the OLE. According to the results of the current study, the dose of 400 ppm mmight be high as the olive leaf extract dose. Therefore, it would be better to determine appropriate doses of OLE in the studies. Some applications such as emulsified systems can also be tested for the usage of OLE as a feed additive into quail diets.

Financial Support

This research received no grant from any funding agency/sector.

Ethical Statement

This study was approved by the Fırat University Animal Research Ethics Committee (Protocol Number: 2016/68).

Conflict of Interest

The authors declared that there is no conflict of interest.

References

1. **Akcicek E, Otles S** (2011): The products of olive tree and health. 163-172. In: National Olive Conference. Akhisar, Turkey.
2. **Altiok E, Baycin D, Bayraktar O, et al** (2008): *Isolation of polyphenols from the extracts of olive leaves (Olea europaea L.) by adsorption on silk fibroin.* Sep Purif Technol, **62**, 342-348.
3. **Andreadou I, Iliodromitis EK, Mikros E, et al** (2006): *The olive constituent oleuropein exhibits anti-ischemic, antioxidative, and hypolipidemic effects in anesthetized rabbits.* J Nutr, **136**, 2213-2219.
4. **Annunziata G, Maisto M, Schisano C, et al** (2018): *Oleuropein as a novel anti-diabetic nutraceutical. An overview*. Archives of Diabetes & Obesity, **1**, 54-58.
5. **AOAC** (2000): Official Methods of Analysis. (17th Edition). The Association of Official Analytical Chemists, Gaithersburg, MD, USA.
6. **Baycin D, Altiok E, Ulku S, et al** (2007): *Adsorption of olive leaf (Olea europaea L.) antioxidants on silk fibroin.* J Agric Food Chem, **55**, 1227-1236.
7. **Baykalir Y, Simsek UG** (2018): *Impact of different rearing systems and age on Bovans White layer's performance, egg quality traits and synthesis of heat shock protein 70 kDa.* Ann Anim Sci, **18**, 1045-1060.
8. **Bee W** (2011): How to make calcium from egg shells. Available at: https://www.healingnaturallybybee.com. (Accessed September 30, 2011).
9. **Carpenter KJ, Clegg KM** (1956): *The metabolizable energy of poultry feeding stuffs in relation to their chemical composition.* J Sci Food Agric, **7**, 45-51.
10. **Coni E, Di Benedetto R, Di Pasquale M, et al** (2000): *Protective effect of oleuropein, an olive oil biophenol, on low density lipoprotein oxidizability in rabbits.* Lipids, **35**, 45-54.
11. **Crampton EW, Maynard LA** (1938): *The Relation of cellulose and lignin content to 21 nutritive values of animal feeds.* J Nutr, **15**, 383-395.
12. **Decker EA** (1997): *Phenolics: prooxidants or antioxidants?* Nutr Rev, **55**, 396-398.
13. **Ding X, Li M, Peng C, et al** (2019): *Uric acid transporters BCRP and MRP4 involved in chickens uric acid excretion.* BMC Vet Res, **15**, 180.
14. **Duman M, Sekeroglu A, Yıldırım A, et al** (2016): *Relation between egg shape index and egg quality characteristics.* Europ Poult Sci, **80**, 1-9.
15. **Durlu-Ozkaya F, Ozkaya MT** (2011): *Oleuropein using as an additive for feed and products used for humans.* J Food Process Technol, **2**, 3.
16. **Erener G, Ocak N, Ozturk E, et al** (2009): The effects of olive leaf extract on performance, some blood parameters and cecal microflora of broilers. The Scientific and Technological Research Council of Turkey, Agriculture, Forestry and Veterinary Research Group, AFVRG-Project No: 1070820 report of final results.
17. **Erol A** (2011): Effect of different calcium sources addition to diets on performance and egg shell quality in layer hens. Thesis (M.Sc.). Selçuk University, Turkey.
18. **Gongruttananun N** (2011): *Effects of eggshell calcium on productive performance, plasma calcium, bone mineralization, and gonadal characteristics in laying hens.* Poult Sci, **90**, 524-529.
19. **Jemai H, Mahmoudi A, Feryeni A, et al** (2020): *Hepatoprotective effect of oleuropein-rich extract from olive leaves against cadmium-induced toxicity in mice.* BioMed Research International, **2**, 1-9.
20. **Jia J, Liu G, Guo ZX, et al** (2012): *Preparation and characterization of soluble eggshell membrane protein/PLGA electrospun nanofibers for guided tissue regeneration membrane*. J Nanomater, 2012, 25.
21. **Kerimi A, Nyambe-Silavwe H, Pyner A, et al** (2018): *Nutritional implications of olives and sugar: attenuation of post-prandial glucose spikes in healthy volunteers by inhibition of sucrose hydrolysis and glucose transport by oleuropein.* Eur J Nutr, **58**, 3, 1315-1330.
22. **Kingori AM** (2011): *A Review of the uses of poultry eggshells and shell membranes*. Int J Poult Sci, **10**, 908-912.
23. **Kodama T, Fukui K, Kometani K** (1986): *The initial phosphate burst in ATP hydrolysis by myosin and subfragment-1 as studied by a modified malachite green method for determination of inorganic phosphate.* J Biochem, **99**, 1465-1472.
24. **Kul S, Seker I** (2004): *Phenotypic correlations between some external and internal egg quality traits in the Japanese Quail (Coturnix coturnix japonica).* Int J Poult Sci, **3**, 400-405.
25. **Lertchunhakiat K, Saenphoom P, Nopparatmaitree M, et al** (2016): *Effect of eggshell as a calcium source of breeder cock diet on semen quality.* Agriculture and Agricultural Science Procedia, **11**, 137-142.
26. **Lichovnikova M** (2007): *The effect of dietary calcium source, concentration and particle size on calcium retention, eggshell quality and overall calcium requirement in laying hens.* Br Poult Sci, **48**, 71-75.
27. **MacNeil J** (1997): *Separation and utilization of waste eggshell. International egg commission annual production and marketing conference.* Toronto, Ontario.
28. **Makkar S, Rath NC, Packialakshmi B, et al** (2015): *Nutritional effects of egg shell membrane supplements on chicken performance and immunity.* Poult Sci, **94**, 1184-1189.
29. **Markopoulos C, Vertzoni M, Agalias A, et al** (2009): *Stability of oleuropein in the human proximal gut.* J Pharm Pharmacol, **61**, 143-149.
30. **Nakano T, Ikama NI, Ozimek L** (2003): *Chemical composition of eggshell and shell membranes.* Poult Sci, **82**, 510-514.

31. NRC (1994): *Nutrient requirements of poultry*. (9th rev ed). National Research Council. National Academy Press, Washington, DC, USA.

32. Oke OE, Emeshili UK, Iyasere OS, et al (2017): *Physiological responses and performance of broiler chickens offered olive leaf extract under a hot humid tropical climate.* J Appl Poult Res, **26**, 376-382.

33. Olgun O, Yildiz AO, Cufadar Y (2015): *The effects of eggshell and oyster shell supplemental as calcium sources on performance, eggshell quality and mineral excretion in laying hens.* Indian J Anim Res, **49**, 205-209.

34. Ozdemir A, Azman MA (2016): *Effects of olive leaf extract and vitamin E supplementation in quail diet on some blood parameters and egg yolk fatty acids composition.* Vet J Ankara Univ, **63**, 31-37.

35. Ozen T, Yildirim K, Toka M (2018): *The impacts of Elaeagnus umbellata Thunb. leaf and fruit aqueous extracts on mice hepatic, extrahepatic antioxidant and drug metabolizing enzymes related structures.* Braz J Pharm Sci, 53, 3.

36. Sangi SM, Sulaiman MI, El-Wahab MF, et al (2015): *Antihyperglycemic effect of thymoquinone and oleuropein, on streptozotocin-induced diabetes mellitus in experimental animals.* Pharmacogn Mag, **11**, 251-257.

37. Saunders-Blades JL, Mac Isaac JL, Korver DR, et al (2009): *The effect of calcium source and particle size on the production performance and bone quality of laying hens.* Poult Sci, **88**, 338-353.

38. Scheideler SE (1998): *Eggshell calcium effects on egg quality and ca digestibility in first- or third-cycle laying hens.* J Appl Poult Res, **7**, 69-74.

39. SPSS 21 (2012): *Licensed materials property of IBM Corporation.* Copyright IBM corporation and other(s), 1989-2012; International.

40. Tunc AE, Cufadar Y (2015): *Effect of calcium sources and particle size on performance and eggshell quality in laying hens.* Turkish JAF Sci Tech, **3**, 205-209.

41. Valvona CJ, Fillmore HL, Nunn PB, et al (2016): *The regulation and function of lactate dehydrogenase A: Therapeutic potential in brain tumor.* Brain Pathol, **26**, 3-17.

42. Wainstein J, Ganz T, Boaz M, et al (2012): *Olive leaf extract as a hypoglycemic agent in both human diabetic subjects and in rats.* J Med Food, **15**, 605-610.

43. Yanti Y, Yayota M (2017): *Agricultural by-products as feed for ruminants in tropical area: nutritive value and mitigating methane emission.* Reviews in Agricultural Science, **5**, 65-76.

44. Zhang B, Coon CN (1997): *The relationship of calcium intake, source, size, solubility in vitro and in vivo, and gizzard limestone retention in laying hens.* Poult Sci, **76**, 1702-1706.

Ankara Univ Vet Fak Derg, **68**, 259-267, 2021
DOI: 10.33988/auvfd.753067

The investigation of fatty acids compositions of Jerusalem artichoke (*Helianthus tuberosus*) herbage harvested at different phenological stages

Kanber KARA

Erciyes University, Faculty of Veterinary Medicine, Department of Animal Nutrition and Nutritional Diseases, Kayseri, Turkey.
ORCID: https://orcid.org/0000-0001-9867-1344

✉Corresponding author: kanberkara@erciyes.edu.tr
Received date: 15.06.2020 - Accepted date: 24.11.2020

Abstract: This study was aimed to determine fatty acid compositions of Jerusalem artichoke herbages (*Helianthus tuberosus*) at five different phenological stages. Jerusalem artichoke was harvested at early vegetative, vegetative, early flowering, full flowering, and early seed stages and its herbage samples were obtained. In the herbages, the saturated fatty acid (∑SFA), unsaturated fatty acid (∑UFA), polyunsaturated fatty acid (∑PUFA), monounsaturated fatty acid (MUFA), medium chain fatty acids (∑MCFA), long chain fatty acids (∑LCFA) and very long chain fatty acids (∑VLCFA) were analyzed. The linoleic acid (C18:2n 6c) concentrations of herbages were changed from about 21 to 23% at different growing stages (P<0.05). The oleic acid (C18:2n 6t) concentrations of this forage increased with plant growing (20 to 34% in total fatty acids) (P<0.001). The ∑PUFA, w-3, w-6, ∑MCFA and ∑VLCFA concentrations of Jerusalem artichoke herbage were positively correlated with plant growing stage (from vegetation to after flowering) (P<0.05). The ∑MUFA, w-9 and ∑LCFA concentrations of this herbage were negatively correlated with plant growing stage of plant (P<0.05). As a result of the study, the ∑UFA, ∑MUFA and w-9 fatty acids compositions of Jerusalem artichoke herbage, harvested at early flowering stage, were high than those of other plant growing stages. Besides, the Jerusalem artichoke herbage, harvested at flowering stage, was rich from ∑PUFA, w-3 and ∑VLCFA fatty acids. Therefore, Jerusalem artichoke herbage, harvested at early flowering and full flowering stages, has high functional properties for ruminants and other herbivorous.
Keywords: Forage, plant growing, polyunsaturated fatty acid, ruminant.

Farklı fenolojik dönemlerde hasat edilen yerelması hasılının (*Helianthus tuberosus*) yağ asiti kompozisyonun araştırılması

Özet: Bu çalışmada farklı fenolojik dönemlerde hasat edilen yerelması (*Helianthus tuberosus*) hasılının yağ asiti kompozisyonunun saptanması amaçlandı. Yerelması vejetasyonun başlangıcı, vejetasyon dönemi, çiçeklenme başlangıcı, tam çiçeklenme ve tohum başlama başlangıcı olmak üzere beş farklı fenolojik dönemde hasat edildi ve örnekleri alındı. Bitki örneklerinde doymuş yağ asitleri (∑SFA), doymamış yağ asitleri (∑UFA), çoklu doymamış yağ asitleri (∑PUFA), tekli doymamış yağ asitleri (∑MUFA), orta zincirli yağ asitleri (∑MCFA), uzun zincirli yağ asitleri (∑LCFA) ve çok uzun zincirli yağ asitleri (∑VLCFA) analiz edildi. Hasılın linoleik asit (C18:2n 6c) konsantrasyonu büyüme dönemine göre %21 ile 23 arasında değişmekteydi (P<0,05). Bu kaba yemin oleik asit (C18:2n 6t) konsantrasyonu bitki büyümesi ile arttı (%20-34, toplam yağ asitleri içinde) (P<0,001). Yerelması hasılının ∑PUFA, w-3, w-6, ∑MCFA ve ∑VLCFA konsantrasyonu bitkinin (vejetasyondan çiçeklenmeye kadar) büyüme dönemiyle pozitif korelasyon içindeydi (P<0,05). Bu hasılın ∑MUFA, w9 ve ∑LCFA konsantrasyonu bitki büyüme dönemiyle negatif korelasyonluydu (P<0,05). Çalışmanın sonucu olarak, çiçeklenme başlangıcında hasat edilen yerelması hasılı ∑UFA, ∑MUFA ve w-9 yağ asitleri kompozisyonu diğer bitki büyüme dönemlerinkinden yüksekti. Bunun yanında, çiçeklenme döneminden hasat edilen yerelması hasılı ∑PUFA, w3 ve ∑VLCFA yağ asitleri açısından zengindi. Bunların göstergesi olarak, çiçeklenme başlangıcı ve tam çiçeklenme döneminde hasat edilen yerelması hasılı ruminantlar ve diğer herbivorlar için fonksiyonel özelliklere sahiptir.
Anahtar sözcükler: Bitki gelişimi, doymamış yağ asitleri, kaba yem, ruminant.

Introduction

Forage-feedstuff resources have major significant effects on diet of dairy cattle. They are important sources for fiber, as well as protein, energy, mineral, vitamin and unsaturated fatty acid (UFA) (22). The amount of lipids in forage feedstuffs reach up to 8% in dry matter (DM).

Lipids in the leaf are often localized in chloroplasts, which contain 22 to 25% lipids on a DM basis. Complex lipids constitute most leaf tissues, mainly as glycolipids and phospholipids (6). The esterified fatty acids (FA) in forages represent two-thirds of the total lipids (5% of DM). Their composition includes simple lipids, i.e. diglycerides, free FA, waxes, and sterol esters (33%), galactolipids, i.e. mono- and digalactosyl diglycerides (50%), and phospholipids (17%). The FA composition of forage lipids is dominated by high proportions of linolenic (C18:3) and linoleic acids (C18:2) from polyunsaturated fatty acids (PUFA), but also small amounts of oleic acid (C18:1) (12, 15). Moreover, forage lipids sometimes contain significant amounts of polyunsaturated fatty acids (FA). Nutritional quality of milk and meat in dairy cattle and beef cattle, which fed with diets based on pasture and grass silage, can be improve by shifting their FA composition toward less saturated FA and more PUFA, particularly toward omega-3 fatty acids (9).

Animal products obtained in such systems contain high levels of fatty acids (FA) which is beneficial to human health, such as conjugated linoleic acid (CLA) and polyunsaturated FA (PUFA) from the omega-3 fatty acids (9). Collomb et al. (7) reported that the concentration of these beneficial FA in milk fat increased with altitude and suggested that they could be related to a higher percentage of herbs in the dairy cow ration. Vanhatalo et al. (26) stated that changes in the rates of grass and legume forages in the dairy cattle ration resulted in differentials in milk FA composition. In conclusion, it is possible to alter the milk fat composition on high-forage-based diets through the selection of forage species and manipulation of the herbage harvesting stage (26). Similarly, the present results suggest that it is possible to manipulate the milk PUFA content by increasing the intake of forage PUFA (26).

Jerusalem artichoke (*Helianthus tuberosus* L.), which is a tuberous plant and belongs to *Asteraceae* family, can grow naturally or be cultivated in various areas of the world and originates from North America (13). Jerusalem artichoke is a perennial plant and it can reach up to 3-4 meters in length. The length of this plant, color of its tubers, the numbers of branches and stems, and the leaf ratio in the plant change according to variety, soil type and climatic conditions (18, 23). It is suitable for various soil types (pH 4.5-8.2 and salinity) and different climatic conditions (about 6-27°C) and also includes natural taste substances in leaves of this plant (14, 24, 30). In addition, Jerusalem artichoke has a number of advantages, such as low input cultivation, high crop yield and strong resistance to pests and plant diseases (30).

The FA concentration in forages depends on many factors, including species and senescence, growth stage, conservation method, as well as wilting, shading, and silage additives (6, 12, 15). Jerusalem artichoke herbage has the potential to be used as quality forage, especially at the vegetative stage, in terms of high/moderate nutrient composition (crude protein, ether extract, ash, non-fibrous carbohydrate, neutral detergent fiber, and lutein, zeaxanthin, lycopene, and α-, β-, and γ-carotenes) and satisfactory digestion values (metabolic energy, true dry matter disappearance, true organic matter disappearance) for both horses and ruminants (11). The present study hypothesizes that the fatty acid profile of the Jerusalem artichoke plants in different growth periods will change and these values can be used to adjust the plant harvesting time for animal nutrition. The aim of this study was to determine fatty acid compositions for different phenological stages (/growing stages) of Jerusalem artichoke herbage, which has the potential of quality forage.

Materials and Methods

The samples of Jerusalem artichoke plant were collected from Karaman province, Turkey. Karaman is located (36°33’50” N, 32°56’52” E) in Turkey’s Central Anatolia region. Arid conditions and desert-like steppe vegetation are dominant in the Karaman province due to temperature and rainfall amounts (2). Plant samples were gathered at five different stages: early vegetative (May 2015) (n=6), vegetative (Jun 2015) (n=6), early flowering (July 2015) (n=6), full flowering (August 2015) (n=6), and early seed (September 2015) (n=6) (Table 1; 11). For each phenological stage, six different plants were gathered, which included all the aerial parts (leaf, stem, and flower). Plants were harvested at above 5 cm from the soil in the morning. The amount of sample was about 3 kg for each phenological stage. Three samples for each different plant were used.

Table 1. Phenological stages of Jerusalem artichoke herbage used in the present study.

Phenological stages	Stage definition
Early vegetative	Stem length <50 cm; no bud or flowers; green leaves
Vegetative	Stem length <100 cm; no bud or flowers; green leaves
Early flowering	Stem length >100 cm; starting of flowering (yellow color); green leaves
Full flowering	Open flowers (yellow color); green leaves
Early seeding	Brown and dried flowers; first green pods; green leaves Leaves near the ground starting to dry

The samples of Jerusalem artichoke herbage were dried (48 hours, 55°C) using a thermostatically controlled cabinet (Lovidond, Dortmund, Germany). The dried samples were milled through a 1 mm sieve (IKA Werke, Staufen im Breisgau, Germany) for analysis. The ether extract (EE) levels were determined according to the method (method 920.39) reported by the AOAC (4) (Velp, Italy). For fatty acid analyses, the EE of dried Jerusalem artichoke herbage were methylated with the modified (17) three stage procedure of Wang et al. (29). According to this procedure, 40 µL of fats in falcon tubes with 15 mL volumes were mixed with 0.7 ml of KOH (10 M) and 5.3 mL of methanol and was vortexed. The mixture was incubated for 45 min at 55°C in an incubator (Nüve, Turkey) and cooled to 21°C. The mixture was combined with 0.58 mL of H_2SO_4 (10 M) and was vortexed. After this mixture was incubated for 45 min at 55°C, 3 mL of n-hexane was added. The tubes were centrifuged for 5 min at 4000 rpm. The 1.5 mL of supernatants was analyzed in a gas chromatograph (Thermo Scientific, USA) with autosampler (Thermo AI 1310, USA). Analyses were conducted by FAME column (Leigh 60 m, I.D: 0.25 mm, film: 0.25 µm and maximum temperature 250-260°C) at an injection split temperature of 255°C and a colon temperature of140 °C with a flow rate of 30 ml/min for 40 min. Fatty acid identification was performed by comparing the peaks in the chromatogram with the retention times at the standard (19). Total saturated fatty acid (∑SFA), unsaturated fatty acid (∑UFA), polyunsaturated fatty acid (∑PUFA), monounsaturated fatty acid (∑MUFA), medium chain fatty acids (∑MCFA), long chain fatty acids (∑LCFA) and very long chain fatty acids (∑VLCFA) were detected.

The experiment data were first subjected to Levene's test to detect the variance homogeneity. One-way variance analyses (ANOVA) were implemented for homogeneous variances by General Linear Model procedures to test treatment differences. The data were analyzed based on the statistical model: $Yij = \mu ij + Si + ei$. Where, Yij = the general mean common for each parameter under investigation. S_i = the ith effect of phenological stages of Jerusalem artichoke herbage on the observed parameters, and ei = the standard error term. Polynomial contrast (linear, quadratic and cubic) of fatty acid values in different plant growing stages were analyzed to reveal the change in fatty acid profile according to the growth period of the plant. Linear relations between the maturity stage and fatty acid compositions of Jerusalem artichoke herbage were determined using Pearson's correlation coefficients (r). Analyses were performed using SPSS 17.0 software (IBM Corp., Armonk, NY, USA). All data were expressed as means ± standard error of means (SEM).

Results

Caprylic, tridecanoic, myristoleic, *cis*-10-pentadecenoic, palmitoleic, heptadecanoic, elaidic, oleic, arachidic and cis-13,16-docosadienoic acid concentrations of Jerusalem artichoke herbage linearly increased to early flowering stage ($P<0.05$) and decreased after early/full flowering stages ($P<0.05$). The palmitic acid (C16:0) concentrations of Jerusalem artichoke herbage was ranged from about 22% to 26% according to the growing stage ($P<0.001$). The linoleic acid (C18:2 n6 cis) concentration of Jerusalem artichoke herbage was changed from about 21% to 23% at different growing stages ($P<0.05$). The concentration of oleic acid (C18:2 n6 trans) of Jerusalem artichoke herbage was changed from about 20% to 34% with plant growing ($P<0.001$). The highest stearic acid concentration (9.66%) of Jerusalem artichoke herbage (C18:0) was determined at the vegetation stage ($P<0.001$). The alpha linolenic acid (C18:3n3) concentration of herbage changed from 0.44% to 5.99%; and the highest alpha linolenic acid concentration of herbage was in full flowering stage ($P<0.001$). The highest fatty acid concentrations in early vegetation, vegetation and early flowering stages were in oleic acid (C18:1n9); but the highest fatty acid concentrations in full flowering and after flowering stages were in palmitic acid (C16:0) (Tables 2 and 3).

The highest eicosapentaenoic acid (C20:5n3), docosahexaenoic acid (C22:6n3), tricosanoic acid (C23:0), lignoceric acid (C24:0) and nervonic acid (C24:1) concentrations of Jerusalem artichoke herbage at full flowering stage were different from other stages ($P<0.001$) (Tables 4 and 5).

The ∑SFA concentration of Jerusalem artichoke herbage was ranged from about 33 to 42% for different phenological stages of plant (linearly; $P<0.001$ and quadratic; $P=0.001$). The highest ∑UFA (67.43%), ∑MUFA (39.42%), w-9 (34.92%) and w-6/w-3 ratio (25.19) of Jerusalem artichoke herbage was at the early flowering stage. The highest ∑LCFA concentration (95.63%) of Jerusalem artichoke was at vegetation stage. The highest ∑PUFA (33.97%), w-3 (9.22%) and ∑VLCFA (10.97%) concentrations of Jerusalem artichoke herbage were at full flowering stage (Tables 6 and 7).

For phenological stages of Jerusalem artichoke herbage from vegetation to after flowering stage, ∑PUFA (r = 0.829), w-3 (r = 0.571), w-6 (r = 0.649), ∑MCFA (r = 0.891) and ∑VLCFA (r = 0.758) concentrations of plant were positively correlated with plant growing ($P<0.05$). The ∑MUFA (r = -0.711), w-9 (r = -0751) and ∑LCFA (r = -0.775) concentrations of Jerusalem artichoke herbage were negatively correlated with plant growing ($P<0.05$) (Table 8).

Table 2. The composition of C8-C15 fatty acids (as % in total fatty acids) of Jerusalem artichoke (*Helianthus tuberosus*) herbage at different growing stages.

	Caprylic acid	Capric acid	Undecanoic acid	Lauric acid	Tridecanoic acid	Myristic acid	Myristoleic acid	Pentadecanoic acid	*ci*- 10 pentadecenoic acid
	C8:0	C10:0	C11:0	C12:0	C13:0	C14:0	C14:1	C15:0	C15:1
Early vegetation	0.06±0.00^{d}	0.05±0.01^{c}	0.01±0.00	0.11±0.00^{d}	0.03±0.01^{a}	1.04±0.01^{e}	0.17±0.01^{a}	0.21±0.01^{c}	0.06±0.01^{c}
Vegetation	0.05±0.00^{e}	0.08±0.01^{a}	0.01±0.00	0.33±0.00^{c}	0.01±0.00^{c}	1.40±0.01^{c}	0.17±0.01^{a}	0.21±0.01^{c}	0.05±0.00^{d}
Early flowering	0.15±0.01^{a}	0.07±0.00^{ab}	0.003±0.00	0.09±0.01^{e}	0.03±0.00^{a}	1.27±0.01^{d}	0.18±0.01^{a}	0.20±0.01^{c}	0.13±0.01^{a}
Full flowering	0.10±0.00^{b}	0.07±0.01^{ab}	0.01±0.00	0.37±0.01^{b}	0.02±0.00^{b}	2.63±0.01^{a}	0.09±0.01^{c}	0.40±0.01^{a}	0.02±0.01^{e}
After Flowering	0.07±0.01^{c}	0.06±0.00^{bc}	0.01±0.00	0.46±0.00^{a}	0.02±0.00^{b}	1.94±0.01^{b}	0.13±0.01^{b}	0.30±0.01^{b}	0.08±0.01^{b}
SD	0.03	0.01	0.004	0.15	0.01	0.58	0.03	0.08	0.04
SEM	0.01	0.003	0.001	0.03	0.002	0.15	0.01	0.02	0.01
Linear	<0.001	0.496	0.628	<0.001	0.005	<0.001	<0.001	<0.001	<0.001
Quadratic	<0.001	<0.001	0.061	<0.001	0.014	<0.001	<0.001	0.285	<0.001
Cubic	<0.001	0.060	0.242	<0.001	<0.001	<0.001	<0.001	<0.001	<0.001

SD: Standard deviation of means, SEM: Standard error of means

[a,e:] Values within a column with different superscripts differ significantly at $P < 0.05$.

Table 3. The composition of C16-C18 fatty acids (as % in total fatty acids) of Jerusalem artichoke (*Helianthus tuberosus*) herbage at different growing stages.

	Palmitic acid	Palmitoleic acid	Heptadecanoic acid	*cis*-10 heptadecanoic acid	Stearic acid	Elaidic acid	Oleic acid	Linolelaidic acid	Linoleic acid	α-Linolenic acid
	C16:0	C16:1	C17:0	C17:1	C18:0	C18:1 n9*t*	C18:1 n9*c*	C18:2 n6*t*	C18:2 n6*c*	C18:3 n3
Early vegetation	23.90±0.03^{c}	3.47±0.01^{b}	0.08±0.01^{b}	0.26±0.001^{d}	7.68±0.01^{b}	0.10±0.01^{b}	31.32±0.01^{b}	0.00±0.00^{c}	23.05±0.02^{b}	0.86±0.01^{c}
Vegetation	26.00±0.04^{ab}	2.96±0.01^{d}	0.06±0.01^{c}	0.32±0.001^{c}	9.66±0.01^{a}	0.10±0.01^{b}	30.13±0.01^{c}	0.01±0.01^{b}	22.16±0.01^{c}	1.02±0.01^{c}
Early flowering	22.21±0.01^{d}	4.25±0.01^{a}	0.31±0.01^{a}	0.05±0.001^{e}	7.37±0.01^{c}	0.16±0.01^{a}	33.73±0.01^{a}	0.02±0.01^{a}	23.01±0.01^{b}	0.44±0.01^{d}
Full flowering	26.22±0.19^{a}	1.88±0.01^{e}	0.02±0.01^{c}	0.45±0.01^{a}	6.13±0.01^{d}	0.15±0.01^{a}	20.45±0.19^{e}	0.01±0.01^{b}	21.43±0.21^{d}	5.99±0.08^{a}
After Flowering	25.62±0.10^{b}	3.33±0.01^{c}	0.03±0.01^{c}	0.41±0.001^{b}	7.71±0.02^{b}	0.14±0.01^{a}	22.29±0.05^{d}	0.01±0.01^{b}	23.64±0.05^{a}	2.12±0.01^{b}
SD	1.58	0.79	0.12	0.16	1.17	0.02	5.42	0.007	0.81	2.10
SEM	0.40	0.20	0.03	0.04	0.30	0.007	1.40	0.001	0.21	0.54
Linear	<0.001	<0.001	<0.001	<0.001	<0.001	<0.001	<0.001	0.031	0.196	<0.001
Quadratic	<0.001	<0.001	<0.001	<0.001	0.078	0.001	<0.001	<0.001	<0.001	<0.001
Cubic	<0.001	<0.001	0.010	<0.001	<0.001	0.003	<0.001	0.850	<0.001	<0.001

SD: Standard deviation of means, SEM: Standard error of means.

[a,e:] Values within a column with different superscripts differ significantly at $P < 0.05$.

Table 4. The composition of C20-C21 fatty acids (as % in total fatty acids) of Jerusalem artichoke (*Helianthus tuberosus*) herbage at different growing stages.

	Arachidic acid	*cis* 11 eicosenoic acid	*cis*11,14-eicosadienoic acid	*cis* 11,14,17 eicosatrienoic acid	Arachidonic acid	*cis* 5,8,11,14,17 eicosapenta enoic	Heneicosanoic acid
	C20:0	C20:1	C20:2	C20:3 n3	C20:4 n6	C20:5 n3	C21:0
Early vegetation	0.06±0.01	0.75±0.01^{b}	0.04±0.001^{a}	0.65±0.01^{c}	0.30±0.01^{b}	0.20±0.01^{b}	0.19±0.01^{c}
Vegetation	0.01±0.01	0.44±0.01^{c}	0.03±0.001^{a}	0.71±0.02^{b}	0.03±0.01^{d}	0.18±0.01^{b}	0.16±0.01^{d}
Early flowering	0.08±0.03	0.42±0.01^{c}	0.03±0.001^{a}	0.38±0.001^{d}	0.18±0.01^{c}	0.10±0.01^{b}	0.22±0.01^{b}
Full flowering	0.01±0.01	0.92±0.01^{a}	0.01±0.001^{b}	0.15±0.003^{e}	0.42±0.01^{a}	1.03±0.01^{a}	0.31±0.01^{a}
After Flowering	0.02±0.01	0.19±0.01^{d}	0.03±0.01^{a}	1.43±0.001^{a}	0.17±0.01^{c}	0.36±0.09^{b}	0.14±0.01^{e}
SD	0.03	0.27	0.02	0.45	0.14	0.36	0.06
SEM	0.01	0.07	0.003	0.12	0.04	0.09	0.02
Linear	0.077	<0.001	<0.001	<0.001	<0.001	<0.001	<0.001
Quadratic	0.709	<0.001	<0.001	<0.001	<0.001	0.220	<0.001
Cubic	0.348	<0.001	0.001	<0.001	<0.001	<0.001	<0.001

SD: Standard deviation of means, SEM: Standard error of means
$^{a,e:}$ Values within a column with different superscripts differ significantly at $P < 0.05$.

Table 5. The composition of C22-C24 fatty acids (as % in total fatty acids) of Jerusalem artichoke (*Helianthus tuberosus*) herbage at different growing stages.

	Erucic acid	Behenic acid	*cis* 13,16 docosadienoic acid	*cis* 4,7,10,13,16,19 docosahexaenoic	Tricosanoic acid	Lignoceric acid	Nervoric acid
	C22:1 n9	C22:0	C22:2	C22:6 n3	C23:0	C24:0	C24:1
Early vegetation	0.69±0.01^{b}	1.66±0.01^{a}	1.17±0.01^{d}	0.42±0.01^{c}	0.30±0.01^{d}	0.93±0.02	0.12±0.01^{b}
Vegetation	0.71±0.01^{b}	0.73±0.01^{d}	0.28±0.01^{e}	0.14±0.01^{d}	0.34±0.01^{c}	1.47±0.02	0.04±0.01^{cd}
Early flowering	0.43±0.01^{c}	0.16±0.003^{e}	3.79±0.02^{b}	0.15±0.01^{d}	0.14±0.01^{e}	0.12±0.01	0.02±0.01^{d}
Full flowering	0.22±0.01^{d}	1.50±0.03^{b}	2.89±0.04^{c}	2.04±0.02^{a}	1.22±0.01^{a}	2.57±0.95	0.22±0.01^{a}
After Flowering	1.52±0.01^{a}	0.96±0.01^{c}	3.95±0.01^{a}	0.58±0.01^{b}	0.69±0.01^{b}	1.52±0.10	0.05±0.01^{c}
SD	0.46	0.56	1.50	0.73	0.40	1.03	0.07
SEM	0.12	0.15	0.38	0.18	0.10	0.26	0.01
Linear	<0.001	<0.001	<0.001	<0.001	<0.001	0.122	<0.001
Quadratic	<0.001	<0.001	<0.001	<0.001	<0.001	0.711	0.030
Cubic	<0.001	<0.001	<0.001	<0.001	<0.001	0.264	<0.001

SD: Standard deviation of means, SEM: Standard error of means
$^{a,e:}$ Values within a column with different superscripts differ significantly at $P < 0.05$.

Table 6. The compositions of total saturated and unsaturated fatty acids (as % in total fatty acids) of Jerusalem artichoke (*Helianthus tuberosus*) at phenological stages.

Phenological stages	∑SFA	∑UFA	∑MUFA	∑PUFA	∑MCFA	∑LCFA	∑VLCFA
Early vegetation	36.33±0.40^{b}	63.66±0.46^{b}	36.95±0.45^{b}	26.71±0.80^{c}	0.23±0.01^{c}	94.23±0.99^{b}	5.49±0.20^{c}
Vegetation	40.48±0.38^{a}	59.51±0.20^{b}	34.93±0.83^{b}	24.58±0.42^{c}	0.46±0.01^{ab}	95.63±0.64^{a}	3.89±0.31^{c}
Early flowering	32.57±0.27^{b}	67.43±0.97^{a}	39.32±0.90^{a}	28.10±0.84^{b}	0.38±0.04^{b}	94.49±0.78^{b}	5.03±0.08^{c}
Full flowering	41.59±0.15^{a}	58.40±1.02^{b}	24.42±0.10^{b}	33.97±1.05^{a}	0.56±0.01^{a}	88.44±0.84^{c}	10.97±0.07^{a}
After Flowering	39.56±0.64^{ab}	60.45±0.81^{b}	28.16±0.23^{b}	32.28±1.10^{b}	0.60±0.02^{a}	89.96±0.49^{c}	9.42±0.49^{b}
SD	3.41	3.41	5.78	3.62	0.13	2.97	2.89
SEM	0.88	0.88	1.49	0.93	0.03	0.76	0.74
Linear	<0.001	<0.001	<0.001	<0.001	<0.001	<0.001	<0.001
Quadratic	0.001	0.001	<0.001	0.001	<0.001	0.009	0.007
Cubic	0.256	0.270	<0.001	<0.001	<0.001	<0.001	<0.001

SD: Standard deviation of means, SEM: Standard error of means, ∑LCFA: Total long chain fatty acids, ∑MCFA: Total medium chain fatty acids, ∑MUFA: Total monounsaturated fatty acids, ∑PUFA: Total polyunsaturated fatty acids, ∑SFA: Total saturated fatty acids, ∑UFA: Total unsaturated fatty acids, ∑VLCFA: Total very long chain fatty acids.
[a,c:] Values within a column with different superscripts differ significantly at $P < 0.05$.

Table 7. The compositions of total omega fatty acids (as % in total fatty acids) of Jerusalem artichoke (*Helianthus tuberosus*) herbage at phenological stages.

Phenological stages	w3	w6	w9	w6/w3
Early vegetation	2.13±0.04^{c}	24.57±0.72^{b}	33.03±0.95^{b}	11.50±0.78^{b}
Vegetation	2.06±0.48^{c}	22.52±0.52^{c}	31.56±0.87^{b}	10.93±1.14^{b}
Early flowering	1.07±0.07^{c}	27.03±0.09^{a}	34.92±1.23^{a}	25.19±0.97^{a}
Full flowering	9.22±0.44^{a}	24.75±0.21^{b}	21.84±0.40^{c}	2.68±0.46^{d}
After Flowering	4.48±0.80^{b}	27.79±0.43^{a}	24.28±0.51^{c}	6.20±0.88^{c}
SD	3.04	1.95	5.30	7.93
SEM	0.78	0.50	1.37	2.04
Linear	<0.001	<0.001	<0.001	<0.001
Quadratic	0.574	<0.001	<0.001	<0.001
Cubic	<0.001	0.007	<0.001	<0.001

SD: Standard deviation of means, SEM: Standard error of means
[a,d:] Values within a column with different superscripts differ significantly at $P < 0.05$.

Table 8. Pearson correlations (*r*) in among fatty acid compositions and phenological stage of Jerusalem artichoke (*Helianthus tuberosus*) herbage.

		∑SFA	∑UFA	∑MUFA	∑PUFA	w3	w6	w9	∑MCFA	∑LCFA	∑VLCFA
Phenological stage	*r*	0.325	-0.323	-0.711	0.829	0.571	0.649	-0.751	0.891	-0.775	0.758
	P value	0.238	0.240	0.003	0.000	0.026	0.009	0.001	0.000	0.001	0.001

∑LCFA: Total long chain fatty acids, ∑MCFA: Total medium chain fatty acids, ∑MUFA: Total monounsaturated fatty acids, ∑PUFA: Total polyunsaturated fatty acids, ∑SFA: Total saturated fatty acids, ∑UFA: Total unsaturated fatty acids, ∑VLCFA: Total very long chain fatty acids.

Discussion and Conclusion

The fatty acids have important biological functions for animals. Fibrous feedstuffs, which must be included in the rations of ruminants (such as cattle, goat, sheep) raised milk production or meat production, are ration components that continuously provide fatty acids for ruminants. Average total fatty acid content in wheat and legume forages used in feeding dairy cattle is in the range of 20-50 g per kg of dry matter. The fatty acid content in forages, which are the cheapest and safest source of fatty acids in ruminant ration, are affected by various different factors such as plant species, plant growing stage, climate, rainfall, soil and fertilization (15). The chemical compositions of in common forage plants change with plant growing stage (16). Ersahince and Kara (11) stated that nutrient composition of Jerusalem artichoke herbage changed by plant maturating. Nutritional quality and quantities of forage in ruminant diet are also not same for different phenological stage of plant. The amount of oil and fatty acid concentration in forage can change depending on plant species, plant growing stage and environmental conditions (9, 10, 21). According to results of the present study, individual fatty acid composition of Jerusalem artichoke herbage, which consist of leaf, stem or bloom/flower, changed depending on the plant growth stage.

The saturated fatty acid in the highest concentration (22-26% in total FA) of Jerusalem artichoke herbage was palmitic acid (C16:0) for all phenological stages in the present study. In a previous study, it was demonstrated that C16:0 concentrations (in total FA) of common forages used in dairy cattle diet were 15-30% for alfalfa (fresh, silage or hay), 16-20% perennial ryegrass (fresh), 14-20% for red clover (fresh, silage or hay), % 16 for white clover (fresh, silage) and 16% for corn silage (10, 12, 25, 26). Palmitic acid concentration of Jerusalem artichoke herbage reached to about 26% in vegetation and full flowering stages can relation with leaf: stem ratio and flower amount of plant. Other high saturated fatty acid of Jerusalem artichoke herbage in the present study was stearic acid (C18:0). The stearic acid concentration of herbage reached to about 9.7% in all fatty acids may connect more leaf amount in vegetation stage in the present study. However, stearic acid concentrations of common legume forages and grasses used in dairy cattle diet were range from about 2 to 4.6% in total fatty acids showed by previous researchers (10, 12, 25, 26). The C18:0 concentration of Jerusalem artichoke herbage in the present study was higher than those of common forages; C16:0 concentration of it was similar to legume forage and higher than that of grass forage (12). Mir et al. (21) stated that the concentrations of saturated C16:0, as weight percentage of the fat, increased in the orchardgrass (*Dactylis glomerata* L.), perennial ryegrass (*Lolium perennne* L.) and tall fescue (*Festuca arundinacea* Schreb.), which used in dairy cattle ration, by increasing plant growth stage. In the present study, ∑SFA, 18:0 and C16:0 fatty acid concentrations of Jerusalem artichoke herbage increased with plant growing stage, expect for early flowering stage. The C14:0, C16:0 and C18:0 concentrations in total FA of Jerusalem artichoke herbage in present study decreased up to full flowering stage of plant were parallel with results of (6).

The oleic acid (C18:1n9c) concentration of Jerusalem artichoke herbage, which was the highest MUFA in plant of the present study, was in about 30-33% in all fatty acids of Jerusalem artichoke herbage up to early flowering stage. The oleic acid and MUFA concentrations in total fatty acid of herbage decreased after lowering stages may relation with plant height, leaf: stem ratio and other environmental conditions. The oleic acid concentrations in fat of orchardgrass (*Dactylis glomerata* L.), perennial ryegrass (*Lolium perennne* L.) and tall fescue (*Festuca arundinacea* Schreb.) were found to be in a minimal amount (about 1.5-5%) and increased with plant growth stage as demonstrated by Mir et al. (21).

The UFA concentration in fatty acids of Jerusalem artichoke herbage increased to about 67% at early flowering stage, which was the highest levels for this plant in the present study,. The concentrations of PUFA, VLCFA and w-3, which are alpha linolenic acid (C18:3n3), EPA (C20:5n3), DHA (C22:6n3), fatty acids of Jerusalem artichoke herbage were found to be in the highest levels in full flowering stage can parallel with flower amount of plant. The alpha linolenic acid (C18:3n3) of Jerusalem artichoke herbage was higher than the value reported for corn silage by Glasser et al. (12). In addition, w6/w3 ratio of Jerusalem artichoke herbage at the full flowering stage decreased to 2.68 value which can be caused by high w-3 concentration in full flowering stage. The MUFA, w-9 and LCFA concentrations in total fatty acids of Jerusalem artichoke herbage lowed with plant growing stage demonstrate rich forage in terms of MUFA (oleic acid) and w-9 fatty acids, which have a positive effect on fertility and embryo implantation in uterus of the ruminant, up to early flowering stage.

Findings of this study shows that the C18:3 fatty acid concentrations of timothy decreased up to early flowering stage stated as reported by a previous study (6). The alpha linolenic acid (C18:3 n3) ratio in total fatty acids of Jerusalem artichoke herbage was increased up to full flowering stage by plant maturating, and then decreased after full flowering stage. In contrast, C18:3 concentrations of some pasture plants decreased with plant maturating by the results of Mir et al. (21). As similar with the results at full flowering and after flowering stages of

the present study, Vanhatalo et al. (26) showed that C18:3 n3 and PUFA concentrations in green herbage harvested early were higher than those of it harvested late.

The dairy cattle diet added with alpha-linolenic acid and rations which are rich in alpha-linolenic acid increases blood progesterone concentration, which is the hormone necessary for the healthy continuation of pregnancy in dairy cattle. Due to this increase, follicular and luteal cells are stimulated, and progesterone synthesis increased (20, 23). Ovarian follicles contain insulin receptors (5) and delay the resumption of postpartum ovarian activity and maintenance of regular estrus cycles in cows with low peripheral insulin levels immediately after calving (27, 28). The high alpha linolenic acid (C18:3, n3) concentration of herbage at full flowering and after flowering stages in the present study show that Jerusalem artichoke herbage at these stages will be a positive effect for the healthy continuation pregnancy in dairy cattle.

In the current study, the high oleic acid concentration of Jerusalem artichoke herbage up to early flowering stage shows that this forage at these stages will be on oocyte quality and fertility in ruminant (1). Aardema et al. (1) investigated the effect of three fatty acids (saturated palmitic and stearic acid and unsaturated oleic acid) on lipid storage and development of oocytes in vitro and showed that palmitic and stearic acid had inhibitory effects on oocyte development, but oleic acid (MUFA) eliminated this adverse effect and showed a positive effect.

As a result of the study, the Jerusalem artichoke herbage, harvested at early flowering stage, was rich from ∑UFA, ∑MUFA and w-9 fatty acids. Besides, the Jerusalem artichoke herbage, harvested at flowering stage, was rich from ∑PUFA, w-3 and ∑VLCFA fatty acids. The Jerusalem artichoke herbage, harvested at these phenological (early flowering and full flowering) stages, demonstrate that it has high functional and nutritional properties for ruminants.

Financial Support

This research received no grant from any funding agency/sector.

Ethical Statement

This study does not present any ethical concerns.

Conflict of Interest

The authors declare that they have no conflict of interest.

References

1. **Aardema H, Vos PL, Lolicato F, et al** (2011): *Oleic acid prevents detrimental effects of saturated fatty acidson bovine oocyte developmental competence.* Biol Reprod, **85**, 62-69.
2. **Altin TB, Barak B, Altin BN** (2012): *Change in precipitation and temperature amounts over three decades in central Anatolia, Turkey.* Atmosph Clim Sci, **2**, 107-125.
3. **Alderman G, Blake JS, France J, et al** (2001): *A critique of the Cornell Net Carbohydrate and Protein System with emphasis on dairy cattle. 2. The post-rumen digestion model*. J Anim Feed Sci, **10**, 203-221.
4. **AOAC** (1995): Official Methods of Analysis of the Association of Official Analytical Chemists. AOAC International. Washington, DC, USA. 1995.
5. **Bossaert P, De-Cock H, Leroy MR, et al** (2010): *Immunohistochemical visualization of insulin receptors in formalin-fixed bovine ovaries post mortem and in granulosa cells collected in vivo*. Theriogenology, **73**, 1210-1219.
6. **Boufaïed H, Chouinard PY, Tremblay GF, et al** (2003): *Fatty acids in forages. I. Factors affecting concentrations*. Can J Anim Sci, **83**, 501-511.
7. **Collomb M, Butikofer U, Sieber R, et al** (2002): *Correlations between fatty acids in cows' milk produced in the lowlands, mountains and highlands of Switzerland and botanical composition of the fodder*. Int Dairy J, **12**, 661-666.
8. **Dewhurst RJ, Scollan ND, Youell SJ, et al** (2001): *Influence of species, cutting date and cutting interval on the fatty acid composition of grasses*. Grass Forage Sci, **56**, 68-74.
9. **Dewhurst RJ, Shingfield KJ, Lee MRF, et al** (2006): *Increasing the concentrations of beneficial poly-unsaturated fatty acids in milk produced by dairy cows in high-forage systems.* Anim Feed Sci Tech, **131**, 168-206.
10. **Dierking RM, Kallenbach RL, Roberts CA** (2010): *Fatty acid profiles of orchardgrass, tall fescue, perennial ryegrass, and alfalfa*. Crop Sci, **50**, 391-402.
11. **Ersahince AC, Kara K** (2017): *Nutrient composition and in vitro digestion parameters of Jerusalem artichoke (Helianthus tuberosus L.) herbage at different maturity stages in horse and ruminant*. J Anim Feed Sci, **26**, 213-225.
12. **Glasser F, Doreau M, Maxin G, et al**. (2013): *Fat and fatty acid content and composition of forages: A meta-analysis.* Anim Feed Sci Tech, **185**, 19-34.
13. **Gunnarsson IB, Svensson SE, Johansson E, et al** (2014): *Potential of Jerusalem artichoke (Helianthus tuberosus L.) as a biorefinery crop*. Ind Crop Prod, **56**, 231-240.
14. **Helmi Z, Azzam KM, Tsymbalista Y, et al** (2014): *Analysis of essential oil in Jerusalem artichoke (Helianthus Tuberosus L.) leaves and tubers by gas chromatography-mass spectrometry.* Adv Pharm Bull, **4**, 521-526.
15. **Kalac P, Samkova E** (2010): *The effects of feeding various forages on fatty acid composition of bovine milk fat: A review*. Czech J Anim Sci, **55**, 521-537.
16. **Kara K, Ozkaya S, Baytok E, et al** (2018): *Effect of phenological stage on nutrient composition, in vitro fermentation and gas production kinetics of Plantago lanceolata* herbage. Vet Med, **63**, 251-260.
17. **Kara K** (2020): *The investigation of milk urea nitrogen and milk fatty acids compositions in dairy cattle with subacute ruminal acidosis*. Vet Med, **65**, 1-8.
18. **Kays SJ, Nottingham SF** (2007): Classification, identification, and distribution. Biology and Chemistry of Jerusalem Artichoke, CRC Press, Boca Raton.

19. **Kramer JK, Feller V, Dugan ME, et al** (1997): *Evaluating acid and base catalysts in the methylation of milk and rumen fatty acids with special emphasis on conjugated dienes and total trans fatty acids*. Lipids, **32**, 1219-1228.
20. **Lopez H, Caraviello D, Satter L, et al** (2005): *Relationship between level of milk production and multiple ovulations in lactating dairy cows*. J Dairy Sci, **88**, 2783-2793.
21. **Mir PS, Bittman S, Hunt D, et al** (2006): *Lipid content and fatty acid composition of grasses sampled on different dates through the early part of the growing season*. Can J Anim Sci, **86**, 279-290.
22. **NRC** (2001): Nutrient Requirements of Dairy Cattle. National Research Council. 7th Revised Edition. National Academy Press, Washington, DC, USA.
23. **Robinson R, Pushpakumara P, Cheng Z, et al** (2002): *Effects of dietary polyunsaturated fatty acids on ovarian and uterine function in lactating dairy cows*. Reproduction, **124**, 119-131.
24. **Szpunar-Krok E, Bobrecka-Jamro D, Grochowska S, et al** (2016): *Yield of the aboveground parts and tubers of Jerusalem artichoke (Helianthus tuberosus L.) depending on plant density*. Acta Sci Pon Agr, **15**, 69-78.
25. **Van Ranst G, Fievez V, Vandewalle M, et al** (2009): *Influence of herbage species, cultivar and cutting date on fatty acid composition of herbage and lipid metabolism during ensiling.* Grass Forage Sci, **64**, 196-207.
26. **Vanhatalo A, Kuoppala K, Toivonen V, et al** (2007): *Effects of forage species and stage of maturity on bovine milk fatty acid composition*. Eur J Lipid Sci Tech, **108**, 856-867.
27. **Vanholder T, Leroy J, Soom AV, et al** (2005): *Effect of non- esterified fatty acids on bovine granulosa cell steroidogenesis and proliferation in vitro.* Anim Reprod Sci, **87**, 33-44.
28. **Vanholder T, Leroy JL, Dewulf J, et al** (2005): *Hormonal and metabolic profiles of high-yielding dairy cows prior to ovarian cyst formation or first ovulation postpartum*. Reprod Dom Anim, **40**, 460-467.
29. **Wang J, Wu W, Wang X, et al** (2015): *An affective GC method for the determination of the fatty acid composition in silkworm pupae oil using a two-step methylation process.* J Serbian Chem Soc, **80**, 9-20.
30. **Yang L, Sophia Q, Corscadden K, et al** (2015): *The prospects of Jerusalem artichoke in functional food ingredients and bioenergy production*. Biotechnol Rep (Amst), **5**, 77-88.

Ankara Univ Vet Fak Derg, **68**, 269-273, 2021
DOI: 10.33988/auvfd.749467

A quantitative evaluation of color changes occurring in the muscle tissue during the stages of S10 silicone plastination technique

Burcu İNSAL[1,a,✉] , R. Merih HAZIROĞLU[1,b]

[1]Ankara University, Faculty of Veterinary Medicine, Department of Anatomy, Ankara, Turkey
[a]ORCID: 0000-0003-3354-6424; [b]ORCID: 0000-0001-9049-4136

✉Corresponding author: burcuinsal@gmail.com
Received date: 10.06.2020 - Accepted date: 24.11.2020

Abstract: There are many preservation techniques that are used to ensure that the changes (odor, color, and elasticity) in the characteristics of the animal or human bodies after death are minimized in the field of anatomy. One of the most modern anatomic specimen preparation methods is the plastination technique. Therefore, primary plastination stages were applied to the muscle tissue in this study. The aim of the current study is to present color changes in muscle tissue quantitatively by using a colorimeter device in every stage of the standard silicone plastination technique until the last product is obtained. Color analyses were performed on the muscle tissue after each stage of the plastination. Throughout the whole process, it was observed that the stage when the value of color change from green to red in the product was the closest to the fresh tissue was the 1st acetone bath. The value of color change from blue to yellow was closest to the fresh tissue at the gas curing and hardening stage. Furthermore, the closest values to the fresh tissue were recorded after the impregnation stage when the variations in plastinates were evaluated in terms of brightness. Color changes in plastinates, which have been described as close to the natural color up to today, were determined through statistical data in this study. Moreover, as a result of this dissertation, it was asserted that colorimeter can be effectively used in the field of anatomy due to the advantages it holds.
Keywords: Colorimeter, plastination, S10.

S10 silikon plastinasyon tekniği aşamalarında kas dokusunda meydana gelen renk değişimlerinin kantitatif olarak değerlendirilmesi

Özet: Anatomi biliminde, ölümden sonra hayvan veya insan bedenlerinde meydana gelen değişikliklerin (koku, renk, elastikiyet) en aza indirilmesini sağlamak için kullanılan birçok koruma tekniği vardır. Bu teknikler arasında, bilinen en modern anatomik örnek hazırlama yöntemlerinden biri, plastinasyon tekniğidir. Bu sebeple bu çalışmada kas dokusuna temel plastinasyon aşamaları uygulandı. Çalışmada, standart silikon plastinasyon tekniğinde son ürün elde edilene kadar geçen her aşamada kas dokusunda meydana gelen renk değişimlerinin kolorimetre cihazıyla sayısal olarak ortaya konulması amaçlandı. Plastinasyonun her aşamasında, kas dokusuna renk analizi yapıldı. İlk aşamadan son aşamaya kadar olan tüm süreç boyunca renk değişimi değerlendirildiğinde; elde edilen son üründeki yeşilden kırmızıya renk değişiminin taze dokuya en yakın olduğu aşamanın; 1. aseton banyosu olduğu gözlemlendi. Maviden sarıya değişimin taze dokuya en yakın olduğu aşamanın ise gaz kürleme ve sertleştirme aşaması olduğu görüldü. Ayrıca plastinatların parlaklık açısından değişimi ele alındığında; taze dokuya en yakın değerleri, vakumla gömme aşamasından sonra kaydedildi. Yapılan bu çalışmayla, bugüne kadar doğal renge yakın olarak tanımlanan plastinatlardaki renk değişimi sayısal verilerle belirlendi. Bununla birlikte bu tez çalışması sonucunda kolorimetre cihazının, sahip olduğu avantajlar sebebiyle, anatomi alanında oldukça etkili bir şekilde kullanılabilir olduğu ortaya konuldu.
Anahtar sözcükler: Kolorimetri, plastinasyon, S10.

Introduction

Preservation of cadavers without disintegration as much as possible is of great importance in the field of anatomy (1, 2, 15, 22). Techniques used to preserve human or animal bodies after death for the purpose of using them as training and research material and exhibiting them in museums date back to ancient times (1, 2, 8, 22). No matter how good preservation it is in, a number of changes occur in the flexibility, color, and tissue integrity of cadavers in classical anatomic methods (4). When the last products obtained as a result of plastination (plastinates) are compared to the specimen

prepared with conventional anatomical techniques, they are not only durable but also preservable for many years (3, 19).

Plastination is a process used to remove water and fat in tissues through chemical dehydrators (acetone, alcohol, etc.) with the help of various chemicals and physical factors. Then, the dehydrators replace them with a chemically active polymer (silicone, epoxy, polypropylene, orthocryl and polyester copolymers) and stabilize them in the tissue (3, 5, 19, 24, 27). Silicone plastination is the most common technique among all plastination techniques. Silicone plastination consists of 5 consecutive stages that are based on chemical and physical laws. These stages are specimen preparation, dehydration, defatting, forced impregnation, and gas curing-hardening (3).

As a result of these processes, plastinates which have visual (transparent/matte) and mechanical (flexible/rigid) characteristics, varying depending on the polymer type used, are obtained as end products which are odorless, durable, preservable for many years and harmless to human health (18, 19). However, one of the most major problems of the plastination technique is its inability to fully preserve the natural color of biological tissues and organs (13, 23). Color is the most important determiner of a product's quality in many fields (7, 10, 28). Colors can be measured through different methods of measurement and can be converted into quantitative data. (12, 14, 28). Colorimetry is defined as a color measurement method which was developed in order to present colors quantitatively and exhibit color differences among specimens. These devices display the brightness ratio as L* (between values of 0 - 100), degree of color change (between the values of -120 – 120) from green to red as a* and from blue to yellow as b* on the coordinates and quantitative values in L*a*b* standards determined by CIE (International Commission on Illumination) (10, 16, 26, 28).

In the studies conducted so far, there has not been enough literature showing that the plastinates are measured by any color analysis system stage by stage. For that reason, the aim of the current study is to quantitatively present various color changes that might occur in any stage of the plastination.

Material and Methods

In this study, muscle tissue belonging to an adult sheep (*Ovis aries*) was obtained from a licensed slaughterhouse (Ethical Committee Number: 2017-3-18). M. longissimus cervicis, thoracis and lumborum sections were used. First, a detailed procedure of dissection was conducted on m. longissimus in order to remove the surrounding adipose and connective tissue. Following this procedure, total of 10 specimens were prepared in a way that 2 cm wide incised sections were removed from the tissue. Each section was marked on 3 points. Initial color analyses were conducted on the marked sections of fresh muscle tissue in the first hour following the slaughter (7, 26) in order to set reference color values. After that, specimens were fixated in a 10% formalin solution at room temperature within a time frame of 24 hours. At the end of this period, second color measurements were performed from the marked points.

Upon the procedure, specimens were kept under running water for 2 days to remove the formaldehyde residue. As the next step, specimens were taken into a pure (99.5 %) acetone bath at -25 ^{o}C. The acetone to tissues ratio was set as 10:1. After acetone concentration was fixated at a certain value, color changes in specimens were remeasured. After that, specimens were taken to the second acetone bath and were measured each day. Since the acetone was fixated at a value of >99 %, specimens were subjected to colorimetric measurement again without requiring a 3rd bath. The defatting process (27) that is a stage applied for tissues and organs with dense adipose tissue, was not applied because the muscle tissue did not contain dense adipose tissue. Then the samples were taken to the impregnation stage. At this stage, acetone that was replacing the tissue fluids was evaporated under negative pressure and removed from the tissue and so replaced with the silicone polymer. While preparing the silicone polymer, a mixture at a ratio of 1:100 was formed from 2 important chemical agents used in this stage: Biodur® S10 silicone polymer and its catalyzer Biodur® S3 chemical agent. The outflow of gas bubbles was adjusted with a valve connected to the vacuum tank in a 5 cm^2 area in a way that it output 1-3 bubbles per second. The outflow of bubbles was observed for 6 days. Since there was no observable bubble outflow when Bennert manometer displayed <5 mm-Hg (21) and the valve was completely shut, impregnation stage was considered as completed. Specimens were left to rest hanging in the silicone tank for 24 hours after being taken out from the mixture of S10/S3 in order for the extra silicone to be filtered from the tissue. Then, specimens were taken into a resting period for 2 more days at room temperature so that the extension of the chemical chain reaction could continue. The main purpose here was to acquire specimens that are more durable. Specimens were subjected to color analysis once more. After that, specimens were placed in the tank of gas curing and hardening. Hardening agent Biodur® S6 in a glass container was placed into the curing tank which was isolated from the external environment. 400 l/hr airflow was given to the curing tank through an air engine externally integrated to the curing tank for an hour two times a day, in order for S6 to evaporate slowly and turn into the gas state and for cross-reactivity to start. Deep surfaces of the specimens that started hardening on the

surfaces were subjected to gas curing and hardening for 10 days in order for the cross-reactivity to start. At the end of this period, specimens were removed and last color analyses were performed to be compared with previous measurements. The data from the color measurements were evaluated with the SPSS 14.01 package software used in the analysis of variance for repeated measures. Whether the data was normally distributed was checked through the Shapiro Wilk test. For all statistical evaluation, P <0.05 was used as the criterion.

Results

For color analysis, the values taken from fresh tissue were first compared with the measurements made after the fixation step. It was observed that value dE*, an indicator of a visible degree of color change, was considerably high as shown in Table 1 (P<0.001). Specimens that were taken to a pure acetone bath were dehydrated at 96.5 % acetone concentration at the end of the 4th day. Before the 2nd acetone bath, the degree of color change in the specimens was recorded as shown in Table 1. The acetone concentration was fixated at 99.2 % on the 3rd day of the second acetone bath. Thus, the 2nd acetone bath was completed at the end of the 6th day. Color analyses were performed again (Table 1). Specimens taken to the resting period following the impregnation were subjected to the measurement again at the end of this chemical process. When the results were compared, it was observed that the L* value was highest in the fixation stage. The difference between L* value recorded after the stage of impregnation and the L* value taken from a fresh tissue was recorded as the closest values of L* with 13.74 units of value. In addition, a*, which is the mean degree of color changes from green to red on fresh tissue, was close to the color red. However, it was observed that while this value was recorded as having moved away from red with 6.6 unit of value on average after fixation. Nevertheless, value a* moved towards the color red again with 5.87 units of value on average after the stage of impregnation. Furthermore, whereas b*, the degree of color change from yellow to blue on the fresh tissue, was close to yellow with 3.74 unit at the beginning of the study. It was recorded that the b* value increased by 6.17 unit after fixation. Additionally, value b* continued to increase by 2.08 units of value in favor of yellow after the impregnation. These changes were shown on the wavelength scatterplot in Figure 1. At the end of 10 days when the impregnation processes were completed, specimens that were moved into the stage of gas curing and hardening were taken to color analysis for the last time. Recent values have been shown in Table 1 and Figure 1. When the color values of the end products were compared with the fresh tissue, it was observed that tissues lost their red color value, a*, by 6,33 units of value. The ratio of tissue brightness, L*, increased by 19.52 units of value. On the other hand, the specimens moved towards yellow color, b*, by 6.01 units of value (P<0.001). After all stages, the specimen's observable color change value, dE; changed by 21.04 units of value (Figure 1). During the whole process, it was observed that the last product was closest to the fresh tissue after the 1st acetone bath in terms

Table 1. Color and brightness measurements of muscle tissue at all stages of plastination.

	S10 Silicone Plastination Steps						
			Dehydration				
Parameters	**Fresh Tissue**	**Fixation**	**1st Acetone Bath**	**2nd Acetone Bath**	**İmpregnation**	**Gas Curing-Hardening**	**P**
L*	32.6 ± 1.02 [d]	54.02 ± 0.46 [a]	52.74 ± 0.42 [b]	52.62 ± 0.49 [b]	46.34 ± 0.32 [c]	51.58 ± 0.31 [b]	<0.001
a*	13.09 ± 0.26 [ab]	6.49 ± 0.16 [c]	13.32 ± 0.44 [a]	12.45 ± 0.39 [b]	12.36 ± 0.34 [b]	6.76 ± 0.23 [c]	
b*	3.74 ± 0.33 [c]	9.91 ± 0.22 [b]	11.95 ± 0.19 [a]	11.89 ± 0.21 [a]	11.99 ± 0.22 [a]	9.75± 0.31 [b]	
dE*	-	23.34 ± 0.62 [a]	21.85 ± 0.83 [b]	21.73 ± 0.69 [b]	16.18 ± 0.83 [c]	21.04 ± 0.82 [b]	

[a,b,c] Values within a row with different superscripts differ significantly at P < 0.05 and N=10.

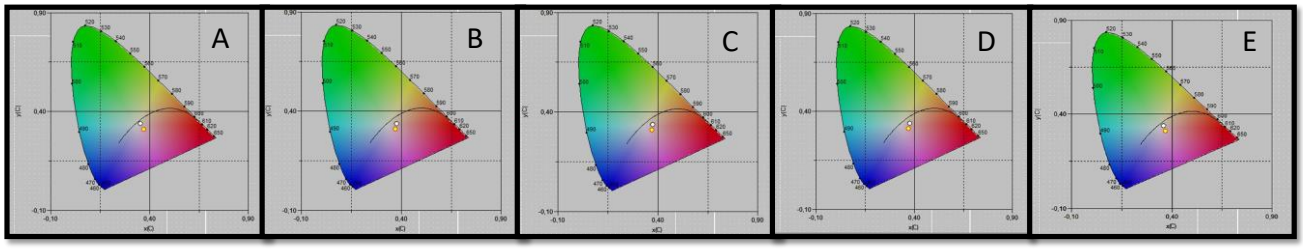

Figure 1. The wavelength distribution graph of the color change at all stages of plastination on the X-Y plane. A: fresh tissue, B: fixation, C: dehydration, D: impregnation, E: gas curing-hardening.

of a* values. In addition, it was observed that the last product was closest to the fresh tissue after the stage of gas curing and hardening in terms of b* value. Moreover, when the variation in plastinates' brightness was examined, the closest values to the fresh tissue were recorded after the stage of impregnation (Figure 1).

Discussion and Conclusion

In many articles, plastinates, obtained through plastination technique, are defined as "odorless, lasting products, harmless to human health and 'identical to natural color", (11, 15, 18-20). However, in response to the statement of identicalness to the natural color, certain researchers (6, 13, 17) stated that some stages of plastination lead to loss of color in plastinates. Therefore, the possible color losses in each stage of the standard silicone technique were observed in this study. Huidobro et al. (7) reported that meat quality and accordingly the color can change depending on the age, race and raising methods in the study they carried out in 2003. For that reason, the material was taken from a single sheep and it consisted of 10 specimens. Turan et al. (25) took specimens from fresh muscle tissue (m. quadriceps femoris) from the goats on the 24th hour and subjected it to color analyses. According to Turan et al. (25), the values obtained from the fresh muscle tissue are L*; 20.86 ± 1.74, a*;1.22 ± 0.57, b*; 2.26 ± 0.95. On the contrary, Karabacak et al. (9), calculated the color of fresh muscle tissue (m. longissimus) taken from Malya lambs on the 24th hour as L*; 39.53 ± 0.511, a*; 15.46 ± 0.322; b*; 2.22 ± 0.421. In this dissertation, results of color analysis of fresh muscle tissue (m. longissimus) belonging to an adult sheep on the 1st hour following death were recorded as L*; 32.6 ± 1.02, a*;13.09 ± 0.26, b*; 3.74 ± 0.33. These results show a significant difference when compared to the results of the study conducted by Turan et al. (25). However, they are strikingly similar to the results of the study of Karabacak et al. (9). According to these data, it was observed that analyses of muscle tissues belonging to the different parts of the body of different species of animals produced dissimilar results. Some studies (2, 25) report that fixation solutions and techniques can cause color changes on the cadaver. According to these studies, tissues lose their color in fixation solutions in which formaldehyde and different densities of formaldehyde are used due to the fact that formaldehyde rapidly coagulates the blood. In this case, tonal variation of the color gray is encountered on the tissues. According to the results of the current study, it was recorded that there was a value of 21.42 brightness on fresh tissues after fixation with a change in the value L*. Furthermore, tissues lost their red color (a*) by 6.6 unit of value whereas they increased their yellow color (b*) by 6.17 unit of value ($P<0.001$). These values confirm that fixation in plastination causes tissues to lose their color as asserted by some researchers (6, 13, 17). When the color changes during the dehydration stage were compared the color changes after fixation, a 1.49 unit of value decrease was observed in dE* value, which is the observable color change in tissues, after the 1st acetone bath. Additionally, it was seen that dE* value decreased by 1.61 unit of value in total at this stage as a result of a 0.12 unit of value decrease after the 2nd acetone bath. This data indicates that after the removal of formaldehyde, in which acetone replaced the tissue fluids, brought the tissue close to its natural color to a certain extent ($P<0.001$). McCreary et al. (13) reported that color changes could occur in tissues (muscle, skin and connective tissue etc.) in fixation and dehydration stages. On the contrary, loss of color because of fixation decreased to a certain extent and it got closer to the values in the fresh tissue according to the color analysis performed after the dehydration stage. As the researchers indicated, whether this stage causes loss of color can be studied in specimens that plastination will be applied to without any fixation on their tissues. With the present study, color changes occurring on the last product, plastinates, which were acquired as a result of standard silicone plastination technique stage by stage were presented statistically.

Brightness ratio in tissues as L*, the degree of color changes from green to red as a* and from blue to yellow as b* were shown on X-Y coordinates with the colorimeter device used in the study and converted to statistical data in the value range determined in L*a*b* standards by CIE. The fact that these data were easily comparable among themselves was revealed in the study. It was proved that colorimetric method can be utilized as an anatomical specimen preparation technique as well as in evaluating the color quality of the end products. Color changes in each stage of plastination technique was analyzed individually and statistical data were compared among each other. Data obtained in the study were interpreted as significant results. Thereby, it was statistically presented that plastinates which are used as training material especially in the field of anatomy are anatomic specimens, similar to the natural color of tissues.

For that reason, it is considered that the data of this study will contribute to the science and training. It will be useful to conduct similar studies in different tissues and organs belonging to mammals and animal species other than mammals as well in terms of using and developing colorimetric analyses in anatomy. That colorimetric measurements can produce results on plastinates suggests the necessity of using this method in different anatomical preparation techniques.

Acknowledgements

This article was developed from the thesis study prepared by Burcu Insal in 2017 (YOKSIS thesis number: 473688).

Finacial support

This research received no grant from any funding agency/sector.

Ethical Statement

This study was approved by the Ankara University Animal Experiments Local Ethics Committee (2017-3-18).

Conflict of Interest

The authors declared that there is no conflict of interest.

References

1. **Ajayi IE, Shawulu JC, Ghaji A et al** (2011): *Use of formalin and modified gravity-feed embalming technique in veterinary anatomy dissection and practicals.* J Vet Med Anim Health, **3**, 79-81.
2. **Brenner E** (2014): *Human body preservation-old and new techniques*. J Anat, **224**, 316-344.
3. **Dejong K, Henry RW** (2007): *Silicone plastination of biological tissue: Cold-temperature technique BiodurTM S10/S15 Technique and Products.* J Int Soc Plastination, **22**, 2-14.
4. **Eisma R, Wilkinson T** (2014): *From ''Silent Teachers'' to Models.* PLOS Bio, **12**, 1-5.
5. **Ezhilarasan S, Jetanthi M, Muthuvel VK** (2017): *Polyester plastination of human cadaveric specimens.* Indian J Clin Anatom, **4**, 26-29.
6. **Henry RW, Janick L, Henry C** (1997): *Specimen preparation for silicone plastination.* J Int Soc Plastination, **12**, 13-17.
7. **Huidobro FR, Miguel E, Onega E, et al** (2003): *Changes in meat quality characteristics of bovine meat during the first 6 days post mortem.* Meat Sci, **65**, 1439-1446.
8. **Jangde S, Arya RS, Paikra S, et al** (2015): *How to provide a safe working condition for medical students and professionals in the anatomy dissection room.* Sch J App Med Sci, **3**, 1867-1870.
9. **Karabacak A, Aytekin İ, Boztepe S** (2012): *Determination of fattening performance with some body measurements and carcass traits of Malya lambs at the open sheepfold.* Arch Zootechnica, **15**, 13-22.
10. **Kays SJ** (1998): *Preharvest factors affecting appearance*. Postharvest Biol Tec, **15**, 233-247.
11. **Kumar M, Kataria SK, Mantri LE, et al** (2017): *Study of plastination to preserve biological specimen in Western Rajasthan.* Int J Appl Res, **3**, 229-232.
12. **Leo´n K, Mery D, Pedreschi F, et al** (2006): *Color measurement in L*a*b* units from RGB digital images*. Food Res, **39**, 1084-1091.
13. **Mccreary J, Iliff S, Hermey D** (2013): *Silicone-based coloration technique developed to highlight plastinated specimens.* J Int Soc Plastination, **25**, 13-20.
14. **Melendez-Martinez AJ, Isabel M. Vicario IM, et al** (2005): *Instrumental measurement of orange juice colour: a review*. J Sci Food Agric, **85**, 894-901.
15. **O'neill GJ, Pais D, Andrade FF, et al** (2013): *Improvement of the embalming perfusion method: the innovation and the results by light and scanning electron microscopy.* Acta Med Port, **26**, 188-194.
16. **Oliveria AC, Balaban MO** (2006): *Comparison of a colorimeter with a machine vision system in measuring color of Gulf of Mexico sturgeon fillets.* Appl Eng Agric, **22**, 583-587.
17. **Oostrom K** (1987): *Fixation of tissue for plastination: general principles.* J Int Soc Plastination, **1**, 3-11.
18. **Pandit S, Kumar S, Mishra BK** (2015): *Comparative study of anatomical specimens using plastination by araldite HY103, polypropylene resin, 6170H19 Orthocryl and silicone-a qualitative study.* Med J Armed Forces India, **71**, 246-253.
19. **Pashaei S** (2010): *A brief review on the history, methods and applications of plastination.* Int J Morphol, **28**, 1075-1079.
20. **Ravi SB, Bhat VM** (2011): *Plastination: A novel, innovative teaching adjunct in oral pathology.* J Oral Maxillofac Pathol, **15**, 133-137.
21. **Riederer BM** (2014): *Plastination and its importance in teaching anatomy. Critical points for long-term preservation of human tissue.* J Anat, **224**, 309-315.
22. **Saeed M, Phil M, Rufai AA, et al** (2001): *Mummification to plastination.* Saudi Med J, **22**, 956-959.
23. **Steinke H, Spanel-Borowski K** (2005): *Coloured plastinates.* Ann Anat, **188**, 177-182.
24. **Stoyanov J, Georgieva A, Sivrev D** (2015): *Use of physical and chemical factors in the development of plastination anatomical preparations.* Trakia J Sci, **13**, 21-22.
25. **Turan E, Gules O, Kilimci FS, et al** (2017): *The mixture of liquid foam soap, ethanol and citric acid as a new fixative–preservative solution in veterinary anatomy.* Ann Anat, **209**, 11-17.
26. **Vanezis P, Trujillo O** (1996): *Evaluation of hypostasis using a calorimeter measuring system and its application to assessment of the post-mortem interval (time of death).* Forensic Sci Int, **78**, 19-21.
27. **Von Hagens G, Tiedemann K, Kriz W** (1987): *The Current Potential of Plastination.* Anat Embryol, **175**, 411-421.
28. **Wu D, Sun DW** (2013): *Colour measurements by computer vision for food quality control-a review.* Trends Food Sci Tech, **29**, 5-20.

Ankara Univ Vet Fak Derg, **68**, 275-281, 2021
DOI: 10.33988/auvfd.708329

Molecular detection and phylogenetic analysis of *Theileria equi* and *Babesia caballi* in wild horses in Konya province of Turkey

Özlem DERİNBAY EKİCİ[1,a], Onur CEYLAN[1,b,✉], Gonca SÖNMEZ[2,c], Bilal DİK[1,d], Ceylan CEYLAN[1,e], Asma SEMASSEL[3,f]

[1]Selçuk University, Faculty of Veterinary Medicine, Department of Veterinary Parasitology, Konya, Turkey; [2]Selçuk University, Faculty of Veterinary Medicine, Department of Zootechnics and Husbandry, Konya, Turkey; [3]Selçuk University, Institute of Health Sciences, Konya, Turkey.

[a]ORCID: 0000-0002-0509-091X; [b]ORCID: 0000-0002-3514-5221; [c]ORCID: 0000-0002-4946-3749; [d]ORCID: 0000-0002-7553-5611; [e]ORCID: 0000-0001-8072-2983; [f]ORCID: 0000-0002-6657-8644

✉Corresponding author: onurceylan@selcuk.edu.tr
Received date: 11.08.2020 - Accepted date: 27.11.2020

Abstract: The aim of this study was to investigate equine piroplasms of wild horses (*Equus ferus caballus*) in Konya province of Turkey in November-December 2017. For this aim, blood samples were collected from 36 wild horses and examined for equine piroplasms by microscopy and multiplex PCR. Some of the PCR products from positive samples were also sequenced. Five (13.89%) out of the 36 horses were infected with either *Theileria equi, Babesia caballi* or both in the microscopical examination. Single infections with *T. equi* and *B. caballi* were detected in three (8.33%) and one horses (2.78%), respectively. Prevalence of *T. equi*, *B. caballi* and mix infections was determined as 50%, 38.8% and 38.8% by multiplex PCR, respectively. Multiplex PCR was found more sensitive than microscopical examination to detect the piroplasms of horses. The results of sequence analysis showed 99.25-100% and 98.23-99.59% nucleotide sequence identity to the previously reported *T. equi* and *B. caballi* 18S rRNA gene sequences, respectively. Consequently, the existence of equine piroplasmosis in wild horses was reported for the first time in Turkey, and high molecular prevalences of *T. equi* and *B. caballi* were reported with this study.

Keywords: *Babesia caballi,* multiplex PCR, *Theileria equi,* Turkey, wild horse.

Türkiye'nin Konya yöresinde yaban atlarında *Theileria equi* ve *Babesia caballi*'nin moleküler tespiti ve filogenetik analizi

Özet: Bu çalışma Türkiye'nin Konya yöresinde yaban atlarının (*Equus ferus caballus*) equine piroplasmlarını tespit etmek amacıyla Kasım-Aralık 2017 tarihlerinde yürütülmüştür. Bu amaçla, 36 yaban atına ait kan örnekeri toplanmış ve bu örnekler mikroskobi ve multiplex PCR yöntemi ile equine piroplasmlar yönünden incelenmiştir. Ayrıca pozitif olduğu tespit edilen bazı örneklere ait PCR ürünleri sekanslanmıştır. Mikroskobik incelemede 36 atın 5'i (13,89%) *Theileria equi, Babesia caballi* veya her ikisiyle birlikte enfekte bulunmuştur. Üç (8,33%) atta *T. equi*, bir (2,78%) atta da *B. caballi* tek tür olarak tespit edilmiştir. *T. equi* ve *B. caballi* ve miks enfeksiyonların prevalansları multiplex PCR ile sırasıyla %50, %38,8 ve %38,8 olarak belirlenmiştir. Çalışmada kan parazitlerinin tespitinde multiplex PCR yönteminin mikroskobik incelemeden daha duyarlı olduğu görülmüştür. Sekans analizleri sonucunda *T. equi* ve *B. caballi* 18S rRNA genleri ile sırasıyla 99,25-100% ve 98,23-99,59%'luk benzerlik tespit edilmiştir. Bu çalışma Türkiye'deki yaban atlarında equine piroplasmosis'in varlığını bildiren ilk çalışmadır ve çalışmada *T. equi* ve *B. caballi*'nin moleküler prevalansları yüksek düzeyde tespit edilmiştir.

Anahtar sözcükler: *Babesia caballi,* multipleks PCR, *Theileria equi,* Türkiye, yaban atı.

Introduction

The origin of domestic horses on the earth is wild horses known as Przewalski and Tarpan horses which are now extinct. But, even today, Przewalski horses (*Equus ferus przewalskii*) (L.S. Poliakov, 1881) live in the forest of Siberia and Mongolia. The Tarpan horse (*Equus ferus ferus*) (Boddaert, 1785), is a subspecies of wild horse and known as Eurasian wild horse. Wild horses are known as "Yılkı horse" in Anatolia (3).

Theileria equi and *Babesia caballi*, the main agents of equine piroplasmosis, are transmitted by ixodid ticks (18). Equine piroplasmosis cause severe symptoms

including fever, anemia, hemoglobinuria, icterus, anorexia, thrombocytopenia, tachypnea tachycardia, loss of appetite, and petechial haemorrhages on mucous membranes (51). The pathogenicity and prevalence of *T. equi* is higher than *B. caballi* in endemic countries (15). Diagnosis of equine piroplasmosis is traditionally made by the detection of piroplasms in Acridine Orange or Giemsa stained peripheral thin blood smears in microscopical examination (45). However, in the case of low parasitemia and mixed infections, microscopy is not sufficient for accurate identification of equine piroplasms (36, 43). Serological tests such as Enzyme-Linked Immunosorbent Assay (ELISA), Complement Fixation Test (CFT), Indirect Fluorescent Antibody Test (IFAT) and Western-blotting (14, 16, 27, 29, 32, 37); and molecular tests like Polymerase Chain Reaction (PCR), Nested PCR and Real Time PCR could be used for the detection of latent and subclinical infections (13, 20). *Babesia* species were detected by PCR in cattle and horses in many studies (10, 17, 21, 22). In the studies conducted with ELISA, IFAT, and CFT in horses in Turkey, the seroprevalences of *T. equi* and *B. caballi* were varied between 0-100% and 0-56.9%, respectively (1, 2, 7, 30, 31, 38, 41, 46). However, the molecular prevalence of *B. caballi* and *T. equi* was detected between 1.97-3% and 2.96-44.6%, respectively in PCR (19, 24, 25, 35, 42). All the studies above were carried out in domestic horses and no data is available on the *Theileria equi* ve *Babesia caballi* of wild horses in Turkey.

This study was aimed to detect the etiological agents of equine piroplasmosis of wild horses in Konya province of Turkey, to provide a molecular characterization of the isolates.

Materials and Methods

***Study area, sample collection, and microscopic examination*:** This study was conducted on the wild horses (*Equus ferus caballus*) brought to Karkın village in Konya (Figure 1) from Karadağ mountain in Karaman in Turkey, between November-December 2017. A total of 36 wild horses caught by the Kazakh horse herdsmen were examined for equine piroplasms. The thin blood smears for each horse were prepared and stained by Giemsa and examined in a light microscope (Leica DM 1000).

***Ethical statement*:** To carry out all procedures in this study, ethical guidelines for the use of animal samples permitted by Selçuk University, Veterinary Medicine (Permit for an animal experiment: 2018/05, Date: 13.02.2018) were tracked.

DNA extraction: 10 ml of blood samples were taken from each horse into tubes including EDTA for molecular studies and all horses were also visually examined in terms of tick infestations. 200 µl of blood samples was utilized for total genomic DNA (gDNA) isolation, using a commercial kit (Quick-DNA Miniprep Plus Kit, Zymo Research D4068). The isolated gDNA was stored at -20ºC until use.

PCR amplification: To detect *T. equi* and *B. caballi*, species-specific primers targeting 18S rRNA genes of these piroplasms were employed. The protocol of Alhassan et al. (4) was used for multiplex PCR. Each reaction consisted of 4 µl of gDNA and 46 µl of PCR mix containing 1.5 mM $MgCl_2$, 30 mM KCl, 250 µM of each dNTP, 10 pmol of each reverse primers for *T. equi* (EquiR:5-TGCCTTAAACTTCCTTGCGAT-3) and for *B. caballi* (CabR:5-CTCGTTCATGATTTAGAATTGC-3), 20 pmol of universal forward primer (UFP:5-TCGAAGACGATCAGATACCGTCG-3) and 1 U of Taq polymerase (Bioline). BioRad thermocycler was used for the reactions with the following programme: 96ºC for 10 min, 36 cycles (96ºC for 1 min, 60.5ºC for 1 min, 72ºC for 1 min) and final extension 72ºC for 10 minutes. As a negative control, distilled water was used. The amplified DNA samples electrophoresed on agarose gel (1%) in TAE buffer, were stained with ethidium bromide and then photographed using UV transilluminator.

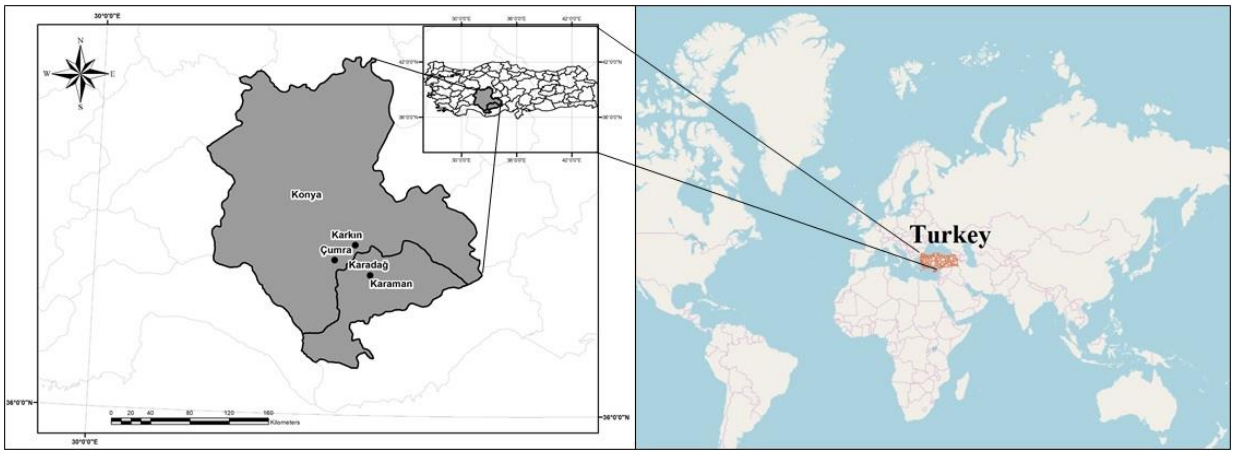

Figure 1. The geographic location of sample collection site.

Phylogenetic analysis: Eight positive products were randomly selected and sequenced. Sequences were analyzed by using NCBI BLAST (https://blast.ncbi.nlm.nih.gov/Blast.cgi). Phylogenetic trees were constructed by using the neighbor-joining method in MEGA version X software generated from the 18S rRNA on aligned sequences of the *T. equi* and *B. caballi* 18S rRNA gene sequences.

Results

As a result of microscopic examination, 5 (13.89%) of the horses were found positive for equine piroplasms. *Theileria equi* in three cases (8.33%), and *B. caballi* in one case (2.78%) were detected as infections with single species in the microscopical examination. Mix infections with these parasites were found in one case (2.78%).

Theileria equi and *B. caballi* were found positive in 18 (50%) and 14 (38.8%) cases, respectively by multiplex PCR. Mix infections were found in 14 cases (38.8%). As a result of the multiplex PCR assay, the presence of bands of 435 bp and 584 bp was determined for *T. equi* and *B. caballi*, respectively (Figure 2). *Theileria equi* was found more prevalent than *B. caballi.* Microscopy and multiplex PCR results are summarized in Table 1.

Theileria equi isolates obtained in this study formed a well-supported clade with the sequences from Turkey, Sudan, South Africa, Brazil, Romania, China, Spain, Switzerland, Jordan, and the USA (Figure 3). The sequences showed 99.25-100% nucleotide sequence identity with the sequences from these countries.

Table 1. Microscopy and multiplex PCR results.

Piroplasm species	Microscopy	Multiplex PCR
B. caballi	1	-
T. equi	3	4
B. caballi + *T. equi*	1	14
Total	5	18

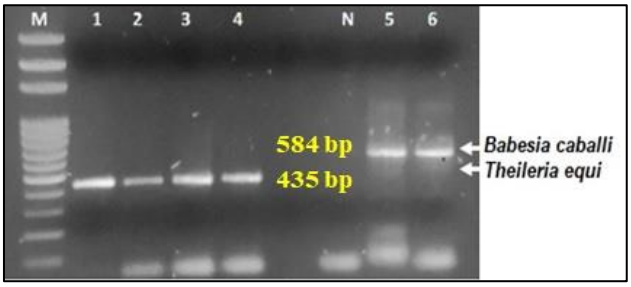

Figure 2. PCR detection of *B. caballi* and *T. equi* with a set of primers. M: 100 bp DNA marker; N: Negative control; Lane 1-4: *T. equi*; Lane 5-6 *B. caballi.*

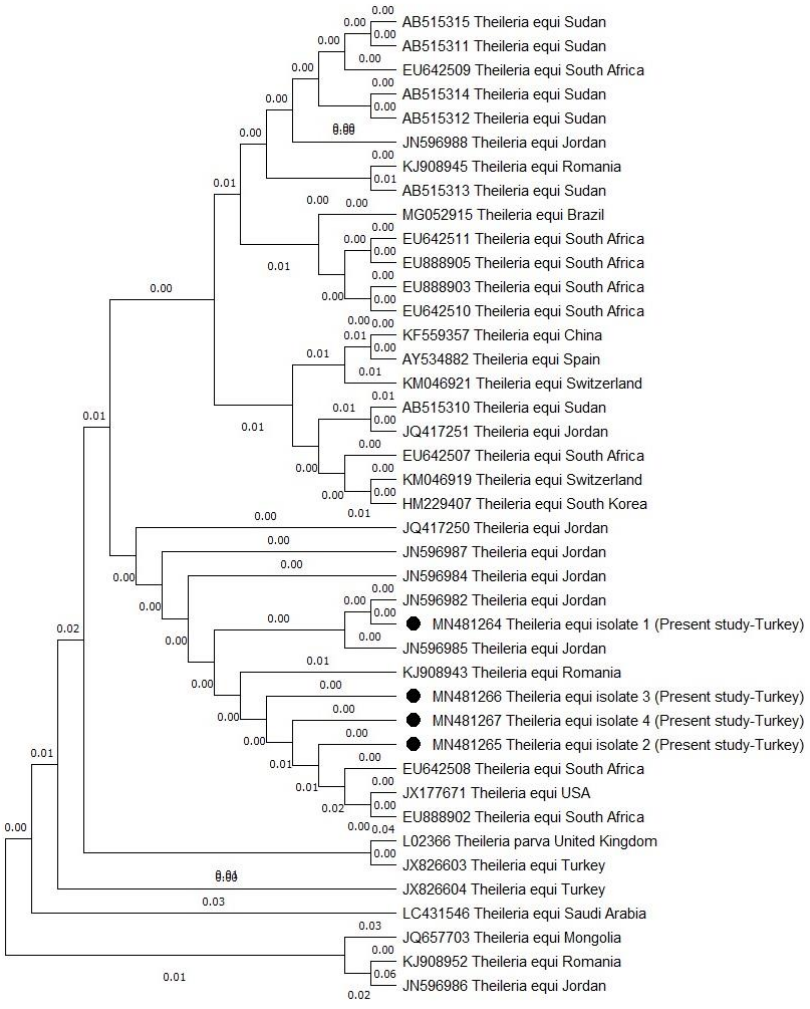

Figure 3. Phylogenetic tree constructed by using the neighbor-joining method in MEGAX software generated from the 18S rRNA on aligned sequence of the *T. equi* 18S rRNA gene. GenBank accession numbers of reference sequences and localities are given. The sequences obtained from this study were marked with the symbol as " •".

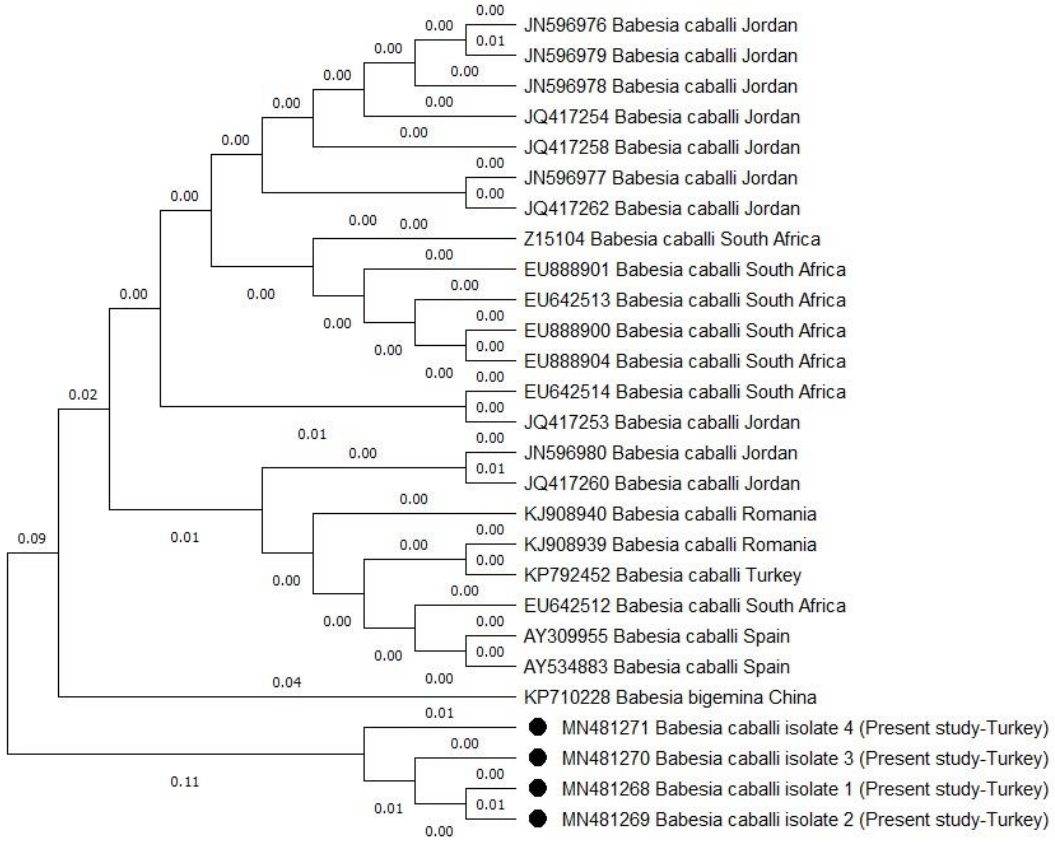

Figure 4. Phylogenetic tree constructed by using the neighbor-joining method in MEGAX software generated from the 18S rRNA on aligned sequence of the *B.caballi* 18S rRNA gene. GenBank accession numbers of reference sequences and localities are given. The sequences obtained from this study were marked with the symbol as " •".

However, *B. caballi* isolates obtained in the present study clustered together in a separate clade (Figure 4) with high proximity to other sequences in the different clades. The nucleotide sequence identity value of *B. caballi* 18S rRNA gene sequences ranged from 98.23-99.59%. The obtained sequences were deposited to Genbank under the accession numbers MN481268-MN481271 for *B. caballi* and MN481264-MN481267 for *T. equi.*

Discussion and Conclusion

So far, only one report (33) on the parasites of wild horses was encountered in Turkey reporting helminth infections. However, no study has been conducted on the *T. equi* ve *B. caballi* in wild horses in Turkey.

Piroplasmosis is a serious disease for all horses, but it is even more crucial for racing horses. The international movement of racing horses increases the probability of disease transmission from infected horses to susceptible ones (23). Previous studies on the diagnosis of piroplasmosis focused on microscopic examination of Giemsa stained preparations. The prevalence of equine piroplasmosis was found to vary between 0-58.18% in Turkey (2, 7, 25, 31, 38). In our study, 5 out of 36 horses were found positive for equine piroplasms, microscopically. *Theileria equi* and *B. caballi* were detected as a single species in three and one cases, respectively and both species were found together in one case. In microscopical examination, the infection rates of *T. equi* and *B. caballi* obtained in this study were found to be higher than the previously reported ones (7, 38). However, the infection rate of *B. caballi* was lower than the result of a previous study conducted in the Central part of Turkey (31). In the microscopy, the low infection rate of *B. caballi* in this study may be due to the latent course of the infection or the season of the study. Since this study was carried out in late autumn and early winter, it is very difficult to find piroplasms in the erythrocytes of the horses in this period of the year. In addition, vector ticks, except *Haemaphysalis* and *Dermacentor* species are inactive in this season in Central Anatolia. The blood samples taken from the vena jugularis may also be another cause of low parasitemia. Microscopic examination may be insufficient in the latent period when parasites are present in the blood in small numbers (14, 28, 47). Stress factors are very important in this infection, and they may temporarily affect the immune system. Some studies

indicating that immunosuppressed animals are more susceptible to infection (28, 34). Since these horses live a relatively remote life from stress in their natural environment, there are no or few conditions that would adversely affect their immune system. In the detection of parasites in the cases of low parasitemia, more sensitive and specific diagnostic techniques such as molecular methods are preferred (12, 18, 26). 18S rRNA gene has been extensively used for the phylogenetic analysis of piroplasms (5). Many researchers stated that the results of PCR based molecular studies were much more sensitive compared to those of microscopic examination (10, 39, 40, 44, 48, 49). In this study, it was also determined that 18S rRNA based multiplex PCR was more sensitive than microscopy in the detection of equine piroplasms. The prevalence of *T. equi* and *B. caballi* was found as 50% and 38.8%, respectively by PCR. The obtained results of the study support the findings of the previously conducted studies in South Africa and Brazil (12, 18, 26) mentioned above that PCR is more sensitive than microscopy. Fifteen blood samples negative in microscopical examination, were *T. equi*-positive in PCR, whereas one microscopy positive sample was negative in PCR. Twelve blood samples, found as negative for *B. caballi* in microscopical examination, were positive in PCR. On the other hand, two *B. caballi* microscopy-positive samples were also positive in PCR. Negative detection in the PCR of one sample found to be *T. equi*-positive on microscopy may be referred to the existence of PCR inhibitors or parasitemia lower than the detection limit of the molecular technique in the circulating blood of hosts (6, 8, 9, 11). The sequencing results obtained from this study were similar to those of equine piroplasms genotypes previously registered to Genbank.

The number of molecular studies on equine piroplasmosis are restricted in Turkey. In these studies, prevalences of *B. caballi* and *T. equi* have been reported as follows: 3% and 7% in PCR; 2.3% and 44.6% in nested PCR; 1.97% and 2.96% in Real Time PCR, respectively (19, 24, 35). In the other studies conducted in Turkey, Guven et al. (25) detected *T. equi* (8.8%) by multiplex PCR in Arabian horses in Erzurum province. Also, Ozubek and Aktas (42) reported the piroplasm infection rate of 33.5% in equids by RLB. No *B. caballi* infection was detected in sampled horses in both of these studies. In the current study, *T. equi* prevalence was 50%, while of *B. caballi* was found as 38.8% in multiplex PCR. These results were higher than the results of the previous studies (24, 35). This may be due to the fact that wild horses have been exposed to continuous tick infestations in nature without veterinary control and treatment. Preimmune horses are reservoirs for healthy horses and therefore infection persists continuously in wild horses.

The etiological agents of equine piroplasmosis are transmitted by some ixodid tick species in the genera of *Rhipicephalus, Hyalomma* and *Dermacentor* (18, 33, 50). *Rhipicephalus* and *Hyalomma* species are seen between spring-autumn in Central Anatolia. Vector tick species of equine piroplasmosis in Turkey are not known well. Four tick species: *Hy. detritum, Hy. marginatum, Rh. turanicus* and *Rh. bursa* were determined in the horses with equine piroplasmosis in the previous studies in Turkey (1, 2, 30, 31). Vector tick species have not been studied in detail in most of those studies on determination of the presence and/or prevalence of equine piroplasmosis.

In conclusion; the wild horses were systematically studied for equine piroplasmosis by using microscopical and molecular techniques for the first time in Turkey. *Theileria equi* was found to be more common than *B. caballi.* The specificity of multiplex PCR was higher than microscopic examination. Wild horses live in nature without veterinary control and these horses are constantly a source of infection for domestic horses. Therefore, further studies are needed to detect the prevalence of equine piroplasms and their relationship with vectors throughout the country.

Acknowledgement

The authors would like to thank Professor Zeki Ogurtan for English editing.

Financial Support

Financial support for the present study was provided by Selcuk University Scientific Research Projects Coordination Office (Project No: 18401042).

Ethical Statement

This study was approved by the Selçuk University Animal Research Ethics Committee, (Permit for animal experiment: 2018/05, Date: 13.02.2018).

Conflict of Interest

The authors declared that there is no conflict of interest.

References

1. **Acici M, Umur S, Guvenc T, et al** (2008): *Seroprevalence of equine babesiosis in the Black Sea region of Turkey*. Parasitol Int, **57**, 198-200.
2. **Akkan HA, Karaca M, Tutuncu M, et al** (2003): *Serologic and microscopic studies on babesiosis in horses in the Eastern border of Turkey*. J Equine Vet Sci, **23**, 181–183.
3. **Aksoy AR** (2016): At yetiştiriciliği ders notları. Available at https://docplayer.biz.tr/22854819-At-yetistiriciligi-ders-notlari-yrd-doc-dr-ali-riza-aksoy-1993-guncelleme-mayis-2016.html. (Accessed March 26, 2020).

4. **Alhassan A, Pumidonming W, Okamura M, et al** (2005): *Development of a single round and multiplex PCR method for the simultaneous detection of Babesia caballi and Babesia equi in horse blood*. Vet Parasitol, **129**, 43–49.
5. **Allsopp MT, Allsopp BA** (2006): *Molecular sequence evidence for the reclassification of some Babesia species*. Ann N Y Acad Sci, **1081**, 509–517.
6. **Allsopp MTEP, Lewis BD, Penzhorn BL** (2007): *Molecular evidence for transplacental transmission of Theileria equi from carrier mares to their apparently healthy foals*. Vet Parasitol, **148**, 130–136.
7. **Balkaya I, Erdogmus Z** (2006): *Investigation of prevalence of Babesia equi (Laveran, 1901) and Babesia caballi (Nuttall 1910) in horses by serological methods in Elazığ and Malatya province*. Fırat Üniv Sag Bil Derg, **20**, 61–63.
8. **Baptista AP, Franco C, Mendes M, et al** (2010): *Subunit composition of Rhodothermus marinus respiratory complex I.* Anal Biochem, **407**, 104–110.
9. **Baptista C, Lopes MS, Tavares AC, et al** (2013): *Diagnosis of Theileria equi infections in horses in the Azores using cELISA and nested PCR.* Ticks Tick Borne Dis, **4**, 242–245.
10. **Bashiruddin JB, Cammà C, Rebêlo E** (1999): *Molecular detection of Babesia equi and Babesia caballi in horse blood by PCR amplification of part of the 16s rRNA gene.* Vet Parasitol, **84**, 75–83.
11. **Bhoora R** (2009): Molecular characterization of Babesia caballi and Theileria equi, the aetiological agents of equine piroplasmosis, in South Africa. PhD. Thesis. University of Pretoria, South Africa.
12. **Bhoora R, Quan M, Franssen L, et al** (2010): *Development and evaluation of real-time PCR assays for the quantitative detection of Babesia caballi and Theileria equi infections in horses from South Africa*. Vet Parasitol, **168**, 201-211.
13. **Boldbaatar D, Xuan X, Battsetseg B, et al** (2005): *Epidemiological study of equine piroplasmosis in Mongolia*. Vet Parasitol, **127**, 29-32.
14. **Bose R, Jorgensen WK, Dalgliesh RJ, et al** (1995): *Current state and future trends in the diagnosis of babesiosis*. Vet Parasitol, **57**, 61-74.
15. **Bruning A** (1996): *Equine piroplasmosis: an update on diagnosis, treatment and prevention.* Br Vet J, **152**, 139-151.
16. **Bruning A, Phipps P, Posnett E, et al** (1997): *Monoclonal antibodies against Babesia caballi and Babesia equi and their application in serodiagnosis*. Vet Parasitol, **58**, 11-26.
17. **Calder JA, Reddy GR, Chieves LP, et al** (1996): *Monitoring Babesia bovis infections in cattle by using PCRbased tests*. J Clin Microbiol, **11**, 2748-2755.
18. **De Waal DT** (1992): *Equine piroplasmosis: A review*. Br Vet J, **148**, 6-14.
19. **Deniz A, Karaer Z, Cakmak A, et al** (2007): Türkiye'de atlarda Babesia etkenlerinin saptanmasında PCR tekniğinin uygulanması (TAGEM, Project number: HS/01/02/06/05/103).
20. **Edwards RZ, Moore H, LeRoy BE, et al** (2011): Equine Babesiosis. Available at http://www.vet.uga.edu/vpp/clerk/edwards/index.php. (Accessed October 15, 2019).
21. **Fahrimal Y, Gott WL, Jamer DP** (1992): *Detection of Babesia bovis carrier cattle by using polymerase chain reaction amplification of parasite DNA*. J Clin Microbiol, **30**, 1374-1379.
22. **Figueroa JV, Chieves LP, Johnson GS, et al** (1993): *Multiplex polymerase chain reaction based assay for the detection of Babesia bigemina, Babesia bovis, and Anaplasma marginale DNA in bovine blood*. Vet Parasitol, **50**, 69-81.
23. **Friedhoff KT** (1988): Transmission of Babesia. 23-52. In: M Ristic (Ed), Babesiosis of Domestic Animals and Man. CRC Press, Boca Raton FL.
24. **Guclu HZ, Karaer Z** (2007): *Detection of Babesia caballi (Nuttall, 1910) and Theileria equi (Syn. Babesia equi, Laveran, 1901) by the Polymerase Chain Reaction (PCR) in show and sport horses in the region of Ankara*. Türkiye Parazitol Derg, **31**, 89-93.
25. **Guven E, Avcioglu H, Deniz A, et al** (2017): *Prevalence and molecular characterization of Theileria equi and Babesia caballi in jereed horses in Erzurum, Turkey*. Acta Parasitol, **62**, 207-213.
26. **Heim A, Passos LMF, Ribeiro MFB, et al** (2007): *Detection and molecular characterization of Babesia caballi and Theileria equi isolates from endemic areas of Brazil*. Parasitol Res, **102**, 63-68.
27. **Hirata H, Xuan X, Yokoyama N, et al** (2003): *Identification of a specific antigenic region of the P82 protein of Babesia equi and its potential use in serodiagnosis.* J Clin Microbiol, **41**, 547-551.
28. **Hodgson J** (2002): Equine exotic diseases, a manual for horse owners. Union Offset, Canberra.
29. **Ikadai H, Osorio CR, Xuan X, et al** (2000): *Detection of Babesia caballi infection by enzyme-linked immunosorbent assay using recombinant 48-kDa merozoite rhoptry protein*. Int J Parasitol, **30**, 633-635.
30. **Inci A** (1997): *Detection of Babesia caballi (Nuttall, 1910) and Babesia equi (Laveran, 1901) in horses by microscopic examination in military farm in Gemlik.* Turk J Vet Anim Sci, **21**, 43-46.
31. **Inci A** (2002): *Investigation of the prevalence of Babesia equi (Laveran, 1901) and Babesia caballi (Nuttall, 1910) in equids by microscopic examination in Kayseri region*. Fırat Üniv Sag Bil Derg, **1**, 85-88.
32. **Kappmeyer LS, Perryman LE, Hines SA, et al** (1999): *Detection of equine antibodies to Babesia caballi by recombinant B. caballi rhoptry-associated protein 1 in a competitive-inhibition enzyme-linked immunosorbent assay*. J Clin Microbiol, **37**, 2285-2290.
33. **Karaman Il Cevre ve Orman Mudurlugu** (2010): Karadağ mevkiindeki Yılkı atlarının durum tespiti, genel sağlık durumları, üremelerinin kontrolü ve çevre üzerindeki etkilerinin değerlendirilmesi projesi. Mevlana Kalkınma Ajansı Teknik Destek Projesi, Referans No: TR52-10-TD01.
34. **Kerber CE, Ferreira F, Pereira MC** (1999): *Control of equine piroplasmosis in Brazil*. Onderstepoort J Vet Res, **66**, 123-127.
35. **Kizilarslan F, Yildirim A, Duzlu O, et al** (2015): *Molecular detection and characterization of Theileria equi and Babesia caballi in horses (Equus ferus caballus) in Turkey*. J Equine Vet Sci, **35**, 830-835.

36. **Krause PJ** (2003): *Babesiosis diagnosis and treatment*. Vector Borne Zoonotic Dis, **3**, 45-51.
37. **Kumar S, Kumar Y, Malhotra DV, et al** (2003): *Standardization and comparison of serial dilution and single dilution elisa using different antigenic preparations of the Babesia equi parasite*. Vet Res, **34**, 71-83.
38. **Kurt C, Yaman M** (2005): *The investigation of the prevalence Babesia equi and Babesia caballi in horses by microscopic and serologic (cELISA) methods in Adana province*. YYU Vet Fak Derg, **23**, 1-4.
39. **Moretti A, Mangili V, Salvatori R, et al** (2010): *Prevalence and diagnosis of Babesia and Theileria infections in horses in Italy: A preliminary study*. Vet J, **184**, 346-350.
40. **Nicolaiewsky TB, Richter MF, Lunge VR, et al** (2001): *Detection of Babesia equi (Laveran, 1901) by nested polymerase chain reaction*. Vet Parasitol, **101**, 9-21.
41. **Oncel T, Vural G, Gicik Y, et al** (2007): *Detection of Babesia (Theileria) equi (Laveran 1901) in Horses in the Kars Province of Turkey*. Türkiye Parazitol Derg, **31**, 170-172.
42. **Ozubek S, Aktas M** (2018): *Genetic diversity and prevalence of piroplasm species in equids from Turkey*. Comp Immunol Microbiol Infect Dis, **59**, 47-51.
43. **Quintao-Silva MG, Ribeiro MF** (2003): *Infection rate of Babesia spp. sporokinetes in engorged Boophilus microplus from an area of enzootic stability in the State of Minas Gerais, Brazil*. Mem Inst Oswaldo Cruz, **98**, 999-1002.
44. **Rampersad J, Cesar E, Campbell MD** (2003): *A field evaluation of PCR for the routine detection of Babesia equi in horses*. Vet Parasitol, **114**, 81-87.
45. **Saal JR** (1964): *Giemsa stain for the diagnosis of bovine babesiosis. II. Changes in erythrocytes infected with Babesia bigemina and B. argentina*. J Protozool, **11**, 582-585.
46. **Sari B, Kirmizigul AH, Deniz A, et al** (2009): *Seroprevalence of Babesia caballi and Theileria equi in horses from Kars and Ardahan provinces during the winter season*. Kafkas Üniv Vet Fak Derg, **16**, 657-661.
47. **Seifi HA, Mohri M, Sardari KA** (2000): *Mixed Infection of Babesia equi and Babesia caballi in a racing colt: a report from Iran*. J Equine Vet Sci, **20**, 858-860.
48. **Sloboda M, Jirků M, Lukešová D, et al** (2011): *A survey of piroplasmids in horses and Bactrian camels in North-Eastern Mongolia*. Vet Parasitol, **179**, 246-249.
49. **Tamzali Y** (2013): *Equine piroplasmosis: an updated review*. Equine Vet Educ, **25**, 590-598.
50. **Uilenberg G** (2006): *Babesia-A historical overview*. Vet Parasitol, **138**, 3-10.
51. **Wise LN, Kappmeyer LS, Mealey RH, et al** (2013): *Review of equine piroplasmosis*. J Vet Intern Med, **27**, 1334-1346.

Ankara Univ Vet Fak Derg, **68**, 283-290, 2021
DOI: 10.33988/auvfd.772685

Detection of tibial fractures in cats and dogs with deep learning

Berker BAYDAN[1,a,✉], Halil Murat ÜNVER[1,b]

[1]Kırıkkale Üniversitesi, Mühendislik Fakültesi, Bilgisayar Mühendisliği Bölümü, Kırıkkale, TÜRKİYE
[a]ORCID: 0000-0003-2806-368X; [b]ORCID: 0000-0001-9959-8425

[✉]Corresponding author: baydanberker@gmail.com
Received date: 21.07.2020 - Accepted date: 21.12.2020

Abstract: The aim of this study is to classify tibia (fracture/no fracture) on whole/partial body digital images of cats and dogs, and to localize the fracture on fracture tibia by using deep learning methods. This study provides to diagnose fracture on tibia more accurately, quickly and safe for clinicians. In this study, a total of 1488 dog and cat images that were obtained from universities and institutions were used. Three different studies were implemented to detect fracture tibia. In the first phase of the first study, tibia was classified automatically as fracture or no fracture with Mask R-CNN. In the second phase, the fracture location in the fracture tibia image that obtained from the first phase was localized with Mask R-CNN. In the second study, the fracture location was directly localized with Mask R-CNN. In the third study, fracture location in the fracture tibia that obtained from the first phase of first study was localized with SSD. The accuracy and F1 score values in first phase of first study were 74% and 85%, respectively and F1 score value in second phase of first study was 84.5%. The accuracy and F1 score of second study were 52.1% and 68.5%, respectively. The F1 score of third study was 46.2%. The results of the research showed that the first study was promising for detection of fractures in the tibia and the dissemination of the fracture diagnosis with the help of such smart systems would also be beneficial for animal welfare.
Keywords: Cat, deep learning, dog, fracture, tibia.

Derin öğrenme ile kedi ve köpeklerde tibia kırıklarının tespiti

Özet: Bu çalışmanın amacı derin öğrenme yöntemleri kullanarak kedilerin ve köpeklerin bütün/kısmi dijital görüntüleri üzerinde tibiayı (kırık/kırık değil) sınıflandırmak ve kırık olarak tespit edilmiş tibialar üzerinde kırığın yerini lokalize etmektir. Bu çalışma klinisyenler için tibiadaki kırığın daha doğru, hızlı ve güvenli bir şekilde teşhis edilmesini sağlar. Bu araştırmada üniversitelerden ve kurumlardan sağlanan toplam 1488 adet köpek ve kedi görüntüsü kullanıldı. Tibia kırığı tespiti için üç farklı çalışma yapıldı. İlk çalışmanın ilk fazında, Mask R-CNN ile otomatik şekilde kırık ve sağlam tibia sınıflandırılması yapıldı. İkinci fazda ilk fazdan elde edilen kırık tibiadaki kırık yeri Mask R-CNN ile lokalize edildi. İkinci çalışmada, Mask R-CNN ile kırığın yeri doğrudan lokalize edildi. Üçüncü çalışmada SSD ile birinci çalışmanın birinci fazından elde edilen kırık tibiadaki kırık yeri lokalize edildi. İlk çalışmanın ilk faz doğruluk ve F1 skor değerleri sırasıyla %74 ve %85, birinci çalışmanın ikinci faz F1 skor değeri ise %84,5 olarak bulundu. İkinci çalışmanın doğruluk ve F1 skor değerleri sırasıyla %52,1 ve %68,5 olarak bulundu. Üçüncü çalışmanın F1 skor değeri ise %46,2 olarak bulundu. Araştırma sonuçları, ilk çalışmanın tibiada kırık tespiti için umut verici olduğunu ve bu tip akıllı sistemler yardımıyla kırık teşhisinin yaygınlaştırılmasının hayvan refahı yönünden de yararlı olacağını gösterdi.
Anahtar sözcükler: Derin öğrenme, kedi, kırık, köpek, tibia.

Introduction

Tibial fractures are common in dogs and cats (4). Tibiofibular and pelvic bone fractures were most common in dogs, pelvic limb fractures were most common in cats (1). Treatment of fractures is important. If the correct intervention is not performed, there may be complications in the fracture improvement process. So, it is essential to make a correct and quick decision (4). In general, x-ray images are used in the diagnosis of fracture in veterinary medicine. But, the diagnosis of bone fracture by taking X-Ray image is risky for clinicians due to radiation exposure. It is also a costly and error-prone method in diagnosis (9). Sometimes, it may be difficult to diagnose a fracture or fracture type due to the low quality of the x-ray image or fatigue cause of demanding workloads for the general orthopedist or even the expert orthopedist (2, 3, 7, 10). These adverse conditions can be minimized by using deep learning technology. Rapid diagnosis and reporting are as important as an accurate diagnosis. The quick procedure will prevent patient harm due to delayed or missed diagnosis. (11).

X-ray images are frequently degraded by Poisson noise, which degrades the visual quality of the image and obscures important information required for an accurate diagnosis. Including a denoising step in automatic fracture detection process was used by several researchers (13). There are different methods for fracture detection based on X-ray and CT images. Some of them are Active contour model (ACM and GACM), Wavelet and Curvelet, Haar, Support Vector Machine (SVM) classifier, X-Ray/CT auto classification of fracture (GLCM), Novel morphological gradient based edge detection technique, Daubechies Wavelet and Fuzzy C-Means (FCM) Clustering, Using Classifiers DT, BN, NB, NN and mixed, Fusion Classification technique, Wavelet and Haar, Combined snake and GVF, Novel approach using binary tree and cuttoff, Using Discrete Wavelet Transform and ring, Using Bi Plane Slicing, Supervised learning based classification (10). Although there are many retrospective studies about the automatic determination of human bone fractures, no many studies have been found on animal fractures. There is a retrospective study only to evaluate the prevalence of appendicular fractures in dogs and cats in Libya (1). But this study does not relate to the automatic determination of bone fracture in animals by computer aided.

The aim of this study is to develop computerized system for classification of dog and cat tibia images whether fracture or no fracture and localization of the location of the fracture with Mask R-CNN and SSD which are the deep learning methods.

Materials and Methods

Dataset: In this study, the dataset was created from scratch. No fracture and fracture tibia images were collected from veterinary faculties and Ankara municipality. In order to get these images, contacted with Surgery Department of Veterinary Faculties of Ankara, Kırıkkale, and Selçuk Universities. Also, most of the images were supplied from Ankara Metropolitan Municipality Sincan Temporary Animal Care Home Rehabilitation Center. A total of 1488 dogs and cats whole/partial body images were selected among thousands of images. These 1488 images consisted of 988 dogs and 500 cats. These images were obtained in Digital Imaging and Communication in Medicine (DICOM) format. The anatomical structures of the dog and cat tibia are almost similar (5). Therefore, there is no difference between them in terms of detecting cat and dog fracture tibia.

Annotation of no fracture, fracture tibia and fracture location of fracture tibia: 1488 tibia images were annotated by a veterinarian. These images consisted of no fracture and fracture tibia. LabelImg (19) is a graphical image annotation tool for labeling image with bounding box. In order to annotate tibia images by using labelImg, 1488 DICOM images were converted to JPEG format. The Angora Viewer software installed on the institution's computer was used to convert DICOM to JPEG.

System architecture: The backbone of deep learning bases on neural networks. The architecture of deep learning that consists of many hidden layers and neurons, provides an advantage to obtain good results on coarse data or image as regards standard neural network (16). There are many deep learning technologies such as Mask R-CNN (6) and SSD (12). Mask R-CNN is a method that allows to detect objects in an image by localizing and masking. Mask R-CNN is the addition of the mask object in parallel with the existing bounding box identifier of Faster R-CNN. In the structure of Mask R-CNN, masks are implemented on each Region of Interest (ROI) to predict segmented part of object. It enables useful framework for implementation and training. Also, it provides fast framework (6). SSD is a deep learning algorithm that generates bounding boxes and their confidence score to detect objects on image and after that non-max suppression is applied on bounding box in order to achieve last detection (12).

Three different studies (S1, S2 and S3) were performed in order to detect, classify tibia and localize fracture location of fracture tibia. S1 is related to detect and localize fracture location of fracture tibia which is obtained automatically by system from whole/partial body digital image by using Mask R-CNN. S1 builds up two stages (Stage 1 and Stage 2). No fracture and fracture tibia were detected and classified by using Mask R-CNN in the first stage. After fracture tibia image was seperated automatically by system from whole/partial body digital image, fracture location was detected and localized by using Mask R-CNN on fracture tibia in the second stage. S2 is related to detect and localize fracture location of fracture tibia directly from whole/partial body digital image by using Mask R-CNN. Mask R-CNN architecture was used in this study (Figure 1). In S3, the SSD algorithm was used instead of the Mask R-CNN that is used in S1-Stage2 to localize the fracture location of fracture tibia which is obtained from S1-Stage1. SSD architecture was shown in Figure 1.

Proposed framework: According to performed studies, S1 is proposed. The flowchart of the proposed framework was shown in Figure 2. The proposed framework works fully automatic in all steps and stages. There is no manual process in the proposed framework. Therefore, this system proposed offers faster, more intelligent and accurate solution for fracture detection on tibia.

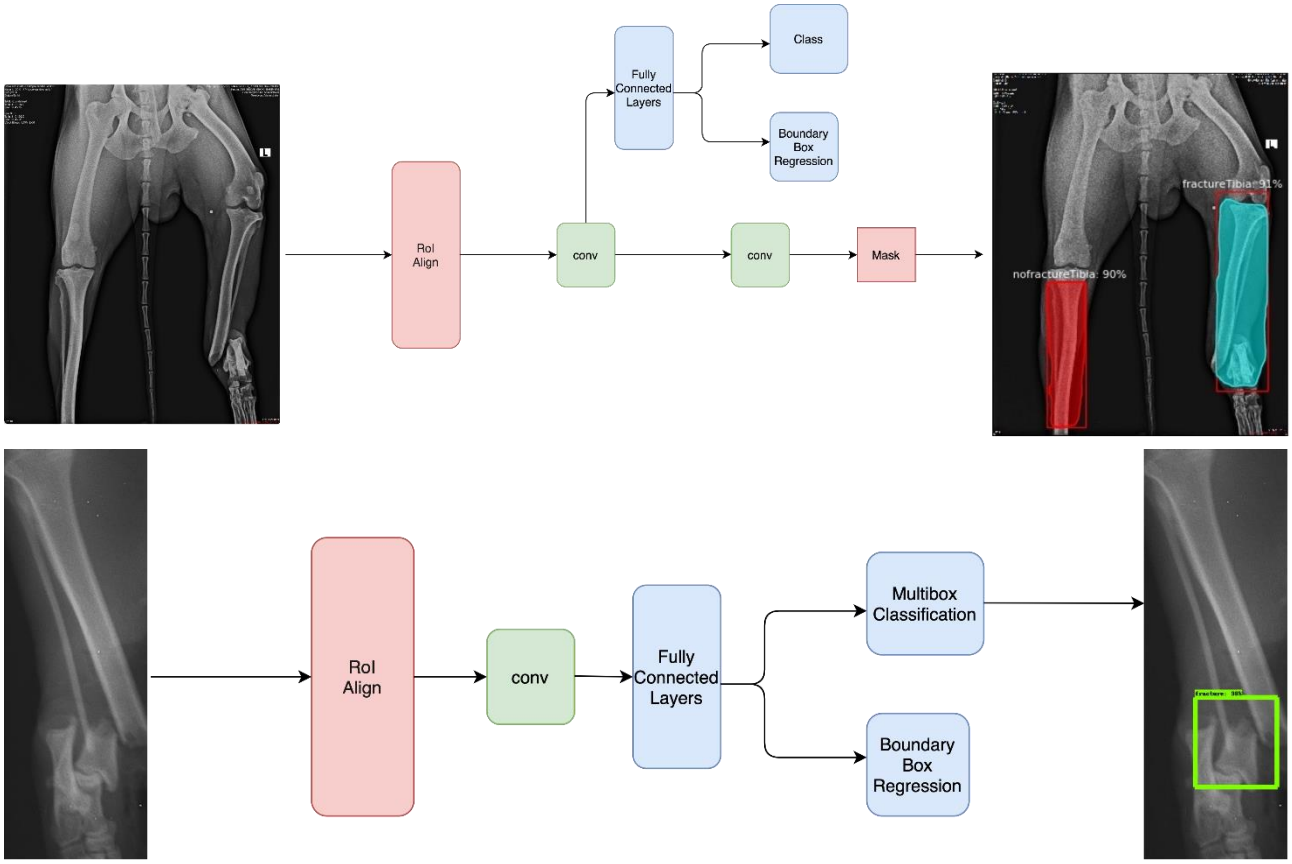

Figure 1. Mask R-CNN and SSD architecture.

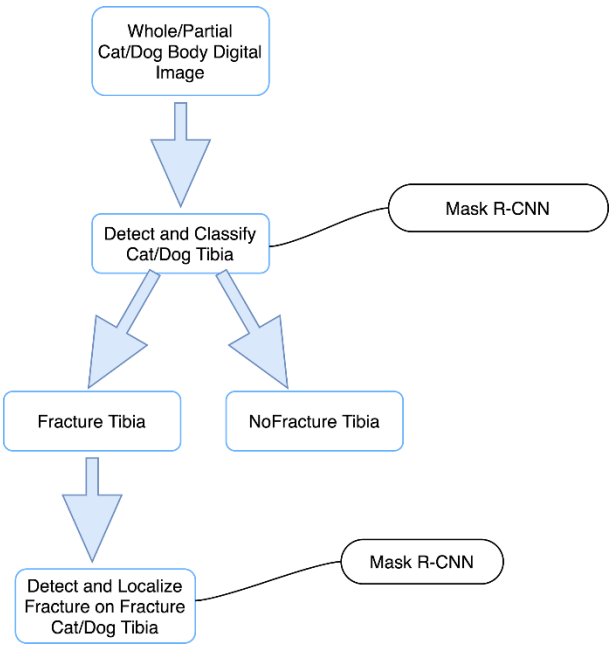

Figure 2. The flowchart illustrating the proposed framework.

Training phase: Tibia dataset was trained by using Mask R-CNN for detection and classification of tibia and detection and localization fracture location of fracture tibia. The dataset consisted of two parts. First part was training and second part was testing. This dataset was re-trained with pre-trained Mask R-CNN model for the detection and localization of no fracture, fracture tibia and fracture location of fracture tibia. Thus, transfer learning process was generated for these studies. The weights of Mask_RCNN_COCO model were used for training. The configuration values of Mask R-CNN were specified during training phase. Batch size: 2, learning rate: 0.001, learning momentum: 0.9, weight decay: 0.0001, epoch: 4000. In order to perform different size of images, image was resized for scaling ratio in Mask R-CNN. Image_min_dim and image_max_dim was set to 800 and 1024 pixel, respectively. Images were scaled that small side was image_min_dim, but scaling doesn't applied if long side is greater than image_max_dim. The system was developed for S1 and S2 by using Keras API. Also, fracture tibia dataset that obtained from first phase of S1 was trained by using SSD for localization fracture on fracture tibia. The configuration values of SSD were specified during training phase. Batch size: 16, learning rate: 0.01, learning momentum: 0.9, weight decay: 0.9, epoch: 4000. Fixed shape resizer was used for scaling different size of images in SSD. Height and width was set to 300 and 300, respectively. The system was developed for S3 by using Tensorflow API. The implementations of these studies were performed on 30.5 GB NVIDIA Tesla M60 GPU and Ubuntu 18.04 operating system.

***Performance evaluation metrics*:** In order to evaluate performance of detection and classification of

tibia and detection and localization of fracture location of fracture tibia, some metrics have to be calculated. Intersection of Union (IoU) is required metric for evaluate performance of system. IoU is part that intersects between the ground truth and the bounding box on the image (18). When the ground truth and bounding box are compared, it is decided on whether the result is True Positive or False Positive through IoU. In this context threshold has to be determined for IoU. IoU was taken as 0.4 for S1, S2 and S3. For instance, if IoU is greater than 0.4, the result is True Positive. Otherwise, it is False Positive. The threshold for the IoU was determined by observing how accurately all the test data cover the fracture between ground truth and the bounding box found by the system. The IoU threshold for the detection of no fracture and fracture tibia and detection of fracture location directly from whole/partial body image was also determined by same method. Confidence score is important metric to evaluate system performance. Confidence score is the probability of detection fracture on fracture tibia or classification of tibia. If the annotated fracture overlaps the location detected as fracture by the system, it is called "True Positive-TP". If the annotated fracture does not overlap the location detected as fracture by system, it is called "False Positive-FP". If the system doesn't detect anything on the image but there is a fracture on the image, it is called "False Negative-FN". If there is no fracture on tibia and system also define "there is no fracture on tibia", it is called "True Negative-TN".

There can be multiple TP and FP on fracture tibia image. Let's assume highest confidence score is TP and second highest confidence score is FP. In this case, since the highest value is TP and it correctly detects the tibia fracture, only the value TP is used to measure the performance of the system. Therefore, FP is not used to calculate system performance. Let's say highest confidence score is FP and second highest confidence score is TP. In this case, both TP and FP are used to calculate system performance. The reason why the TP value is taken here is the correct detection of the tibia fracture with the second highest probability. Accuracy (15) is calculated for how system detect accurately. Accuracy is the ratio of cases that are True Positive and True Negative to all cases. In the light of these obtained metrics, F-Score (17) is calculated to determine the overall performance of the system.

Results

In the first stage of S1, 1488 no fracture and fracture tibia dataset were used. Total dataset was seperated as 595 no fracture and 595 fracture tibia images for training, 149 no fracture and 149 fracture tibia images for test. Dog dataset was seperated as 286 no fracture and 514 fracture tibia images for training, 76 no fracture and 112 fracture tibia images for test. Cat dataset was seperated as 309 no fracture and 81 fracture tibia images for training, 73 no fracture and 37 fracture tibia images for test. Mask R-CNN was used to detect and classify no fracture and fracture tibia from whole/partial body image. IoU rate was specified as greater than 0.4. The accuracy and F1 score of model on the total dataset were 74% and 85% respectively. Only 7 images out of 149 could not make a prediction for the classification of fracture tibia. Only 2 images out of 149 were unable to make a prediction for classification of no fracture tibia. The accuracy and F1 score of model on the dog dataset were 72.4% and 84% respectively. Only 2 images out of 112 could not make a prediction for the classification of fracture tibia. Only 1 images out of 76 were unable to make a prediction for classification of no fracture tibia. The accuracy and F1 score of model on the cat dataset were 76.6% and 86.7% respectively. Only 1 images out of 37 could not make a prediction for the classification of fracture tibia. Only 1 image out of 73 were unable to make a prediction for classification of no fracture tibia. Thus, 518 fracture tibia (441 dog and 77 cat) images were detected automatically by system from 744 fracture tibia (626 dog and 118 cat fracture tibia) images. 744 fracture tibia images consisted of training and testing sets. 518 fracture tibia images obtained as a result of training and testing were automatically extracted from the whole/partial body image by the coordinates of the bounding box. The detected and classified no fracture and fracture tibia from a whole body image was shown in Figure 3.

No fracture and fracture tibia in 298 total test data were detected and classified within 433.1 seconds. It took an average of 1.45 seconds for an image. No fracture and fracture tibia in 188 dog test data were detected and classified within 272.6 seconds. No fracture and fracture tibia in 110 cat test data were detected and classified within 159.5 seconds. In second stage of S1, a total of 518 fracture tibia were divided into 415 training (360 dog and 55 cat) and 103 test (81 dog and 22 cat) data on the images of the fracture tibia. IoU rate was specified as greater than 0.4. The F1 score of model on the total dataset was 84.5%. Only 8 images out of 103 could not make a prediction for the detection of fracture on the fracture tibia. The F1 score of model on the dog dataset was 87.1%. Only 6 images out of 81 could not make a prediction for the detection of fracture on the fracture tibia. The F1 score of model on the cat dataset was 74.3%. Only 2 images out of 22 could not make a prediction for the detection of fracture on the fracture tibia. The detected fracture location on fracture tibia which was obtained automatically by system from whole/partial body image by using Mask R-CNN was shown in Figure 4.

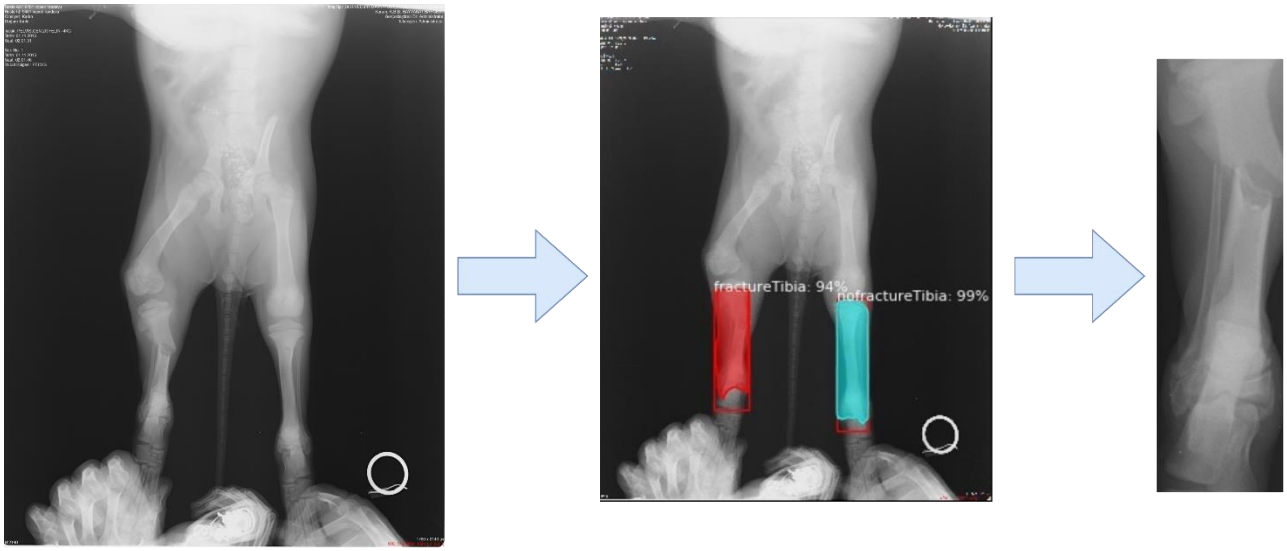

Figure 3. The detected and classified nofracture and fracture tibia from whole body image by using Mask R-CNN.

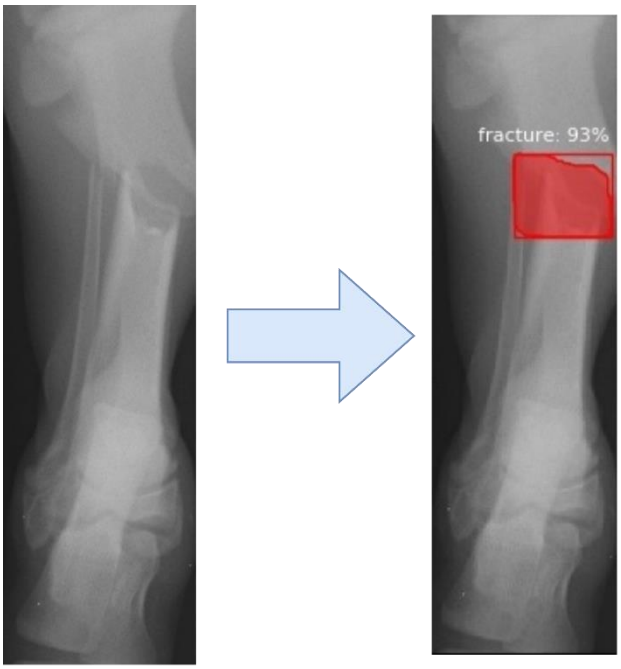

Figure 4. The detected fracture location on fracture tibia which was obtained automatically by system from whole/partial body image by using Mask R-CNN.

Fracture location of fracture tibia in 103 test data were detected and localized within 375.3 seconds. It took an average of 3.6 seconds for an image. Fracture location of fracture tibia in 81 dog test data were detected and localized within 291.6 seconds. Fracture location of fracture tibia in 22 cat test data were detected and localized within 79.2 seconds. The full cycle composed of two stages. No fracture and fracture tibia were detected and classified by using Mask R-CNN in the first stage and fracture location of fracture tibia which was obtained automatically by system from whole/partial body images by using Mask R-CNN was detected and localized in the second stage. The full cycle of automatic fracture detection by system on fracture tibia took an average of 5.05 seconds for an image.

In S2, 744 images containing total dataset fracture tibia were seperated as 595 training data and 149 test data. 149 test data were used as no fracture tibia. Dog dataset was seperated as 514 training data and 112 test data. 76 dog test data were used as no fracture tibia. Cat dataset was seperated as 81 training data and 37 test data. 73 cat test data were used as no fracture tibia. IoU rate was specified as greater than 0.4. The accuracy and F1 score of model on the total dataset were 52.1% and 68.5% respectively. Only 35 images out of 149 could not make a prediction for the detection of fracture location of fracture tibia directly from whole/partial body. The accuracy and F1 score of model on the dog dataset were 51.7% and 68.1% respectively. Only 28 images out of 112 could not make a prediction for the detection of fracture location of fracture tibia directly from whole/partial body. The accuracy and F1 score of model on the cat dataset were 53% and 69.3% respectively. Only 7 images out of 37 could not make a prediction for the detection of fracture location of fracture tibia directly from whole/partial body. The detected and localized fracture location of fracture tibia directly from whole/partial body image by using Mask R-CNN was shown in Figure 5.

Fracture location of fracture tibia directly from whole/partial body images in 149 test data were detected and localized within 2991.8 seconds. It took an average of 20 seconds for an image. Fracture location of fracture tibia directly from whole/partial body images in 112 dog test data were detected and localized within 2520 seconds. Fracture location of fracture tibia directly from whole/partial body images in 37 cat test data were detected and localized within 460 seconds.

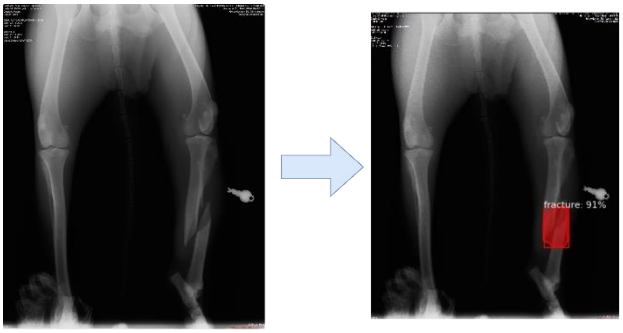

Figure 5. The detected and localized fracture location of fracture tibia directly from whole/partial body image by using Mask R-CNN.

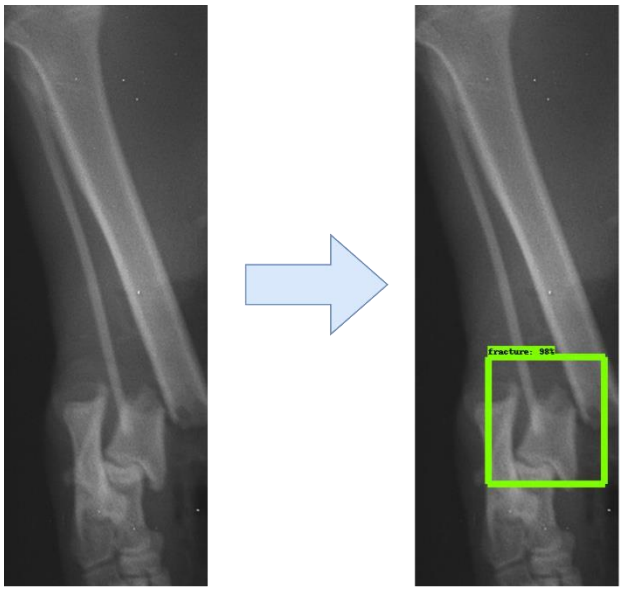

Figure 6. The detected fracture location on fracture tibia which was obtained automatically by system from whole/partial body image by using SSD.

Table 1. Detection, classification and localization studies of fracture in tibia using Mask R-CNN.

Studies (S)	Mask R-CNN																				
	Dog							Cat								Total					
	P (%)	R (%)	A (%)	Se (%)	Sp (%)	F1 (%)	ART (sec)	P (%)	R (%)	A (%)	Se (%)	Sp (%)	F1 (%)	ART (sec)	P (%)	R (%)	A (%)	Se (%)	Sp (%)	F1 (%)	ART (sec)
S1-St1	74.5	96.2	72.4	92.4	84.8	84	1.45	77.6	98.3	76.6	94.4	89.3	86.7	1.45	75.7	97	74	92.7	86.9	85	1.45
S1-St2	83.1	91.4	-	-	-	87.1	3.6	65	86.6	-	-	-	74.3	3.6	79.3	90.5	-	-	-	84.5	3.6
S2	59.6	79.5	51.7	73.2	40.7	68.1	20	57.7	86.6	53	61.9	53.4	69.3	20	59	81.7	52.1	71.3	46.9	68.5	20

P: Precision R: Recall A: Accuracy Se: Sensitivity Sp: Specificity F1: F1 Score ART: Average Response Time.

In S3, fractures on fracture tibia were detected using SSD deep learning algorithm instead of Mask R-CNN as in the second phase of S1. IoU rate was specified as greater than 0.4. The F1 score of model on the total dataset were 46.2%. Only 36 images out of 103 could not make a prediction for the detection of fracture on the fracture tibia. The F1 score of model on the dog dataset was 48.1%. Only 26 images out of 81 could not make a prediction for the detection of fracture on the fracture tibia. The F1 score of model on the cat dataset was 42.9%. Only 10 images out of 22 could not make a prediction for the detection of fracture on the fracture tibia. The detected fracture location on fracture tibia which was obtained automatically by system from whole/partial body image by using SSD was shown in Figure 6.

Fracture location of fracture tibia in 103 test data were detected and localized within 7.8 seconds. It took an average of 0.075 seconds for an image. Fracture location of fracture tibia in 81 dog test data were detected and localized within 6.15 seconds. Fracture location of fracture tibia in 22 cat test data were detected and localized within 1.575 seconds. The metrics of these studies were given in Table 1 and 2.

Table 2. Fracture detection on tibia using SSD.

Study (S)	SSD																				
	Dog							Cat								Total					
	P (%)	R (%)	A (%)	Se (%)	Sp (%)	F1 (%)	ART (sec)	P (%)	R (%)	A (%)	Se (%)	Sp (%)	F1 (%)	ART (sec)	P (%)	R (%)	A (%)	Se (%)	Sp (%)	F1 (%)	ART (sec)
S3	46.4	50	-	-	-	48.1	0.075	50	37.5	-	-	-	42.9	0.075	46.2	46.2	-	-	-	46.2	0.075

P: Precision R: Recall A: Accuracy Se: Sensitivity Sp: Specificity F1: F1 Score ART: Average Response Time.

Discussion and Conclusion

Automatic fracture detection system is remarkable subject in diagnosis of fracture. There are many studies performed in human fracture. However, there are not many studies in animals regarding automatic fracture detection system using deep learning method. This is the first automatic fracture detection smart system on dogs and cats. In current research, no preprocess and data augmentation methods were applied. According to test results, tibia fracture detection performance of the proposed framework which was related to combination of first stage and second stage of S1 (84.5%) was higher than tibia fracture detection performance of S2 (68.5%) and S3 (46.2%). Also, the response time of proposed framework (5.05 seconds) was faster than the response time of S2 (20 seconds). Although the performance of the S3 was the lowest, the response time was obtained to be faster than the S1 and the S2. When the dog and cat dataset were evaluated separately using both Mask R-CNN and SSD in all studies, it was observed that the performance of the detection of fracture location of fracture tibia in dog was higher than in cats (Table 1 and 2). The reason for this may be that the number of cats in total dataset is less than the number of dogs. In various human clinical studies involving computer-aided fracture detection had been found different performance (metric) values (8). In some of these research by using radiographs as modality, accuracy, sensitivity and specificity were found as 0.83 (14), 0.90 and 0.88 (11), respectively for Wrist/Hand/ Ankle. In the study of proximal humerus by Chung et al., accuracy, sensitivity and specificity for detection were found as 0.96, 0.99 and 0.97, respectively. According to results of S1 of this research, accuracy was less than the result of previous some researches, but sensitivity and specificity were similar (Table 1). On the other hand, the detection performance (F1-score) of fracture location on the fracture tibia in this research was high 84.5%. The low accuracy in this study may be due to the fact that the digital images used belong to very different dog and cat breeds and the difference in the method used.

The most important aspect of this study compared to the other researches (i.e fracture detection on proximal humerus which is cropped manually from radiograph (2)) was to detect fracture tibia automatically from whole/partial body image and then localize fracture location automatically on fracture tibia.

As far as the result of proposed system, the metrics were promising regarding to detect and localize fracture on tibia of cats and dogs. The dissemination of the fracture diagnosis with the help of such smart systems would also be beneficial for animal welfare.

Finacial support

This research received no grant from any funding agency/sector.

Ethical Statement

This study was approved by the Kırıkkale University Animal Experiments Local Ethics Committee (60821397-010.99).

Conflict of Interest

The authors declared that there is no conflict of interest.

References

1. **Bennour EM, Abushhiwa MA, Ben Ali L, et al** (2014): *A retrospective study on appendicular fractures in dogs and cats in Tripoli – Libya.* J Vet Adv, **4**, 425-431.
2. **Chung SW, Han SS, Lee JW, et al** (2018): *Automated detection and classification of the proximal humerus fracture by using deep learning algorithm*. Acta Orthop, **89**, 468-473.
3. **Eksi Z, Dandil E, Cakiroglu M** (2012): Computer aided bone fracture detection. In: 2012 20th Signal Processing and Communications Applications Conference (SIU). Muğla, Turkey.
4. **Glyde M, Arnett R** (2006): *Tibial fractures in the dog and cat: options for management.* Ir Vet J, **59**, 290-295.
5. **Hayashi K, Kapatkin AS** (2012): Fractures of the tibia and fibula, 999-1014. In: KM Tobias, SA Johnston (Eds), Veterinary Surgery Small Animal. Volume One, E-BOOK: 2-Volume Set, Elsevier Inc., Canada.
6. **He K, Hkioxari G, Dollar P et al** (2018): Mask R-CNN. 2980-2988. In: IEEE International Conference on Computer Vision (ICCV). Venice, Italy. arXiv:1703.06870v3 [cs.CV].
7. **Joshi D, Singh T** (2020): *A survey of fracture detection techniques in bone x-ray images.* Artif Intell Rev, **53**, 4475–4517.
8. **Kalmet PHS, Sanduleanu S, Primakov S et al** (2020): *Deep learning in fracture detection: a narrative review*. Acta Orthop, **91,** 215-220.

9. **Khan M, Sirdeshmukh, SPSMA, Javed K** (2016): Evaluation of Bone Fracture in Animal Model Using Bio-electrical Impedance Analysis. Perspectives in Science, **8**, 567-569.
10. **Khatik I** (2017): A *study of various bone fracture detection techniques.* Int J Eng Comput Sci, **6**, 21418-21423.
11. **Kim DH, MacKinnon T** (2017): *Artificial intelligence in fracture detection: transfer learning from deep convolutional neural networks*. Clin Radiol, **73**, 439-445.
12. **Liu W, Anguelov D, Erhan D et al** (2016): *SSD:* Single Shot MultiBox Detector. arXiv:1512.02325 [cs.CV]. Available at https://arxiv.org/pdf/1512.02325.pdf. (Accessed October 21, 2020).
13. **Mahendran SK, Santhosh Baboo S** (2011): *An enhanced tibia fracture detection tool using image processing and classification fusion techniques in x-ray images*. GJCST, **11**, 23-28.
14. **Olczak J, Fahlberg N, Maki A et al** (2017). *Artificial intelligence for analysing orthopaedic trauma radiographs.* Acta Orthop, **88**, 581-586.
15. **Rani S, Kumari M, Amulya G et al** (2019): *Leg bone fracture segmentation and detection using advanced morphplogical techniques.* Int J Recent Technol Eng, **8**, 1246-1249.
16. **Ravi D, Wong C, Deligianni F et al** (2017): *Deep Learning for Health Informatics.* IEEE J Biomed Health, **21**, 4-21.
17. **Tsuruoka Y, Tsujii J** (2003): Boosting precision and recall of dictionary-based protein name recognition. 41-48. In: Proceedings of the ACL 2003 workshop on Natural language processing in biomedicine. Sapporo, Japan.
18. **Tychsen-Smith L, Petersson L** (2018): Improving object localization with fitness nms and bounded IOU loss. arXiv:1711.00164v3 [cs.CV]. Available at https://arxiv.org/pdf/1711.00164.pdf. (Accessed July 21, 2020).
19. **Tzutalin** (2015): LabelImg. Git code. Available at https://github.com/tzutalin/labelImg. (Accessed February 27, 2020).

Ankara Univ Vet Fak Derg, **68**, 291-296, 2021
DOI: 10.33988/auvfd.755670

Anatomical and histological structure of ovary and salpinx in Red Foxes *(Vulpes vulpes) (Linnaeus, 1758)*

Gülseren KIRBAŞ DOĞAN[1,a,*], Mushap KURU[2,b], Buket BAKIR[3,c], Ebru KARADAĞ SARI[4,d]

[1]Kafkas University, Faculty of Veterinary Medicine, Department of Anatomy, Kars; [2]Kafkas University, Faculty of Veterinary Medicine, Department of Obstetrics and Gynecology, Kars; [3]Tekirdağ Namık Kemal University, Faculty of Veterinary Medicine, Department of Histology and Embryology, Tekirdağ; [4]Kafkas University, Faculty of Veterinary Medicine, Department of Histology and Embryology, Kars, Turkey.
[a] ORCID:0000-0003-3770-9956; [b] ORCID:0000-0003-4409-251X; [c] ORCID:0000-0003-3637-3688;
[d] ORCID:0000-0001-7581-6109.

✉Corresponding author: glsrn36@gmail.com
Received date: 20.06.2020 - Accepted date: 26.11.2020

Abstract: The Red fox is the largest of the true foxes and the most abundant wild member of the carnivora. This study aimed to determine the anatomical and histological structure of the ovary and salpinx of the Red foxes. The ovary and salpinx of four Red foxes of similar ages, which could not be rescued by the Center despite all interventions, were dissected. Measurements were taken from the right-left ovary and salpinx using digital callipers. The weights of each ovary and salpinx were measured using a precision scale (min: 0.0001 g, max: 220 g). The mean length of the ovary was 13.43 ± 2.38 mm, the width was 6.28 ± 1.99 mm, the thickness was 4.89 ± 0.18 mm, and weight was 0.93 ± 0.14 g. The mean length of the salpinx was 76.22 ± 3.02 mm, the width was 1.98 ± 0.07 mm, and the weight was 0.53 ± 0.31 g. Crossman's triple staining method was applied for histological examination of the ovary tissue. It was observed that the ovary was surrounded by germinative epithelium from the outside and consisted of the cortex with different follicles in the development stage, and the medulla layer with plenty of blood vessels and nerve plexuses inside. In conclusion, we believe that the findings of this study may be useful for further studies on foxes and surgical operations (ovariectomy, ovariohysterectomy). In addition, it is aimed to eliminate the insufficient information regarding the reproductive system of wild animals in this study.
Keywords: Anatomy, histology, ovary, Red fox, salpinx.

Kızıl tilkilerde (*Vulpes vulpes) (Linnaeus, 1758)* ovaryum ve salpinx'in anatomik ve histolojik yapısının incelenmesi

Özet: Kızıl tilki, tilkilerin en büyüğü ve vahşi yaşamın bir üyesi olan carnivorların en çok görülenidir. Bu çalışma ile kızıl tilki ovaryum ve salpinx'inin anatomik ve histolojik yapısını belirlemek amaçlandı. Tüm müdahalelere rağmen merkez tarafından kurtarılamayan benzer yaşlardaki 4 adet kızıl tilki ovaryum ve salpinx'i diseke edildi. Ölçümler digital kumpas yardımıyla sağ-sol ovaryum ve salpinx'ten alındı. Her bir ovaryum ve salpinx'in ağırlığı digital hassas terazide tartıldı (min: 0,0001 g, max: 220 g). Ortalama ovaryum uzunluğu 13,43 ± 2,38 mm, genişliği 6,28 ± 1,99 mm, kalınlığı 4,89 ± 0,18 mm ve ağırlığı 0,93 ± 0,14 g idi. Ortalama salpinx uzunluğu 76,22 ± 3,02 mm, genişliği 1,98 ± 0,07 mm ve ağırlığı 0,53 ± 0,31 g olarak belirlendi. Ovaryum dokusuna histolojik olarak incelenmesi amacıyla Crossman'ın üçlü boyama yöntemi uygulandı. Ovaryum'un dıştan germinatif epitelle çevrili olduğu, korteksinde farklı gelişim aşamasındaki foliküllerin bulunduğu ve içte bol miktarda kan damarı ve sinir pleksuslarının yer aldığı medulla tabakasından oluştuğu gözlendi. Sonuç olarak bu çalışmaya ait bulguların tilkiler üzerinde yapılacak olan cerrahi operasyonlarda (ovariektomi, ovaryohisterektomi) faydalı olacağı düşünülmektedir. Ayrıca, yapılan çalışma ile özellikle yaban hayvanlarının üreme sistemi ile ilgili bilgi yetersizliğinin giderilmesi amaçlanmaktadır.
Anahtar sözcükler: Anatomi, histoloji, Kızıl tilki, ovaryum, salpinx.

Introduction

The red fox (*Vulpes vulpes*) is a mammal of the Canidae family of carnivora, 70-90 cm tall and 7-10 kg of weight. This species, which can be seen in many regions of the world, is also available in Turkey. It is in the Canidae family. There are species living on the continent of Europe, Asia, North Africa, and America. It is a seasonally monogamous carnivores with big ears and a

long tail, famous for its intelligence and fraud (17). It has a 3-month gestation period and reaches sexual maturity at the age of 7-10 months (3).

The ovaries, which are the female reproductive organs, are a small, longitudinal, oval located in the caudal of the kidneys in the abdominal cavity (*cavum abdominis*) (28). In medium-sized adult bitches, the left ovary is located approximately 12 cm behind the 13th rib (*costa*) and 1-3 cm caudal of the kidney (*ren*), while the right ovary is located approximately 10 cm caudal of the last rib (*costa*) on the right (10). Its mean length is 20 mm in dogs and 10 mm in cats (28). It is a mean of 3-12 g in weight and 15 mm in diameter. Canine ovary length is 2 mm, while feline is 8-9 mm (4). The mean length of ovaries is 15 mm, width 7 mm, thickness 5 mm, weight 0.3 gr in dogs of 25 kg (10, 13). Each caudal end is associated with the kidneys (*renes)*. It is located at the level of the third and fourth lumbar vertebrae (*vertebrae lumbalis*) or between the last rib (*costa*) and iliac crest (*crista iliaca*) (28). The left ovary is usually larger than the right. The left ovary participates with the lateral of the spleen (*lien*) (28). The right ovary is located between the right part of the duodenum and the right abdominal wall. In bitches, each ovary is hidden inside the ovarian bursa (*bursa ovarica*), which is a completely peritoneal pouch (*peritoneum)*, while the cat is partially located in this pouch (28). Ovaries are connected by their mesovarium, which is the cranial part of the broad ligament of the uterus, (*ligamentum latum uteri*), which connects the reproductive organs to the abdominal wall and is a peritoneum wrap. Ovaries are found in the ovarian bursa (*bursa ovarica*), which formed by the mesosalpinx externally, the mesovarium with the round ligament of the ovary (*ligamentum ovarii proprium*) and the mesovarium internally. It has exocrine and endocrine functions. It is the exocrine function giving ovum from ovary to genital canal with oogenesis, endocrine function that produces its own hormones (23). It consists of two parts in the ovary: cortex ovarii (*zona parenchymatosa*) on the outside and medulla ovarii (*zona vasculosa*) on the inside (4). In all mammals except for mare, the cortex settles in the periphery. The structure of the cortex and medulla is very variable according to the stages of the sexual cycle, age, and type (23). Ovarian tissue is surrounded by surface epithelial cells that change from outer to cubic to prismatic or flattened, and this area is called stratum germinativum. The cells in this area are also called germinative epithelium (9). Germinative epithelial cells can be cubic-prismatic in developing females, prismatic in adults and flattening epithelium at later ages (12, 23). Under the stratum germinativum, tunica albuginea is found with connective tissue (5, 29). In most mammalian species, cortex and medulla can be distinguished. The cortex forms the follicles at different stages of development and the reticulum threads with collagen surrounding them (13). The medulla consists of blood vessels, lymph vessels, nerves, elastic, and reticular connective tissue fibers (5, 20).

Salpinx (*oviduct, tuba uterina*) is the closest part of the ovum paths to the ovary. It has an environment suitable for fertilization. Macroscopically, it has 3 parts the infundibulum, ampulla, and isthmus (23). There are many extensions called fimbria at the ends of the infundibulum, which is closest to the ovary. The infundibulum opens to the ampulla where fertilization takes place with ostium abdominale. After the ampulla, oocyte proceeds to isthmus, which is narrow and curved. Isthmus opens to cornu uteri with opening of the uterin tubae (*ostium uterinum tuba*) (15). In carnivores, salpinx (*oviduct, tuba uterina*) is small and mean length 50-80 mm (27, 28) or 60-100 mm and 1-3 mm in diameter (13). Salpinx (*oviduct, tuba uterina*) epithelium plays an important role in early embryonic development, in the opposite direction of ovum and spermatozoon, providing an appropriate environment for oocyte maturation and sperm capacitation (23).

There are studies on female genital system in various animal species (1, 6, 14, 26). However, in the literature searches, a study on the anatomy and histology of the female genital system in red foxes was not found. In this study, the red fox is a member of the wildlife (*Vulpes vulpes*) was conducted to examine the ovaries and salpinges of the anatomical and histological structure. Literature information reporting the morphological and histological features of the reproductive system of the red fox, which has an important place in the wildlife, especially in hunting, has not been obtained. We think that we will add new literature knowledge to the scientific world in order to overcome the mentioned deficiency with the presented study. In addition, the differences between the red foxes and other carnivores genital ducts were compared with the morphological and histological similarities. Considering these similarities and differences, it is thought that the findings obtained during the interventions (ovarian cysts or tumors) (18) may be a reference value or may help ovariectomy operations due to genital canal problems.

Material and Methods

These foxes (n=4) were brought to Kafkas University Wildlife Rescue and Rehabilitation Centre (Kars, Turkey) for various reasons such as traffic accidents and firearm injury, but could not be saved or needed to be euthanised according to the Wildlife Rescue and Rehabilitation Centre staff. This study was carried out after the approval from the Ministry of Agriculture and Forestry, General Directorate of Nature Conservation and National Parks (21264211-288.04-E.115365) and Ethical

Committee of Animal Experiments of Kafkas University, Kars, Turkey (KAÜ-HADYEK / 2019-018).

Anatomical examination: The study was carried out in Kafkas University Veterinary Faculty Anatomy Department and Histology and Embryology Department laboratory. The ovaries and salpinges (*oviduct, tuba uterina*) of red foxes of a similar age were dissected. Measurements were taken using a digital calliper (0.01, BTS, UK.). The ovaries lengths were determined from the extremitas uterina and extremitas tubaria. The ovaries width were measured between the margo mesovaricus and margo liber. Ovaries thickness were standard between the facies medialis and facies lateralis. Salpinges (*oviduct, tuba uterina*) length was measured from the between infundibulum and cornu uteri. The weights of the organs were measured using precision scales (min: 0.0001 g – max: 220 g, code: XB220A, Precisa®, Swiss). Nomina Anatomica Veterineria 2017 is used for scientific terms (22).

Histological examination: Ovarian tissue samples taken for histological examinations were determined in 10% formalin solution for 24 hours, then routine histological follow-up solutions and then blocked in paraffin. Crossman's triple staining (19) was applied to examine the histological structure of the 5 µm thick sections taken from paraffin blocks. The slides were examined under an Olympus EP50 microscope and their photos were taken.

Statistical analysis: The mean and standard error values of the morphometric measurements taken were determined in the SPSS® (20.0 version) package program. All morphometric parameters were expressed as mean ± standard error (SE). Lengths were expressed in millimeters and weights were stated in grams.

Results

Anatomical results: In anatomical examinations, it was observed that ovaries were oval shaped, completely in the ovarian bursa (*bursa ovarica*) between the 13th rib (*costae)* and the first lumbar vertebrae (*vertebrae lumbalis*). Ovary mean length is 13.43 ± 2.38 mm, width of 6.28 ± 1.99 mm (Figure 1), thickness 4.89 ± 0.18 mm, weight 0.93 ± 0.14 g, as determined (Table 1). The mean salpinx (*oviduct, tuba uterina*) length was 76.22 ± 3.02 mm, the width was 1.98 ± 0.07 mm, and the weight was 0.53 ± 0.31 g (Figure 2).

Histological results: The ovarian tissue of the foxes was surrounded by cubic germinative epithelial cells from the outside. In addition, a layer of connective tissue tunica albuginea was observed under the germinative epithelium. It was determined that the cortex layer was outside, and the medulla layer was inside (Figure 3). Follicles at different stages of development in the cortex layer (*primary, secondary, tertiary = Graafian follicles*) (Figure 4) and also the corpus luteum (Figure 5) were seen. While primordial follicles were distinguished in the periphery of the cortex, abundant blood vessels and nerve plexuses in the medulla attracted attention (Figures 3, 4, 5). It was observed that the intermediary tissue in the cortex and the medulla consisted of connective tissue.

Figure 1. Red fox ovary length (L) and width (W).

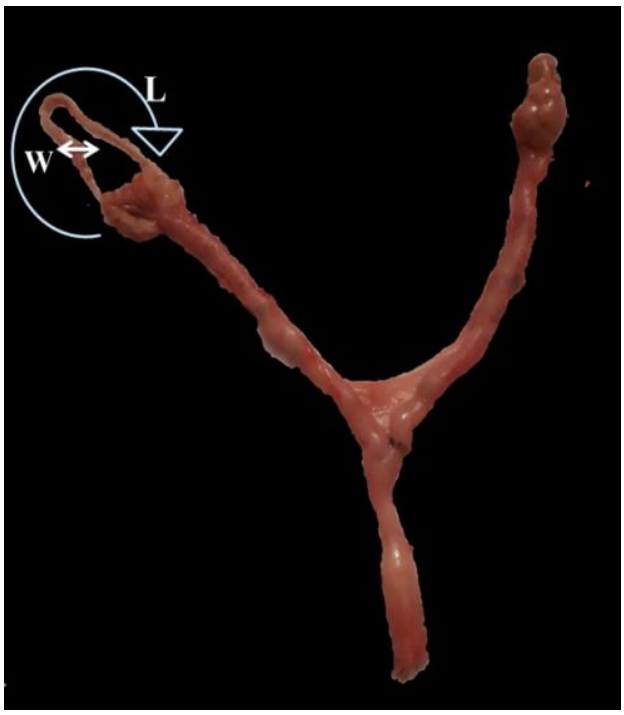

Figure 2. Red fox salpinx length (L) and width (W).

Table 1 Statistical results of some parameters of red fox ovary and salpinx.

Measurement	Mean ± SE		General mean ± SE
	Right	Left	
OV lengths (mm)	13.72 ± 0.79	13.14 ± 1.99	13.45 ± 0.96
OV width (mm)	6.84 ± 1.62	5.71 ± 0.79	6.28 ± 0.84
OV thickness (mm)	5.10 ± 0.53	4.69 ± 0.32	4.89 ± 0.29
OV weight (g)	1.08 ± 0.19	0.78 ± 0.04	0.93 ± 0.11
SAL lengths (mm)	74.96 ± 2.64	77.48 ± 1.05	76.22 ± 1.39
SAL width (mm)	1.93 ± 0.09	2.02 ± 0.02	1.98 ± 0.05
SAL thickness (mm)	0.68 ± 0.01	0.64 ± 0.02	0.66 ± 0.01
SAL weight (g)	0.50 ± 0.17	0.57 ± 0.19	0.53 ± 0.12

OV: Ovaryum, **SE:** Standard error, **SAL:** Salpinx.

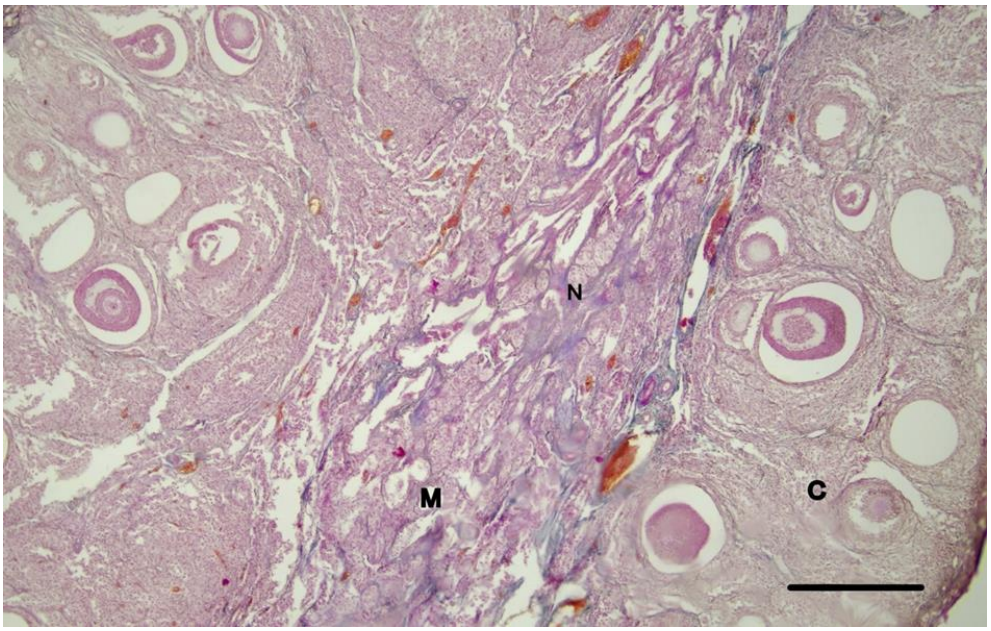

Figure 3. Red fox ovarian tissue. Medulla (M), cortex (C), nerve plexus (N), Triple Staining, Bar=500 µm.

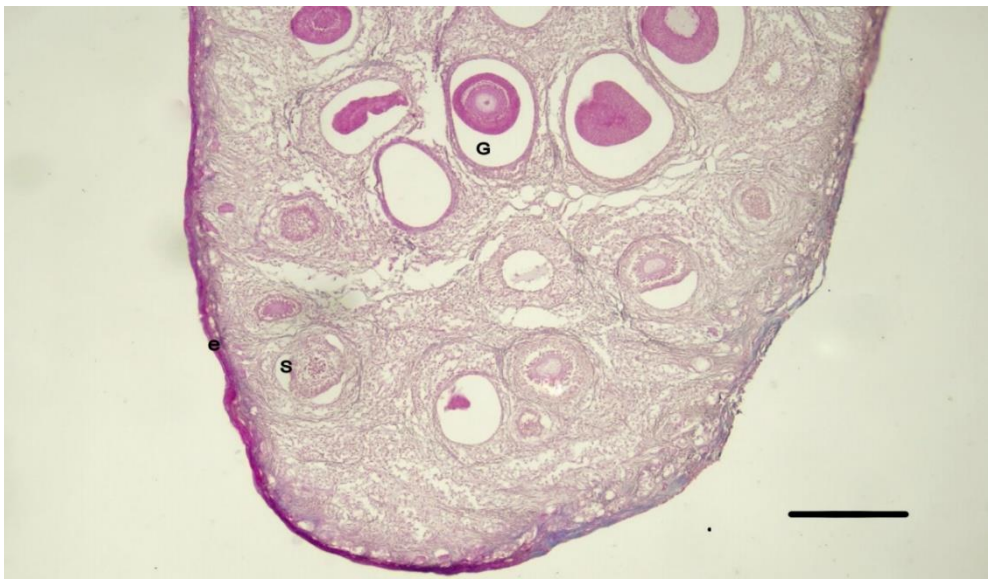

Figure 4. Red fox ovarian tissue. Germinative epithelium (e), secondary follicle (S), Graafian follicle (G). Triple Staining, Bar=500 µm.

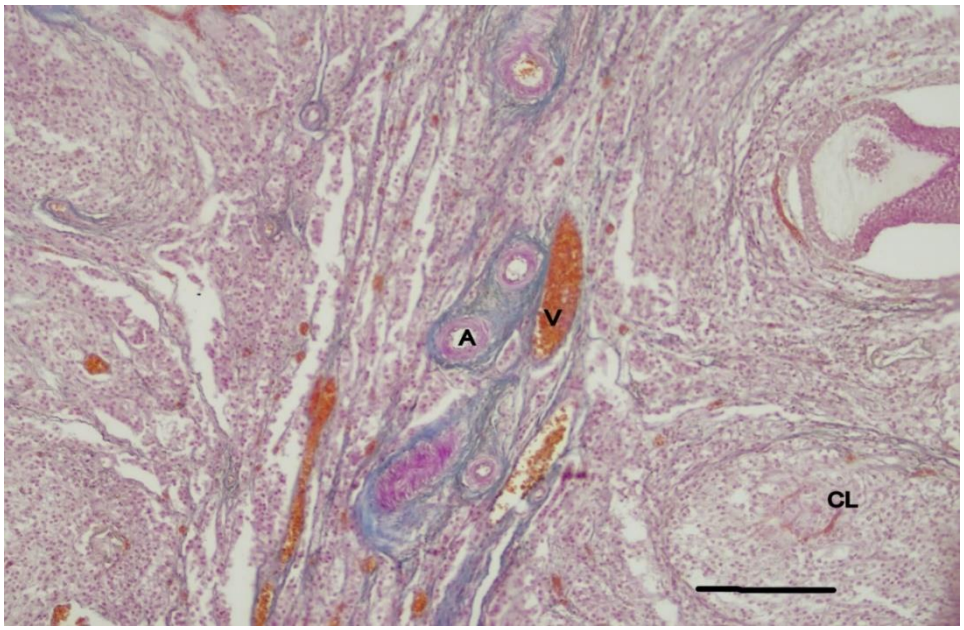

Figure 5. Red fox ovarian tissue. Arteriole (A), venule (V), corpus luteum (CL). Triple Staining, Bar=200 µm.

Discussion and Conclusion

Although there are about 270 species belonging to the Carnivora team, the Mustelidae, Felidae, Canidae and Ursidae families are mostly known. Most assisted reproductive technology development studies are used as models of pet dogs and farm foxes from the Canidae family. Farm foxes also have an economically important place in the fur industry. Artificial insemination in fox farming is one of the main methods applied in Scandinavian countries (2).

The shape of the ovaries was reported as kidney in horses and ellipsoids in other domestic mammals, while foxes were found to be oval (15). The mean ovary length is 10-20 mm in bitches (4) and 8-10 mm in cats (4, 15, 28). In another study in bitches, the length of the left ovary was 14.30 ± 2.20 mm and the right ovary was measured as 14.00 ± 2.00 mm (30). In foxes, the length of the ovaries was measured as 13.43 mm and the data obtained was between the mean length of the cat-dog ovaries. In bitches of 25 kg, the width of the ovary was 7 mm, the thickness was 5 mm (10, 13), while the foxes were 6.27 mm wide and 4.89 mm thick. In the bitches, the mean ovary weighs of 0.3-12 g (4, 10, 13). In our study, ovaries in foxes were determined as 1.12 g. It was determined that the mean weight of this ovaries obtained from the foxes was within the mean values determined for the bitches.

The mean length of salpinx (*oviduct, tuba uterina*) in carnivores is 50-80 mm (27, 28). However, there are sources reporting that the length of salpinx (*oviduct, tuba uterina*) varies between 60-100 mm in bitches (13). In foxes, the length of salpinx (*oviduct, tuba uterina*) was determined as 76.22 mm and was among the averages reported in the literature. While the width of salpinx (*oviduct, tuba uterina*) was 1-3 mm (13) in carnivores, this study was 1.97 mm in foxes. It is generally understood that the data obtained for salpinx (*oviduct, tuba uterina*) from foxes are similar to bitches.

The ovary is the organ where female germ cells (egg cells = ovum) are formed, at the same time, the genital cycle is regulated, and the hormones of the sex are released (8, 23). The ovary is covered with germinative epithelium ranging from prismatic to cubic to cubic to flattening. Under the germinative epithelium is found tunica albuginea which consisting of connective tissue. It has been reported that there are medulla inside and cortex outside in histological sections. It is stated that there are abundant blood vessels, lymph vessels, collagen, elastic fibers and nerve plexuses in the medulla. In cortex, it has been suggested that interstitial tissue rich in connective tissue where fibroblasts are abundant and follicles (primary, secondary, Graafian) at various stages of development are seen (5, 7, 29). In our study, findings similar to the information mentioned were observed. The corpus luteum, as well as the primary, secondary, Graafian follicles of the ovary, surrounded by cubic germinative epithelial cells from the outside, was seen in the cortex. In the medulla, abundant blood vessels and nerve plexuses attracted attention.

In conclusion with the presented study, information was given about the anatomical and histological structures of ovaries and salpinges from the female genital organs of the Red fox. Working with wild animals is very few in number due to difficulties in procuring materials. Therefore, it is difficult to compare the similarities and differences of other animals with regard to organs, systems and their functioning. It is noteworthy that the studies conducted are mostly based on observation. In addition, no study has been found to examine the

morphological and histological examinations of the genital systems of red foxes which are examples of wildlife. With this study, it is aimed to overcome the lack of literature in this regard. In addition, findings obtained during interventions (ovarian cysts or tumors) that can form in the genital canal (ovarian cysts or tumors), especially in red foxes, may be reference values. We believe that oocyte storage (25), cloning (11, 16), ovarian transplantation (21, 24) operations and ovariectomy operations that will be performed due to genital canal problems will be contributed.

Financial Support

This research received no grant from any funding agency/sector.

Ethical Statement

This study was carried out after the approval from the Ministry of Agriculture and Forestry, General Directorate of Nature Conservation and National Parks (21264211-288.04-E.115365) and Ethical Committee of Animal Experiments of Kafkas University, Kars, Turkey (KAÜ-HADYEK / 2019-018).

Conflict of Interest

The authors declared that there is no conflict of interest.

References

1. **Abiaezute CN, Nwaogu IC, Okoye CN** (2017): *Morphological features of the uterus during postnatal development in the West African Dwarf goat* (*Capra hircus*). Anim Reprod, **14**, 1062-1071.
2. **Amstislavsky S, Lindeberg H, Luvoni GC** (2012): *Reproductive technologies relevant to the genome resource bank in carnivora*. Reprod Dom Anim, **47,** 164-175.
3. **Angela W** (2019): The Reproductive System - The Red Fox Resource. Available at http://redfoxofficial.weebly.com/the-reproductive-system.html. (Accessed Mar 21, 2019).
4. **Bahadır A, Yıldız H** (2014): Veterinary Anatomy (Locomotor system & Internal organs), Ezgi bookstore, Bursa.
5. **Banks WJ** (1993): Female reproductive system. Applied Veterinary Histology. Mosby, St. Louis.
6. **Dayan MO, Beşoluk K, Eken E, et al** (2010): *Anatomy of the cervical canal in the Angora goat* (*Capra hircus*). Kafkas Univ Vet Fak Derg, **16**, 847-850.
7. **Delmann HD, Brown EM** (1981): Textbook of Veterinary Histology. Lea and Febiger, Philadelphia.
8. **Duke KL** (1980): Comparative Aspects of Mammalian Ovary. In: Motta PM, Hafez ESE, Editors. Biology of the ovary. Springer, Netherlands.
9. **Dyce KM, Sack WO, Wensing CJG** (2010): The female reproductive organs-The pelvis a reproductive organs of dog and cat. Textbook of Veterinary Anatomy. Saunders, St. Lou.
10. **Evans HE, de Lahunta A** (2013): Millers Anatomy of the Dog. WB Sunders Company, Philadelphia.
11. **Ibtishama F, Fahd Qadirb MM, Xiaoa M, et al** (2017): *Animal cloning applications and issues.* Russ J Genet, **53**, 965–971.
12. **Jennigs R, Premanandan C** (2017): Veterinary Histology. The Ohio State University, Columbus, USD.
13. **Kaymaz M, Fındık M, Rişvanlı A, et al** (2013): Obstetric and Gynecology in Cats and Dogs. Medipres, Malatya.
14. **Kırbaş Doğan G, Kuru M, Bakır B, et al** (2019): *Anatomical and histological analysis of the salpinx and ovary in Anatolian wild goat* (*Capra aegagrus aegagrus*). Folia Morphol, **78**, 827–832.
15. **König HE, Liebich HG** (2015): Veterinary Anatomy (Domestic Mammals). Medipres, Malatya.
16. **Kukekova AV, Johnson JL, Xiang X, et al** (2018). *Red fox genome assembly identifies genomic regions associated with tame and aggressive behaviours*. Nat Ecol Evol, **2,** 1479-1491.
17. **Larivière S, Pasitschniak-Arts M (**1996): *Vulpes vulpes. Mammalian Species*, **537**, 1-11.
18. **Lee SY, Jung DH, Park SJ, et al** (2014): *Unilateral laparoscopic ovariectomy in a red fox (vulpes vulpes) with an ovarian cyst.* J Zoo Wild Med, **45**, 678-681.
19. **Luna LG** (1968): Manual of Histologic Staining Methods of Armed Forces Institute of Pathology. Mc Graw- Hill Book Comp, London.
20. **McEntee K** (1990): Reproductive Pathology of Domestic Mammals. Academic Press, New York.
21. **Mohammed AEN** (2018): *Ovarian tissue transplantation in mice and rats: Comparison of Ovaries Age.* Pakistan J Zool, **50**, 481-486.
22. **NAV** (2017): International Committee on Veterinary Gross Anatomical Nomenclature. Nomina Anatomica Veterinaria (NAV). 6th ed., World Association of Veterinary Anatomists, Hanover (Germany), Ghent (Belgium), Columbia, MO (U.S.A.), Rio de Janeiro (Brazil).
23. **Özer A** (2010): Veterinary Special Histology, Nobel Publishing, Ankara.
24. **Picton HM** (2018): *Preservation of female fertility in humans and animal species.* Anim Reprod, **15**, 301-309.
25. **Piras AR, Burrai GP, Ariu F, et al** (2018): *Structure of preantral follicles, oxidative status and developmental competence of in vitro matured oocytes after ovary storage at 4°C in the domestic cat model*. Reprod Biol Endocrin, **16,** 76.
26. **Saleem R, Suri S, Sarma K** (2017): *Gross and biometrical studies on internal female genitalia of adult Bakerwali goat in different phases of estrus cycle*. Indian J Vet Anat, **229**, 23-25.
27. **Sission S** (1910): A Textbook of Veterinary Anatomy, W.B. Saunders Company, Philadelphia.
28. **Getty R, Sission S** (1975): Sisson and Grossman's the Anatomy of the Domestic Animals. W.B. Saunders, Nottingham.
29. **William JB** (1986): Female reproductive system. Applied Veterinary Histology. Williams and Wilkins, London.
30. **Yılmaz O, Uçar M, Çelik HA** (2006): *Ultrasonographic and postoperative examinations of the ovaries in dogs.* Uludag Univ J Fac Vet Med, **25,** 1-6.

Ankara Univ Vet Fak Derg, **68**, 297-300, 2021
DOI: 10.33988/auvfd.714308

Short Communication / *Kısa Bilimsel Çalışma*

Marine fish parasite, *Lernanthropus kroyeri* (Copepoda) is a repository of *Vibrio anguillarum* as evidenced by Loop-Mediated Isothermal Amplification method

Hijran YAVUZCAN YILDIZ[1,a,✉], Özge OTGUCUOĞLU[2,b]

[1]Ankara University, Faculty of Agriculture, Department of Fisheries and Aquaculture, Ankara; [2]Ak-Ya Veterinary Laboratory and Consultancy, Milas, Muğla, Turkey
[a]ORCID:0000-0001-6567-7467; [b]ORCID: 0000-0002-1432-4693

✉Corresponding author: yavuzcan@ankara.edu.tr
Received date: 03.04.2020 - Accepted date: 13.07.2020

Abstract: Fish parasites act as a vector of other pathogenic diseases such as bacteria and virus in fish. Although it has been long known that fish parasites can act as a vector for bacterial pathogens, their role in the transmission of specific bacterial pathogens via particular parasites in the off-host stage has been neglected. The aim of the present study was to disclose that if the copepod parasite, *Lernanthropus kroyeri* in the off-host stage, can store up the aquatic bacterial pathogens: *Aeromonas hydrophila, Photobacterium damsela* subsp. *piscicida*, *Vibrio (Listonella) anguillarum*, *V. harveyi*, *V. vulnificus*, and *V. alginolyticus*. Our results using the Loop-mediated Isothermal Amplification (LAMP) method demonstrated that the bacteria, *V. anguillarum* is internally present in the off-host copepod parasites, *L. kroyeri*. It was also found that the parasite, *L. kroyeri* could survive in the off-host stage for a given time with its potential of vectoring ability in terms of transmission of the bacterium to the fish. This study demonstrates evidence that the copepod parasite in the off-host stage on the gills of sea bass is a reservoir of pathogen bacteria, *Vibrio anguillarum*.
Keywords: *Lernanthropus*, parasitic copepod, vector, *Vibrio anguillarum*.

Deniz balıkları paraziti, *Lernanthropus kroyeri* (Copepoda)'nın *Vibrio anguillarum* için bir depo olabileceğinin Loop-Mediated Isothermal Amplification metodu ile kanıtlanması

Özet: Balık parazitleri bakteri, virus gibi patojenler için vektör olarak hareket edebilmektedirler. Balık parazitlerinin bakteriyel patojenler için vektör olarak hareket ettiği uzun zamandır bilinmesine karşın bazı parazitlerin konakçı (balık) dışındaki dönemlerinde spesifik bakteriyel patojenleri bulaştırmasına ilişkin rolleri yeterince çalışılmamıştır. Bu çalışmadaki temel amacımız bir kopepod parazit olan *Lernanthropus kroyeri* 'nin konakçı dışında yaşadığı dönemde sucul bakteriyel patojenlerden: *Aeromonas hydrophila, Photobacterium damsela* subsp. *piscicida, Vibrio (Listonella) anguillarum, V. harveyi, V. vulnificus* ve *V. alginolyticus'*u bünyesinde tutup tutmadığının ortaya çıkarılmasıdır. Loop-mediated Isothermal Amplification (LAMP) metodu ile elde ettiğimiz sonuçlar, araştırılan bakterilerden, *V. anguillarum'*u kopepod parazit, *L. kroyeri'*nin taşıdığını göstermektedir. Ayrıca parazit *L. kroyeri* belli bir süre, balığa bakteri bulaştırma açısından potansiyel vektörel yeteneğini muhafaza ederek konakçı dışında hayatta kalabilmektedir. Bu çalışma levreklerin solungaçlarında bulunan kopepod parazitin konakçı dışında, patojen bakteri *V. anguillarum* için bir taşıyıcı olduğunu kanıtlamaktadır.
Anahtar sözcükler: *Lernanthropus*, parazitik kopepod, vektör, *Vibrio anguillarum.*

Intensive aquaculture is under the pressure of a huge diversity of the pathogens, evidenced by the propagations with a multiplication of disease outbreaks. Infections, particularly co-infections of parasites and bacteria, are common in aquaculture systems. The prevalence of copepod parasite, *Lernanthropus kroyeri* is high in sea bass, *Dicentrarchus labrax* culture, leading to economic losses due to impaired growth rate, feed conversion ratio and mortality associated with secondary pathogens (5, 11, 16). *Vibrio anguillarum*, also known as *Listonella anguillarum* is the aetiological agent of vibriosis, a systemic disease in fishes characterized by severe hemorrhagic septicemia in different fish from marine and fresh/brackish water. *V. anguillarum* has been one of the

challenging pathogens in mariculture for a long time as its serious effects on the economy in addition to the sustainability of aquaculture (7).

Loop-mediated Isothermal Amplification (LAMP) is a specific DNA-based detection method, providing technically superior to the others such as fast results on-site, a simplified amplification reaction, even more, specific than qPCR and immunoassays (1, 8). LAMP, with its high sensitivity and specificity, has been used for the detection of aquatic pathogens such as *Mycobacterium marinum* (12), infectious hematopoietic necrosis virus (IHNV) (6) and *Cyprinid herpesvirus* (8).

Synergistic interaction between parasites and bacterial infections in fish has been known as a result of the stress caused by parasites disrupting immune reactions and osmoregulatory mechanisms to other secondary bacterial infections (9). Parasite vectors in fish increase the transmission efficiency of bacterial pathogens by forming an entry portal (4). Hence, previous evidence of parasites acting as vectors is available. Parasitic crustaceans of fish are well-known vectors of a range of bacterial pathogens; however, the answers of the following questions are less studied: i) are the bacteria present in water or surface of the parasite and fish affected by mechanical damage of copepod parasite to fish? ii) Or is a copepod parasite a perpetual reservoir of the pathogenic bacteria? Theoretically, the simultaneous presence of Vibrio species and copepod parasites is known in cultured sea bass; however, the empirical evidence of the potential role of the parasite, *L. kroyeri* in transmitting pathogens does not exist. The purpose of this study is to ascertain that the copepod parasite, *L. kroyeri* can harbor the aquatic pathogen bacteria in the condition of off-host. We provide empirical evidence of the presence of *V. anguillarum* within the copepod parasite, *L. kroyeri* using the LAMP method.

Parasitized European sea bass *(Dicentrarchus labrax)* were obtained from a commercial marine aquaculture company located in Güllük Bay. The females of the copepod parasite *L. kroyeri* were carefully collected from the gills by using forceps in newly harvested fish. All collected females of the *L. kroyeri* were with egg-sacs. Parasites were checked for their species and sex, under the microscope. Collected female *L. kroyeri* individuals (N=20) were kept in distilled water for 15 days at 4 ºC and water exchanged every day. Parasites were washed with the antibiotic solution (1 mg/ml sulfadiazine/ trimethoprim) for one hour to remove the external bacteria on the surface of the parasites. After three washes with sterile distilled water, parasites were homogenized at Vortex for 1 minute for LAMP PCR. The LAMP assay was carried out in the instrument Genie II (Optigene, UK). Bacteria were purchased from DSMZ, Germany. Design of primers for the bacteria; *Aeromonas hydrophila* (ATCC 15338), *Photobacterium damsela* subsp. *piscicida* (ATCC 33539), *V. anguillarum* (ATCC 19264), *V. harveyi* (ATCC 27562), *V. vulnificus* (ATCC 27562) *and V. alginolyticus* (ATCC 17749) were carried out in Ak-YA Veterinary Laboratory, Muğla, Turkey. The gene region of 16s rRNA was selected as the target region. Extraction, amplification, and analysis of the results were carried out with LAMP PCR analyzer (Genie II, OptiGene, UK). All the procedures were completed within 90 minutes. Result graphics were automatically obtained from the LAMP PCR analyzer at the end of the procedures. Six primer sets: two outer primers (F3 and B3), two inner primers (FIP and BIP), and two loop primers (loop F and loop B) were arranged by using software LAMP Designer. Recommendations of the manufacturer were followed in optimization: the reaction was performed in a 50 μL mixture containing 4 μL each of FIP and BIP; 1 μL each of F3 and B3; 2 μL loop F and loop B, respectively; 15 L 1× Isothermal Master Mix (OptiGene, UK) and 5x DNA template. The mixture was incubated at 75 ℃ for 15 min and at 95 ℃ for 5 min, respectively. At the stage of lamp and anneal, the incubation was at 65 ℃ for 60 min, and then termination was from 98 ℃ to 80 ℃ in 1 min. To assess off-host survival period, parasites following to detach from the gills of sea bass were transferred to a flask containing seawater at 22 ℃ and kept for 10 days with light aeration. They were daily checked for their death.

LAMP assay in the GenieII showed that the set of primers (*A. hydrophila, P. damsela* subsp. *piscicida, V. anguillarum, V. harveyi, V.vulnificus,* and *V. alginolyticus*) was only specific to *V. anguillarum.*

The optimization of LAMP reaction temperature for the primers is shown in Figure 1, and the obtained amplification rates in Figure 2. Figure 3 shows that none of the DNA samples of *A. hydrophila, P. damsela* subsp. *piscicida, V. harveyi, V. vulnificus,* and *V. alginolyticus* culminated with a positive response in the LAMP reactions. The set of primers was only specific to *V. anguillarum,* with a peak value of 85.9.

We have provided the empirical evidence that bacterial pathogen, *V. anguillarum,* could be found internally in the parasite, *L. kroyeri,* demonstrating that off-host copepod parasites exist as a repository in the aquaculture environment. The presence of bacteria within the parasitic copepod is a strong sign to their vectoring potential and the transmission efficiency for the bacterial pathogens. Vector-pathogen interactions in fish have been studied in different fish and parasites species, providing the findings in line with our results. Three pathogenic bacteria; *Tenacibaculum maritimum, Pseudomonas fluorescens and Vibrio* spp. isolated from sea lice, *Lepeophtheirus salmonis* (Copepoda: Caligidae), and their salmon hosts had been isolated by Barker et al. (3), supporting the fact about potential role of parasitic diseases associated with bacterial infections in salmon aquaculture. Similarly, the presence of *Flavobacterium*

columnare in *Argulus coregoni* in *Oncorhynchus mykiss* has been reported by Bandilla et al. (2). Moreover, Xu et al. (15) provided scientific evidence to prove that a ciliate parasite, *Ichthyophthirius multifiliis* can act as vector of *Edwardsiella ictaluri* in channel catfish. Pylkkö et al. (10) also mentioned another example of bacterial interference occuring in infection by diplostomids, *Diplostomum spathaceum*, leading to increase in atypical *Aeromonas salmonicida* infections in fish.

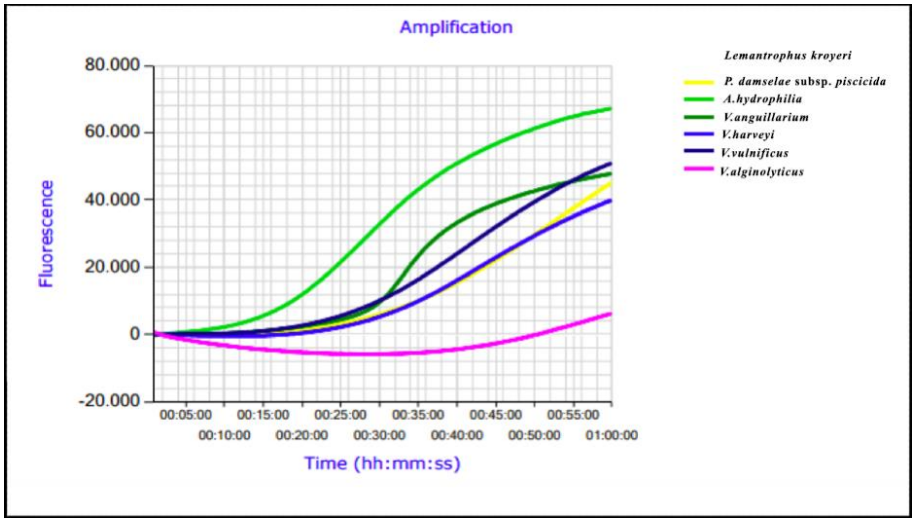

Figure 1. Optimization of LAMP reaction temperature for the primers.

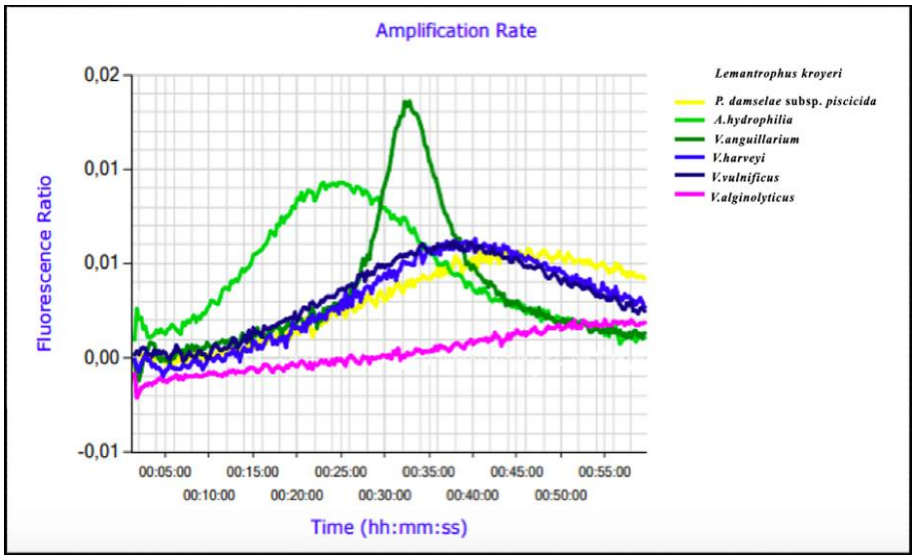

Figure 2. The obtained amplification rates for testing bacteria species.

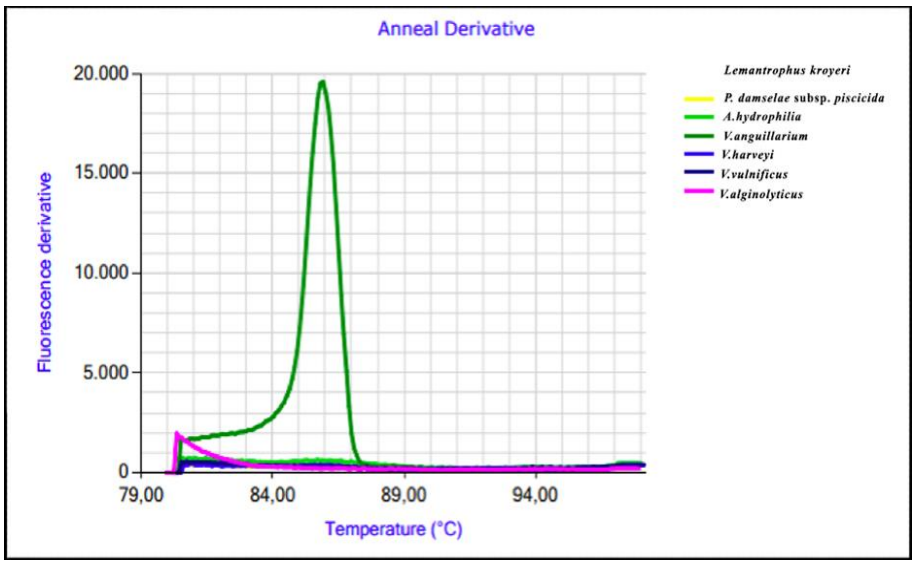

Figure 3. Specificity of the LAMP assay tested with DNA samples of different bacteria species.

On the other hand, crustacean parasites have the ability to survive off-host. Tully& Nolan (13) reported that pre-adult and adult lice *Lepeophtheirus salmonis* (Copepoda: Caligidae) can survive off-host for several days and can change their hosts. Similarly, adult Argulus species (Crustacea: Branchiura) can continue to live without any host up to two weeks (14). In our observations, *L. kroyeri* could survive more than seven days at 22 ^{o}C seawater temperature without any host and swim freely. It indicates a potential danger of dispersing *V. anguillarum* to various marine fish species as *L. kroyeri* may deliver pathogen bacteria to new hosts.

Surprisingly, the transmission dynamics or delivery models of vectors and their specificity have been neglected in parasitological studies in an aquatic environment, although co-infections of bacteria and parasites in fish is well-recognized in aquaculture. Thus, a more integrated approach to revealing the transmission dynamics of vector parasites in aquatic animals is needed to ensure the sustainability of the aquaculture. This research defined our study of LAMP for the detection of pathogen bacteria in a parasite in marine fish with high sensitivity and specificity for the first time. Conclusively, copepod parasite *L. kroyeri* on species of *D. labrax* is a potential reservoir and acts as a vector by perpetuating the pathogenic bacteria, *V. anguillarum*. In order to overcome the bacterial problems in aquaculture, the elimination strategy for parasites should take priority over all bacterial fish disease treatment methods.

Acknowledgements

We thank Agro-Mey Company (Turkey) for providing fish.

Financial Support

This research received no grant from any funding agency/sector.

Ethical Statement

This study does not present any ethical concerns.

Conflict of Interest

The authors declared that there is no conflict of interest.

References

1. **Aartse A, Scholtens IMJ., van der AHJG, et al** (2017): *Evaluation of a loop-mediated isothermal amplification (LAMP) method for rapid on-site detection of horse meat.* Food Control, **81**, 9-15.
2. **Bandilla M, Valtonen ET, Suomalainen LR, et al** (2006): *A link between ectoparasite infection and susceptibility to bacterial disease in rainbow trout.* Int J Parasitol, **36**, 987-991.
3. **Barker DE, Braden LM, Coombs MP, et al** (2008): *Little bugs with smaller bugs: preliminary studies on the role of sea lice as a vector of bacterial pathogens.* Aquaculture Canada 2008. Proceedings of the contributed papers of the 25th Annual Meeting of the Aquaculture Association of Canada, Saint John, NB, 11-14 May 2008.
4. **Cusack R, Cone DK** (1986): *A review of parasites as vectors of viral and bacterial diseases of fish.* J Fish Diseases, **9**, 169-171.
5. **Er A, Kayiş Ş** (2015): *Intensity and prevalence of some crustacean fish parasites in Turkey and their molecular identification.* Turkish J Zool, **39**, 1142-1150.
6. **Gunimaladevi I, Kono T, LaPatra SE, et al** (2005): *A loop mediated isothermal amplification (LAMP) method for detection of infectious hematopoietic necrosis virus (IHNV) in rainbow trout (Oncorhynchus mykiss).* Arch Virology, **150**, 899-909.
7. **Frans I, Michiels CW, Bossier P, et al** (2011): *Vibrio anguillarum* as *a fish pathogen: virulence factors, diagnosis and prevention.* J Fish Diseases, **34,** 643-661.
8. **He J, Shi X, Yu L, et al** (2013): *Development and evaluation of a loop-mediated isothermal amplification assay for diagnosis of Cyprinid herpesvirus 2*. J Virol Methods, 1**94**, 206-210.
9. **Kotob MH, Menanteau-Ledouble S, Kumar G, et al** (2016): The impact of co-infections on fish: a review. *Veterinary Research*, **47**, 1-12.
10. **Pylkkö P, Suomalainen LR, Tiirola M, et al** (2016): E*vidence of enhanced bacterial invasion during Diplostomum spathaceum infection in European grayling, Thymallus thymallus (L.)*. J Fish Diseases, **29,** 79-86.
11. **Toksen E** (2007): *Lernanthropus kroyeri van Beneden, 1851 (Crustacea: Copepoda) infections of cultured sea bass (Dicentrarchus labrax L.).* Bull Eur Assoc Fish Pathol, **27**, 49-53.
12. **Tsai MA, Wang PC, Yoshida S, et al** (2019): *Establishment of loop-mediated isothermal amplification for rapid and convenient detection of Mycobacterium marinum complex.* J Microbiol Methods, **164**, 105671.
13. **Tully O, Nolan DT** (2002): *A review of the population biology and host–parasite interactions of the sea louse Lepeophtheirus salmonis (Copepoda:Caligidae).* Parasitology, **124**, 165-182.
14. **Walker PD, Russon IJ, Duijf R, et al** (2011): T*he off-host survival and viability of a native and non-native fish louse (Argulus, Crustacea: Branchiura).* Curr Zool, **57**, 828-835.
15. **Xu DH, Shoemaker CA, Klesius PH** (2012): *Ichthyophthirius multifiliis as a potential vector of Edwardsiella ictaluri in channel catfish.* FEMS Microbiol Lett, **329**, 160-167.
16. **Yardımci B, Pekmezci G** (2012): *Gill histopathology in cultured sea bass (Dicentrarchus labrax (L.) co- infected by Diplectanum aequans (Wagener, 1857) and Lernanthropus*. Ankara Univ Vet Fak Derg, **59**, 61-64.

Ankara Univ Vet Fak Derg, **68**, 301-306, 2021
DOI: 10.33988/auvfd.772831

Case Report / *Olgu Sunumu*

Non-taurine responsive dilated cardiomyopathy in 2 cats

Kadir SEVİM[1,a], Ekrem Çağatay ÇOLAKOĞLU[1,b,✉]

[1]Ankara University, Faculty of Veterinary Medicine, Department of Internal Medicine, Ankara, Turkey
[a]ORCID: 0000-0002-1959-1010; [b]ORCID: 0000-0003-2789-035X

[✉]Corresponding author: colakoglu@ankara.edu.tr
Received date: 23.07.2020 - Accepted date: 13.10.2020

Abstract: Feline dilated cardiomyopathy (DCM) is a rare disease characterized by myocardial failure and systolic dysfunction. Taurine deficiency is the most important cause of DCM phenotype in cats. A 2 year-old Scottish fold and a 8 month-old domestic shorthair cat were referred to hospital with anorexia, weakness and increased respiratory effort. Based on electrocardiographic, radiographic and echocardiographic findings, the both cases were diagnosed with DCM. The cases were managed with pimobendan, furosemide, acetylsalicylic acid and taurine. The cats were more active and clinically healthy during 15 days follow-up. No remarkable changes were observed in follow up echocardiographies. The cases presented here reflect the clinical signs, cardiological examination findings, diagnosis and management of idiopathic DCMin 2 cats.
Keywords: Cat, dilated cardiomyopathy, taurine.

İki kedide taurine yanıt vermeyen dilate kardiyomiyopati

Özet: Kedilerin dilate kardiyomiyopatisi (DCM) myokardiyal yetmezlik ve sistolik disfonksiyonla karakterize nadir bir hastalıktır. Taurin yetmezliği kedilerde dilate kardiyomiyopati fenotipinin en önemli nedenidir. İki yaşında Scottish Fold ırkı ve 8 aylık yaştaki Melez ırk kedi; anoreksi, halsizlik ve solunum güçlüğü şikayetleri ile hastaneye getirildi. Elektrokardiyografik, radyografik ve ekokardiyografik bulgular ile her iki olguda da dilate kardiyomiyopati teşhisi koyuldu. Olgular; pimobendan, furosemid, asetilsalisilik asit ve taurin ile sağaltıldı. Kediler on beş gün süresinceki takiplerde daha aktif ve klinik olarak sağlıklıydı. Kontrol ekokardiyografilerinde önemli bir değişiklik belirlenmedi. Burada sunulan olgular; idiyopatik dilate kardiyomiyopatili iki kedideki klinik bulgular, kardiyolojik muayene sonuçları, tanı ve tedaviyi yansıtmaktadır.
Anahtar sözcükler: Dilate kardiyomiyopati, kedi, taurin.

Feline dilated cardiomyopathy (DCM) is a disease characterized by primary myocardial failure. Severe enlarged left ventricle and hypocontractile myocardium are the main features of DCM phenotype in cats (8). It was proved in 1987 that taurine deficiency was the most important cause of DCM phenotype (17). After this scientific data, the incidence of the disease has decreased considerably by adding taurin to commercial cat food (3, 8, 13). However, DCM cases were also recognized in small number of cats feeding with an appropriate diet. Signs of respiratory distress, tachycardia, hypotension, collapse and lethargy indicating congestive heart failure and, thromboembolism may seen in cats with DCM (9, 13, 19). Gallop sounds and systolic murmur can also be predictable for DCM cats (13). Increased left ventricle internal dimension at end-systole and reduced fractional shortening as typical echocardiographic features of cats with DCM (8, 9, 13). The cases presented here reflect the process of clinical signs, cardiological examination findings, diagnosis and management of non-taurine responsive DCM in 2 cats.

A 2-year-old intact female Scottish Fold cat feeding with commercially available food referred to Small Animal Veterinary Teaching Hospital with complaints of anorexia and weakness. Mucosal pallor, normothermia (38^0 C) and increased capillary refill time (>3s) with increased respiratory effort were noticed in physical examination. The cat was tachycardic (Heart rate > 250 bpm). Femoral arterial pulses were slightly weak. The cat had also bilaterally auscultated systolic heart murmurs and precordial thrill. Routine complete blood count, serum profiles and serum cardiac troponin-I concentration were showed in Table 1. Thoracic radiographs indicated severe cardiomegaly with pulmonary edema (Figure 1). 6-lead

clinic electrocardiography displayed sinus tachycardia and ST-segment elevation (Figure 2). Echocardiography revealed thinning of interventricular septum and left ventricular free wall and, regurgitant jet detected over the mitral and tricuspid valve with doppler-detected pressure gradients (Figure 3, Table 2). Spontaneous echogenic contrast (smoke) was also visible in dilated left atrium and left ventricle (Figure 3). A definitive diagnosis of DCM was made based on the history, examination findings and diagnostic applications and the following medications assigned as: pimobendan (0.2 mg/kg BID, PO), furosemide (2 mg/kg BID, PO), acetylsalicylic acid (25 mg/cat q72h PO) and taurine (250 mg, BID, PO). The owner reported that the cat was more active and were able to breath easily during 15 days follow-up. No remarkable changes observed in follow up echocardiographies.

Table 1. Blood analyses in cases.

CBC	Results (Case 1)	Results (Case 1)	Reference ranges	Serum Profiles	Results (Case 1)	Results (Case 2)	Reference ranges
WBC (10^9/l)	15	14.8	5.5-19.5	**Glucose** (g/dl)	87	109	70-110
LYM (10^9/l)	2.4	1.9	1.1-7	**Urea** (mg/dl)	42.9	49.1	42.8-64.2
MON (10^9/l)	0.9	0.8	0.2-1.5	**Creatinin** (mg/dl)	0.9	0.86	0.8-1.8
NEUT (10^9/l)	11.2	12	2.8-13	**T. Protein** (g/dl)	5.8	6.8	5.4-7.8
EOS (10^9/l)	0.5	0.1	0.1-2.5	**Albumin** (g/dl)	2.9	3.1	2.4-3.8
RBC (10^{12}/l)	9.12	8.5	5-11	**T. Bilirubin** (mg/dl)	0.1	0.13	0.1-0.2
HGB (g/dl)	13.7	11	8-15	**ALP** (IU/L)	46	57	<70
HCT (%)	33.2	29	25-45	**ALT** (IU/L)	25	35	<50
MCV(fl)	36.3	48.4	39-50	**AST** (IU/L)	23	21	<40
MCH (pg)	15.1	13.2	12.5-17.5	**GGT**(IU/L)	7	8	6-28
MCHC (g/dl)	37.5	35.3	31-38.5	**Na** (mmol/l)	149	151	147-156
RDW(%)	14.8	14.9	14-18.5	**K** (mmol/l)	3.8	3.9	3.6-5.6
PLT (10^9/l)	250	350	200-500	**CK** (IU/L)	323	296	<200
MPV(fl)	8.8	8.2	8-12	**tT4** (µg/dl)	2.3	3.8	0.8-4.7
				cTnI (ng/ml)	0.1	-	0.03-0.1 (2)

Table 2. Echocardiographic measurements in cases.

Variables	Case 1	Case 2
IVSd (mm)	6.9	2.51
LVIDd (mm)*	22.5	27
LVWd (mm)	6.9	5
IVSs (mm)	8.1	3.04
LVIDs (mm)*	11.3	13.8
LVWs (mm)	6.6	5.9
LA (mm)	22.2	26.9
Ao (mm)	12.2	7.72
LA/Ao (mm)	1.81	3.48
FS (%)	14.3	28.9
EF (%)	40.7	58.7
High MV E:A Ratio	Restrictive pattern	Restrictive pattern
MR Jet velocity	6.85 m/sec	6.70 m/sec
MR Max PG	187,69 mmHg	179,56 mmHg
Aortic flow velocity	1.75 m/sec	1.45 m/sec

IVSd, interventricular septum diameter during diastole; LVIDd, left ventricular internal dimension during diastole; LVWd, left ventricular wall diameter during diastole; IVSs, interventricular septum diameter during systole; LVIDs, left ventricular internal dimension during systole; LVWs, left ventricular wall diameter during systole (M mode Teich, 2D right parasternal short-axis view); LA, left atrial diameter; Ao, aortic diameter (2D right parasternal short-axis of the heart base); MV, mitral valve; MR, Mitral regurgitation.

* DCM diagnosis based on the measurements of LVIDd > 16 mm and LVIDs > 11 mm (7).

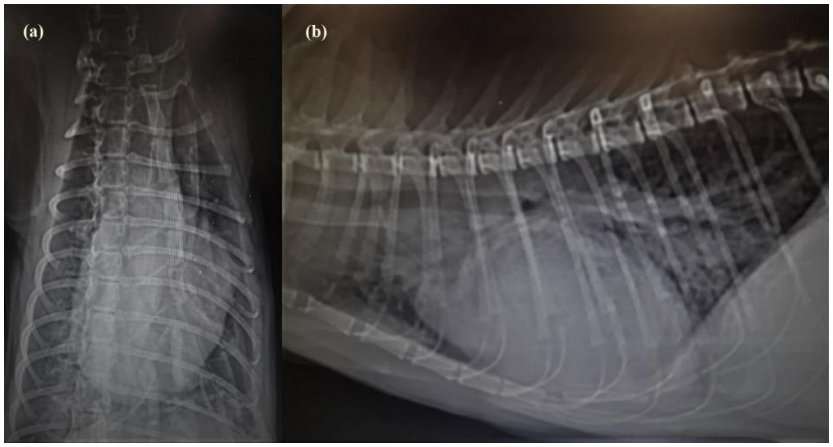

Figure 1. Cardiomegaly in ventrodorsal view (a). Marked pulmonary edema on caudal lung fields. Dorsoventral view (b).

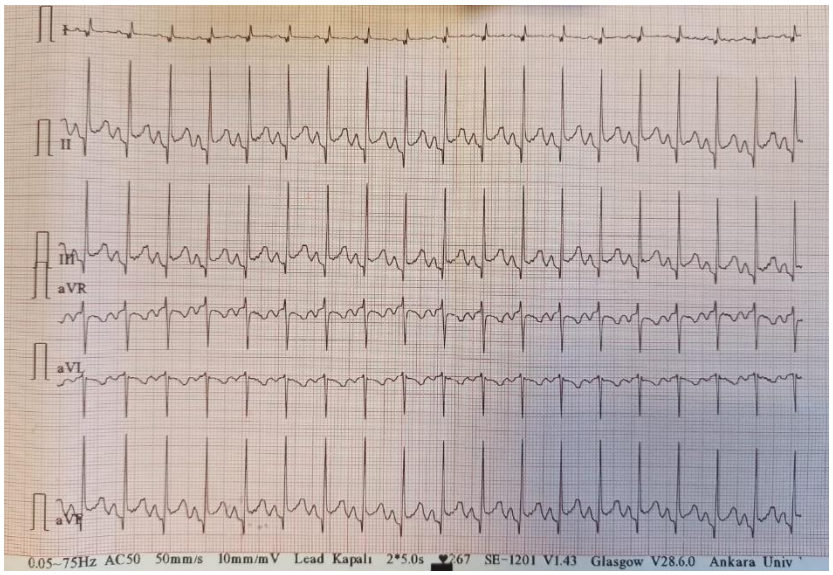

Figure 2. Sinus tachycardia with interatrial conduction delay (P mitrale and P pulmonale) indicating biatrial dilatation.
P wave amplitude 0.3 mV (reference range < 0.2 mV) and P duration 64 ms (reference range < 35ms). Increased R wave amplitude and QRS duration revealed left ventricular enlargement. QRS amplitude 2.2 mV (reference range < 0.9 mV), QRS duration 60 ms (reference range < 40 ms). ST-segment elevation associated with hypoxia is also remarkable in all leads.

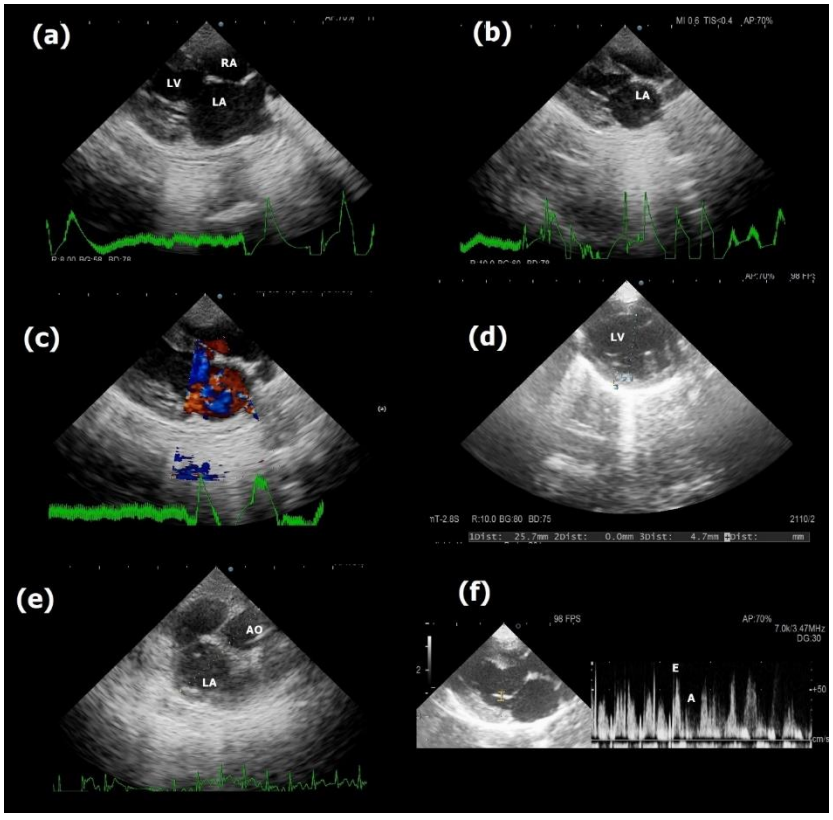

Figure 3. Marked LA dilatation compared to RA and, pulmonary vein dilatation.
Visible smoke in LA. Right PLAX (a,b). Mitral regurgitant jet detected over mitral valve leaflets. Right PLAX (c). Thinning of interventricular septum and left ventricular free wall. Right PSAX papillary muscle level (d). LA (22.2 mm)/AO (12.8) rate: 1.73. Right PSAX heart base (e). Restrictive pattern PW E > A (f). LA: Left atrium, LV: Left ventricle, RA: Right atrium, AO: Aort, PLAX: Parasternal long axis view, PSAX: Parasternal short axis view.

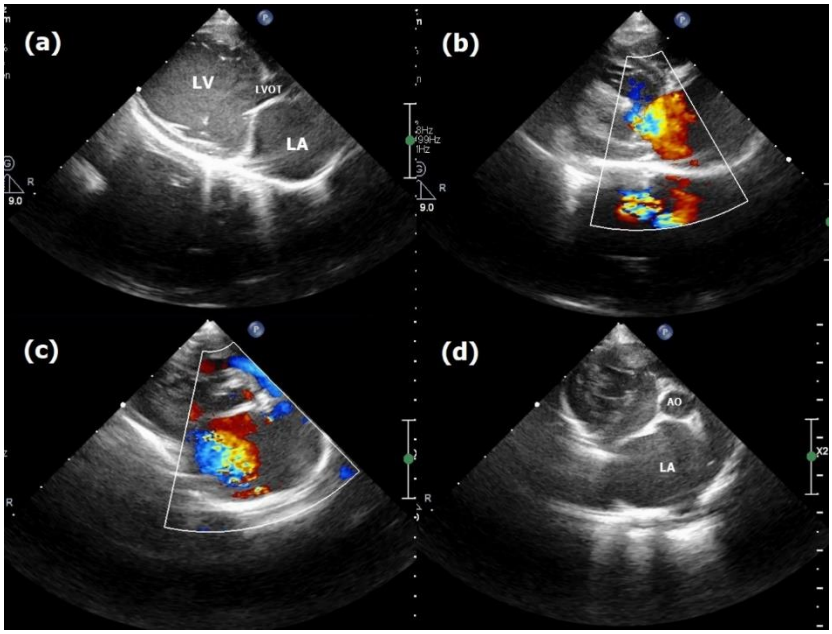

Figure 4. Severe LA and LV dilatation with thinning of interventricular septum and left ventricular free wall.
Visible smoke in LA and LV. Right PLAX (a). Mitral regurgitant jet over mitral valve. Right PLAX (b,c). Increased LA/Ao rate. Right PSAX heart base (d). LA: Left atrium, LV: Left ventricle, AO: Aort, LVOT: Left ventricle outflow tract, PLAX: Parasternal long axis view, PSAX: Parasternal short axis view.

A 8-month-old domestic shorthair cat referred to hospital with anorexia and intermittent open-mouth breathing. Physical examination revealed normothermia (38.3 ^{0}C), hypokinetic femoral pulses, tachycardia (> 240 bpm), gallop rhythm with precordial thrill and increased respiratory effort. Routine complete blood count and serum profile analysis were also performed as showed in Table 1. Thoracic radiographs showed cardiomegaly with increased sternal contact surface. Echocardiography confirmed DCM with smoke formation (Figure 4, Table 2). The cat was initiated the following medications: pimobendan (0.2 mg/kg BID, PO), furosemide (1 mg/kg BID, PO), acetylsalicylic acid (25 mg/cat q72h PO), taurine supplementation (250 mg, BID, PO) and oxygen support. The cat was alive and clinically active during 15 days follow up. No remarkable changes observed in follow up echocardiographies.

DCM phenotype is a myocardial disorder characterized by enlargement of the left ventricular lumen and decreased systolic myocardial function. It was the most common myocardial disease in cats until its relationship with taurine deficiency was determined (17). With the addition of taurine to commercial foods, the incidence of the disease decreased in cats (7, 15). Nevertheless, cats with DCM are encountered although they are fed with a balanced diet. Since the factors causing myocardial dysfunction are often undetectable, non-taurine responsive feline DCM is referred to as idiopathic (13). DCM phenotype can also be possible in the end stage valvular diseases (7). In cases presented here, there is no evidence of pre-existing heart murmur or echocardiographic evidence the valvular pathology to suggest the valvular insufficiency resulting in DCM phenotype or systolic dysfunction. It has been also reported the possibility of infectious etiology and genetic predisposition in occurrence of feline DCM (14, 16). The increase in thyroid hormone levels causes an increase in heart rate and a stronger contraction of the heart muscle. Untreated or unmanaged cases of hyperthyroidism, heart functions deteriorate over time and heart failure may occur (11). In cases here, free thyroxine levels were also within reference ranges. Sustained tachycardia and tachyarrhythmias can also damage myocardial function, causing secondary AV insufficiency or heart failure. This pathological sequela is called tachycardia-induced cardiomyopathy. Arrhythmias can occur due to myocardial diseases, such as DCM or vice versa. Sustained tachycardia can cause DCM (10, 12). It is difficult to distinguish between these two situations. Greet et al. (12) have set criteria for diagnosing supraventricular tachycardia including narrow complex tachycardia with a regular R-R interval and a HR value of more than 260 bpm in the ECG recording, a sudden onset or exit from a narrow complex tachycardia, presence of a permanent atrial depolarization at a rate greater than 260 bpm and the determination of a wide complex tachycardia suggesting intraventricular conduction disturbance. No evidence of supraventricular tachycardia was observed in electrocardiographic evaluations. Congestive signs of respiratory distress, tachycardia, hypotension and collapse and, lethargy and thromboembolism may be seen in cats with DCM (9, 13, 19). Gallop sounds and systolic murmur can also accompany to DCM phenotype in cats (7, 15). In the cases here, congestive signs, gallop rhythm with various degrees of systolic murmur were remarkable as well. Although ECGs are nonspecific in cats with DCM,

sinus tachycardia, atrial or ventricular premature beats, ventricular tachyarrhythmias and atrial fibrillation could be present (5-7, 9, 13). In the first case with ECG, the findings were consistent with the reports previously described. Aroch et al. (4) reported that creatine kinase is a reliable marker of myocardial damage in cats. In accordance with this view, the increase in creatine kinase levels in the case confirms myocardial damage. Cardiac troponins are used as the gold standard in humans to determine myocardial damage (12). Wells et al. (20) reported that reference ranges in healthy cats were 0-0.17 ng / ml in their study of cardiac troponin-I. The absence of any study on cardiac troponin levels in cats with DCM suggests that further studies are needed to determine the diagnostic and prognostic significance of the data we obtain. As DCM progresses, thinning of the atrioventricular area causes dynamic valve insufficiency (9). Mitral insufficiency in echocardiography is the result of this condition. Diagnosis can be made on echocardiography when an enlargement of the left ventricle diameter (> 11 mm in systole and or > 16 mm in diastole) (7). The data we obtained are compatible with this information. In cases with DCM, reduction of fractional shortening (FS <20%) is an expected result (7). In these cases, the differences of FS can be explained by the fact that fractional shortening is affected by hemodynamic status (15). Decreasing myocardial contractility may cause increased fractional shortening. Since it was known that the cat was feeding with a balanced diet, that the limitations of the test were used to identify taurine deficiency and that the response to taurine appears the most reliable method in deficiency, taurine supplementation recommended to the owners regardless of the whole blood concentration (1, 18). The prognosis of idiopathic DCM is poor. In one study, the median survival time was reported to be 11 days (9) while in another one it was 49 days in cats treated with pimobendan (13). Cases presented here remains alive at 1 month following the diagnosis.

In conclusion the cases presented here reflect clinical signs, cardiological examination findings, diagnosis and management of idiopathic dilated cardiomyopathy in 2 cats. We hope that this study will contribute to determining the feline idiopathic dilated cardiomyopathy and help veterinary practitioners.

Financial Support

This research received no grant from any funding agency/sector.

Ethical Statement

This study does not present any ethical concerns.

Conflict of Interest

The authors declared that there is no conflict of interest.

References

1. **An S, Jang H, Lee H, et al** (2016): *Clinical and echocardiographic findings for dilated cardiomyopathy induced by taurine deficiency in a cat*. J Vet Clin, **33**, 205-209.
2. **Andrei B, Angela D, Di Loria A, et al** (2016): *Cardiac biomarkers in clinical practice of dog and cat – a review*. Hum Vet Med, **8**, 50-58.
3. **Andrei B, Turcu C, Vulpe V** (2020): *Nutritional dilated cardiomyopathy in cats -a report of two cases.* Hum Vet Med, **12**, 28-32.
4. **Aroch I, Keidar I, Himelstein A, et al** (2010): *Diagnostic and prognostic value of serum creatine-kinase activity in ill cats: a retrospective study of 601 cases*. J Feline Med Surg, **12**, 466-475.
5. **Côté E, Harpster NK, Laste NJ, et al** (2004): *Atrial fibrillation in cats: 50 cases (1979-2002)*. J Am Vet Med Assoc, **225**, 256-260.
6. **Côté E, Jaeger R** (2008): *Ventricular Tachyarrhythmias in 106 Cats: Associated Structural Cardiac Disorders*. J Vet Intern Med, **22**, 1444-1446.
7. **Côté E, MacDonald KA, Meurs KM, et al** (2011): Dilated Cardiomyopathy. 183-187. In: Cote E. (Ed), Feline Cardiology. John Wiley & Sons, Inc, West Sussex.
8. **Ferasin L** (2012): *Feline cardiomyopathy*. In Pract, **34**, 204-213.
9. **Ferasin L, Sturgess CP, Cannon MJ, et al** (2003): *Feline idiopathic cardiomyopathy: a retrospective study of 106 cats (1994-2001)*. J Feline Med Surg, **5**, 151-159.
10. **Foster SF, Hunt GB, Thomas SP, et al** (2006): *Tachycardia-induced cardiomyopathy in a young Boxer dog with supraventricular tachycardia due to an accessory pathway.* Aust Vet J, **84**, 326-331.
11. **Gordon G** (2019): *Hyperthyroidism in cats: should we be routinely testing for early diagnosis?*. Vet Nurse, **10**, 444-452.
12. **Greet V, Sargent J, Brannick M, et al** (2020): *Supraventricular tachycardia in 23 cats; comparison with 21 cats with atrial fibrillation (2004–2014)*. J Vet Cardiol, **30**, 7-16.
13. **Hambrook L, Peter B** (2012): *Effect of pimobendan on the clinical outcome and survival of cats with non-taurine responsive dilated cardiomyopathy.* J Feline Med Surg, **14**, 233-239.
14. **Lawler DF, Templeton AJ, Monti KL** (1993): *Evidence for genetic involvement in feline dilated cardiomyopathy*. J Vet Intern Med, **7**, 383-387.
15. **Madron É** (2015): Global Left Ventricular Systolic Function Assessment. 111–125. In: De Madron É, Chetboul V, Bussadori C (Eds), Clinical Echocardiography of the Dog and Cat**.** Elsevier Masson, St. Louis.
16. **Meurs KM, Fox PR, Magnon AL, et al** (2000): *Molecular screening by polymerase chain reaction detects panleukopenia virus DNA in formalin-fixed hearts from cats with idiopathic cardiomyopathy and myocarditis*. Cardiovasc Pathol of J Soc Cardiovasc Pathol, **9**, 119-126.

17. **Pion PD, Kittleson MD, Rogers QR, et al** (1987): *Myocardial failure in cats associated with low plasma taurine: a reversible cardiomyopathy*. Science, **237**, 764-768.
18. **Sisson DD, Knight DH, Helinski C, et al** (1991): *Plasma taurine concentrations and M-mode echocardiographic measures in healthy cats and in cats with dilated cardiomyopathy*. J Vet Intern Med, **5**, 232-238.
19. **Smith S, Tobias A, Jacob K, et al** (2003): *Arterial thromboembolism in cats: acute crisis in 127 cases (1992-2001) and long-term management with low-dose aspirin in 24 cases*. J Vet Intern Med, **17**, 73-83.
20. **Wells SM, Shofer FS, Walters PC, et al** (2014): *Evaluation of blood cardiac troponin I concentrations obtained with a cage-side analyzer to differentiate cats with cardiac and noncardiac causes of dyspnea*. J Am Vet Med Assoc, **244**, 425-430.

Ankara Univ Vet Fak Derg, **68**, 307-310, 2021
DOI: 10.33988/auvfd.764656

Case Report / *Olgu Sunumu*

A case of vaginal hyperplasia occurred the last trimester of pregnancy in a Kangal bitch

Tarık ŞAFAK[1,a,✉], Öznur YILMAZ[2,b], Kerem ERCAN[3,c], Burak Fatih YÜKSEL[1,d], Halis ÖCAL[1,e]

[1]Fırat University, Faculty of Veterinary Medicine, Department of Obstetrics and Gynecology, Elazığ; [2]Siirt University, Faculty of Veterinary Medicine, Department of Obstetrics and Gynecology, Siirt; [3]Siirt University, Faculty of Veterinary Medicine, Department of Internal Medicine, Siirt, Turkey.
[a]ORCID: 0000-0002-6178-4641; [b]ORCID: 0000-0003-0424-9471; [c]ORCID: 0000-0003-4914-8578;
[d]ORCID: 0000-0002-7256-9189; [e]ORCID: 0000-0002-9885-6303

[✉]Corresponding author: tsafak@firat.edu.tr
Received date: 06.07.2020- Accepted date: 15.10.2020

Abstract: Vaginal hyperplasia is characterized clinically as the protrusion of edematous hyperplastic mucosa tissue through the vulvar lips. Generally, it is formed during the proestrus and estrus periods in dogs. In this case report, 12 months old, pregnant Kangal breed dog with a mass in the vagina was presented with pre and postoperative findings. The bitch without any genital problems at pro/estrus stages was mated about two months ago. During the clinical examination, it was detected that bitch was in the second stage of labor and had type III vaginal hyperplasia. After the delivery of nine puppies without complication, the bitch was placed under general anesthesia and the hyperplasic tissue was removed surgically. Although no hyperplasia history at pro/estrus stages of the bitch, the fact that vaginal hyperplasia was observed in the last trimester of pregnancy is remarkable. Interestingly, this hyperplastic mass did not cause dystocia during all the puppies' delivery in this case. In conclusion, in pregnant dogs, routine genital exams should be performed once at least until parturition to control vaginal structural integrity.
Keywords: Bitch, pregnancy, vaginal hyperplasia.

Kangal ırkı bir köpekte gebeliğin son trimesterinde meydana gelen bir vajinal hiperplazi olgusu

Özet: Vajinal hiperplazi, klinik olarak ödematöz hiperplastik mukoza dokusunun vulva dudaklardan dışarı çıkması olarak karakterize edilir. Genellikle köpeklerde pro/östrüs dönemlerinde şekillenir. Bu olgu raporunda, 12 aylık, vajinasında kitle bulunan Kangal ırkı gebe bir köpeğin ameliyat öncesi ve sonrası bulguları sunuldu. Proöstrüs ve östrüs dönemlerinde herhangi bir genital problemi olmayan köpek yaklaşık iki ay önce çiftleştirildi. Muayene sırasında, köpek doğumun ikinci aşamasında idi ve tip III vajinal hiperplazisi vardı. Dokuz yavrunun sorunsuz şekilde doğmasından sonra, köpek genel anestezi altına alındı ve hiperplazik doku cerrahi yolla uzaklaştırıldı. Siklusun pro/östrüs dönemlerinde hiperplazi öyküsü olmamasına rağmen, gebeliğin son trimesterinde vajinal hiperplaziye rastlanması dikkat çekicidir. İlginç şekilde, bu hiperplastik kitle hiçbir yavrunun doğumunda güç doğuma neden olmamıştır. Sonuç olarak, gebe köpeklerde doğuma kadarki süreçte vajinal yapının bütünlüğünü kontrol etmek amacıyla en az bir kez rutin genital muayeneler yapılmalıdır.
Anahtar sözcükler: Dişi köpek, gebelik, vajinal hiperplazi.

Vaginal hyperplasia is defined as a protrusion of edematous vaginal tissue into the vaginal lumen and often through the vulvar lips of the bitch. It has been reported as the high estrogen level during the follicular phase of cycles in young bitches, etiologically (4, 10). Clinically, there are three types: type I, type II, and type III. In cases of type I vaginal hyperplasia, the hyperplasic tissue has progressed slightly towards the base of the vagina but is not seen between the vulvar lips. Type II is characterized by protrusion of anterior floor and lateral walls of the vagina through the vulvar opening giving protruding mass the shape of a pear. In type III, the vaginal wall is fully eversion and is visible the entire circumference of the vaginal mucosa outside of the vulvar lips (7). The initial treatment schedule includes hormonal therapy with GnRH (Gonadotropin-Releasing Hormone) analogue or hCG (Human Chorionic Gonadotropin) analogue that causes induction of ovulation and shortening of the estrus. But,

the radical treatment of vaginal hyperplasia is to surgically remove the mass. The operative method consists of submucosal resection or vaginal amputation. Nevertheless, there is a possibility of recurrence during the next follicular phase (1, 7). Another treatment option is ovariectomy or ovariohysterectomy in bitches that do not want to conceive (12). The objective of this case was to determine the effect of type III vaginal hyperplasia events that occurred on the 40-45th days of pregnancy on parturition.

The material of this case presentation was a bitch that 12 months old, Kangal breed, weighing 36 kg. The bitch was referred with protruded mass from the vagina to the Clinic of Obstetrics and Gynecology, Faculty of Veterinary Medicine, Fırat University. According to the owners, she mated about 60 days ago without any genital problems at mating day, also the following days. But, at 40-45th days postcoitally, a pink-red colored formation emerged from the vulva has seen. On clinical examination, rectal temperature, heart rate, respiratory rate, and blood tests were within normal limits. The vaginal wall is fully eversion and is visible the entire circumference of the vaginal mucosa outside of the vulvar lips. Vaginoscopy and digital palpation were performed to identify any lacerations, perforations or ruptures and no such lesions were found. Cervix was found to be dilated during vaginoscopy. Also, a fetus inside the amniotic sac was seen. The case was diagnosed as type III vaginal hyperplasia and the bitch was being in the second stage of labor (Figure 1). To obtain information about signs of fetal viability and fetal stress, fetal heart rates were evaluated from each visible fetus by using a 5 MHz convex probe in M-mode by transabdominal ultrasonography (Mindray DC-T6 Color Doppler Ultrasound System; Shenzhen, China) as described by Gil et al. (8). It was found that fetal distress had not started yet, because the fetal hearts in the fetuses were more than 200 beats per minute (bpm) in each visible fetus. Moreover, according to the results of X-rays, the presentation, position, and posture of the first fetus entering the birth canal were found suitable for vaginal delivery. Additionally, nine puppies were determined by counting the fetal heads. To take the support of the Ferguson reflex, it was massaged to the dorsal wall of the vagina. A total of nine live puppies were born through the birth canal in six hours. After delivery, the dam and puppies were hospitalized. To remove surgical treatment of the protruded mass, she was undergone general anesthetized with Xylazine hydrochloride 2 mg/kg IM (Rompun® 2%, Bayer, Turkey) and 10 minutes later Ketamine hydrochloride (Ketasol®10%, Richterpharma, Austria) at the dose of 10 mg/kg. Preoperatively, a catheter (size 8 gauze number) was applied to the *orificium urethra externa* to prevent damage to the urethra. As described by Ahuja et al. (1), the horizontal-U suture was applied, covering all layers of the mass and passing through each other with absorbable sewing thread (PGLA, USP:2, Medeks, Turkey). After the sutures were completed, protruded mass was carefully excised in a circumferential pattern (Figure 2). The urinary catheter was removed after the completion of the surgery. Postoperatively, Penicillin G-Streptomycin sulphate (Vetimisin, Vetas, Turkey) was administered intramuscularly at the dose of 0.25ml/2.5kg for 5 days and Meloxicam (Meloxicam, Bavet®, Turkey) was administered subcutaneously at the dose of 0.2 mg/kg for 3 days. Although a spaying operation was recommended to reduce the risk of recurrence, it was not performed because of the owner's refusal. The bitch was observed that she was followed up periodically in the postoperative period and the general condition of the bitch was good without any complication.

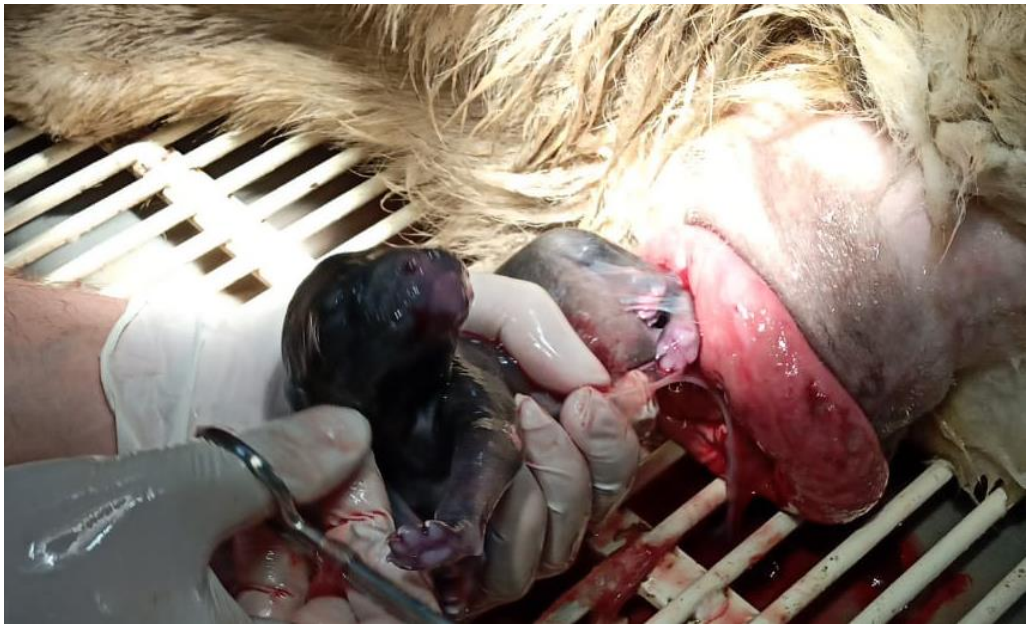

Figure 1. The extraction of the puppy from the vagina with type III hyperplasia.

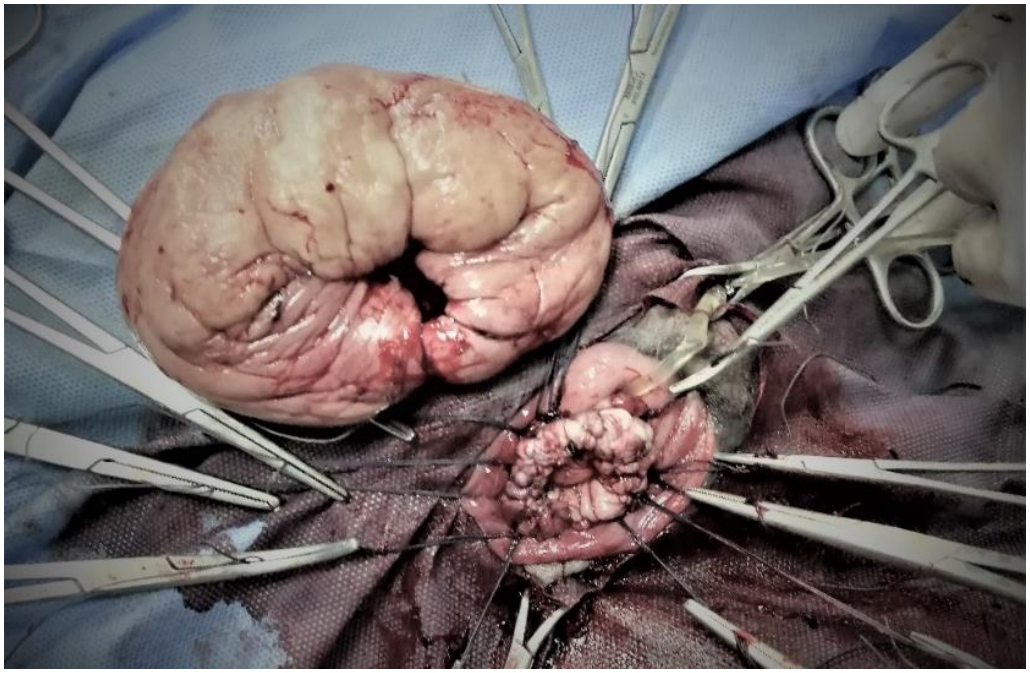

Figure 2. The macroscopy of the excised mass after removing by circumferential incision.

Vaginal hyperplasia is a rather uncommon condition in pregnant bitches and many factors play role in its formation, and usually occur in young bitches during the proestrus or estrus stages when blood estrogen levels are high (10). In the case presented by Ajadi et al. (2), similar to the case presented by us, vaginal hyperplasia was observed in a young bitch. But, in this case, vaginal hyperplasia was in the pregnant dog, and it was without dystocia. The incidence of dystocia in canine practice varies between 2-5%. As evaluating etiologically, it has been reported that the dystocia cases occur caused by maternal (75.3%) and fetal (24.7%) reasons, respectively (4, 10). Among maternal disorders, vaginal hyperplastic masses are known to make the birth canal shrinking and cause dystocia. In such cases, it is recommended to remove the fetuses by cesarean section (3, 5, 6). In the presented case, vaginal hyperplasia did not cause canal stenosis although it was type III. It was observed that the puppies were born through the normal birth canal without the need for cesarean section. Likewise, some researchers reported that they did not encounter dystocia (9, 11). In the case presented by Gouletsou et al. (9), in 47th days of pregnancy, in a case of vaginal hyperplasia, the bitch was hospitalized and local therapy was continued for four days until parturition of four healthy puppies. In the case we presented, it is thought that the hyperplastic tissue begins to form due to the increased estrogen level in the last period of pregnancy. In the presented case, a spaying operation was recommended to reduce the risk of recurrence, but the owner was reluctant to allow it. Only the hyperplasic tissue was removed by operation. In the case presented by Samal et al. (13), only the hyperplasic tissue was amputated without ovariohysterectomy. Similar studies support this knowledge (2, 11, 14). In the presentations of some researchers, ovariohysterectomy was performed to prevent the recurrence of vaginal hyperplasia and because the animal owners did not want to conceive (5, 6).

In conclusion, although the canine vaginal hyperplasia cases were generally seen during the proestrus and estrus stages of the cycle, what makes this case important is that the vaginal hyperplasia was seen in the last trimester of pregnancy, and the mass was first noticed approximately 15 days before parturition. Also, it was observed that the vaginal hyperplasia that occurred in the last trimester of pregnancy was not an obstructive effect in the parturition process in this case. To control vaginal structural integrity, routine genital exams should be performed once at least during pregnancy. In cases with vaginal hyperplasia, the whole parturition process should be monitoring with a clinician accompanied. Following deliveries, removing of vaginal mass and spaying operation should be done for recurrence management.

Acknowledgements

This case report was presented as a poster presentation at "VIII. National & II. International Congress of Turkish Society of Veterinary Gynecology" between 10-13 October 2019 in Antalya/Turkey.

Financial support

This research received no grant from any funding agency/sector.

Ethical Statement

This study does not present any ethical concerns.

Conflict of Interest

The authors declared that there is no conflict of interest.

References

1. **Ahuja AK, Dhindsa SS, Kumar A, et al** (2018): *Surgical approach for vaginal hyperplasia and vaginal fold prolapse in bitch.* J Anim Health Prod, **6**, 86-89.
2. **Ajadi TA, Ajayi OL, Adeniyi AA, et al** (2016): *Vaginal wall hyperplasia with fold prolapse in an eight-month-old Cane Corso dog.* Bulg J Vet Med, **19**, 252-258.
3. **Alan M, Cetin Y, Sendag S, et al** (2007): *Short communication true vaginal prolapse in a bitch.* Anim Reprod Sci, **100**, 411-414.
4. **Arthur GH** (1996): Maternal dystocia and treatment. 228-244. In: GH Arthur, DE Noakes, HA Pearson, TJ Parkinson (Eds), Veterinary Reproduction and Obstetrics. WB Saunders, Philadelphia.
5. **Baki-Acar D, Birdane MK** (2017): *Urinary bladder retroflexion and dystocia in a bitch with the vaginal supportive connective tissue failure.* Ankara Univ Vet Fak Derg, **64**, 61-64.
6. **Canatan HE, Ergin I, Polat IM, et al** (2015): *Unusual cases of vaginal prolapse concurrent with cystocele in two dogs.* Revue Med Vet, **166**, 43-46.
7. **Canooğlu E** (2013): *Köpeklerde vajinal hiperplazi: tanı ve teşhis seçenekleri*. Erciyes Univ Vet Fak Derg, **10**, 177-183.
8. **Gil EM, Garcia DA, Giannico AT, et al** (2014): *Canine fetal heart rate: do accelerations or decelerations predict the parturition day in bitches?* Theriogenology, **82**, 933-941.
9. **Gouletsou PG, Galatos AD, Apostolidis K, et al** (2009): *Vaginal fold prolapse during the last third of pregnancy, followed by normal parturition, in a bitch*. Anim Reprod Sci, **112**, 371-376.
10. **Johnston SD, Kustritz MVR, Olson PNS** (2001): Canine and Feline Theriogenology. W.B. Saunders Company, London.
11. **Konig GJ, Handler J, Arbeiter K** (2004): *Rare case of a vaginal prolapse during the last third of pregnancy in a Golden Retriever bitch.* Kleintierpraxis, **49**, 299-305.
12. **Mostachio GQM, Vicente WRR, Cardilli DJ, et al** (2007): *Anovulvar cleft and vaginal prolapse-hyperplasia in a bitch.* J Small Anim Pract, **48**, 713–715.
13. **Samal P, Jena D, Singh J, et al** (2016): *Vaginal hyperplasia in a Pug: a case report.* Indian Vet J, **93**, 81-82.
14. **Singh J, Poyam MR, Ratre HK, et al** (2017): *Surgical management of vagina prolapse in a nulliparous dog.* ISACP, **9**, 167-168.

Ankara Univ Vet Fak Derg, **68**, 311-320, 2021
DOI: 10.33988/auvfd.909936

Review / *Derleme*

Novel ultrasonographic imaging technique in cat and dog intensive care patients: A-FAST^3

Yusuf ŞEN[1,a, ✉], Medine İrem BAŞER[1,b], Büşra KİBAR KURT[2,c], Ali BUMİN[1,d]

[1]Ankara University, Faculty of Veterinary Medicine, Surgery Department, Ankara, Turkey; [2]Aydın Adnan Menderes University, Faculty of Veterinary Medicine, Surgery Department, Ankara, Turkey
[a]ORCID: 0000-0002-8137-3858; [b]ORCID: 0000-0002-3784-9820; [c]ORCID: 0000-0002-1490-8832; [d]ORCID: 0000-0001-8468-1330

✉Corresponding author: dr.yusufsen@gmail.com
Received date: 05.04.2021 - Accepted date: 25.06.2021

Abstract: Focused Assessment with Sonography for Trauma (FAST) and Veterinary point-of-care ultrasonography (POCUS) are fast ultrasonographic diagnostic tools developed to discover pathologies in trauma patients in veterinary medicine and direct veterinarians to accurate treatment plans. Aside from detection, scoring and treatment protocol establishment in traumatic and non-traumatic hemoabdomen cases, AFAST (abdominal FAST) sonography is used effectively to define anaphylaxis, pericardial effusions and cardiac tamponade and pleural effusion symptoms. This technique when implemented every 4 hours for 3 to 5 minutes assists in identification of patient prognosis and treatment protocols through focused imaging.

With this review, we aimed to explain and deliver in detail indications for AFAST^3 technique, know-how and clinical benefits for trauma patients.

Keywords: A-Fast, diagnostic imaging, emergency protocols, ultrasound.

Kedi ve köpek yoğun bakım hastalarında yeni ultrasonografik görüntüleme tekniği: A-FAST3

Özet: Focused Assesment with Sonography for Trauma (FAST) ve Veterinary point-of-care ultrasonography (POCUS), veteriner hekimlikte travma hastalarında patolojileri çabuk bulma ve yol göstermek için geliştirilmiş, hızlı ultrasonografi tanı yönlemleridir. AFAST (abdominal FAST) ultrasonografi yöntemi ile travmatik ve travmatik olmayan hemabdomen durumlarının belirlenmesi, skorlanması ve sağaltım protokolünün oluşturulması dışında, anafilaksi, perikardiyal efüzyonlar ve kardiak tamponad, plevral efüzyonun belirtilerinin de belirlenmesinde etkin şekilde kullanılmaktadır. Her 4 saatte, 3-5 dakikalık odaklanmış (focused) görüntüleme ile hastanın prognozu ve sağaltım protokollerinin belirlenmesine yardımcı olur.

Bu yazıda, AFAST^3 tekniğinin hangi durumlarda kullanıldığını, nasıl yapıldığını ve travma hastalarına klinik faydalarını detaylı şekilde aktarmayı amaçladık.

Anahtar sözcükler: A-Fast, acil protokolleri, diagnostik görüntüleme, ultrason.

Introduction

Doctors in human medicine have been conducting ultrasonographic assessments in trauma patients since the 1980s (11). FAST (focused assessment with sonography for trauma) was studied in detail in the early 1990s and has developed to be the diagnostic tool of choice for assessment of free fluid in peritoneal and pleural cavities (25), followed by a study performed to determine pneumothorax, pleural and pericardial effusions in thoracic trauma (E-FAST) (13). New intensive care protocols have been developed (FAST-ABCDE) in order to determine respiratory and circulatory disorders and airway obstructions more urgently (31). In line with these advances in human medicine, it is considered a necessity to establish fast diagnostic protocols to identify pathologies in trauma patients in small animals.

Focused assessment with sonography for trauma (FAST) has been identified prospectively by Boysen in 2004 in dogs with trauma (3). Boysen has reported with this study that intraabdominal traumas, particularly hemoabdomen occur more frequently despite previous studies. Lisciandro has supported Boysen's findings with a similar study he conducted on dogs. These two authors have used the term A-FAST (abdominal FAST) for the fast sonography scanning technique they have developed for trauma patients. They have named the technique

performed for the thoracic region in order to better identify this fast scan as T-FAST (thoracic FAST) (21). Authors preferred and globalized these abbreviations to avoid any possible confusion with similar terms in human medicine. Again in 2009 Lisciandro has performed intraabdominal hemorrhage assessment using this scanning technique every 4 hours in all hospitalized dogs beginning from their initial evaluation and established a scoring system. With this study, he was able to differentiate small size hemorrhages from traumas with serious blood loss (22).

With the same study, AFAST has been considered an excellent diagnostic method to determine hemorrhages occurring during the following process in patients with no initial intraabdominal bleeding. Based on the results of scoring, it was possible to evaluate developing anemia in patients with severe blood loss and present their need for blood transfusion or an exploratory laparotomy with this novel diagnostic method (22).

Researchers have compared their results with the research of 2011 to form a triage system by determination of the need for blood transfusion in dogs with hemoabdomen, or by regulation of present fluid therapy protocol (15).

AFAST sonographic technique lasts approximately 3 to 5 minutes and other than determination, scoring, and treatment protocol establishment of traumatic or non-traumatic hemoabdomen cases, it is also facilitated effectively for identification of anaphylaxis, pericardial effusions and cardiac tamponade, pleural effusion. This technique is not performed only for trauma, but its diagnostic value for critically ill dogs or cats has also been demonstrated (27). Based on all these reasons, current terminology as AFAST has been converted to AFAST^3. "T^3" represents AFAST use for trauma, triage, and tracking (6, 17).

What does AFAST^3 ultrasonography method provide us?

AFAST^3 can detect free fluid even in small quantities superior to physical examination and abdominal radiography techniques, on a level equal to computed tomography (CT) which is accepted as the golden standard (40).

- Predicts the degree of anemia following trauma in patients with no previous apparent anemia by performing an abdominal fluid scoring (AFS). Low levels of bleeding are scored as AFS1 and AFS2, whereas severe blood accumulations are scored as AFS3 and AFS4.
- Using the same scoring provides information regarding the degree of anemia formation in non-trauma patients with hemoabdomen (ruptured spleen, coagulopathy, etc.).
- Scoring is possible after checking the development of any effusion in postoperative period controls (complications such as peritonitis) (2, 22).
- While performing an assessment through diaphragm-liver window, pericardial and pleural effusions with clinical significance do not go unnoticed. Changes in gall bladder indicative of anaphylaxis can be defined and possible hepatic venous tension and right heart pathologies can be noticed even with the evaluation of estimated caudal vena cava size (2, 33).

Most importantly, with this assessment performed every four hours which lasts only for 3 to 5 minutes, sensitivity to the patient increases, and any possible pathology can be detected at the very beginning of the process (2).

What is not possible to achieve with AFAST^3 and AFS scoring?

- We cannot determine free fluid characteristics; therefore, it is obligatory to perform an ultrasound-guided abdominocentesis to obtain a sample for analysis.
- Scoring is not objective in penetrating traumas in contrast to blunt traumas. Degrees of anemia can be deceiving.
- Can be insufficient to the determination of the degree of anemia in cats with trauma because in cats the source of free fluid can be urine due to a ruptured bladder (2).

When we should perform AFAST^3?

- As standard assessment of intraabdominal free fluid in all patients with blunt trauma
- In patients with unexplained hypotension, tachycardia and mental alterations
- All patients with anemia
- Cases with risk of hemorrhage following surgery and biopsy
- Patients with risk of peritonitis
- Cases requiring abdominocentesis (2).

How to perform AFAST^3 sonography method

Ultrasonographic method and probe preferences: Convex, micro convex, or linear probes with a range of 5–10 MHz are suitable. For cats, linear probes, and particularly for especially large breed dogs, convex probes should be selected. These selections for sure change based on the ultrasound machine at hand and size of the patient, however ultrasound machine gain (d2) is set to 70%. This adjustment enables imaging even in the light environment (2, 3).

Patient positioning: Hair is usually not trimmed alcohol and ultrasound gel are sufficient. However, in patients with heavy fur such as Anatolian Shepherds and

Siberian huskies, trimming may be needed. Image quality may be enhanced in these patients with small trimming points (15, 22). If it is anticipated to use a defibrillator in a patient, alcohol use must be avoided. Otherwise, severe burns may occur. In addition, it must be kept in mind that alcohol use will cause damage on probe tips in elongated periods.

The patient is assessed on lateral recumbency. There is no difference in practice among patients in right lateral or left lateral recumbency. However, if electrocardiographic and echocardiographic examinations will also be performed on the patient, right lateral recumbency position is more suitable. Left kidney, gall bladder, and bladder assessment are more comfortable in patients in right lateral recumbency. Again, in this position, abdominocentesis is safer because the spleen is anatomically located on the left side of dogs and cats (2, 18).

- Modified sternal position can also be preferred in stressed patients where it is difficult to create lateral recumbency. In dorsal recumbency, acoustic windows used in AFAST assessment cannot be facilitated correctly, therefore free fluid cannot be assessed accurately. In these cases, AFS scoring is misleading. Again, in patients with respiratory distress, dorsal recumbency can elevate stress (15, 37).

AFAST[3] window nomenclature: AFAST examination is performed by assessment of diaphragm, liver, gall bladder, spleen, kidneys, intestinal segments, and bladder circumference in order to detect free fluid in the peritoneal cavity (2).

Free fluid is anechoic and is detected around organs as independent black areas. Assessment usually begins with the diaphragm and continued clockwise in the right lateral recumbency patient (28).

1. Diaphragmatic-hepatic (DH) window
2. Spleno-renal (SR) window
3. Cysto-colic (CC) window
4. Hepato-renal (HR) window, assessment is concluded with this window and this window is the most appropriate window for abdominocentesis.

To start the assessment, a probe marker is placed into the sonographic window in a manner to locate cranially. This is how longitudinal assessment is performed and then the probe is turned to right 90 degrees to realize a transversal scan. Longitudinal assessment is solely successful and sufficient to evaluate fluid presence (3).

Diaphragmatic-hepatic window (DH): Place probe under subxiphoid (Figure 2). Enhance image depth in the ultrasound machine. The objective in this window is to observe fluid accumulation between the liver and diaphragm. The liver is in contact with the diaphragm in a healthy animal. If there is fluid present, an anechoic line is observed between these two structures (Figure 3).

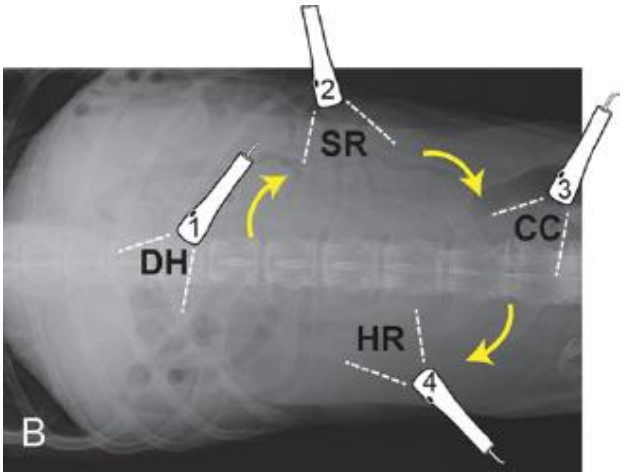

Figure 1. Ultrasonography views for Afast. DH= diaphragmatic-hepatic view, SR= Spleno-renal view, CC=cystocolic view, HR= hepato-renal view (2).

Figure 2. Placement of probe for diaphragmatic-hepatic window.

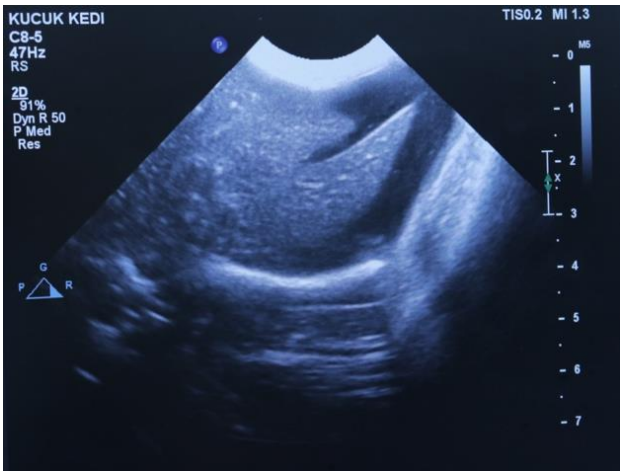

Figure 3. Diaphragmatic-hepatic window showing liver (L), diaphragm (D) and large amounts of interposed peritoneal effusion (E).

Gall bladder, caudal vena cava, pleural and pericardial cavities are also assessed through DH window (16, 20). The gall bladder is located between the right median and quadrate lobes of the liver in dogs, and in the right median lobe right to linea alba in cats. In normal gall bladder of dogs and cats appears as an anechoic, thin-walled, oval-round structure.

Gall bladder shape and structure must be noted. In cases where it is not possible to visualize the gall bladder, it must be kept in mind that a rupture may be present, as well as a dislocation as a result of a diaphragmatic hernia.

Small quantities of fluid are typically located in between the liver and diaphragm and also liver lobes. Even though a marked free fluid is absent between the diaphragm and liver, attention must be paid to fluid presence between lobes. Following fluid presence assessment between diaphragm and liver, evaluate thoracic cavity by enhancing ultrasound machine depth. Pleural and pericardial effusions can be identified through this window.

In a clinical study, it was demonstrated that 88% of pericardial effusions can be identified through DH window (16). However pericardial effusion, pleural effusion, and dilated cardiomyopathy (DCM) images may be melded in this window image. Any interventional centesis procedure must be avoided solely based on DH window image. Once fluid presence is determined in the thoracic cavity, thorax examination for such patient must be continued through the thoracic cavity (with T-FAST method). Thorax imaging may not always be possible due to the depth insufficiency of ultrasound machines used in large animals.

Finally, caudal vena cava (CVC) diameter can be subjectively evaluated and hepatic venous distension is identified. CVC wall is observed as two parallel echoic lines and resembles a big “equal to” mark. Hepatic veins are present in the liver as branches of CVC (8, 12, 30). If hepatic veins are observed large like tree branches, right heart failure, obstructive pathologies between right atrium and liver, caval syndrome, Budd-Chiari-like syndrome, and pathologies like liver cirrhosis must be considered (1, 9).

There are also artifacts while assessing DH window which can mislead the veterinary surgeon. The sound wave is refracted while passing through a solid tissue like a diaphragm to a thoracic cavity filled with gas and causes the appearance of an identical reflection of an image in the abdominal cavity in the thorax (mirror artifacts). This condition can cause false positive scoring or false diagnoses such as pleural effusion and diaphragmatic hernia (4, 26, 32).

Veterinary surgeons in charge of sonography must not forget that these artifacts may occur. Occasionally side lobes of the gall bladder can reflect inside the gall bladder (side-lobe artifacts) and can cause images as if there is mud or sedimentation within. In order to avoid this situation, slightly change probe angle and re-evaluate inside of gall bladder.

Figure 4. Probe position for Spleno-renal window.

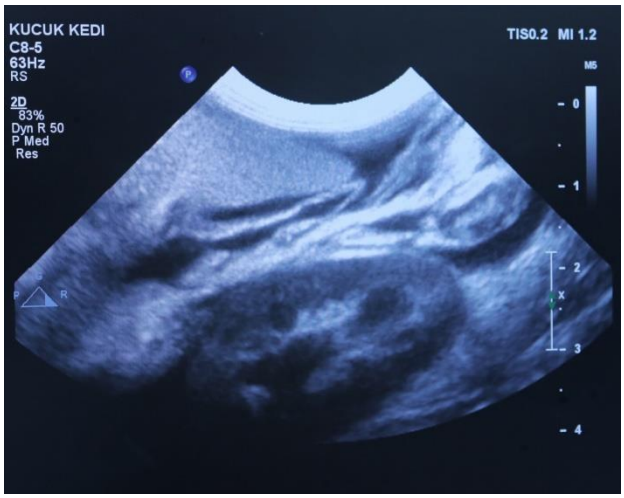

Figure 5. An image of effusion evaluated from Spleno-renal penrece. LK = left kidney, E= effusion.

Spleno-Renal window (SR): Spleno-renal (SR) window demonstrates the presence of free fluid both around the spleen (peritoneal cavity) and left kidney (retroperitoneal cavity). The probe is positioned caudal to final rib and ventral to lumbar hyperaxial muscle to form a long axis image. Anechoic areas around the kidney or spleen, but generally between small intestine segments represent effusion (Figure 5). the presence of a cavity mass

in this area usually indicates spleen tumors (23). It may pose some difficulty to differentiate small fluid accumulations right adjacent to the kidney as peritoneal or retroperitoneal. Retroperitoneal fluid at this particular area must raise doubts for hemorrhage, urine, and sterile and septic effusions (17).

Large veins (aorta and caudal vena cava) progressing immediately medial to left kidney should also be assessed through SR window. Veins are observed as anechoic areas in between hyperechoic straight lines. The probe is turned counter-clockwise to see transversal cross-sections of veins that appear as anechoic areas. If the probe is held in a stationary position, pulsation in the aorta can be easily noticed.

Colon localizes to the right side in a right lateral recumbency patient, which facilitates spleno-renal area assessment. In very small cats, the right kidney can also appear in the image during assessing the left kidney. It must be acknowledged by the veterinary surgeon in charge of sonography that this image is not a mirror artifact (32).

Cysto-Colic window (CC): Cysto-colic (CC) window aims to detect free fluid presence in Greg pouch positioned between urinary bladder and ventral wall. In small-volume effusions when CC window score is positive, fluid accumulation in a triangle shape is observed between urinary bladder apex and ventral abdominal wall (Greg pouch). In large volume fluid accumulations, fluctuation movement of small intestines and omentum in free fluid is observed. This is one of two windows that generally present a positive outcome in small volume fluid accumulations (the other is DH window).

One should be careful during assessment when moderate fluid accumulation is present around the urinary bladder. The anechoic fluid image both inside the urinary bladder and around can cause refraction artifact and result in obstruction of visualization of a part of the urinary bladder wall. This may be falsely interpreted as a urinary bladder rupture. Urinary bladder wall integrity must be assessed in multiple different angles, and it must be kept in mind that the urinary bladder sustains a collapsed appearance in ruptures (2, 32).

Hepato-Renal window: Hepatorenal (HR) window is a relatively difficult window for assessment especially in large breed dogs. The probe must be directed to the table, which means ventral direction in patients with right lateral recumbency (Figure 8). Right kidney is located in caudate lobe of liver in fossa renalis in dogs; in cats, is typically separated from caudate lobe of liver with retroperitoneal fat. Right kidney is generally positioned more cranially and laterally compared to left kidney. Therefore, it may defy imaging right kidney and liver juncture in large breed dogs (15, 22).

Figure 6. Positioning of probe for cystocolic acoustic window.

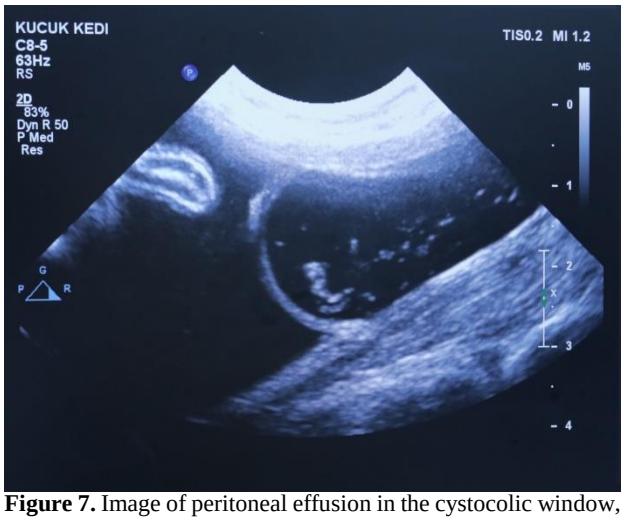

Figure 7. Image of peritoneal effusion in the cystocolic window, UB= bladder, C= colon pattern, e= peritoneal effusion.

Figure 8. Position of probe for Hepatorenal acoustic window.

Table 1. Goal-Directed Template for AFAST[3] (18).

Patient positioning	Right or left lateral recumbency	
Gallbladder	Present or absent, contour (normal or not) and wall (normal or not)	
Urinary bladder	Present or absent, contour (normal or not) and wall (normal or not)	
Diaphragmaticohepatic view	Pleural fluid	Present or absent (mild, moderate, severe) or indeterminate
	Pericardial fluid	Present or absent (mild, moderate, severe) or indeterminate
	Hepatic veins	Unremarkable or distended or indeterminate
Positive or negative at the four views (0 negative, 1 positive)		
Diaphragmaticohepatic site	0 or 1	
Splenorenal site	0 or 1	
Cystocolic site	0 or 1	
Hepatorenal site	0 or 1	
Abdominal fluid score: 0–4 (0 negative all quadrants to a maximum score of 4 positive all quadrants)		
Comments: _____.		

The AFAST[3] examination is an ultrasound scan used to detect the presence of free abdominal fluid and other conditions to better direct resuscitation efforts and patient care. AFAST[3] allows indirect assessment for evidence of intra-abdominal injury or disease and intrathoracic injury or disease. The AFAST[3] examination is not intended to replace a formal abdominal ultrasound.

Table 2. Decision-making algorithm for dogs correlating the abdominal fluid score to the anticipated degree of anemia in bluntly traumatized and post-interventional (surgery, percutaneous biopsy, laparoscopy) canine cases (2).

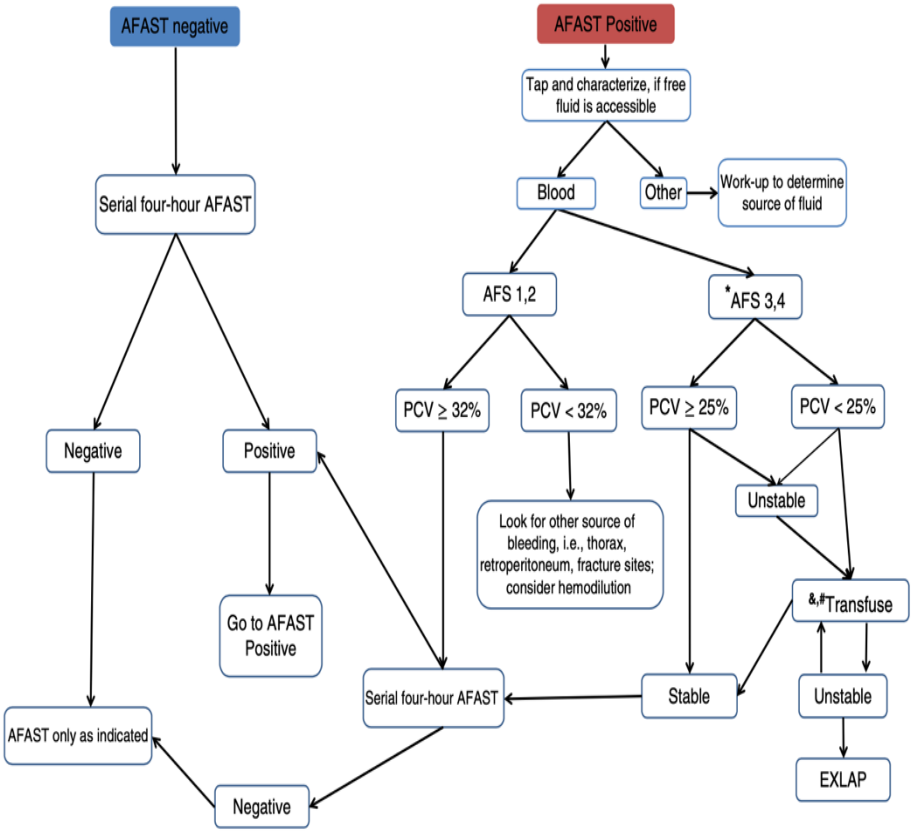

Fluid presence between liver and kidney indicates retroperitoneal and peritoneal effusion (Figure 9). While scanning this particular area, fluid presence is investigated rather than focusing on liver and kidney. It has been reported that scans performed with the transversally positioned probe are more effective in detecting free fluid (22). Scanning is concluded with this window. Even mild volumes of fluid can be observed through this window under influence of gravity. If abdominocentesis is in question, it is generally performed with guided sonography through this window (2).

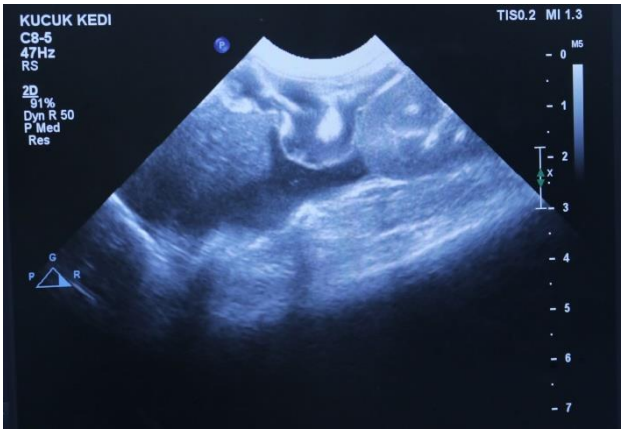

Figure 9. Peritoneal effusion image from Hepatorenal acoustic window. RK= right kidney, L= liver, * = peritoneal efüyon.

In cases where it is necessary to image right kidney, recumbency position is converted to dorso-lateral in small-size dogs and cats. In cases where it is not possible to assess the kidney, the dog is positioned to left lateral position as in larger breed patients.

How to perform Abdominal Fluid scoring (AFS)?

Although the abdominal fluid scoring system is used predominantly for hemoabdomen assessment, urine or bile can also be present as free fluid, therefore fluid scoring terminology is deliberately used.

Following is how AFS scoring is done; each window has 1 point. If all windows are negative, 0, if all of them are positive, maximum AFS is scored 4 (10, 22).

AFS evaluation in dogs: In dogs, AFS 1 and 2 represent small and AFS 3 and 4 severe hemorrhages. In dogs with AFS scored 1 and 2, if there is no previous anemia and hemorrhages if AFS score remains 1 or 2 in the assessment series (A-FAST once every 4 hours), these patients do not develop severe anemia. No blood transfusion or exploratory laparotomy is required. in more recent research, scores 1 and 2 have been categorized for very small amounts of liquids (19). The patient's condition is regarded as stable. In cases where packed cell volume (PCV) is less than 30%, and if there is no history of known anemia, the veterinary surgeon must focus on lungs and fracture sites for hemorrhage. If AFS is 3 and 4, there is no previous anemia and PCV is less than 25% blood transfusion or exploratory laparotomy is needed (3, 22, 38). It is mandatory to assess such patients surgically.

Boysen and Lisciandro have published a decision tree associating abdominal fluid score to the anticipated degree of anemia.

Clinical Significance of Abdominal Fluid Scoring (AFS) in Cats: In an assessment conducted with 49 trauma-cats, no clear connection between anemia and AFS score was identified, as was contrary in dogs (16). However; cats with hemoabdomen appear less than dogs. The reason for this is that cats have a much smaller chance of survival after car accidents compared to dogs (24). In cats with identified free fluid, the possibility of said free fluid to be urine is as high as blood.

Abdominal Fluid Score Use in Non-Traumatic cats and dogs: In non-trauma cats and dogs, abdominal fluid accumulation may occur following organ ruptures, coagulopathy (active bleeding) or surgical operation-biopsy processes and AFS can be facilitated in such patients as well. In the determination of such abdominal bleeding, AFAST^3 is much more reliable and a lot faster compared to laboratory findings (PCV), physical examination outcome, and radiography (22, 35, 36). In contrary to dogs, the prognosis for non-trauma hemoabdomen is generally bad in cats (7) and therefore AFS credibility in cats is yet to be established.

AFAST^3 can be used both in dogs and cats as an auxiliary tool to assist in physical examination for early diagnosis of hemorrhage and other complications. AFAST success regarding this particular issue has been well documented in human medicine (35, 36). Initial AFAST^3 application and series of examinations to establish an AFS score will aid in the early identification of the amount of hemorrhage. Moreover, this technique helps to define severe bleeding and directs veterinary surgeons to perform blood transfusion or laparotomy. In humans, it has been reported that even blood loss of up to 30% of total blood volume may not show with marked clinical symptoms, and attending physicians my fall into erroneous judgement (29). Blood reserves manifest with splenic contractions in dogs and prevent the patient from displaying clinical symptoms even in severe blood losses.

Coincidental lesions are frequently observed during routine AFAST examinations. These are predominantly tumors, spleen hematoma and blood clots in the urinary bladder lumen. This condition is also reported in human medicine (14).

AFAST use in Penetrating Traumas: In a study conducted with 145 dogs with penetrating trauma, it is reported that AFAST failed to identify serious intraabdominal injury in need of surgical intervention (21). The reason for this failure lies in the nature of trauma. Blood is quickly defibered in blunt force traumas and even small amounts of blood can be detected through sonography. The tissue is crushed and torn in penetrating traumas, which enhances blood clotting. Congealed blood does not appear anechoic, rather it displays shades of grey similar to soft tissue. It is possible to miss with sonography. However, in time, congealed blood can de-fibrine and may be defined between organs with sonography. Therefore, it is recommended to use a series of AFAST examinations in penetrating traumas as well. In addition, in penetrating cases where AFAST is positive, the patient needs an emergency laparotomy (13, 25, 39). The evaluation must continue for 12-24 hours, every 4 hours after patient admission.

AFAST use in anaphylaxis in dogs: Anaphylaxis is a condition that requires different medical treatment in dogs (5, 10, 34). In 2009, clinical use of ultrasound in dogs for anaphylaxis diagnosis is documented and it has been shown of service. Since shock organs in dogs are the liver and gastro-intestinal system, hepatic venous congestion (in a few seconds experimentally) immediately occurs with massive histamine release in portal circulation (33). As a result, gall bladder wall is thickened and a double-layer wall image appears.

This pathology in gall bladder wall develops much faster (less than two to four minutes) than shock indicators such as alanine transaminase (ALT) level (peak level in two to four hours). This alteration in gall bladder is called “halo sign” (33). It must be acknowledged that other factors including conditions that cause venous and lymphatic obstruction such as cardiac tamponade and congestive heart failure will manifest in halo sign appearance (normal thickness in dogs is less than 2-3 mm); Halo sign can be noticed in diseases affecting regional anatomy such as pancreatitis, cholangiohepatitis and primary gall bladder pathologies, severe hypoalbuminemia and excessive resuscitation (30).

In addition to halo signs in dogs with anaphylactic shock, fluid accumulation generally with low AFS score (AFS1 or AFS2) is noticed through DH window. Although rarely, AFS 3 and AFS 4 can also be detected. Ensuring the presence of anaphylaxis at this point will avoid a false experimental laparotomy. Clotting time increases, ALT levels are significantly high and hemoconcentration is detected in anaphylaxis (5).

It is crucial to determine whether the patient with halo sign has anaphylaxis or cardiac tamponade. Once halo sign is noticed in the gall bladder, it is recommended to perform an obligatory heart examination (with T-FAST). Because if treatment is initiated assuming the presence of anaphylaxis, but actually there is cardiac tamponade, this treatment may prove to be fatal (20, 30).

AFAST^3 use and DH appearance for Pericardial Effusions: DH window provides a good acoustic window to image the heart. To monitorize the apical aspect of the heart in cats and in small to medium-size dogs, the depth and focus of the ultrasound machine must be adjusted. Pericardial effusion appears as a thin line of anechoic area around the cardiac apex. Using only this window, it may not be possible to differentiate between pericardial and pleural effusion; that’s why when pleural and pericardial effusion is present, T-FAST examination is a must in dogs or cats (17).

Conclusion

AFAST^3 is a sonographic imaging technique more superior to other imaging methods due to its ability to provide rapid information associated with patient prognosis and to direct the surgeon to more accurate treatment.

- A-FAST must routinely be used in cats and dogs with blunt traumas in addition to clinical examination.
- Examination duration must be limited to 3-5 minutes.
- Series of AFAST examinations in trauma patients must always continue in 4-hour intervals starting from patient admission. Including peritonitis cases, following re-hydration and resuscitation of patients with penetrating trauma and patients with non-trauma risk, A-FAST assessment must be initiated and be followed for 12-24 hours.
- AFS system utilization is effectively applicable for hemorrhage in traumatized and non-traumatized dogs to estimate the degree of anemia (not reliable in cats). In addition, it can be a tracking tool for peritonitis or other effusive cases.
- Thoracic assessment should be carried out with T-FAST in patients with pericardial or pleural effusion.
- Anaphylaxis diagnosis in dogs may be supported with a gall bladder halo sign; however, one must ensure that there is no cardiac tamponade-mediated halo sign.

References

1. **Bayraktar UD** (2007): *Hepatic venous outflow obstruction: Three similar syndromes*. World J Gastroenterol, **13**, 1912.
2. **Boysen SR, Lisciandro GR** (2013): *The Use of Ultrasound for Dogs and Cats in the Emergency Room*. Vet Clin North Am Small Anim Pract, **43**, 773–97.
3. **Boysen SR, Rozanski EA, Tidwell AS, et al** (2004): *Evaluation of a focused assessment with sonography for*

trauma protocol to detect free abdominal fluid in dogs involved in motor vehicle accidents. J Am Vet Med Assoc, **225**, 1198–1204.

4. **Browne JE** (2011): *Book Review: Sonography – Principles and Instruments (8th Edition)*. Ultrasound, **19**, 242–242.
5. **Caldwell DJ, Petras KE, Mattison BL, et al** (2018): *Spontaneous hemoperitoneum and anaphylactic shock associated with Hymenoptera envenomation in a dog*. J Vet Emerg Crit Care, **28**, 476–82.
6. **Côté E** (2015): Clinical veterinary advisor. Dogs and cats St. Louis, Missouri: Elsevier Mosby, 3rd ed.
7. **Culp WTN, Weisse C, Kellogg ME, et al** (2010): *Spontaneous hemoperitoneum in cats: 65 cases (1994–2006)*. J Am Vet Med Assoc, **236**, 978–82.
8. **Darnis E, Boysen S, Merveille A-C, et al** (2018): *Establishment of reference values of the caudal vena cava by fast-ultrasonography through different views in healthy dogs*. J Vet Intern Med, **32**, 1308–18.
9. **Dillon RA, Tillson DM, Wooldridge A, et al** (2014): *Effect of pre-cardiac and adult stages of Dirofilaria immitis in pulmonary disease of cats: CBC, bronchial lavage cytology, serology, radiographs, CT images, bronchial reactivity, and histopathology*. Vet Parasitol, **206**, 24–37.
10. **Hnatusko AL, Gicking JC, Lisciandro GR** (2021): *Anaphylaxis-related hemoperitoneum in 11 dogs*. J Vet Emerg Crit Care, **31**, 80–85.
11. **Jehle D, Davis E, Evans T, et al** (1989): *Emergency department sonography by emergency physicians*. Am J Emerg Med, **7**, 605–11.
12. **Kim SY, Park KT, Yeon SC, et al** (2014): *Accuracy of sonographic diagnosis of pneumoperitoneum using the enhanced peritoneal stripe sign in beagle dogs*. J Vet Sci, **15**, 195.
13. **Kirkpatrick AW, Sirois M, Ball CG, et al** (2004): *The hand-held ultrasound examination for penetrating abdominal trauma*. Am J Surg, **187**, 660–65.
14. **Lanitis S, Zacharioudakis C, Zafeiriadou P, et al** (2012): *Incidental Findings in Trauma Patients during Focused Assessment with Sonography for Trauma*. Am Surg, **78**, 366–72.
15. **Lisciandro GR** (2011): *Abdominal and thoracic focused assessment with sonography for trauma, triage, and monitoring in small animals*. J Vet Emerg Crit Care, **21**, 104–22.
16. **Lisciandro GR** (2012): *Evaluation of initial and serial combination focused assessment with sonography for trauma (CFAST) examinations of the thorax (TFAST) and abdomen (AFAST) with the application of an abdominal fluid scoring system in 49 traumatized cats.* J Vet Emerg Crit Care, **22**, 11.
17. **Lisciandro GR** (2020): *Cageside Ultrasonography in the Emergency Room and Intensive Care Unit*. Vet Clin North Am Small Anim Pract, **50**, 1445–67.
18. **Lisciandro GR, Country H, Specialists V** (2017): Abdominal FAST (AFAST ®) and Its Fluid Scoring System for Trauma , Triage , and Tracking - Parts I and II Southwest Veterinary Symposium 2017.
19. **Lisciandro GR, Fosgate G, Romero L, et al** (2015): *Abdominal FAST (AFAST) and Abdominal Fluid Scores in Adult and Juvenile Cats*. J Vet Emerg Crit Care, **25**, 7–8.
20. **Lisciandro GR, Gambino JM, Lisciandro SC** (2021): *Thirteen dogs and a cat with ultrasonographically detected gallbladder wall edema associated with cardiac disease*. J Vet Intern Med, **35**, 1342–1346.
21. **Lisciandro GR, Lagutchik MS, Mann KA, et al** (2008): *Evaluation of a thoracic focused assessment with sonography for trauma (TFAST) protocol to detect pneumothorax and concurrent thoracic injury in 145 traumatized dogs*. J Vet Emerg Crit Care, **18**, 258–269.
22. **Lisciandro GR, Lagutchik MS, Mann KA, et al** (2009): *Evaluation of an abdominal fluid scoring system determined using abdominal focused assessment with sonography for trauma in 101 dogs with motor vehicle trauma.* J Vet Emerg Crit Care (San Antonio), **19**, 426–437.
23. **Lux CN, Culp WTN, Mayhew PD, et al** (2013): *Perioperative outcome in dogs with hemoperitoneum: 83 cases (2005-2010).* J Am Vet Med Assoc, **242**, 1385–91.
24. **Mandell DC, Drobatz K** (1995): *Feline Hemoperitoneum 16 Cases (1986-1993)*. J Vet Emerg Crit Care, **5**, 93–97.
25. **Matsushima K, Frankel HL** (2011): *Beyond focused assessment with sonography for trauma*. Curr Opin Crit Care, **17**, 606–12.
26. **Mattoon JS, Nyland TG** (2021): Small Animal Diagnostic Ultrasound Elsevier.
27. **McMurray J, Boysen S, Chalhoub S** (2016): *Focused assessment with sonography in non-trauma dogs and cats in the emergency and critical care setting.* J Vet Emerg Crit Care, **26**, 64-73.
28. **Milley E, Boysen S, Stillion J** (2017): *A general practitioner's guide to FAST cageside ultrasound techniques*. Companion Anim, **22**, 388–93.
29. **Muir W** (2006): *Trauma: physiology, pathophysiology, and clinical implications*. J Vet Emerg Crit Care, **16**, 253–63.
30. **Nelson NC, Drost WT, Lerche P, et al** (2010): *Noninvasive estimation of central venous pressure in anesthetized dogs by measurement of hepatic venous blood flow velocity and abdominal venous diameter*. Vet Radiol Ultrasound
31. **Neri L, Storti E, Lichtenstein D** (2007): *Toward an ultrasound curriculum for critical care medicine*. Crit Care Med. **35**, S290–304.
32. **Powles AE, Martin DJ, Wells IT, et al** (2021): *Physics of ultrasound*. Anaesth Intensive Care Med. **22**, 58–63.
33. **Quantz JE, Miles MS, Reed AL, et al** (2009): *Elevation of alanine transaminase and gallbladder wall abnormalities as biomarkers of anaphylaxis in canine hypersensitivity patients*. J Vet Emerg Crit Care, **19**, 536–44.
34. **Rachael B, Thomas G, Karen H, et al** (2019): *Haemoabdomen due to suspected anaphylaxis in four dogs.* Vet Rec Case Reports, **7**, 1-5.
35. **Rozycki GS** (1998): *Surgeon-Performed Ultrasound*. Ann Surg, **228**, 16–28.
36. **Rozycki GS, Pennington SD, Feliciano DV.** (2001): *Surgeon-Performed Ultrasound in the Critical Care Setting: Its Use as an Extension of the Physical Examination to Detect Pleural Effusion*. J Trauma Inj Infect Crit Care, **50**, 636–42.
37. **Sigrist NE, Adamik KN, Doherr MG, et al** (2011): *Evaluation of respiratory parameters at presentation as clinical indicators of the respiratory localization in dogs*

and cats with respiratory distress. J Vet Emerg Crit Care, **21**, 13–23.

38. **Simpson SA, Syring R, Otto CM** (2009): *Severe blunt trauma in dogs: 235 cases (1997-2003)*. J Vet Emerg Crit Care, **19**, 588–602.

39. **Udobi KF, Rodriguez A, Chiu WC, et al.** (2001): *Role of Ultrasonography in Penetrating Abdominal Trauma: A Prospective Clinical Study*. J Trauma Inj Infect Crit Care, **50**, 475–79.

40. **Walters AM, O'Brien MA, Selmic LE, et al.** (2018): *Evaluation of the agreement between focused assessment with sonography for trauma (AFAST/TFAST) and computed tomography in dogs and cats with recent trauma.* J Vet Emerg Crit Care (San Antonio), **28**, 429–35.

Veterinary Journal of Ankara University

E-ISSN 1308-2817 Cilt/Volume 68 ● Sayı/Number 3 ● 2021

Ankara Univ Vet Fak Derg - vetjournal.ankara.edu.tr - Open Acsess